UNIVERSITY OF SOUTHAMPTON

# SPATIAL AND TEMPORAL VARIABILITY OF PHYTOPLANKTON COMMUNITY COMPOSITION IN THE TROPICAL AND SUBTROPICAL ATLANTIC OCEAN (40°N - 40°S)

By

Alex James Poulton

This thesis is submitted for

Doctor of Philosophy

Faculty of Science

School of Ocean and Earth Sciences

June 2002

UNIVERSITY OF SOUTHAMPTON

ABSTRACT

FACULTY OF SCIENCE

SCHOOL OF OCEAN AND EARTH SCIENCES

Doctor of Philosophy

# SPATIAL AND TEMPORAL VARIABILITY OF PHYTOPLANKTON COMMUNITY COMPOSITION IN THE TROPICAL AND SUBTROPICAL ATLANTIC OCEAN (40°N - 40°S)

By Alex J. Poulton

Routine measurements of the phytoplankton community from the first 10 cruises (1995 - 2000) of the Atlantic Meridional Transect (AMT) programme were examined in the context of spatial and temporal variations in community composition within the subtropical (10 - 40°N/S) and tropical equatorial (10°N - 10°S) Atlantic Ocean. Measurements include size-fractionated chlorophyll *a* concentration, High-Performance-Liquid-Chromatography (HPLC) determined pigment concentration and large (>5 μm) phytoplankton species abundance and identification. Ancillary measurements (density structure, nutrient concentrations and light levels) are used to examine spatial and temporal variations in the hydrographic environment and provide a spatial framework for analysis of variations in the phytoplankton community composition. Multivariate statistical analysis (Bray-Curtis similarity) of (HPLC) pigment measurements and large (>5 μm) phytoplankton species show both latitudinal and vertical differences in composition; an upper and deep flora in subtropical and equatorial Atlantic waters with a reduction in depth differences in upwelling waters off NW Africa. Such spatial differences are associated with regional changes in the mechanisms important for the formation of the ubiquitous chlorophyll *a* maximum. Analysis of the time-series measurements collected in South Atlantic Subtropical Waters (0 - 30°S) show marked interannual (post-winter) differences in the depth of the mixed layer. Analysis of the phytoplankton community in South Atlantic Subtropical Waters indicates interannual variations in the phytoplankton community composition. It is hypothesised that a decrease in winter mixing associated with climatic variability in the South Atlantic Ocean lead to a reduction in seasonal new nutrient inputs and favoured oligotrophic components (taxa) of the phytoplankton community.

# Acknowledgements:

Well, where do you start? Firstly, I would like to thank my supervisors for their advice and support, Patrick Holligan, Jim Aiken, Duncan Purdie. Thanks to Nigel Rees and Chris Gallienne for their trust, advice and lack of prohibition during the cruises, and Toby Tyrrell for his curing my fear of modelling and keeping me on my toes for 7 weeks. This thesis would not be possible without the dedication and hard-work of all those involved in the AMT cruises and I am indebted to them for the data they have collected and made available; Emilio Maranon, Stuart Gibb, Guy Westbrook, Ray Barlow, Chuck Trees, Stan Hooker, Mike Zubkov, Tim O'Higgins, Toria Hill, Hester Willson, Malcolm Woodward, Mike Lucas and all the others I have encountered in my travels. I would also like to thank the professional approach, enlightenment and sheer luxury provided by the crew and officers of the RRS James Clark Ross. My days and nights at the microscope would have been decades if not for the help of Derek Harbour, Russell Davidson, Jeremy Young and Sandra Broerse. I thank Dave Suggett and Mark Moore for sorting out the muddle of algal photophysiology, and providing much needed advice and beer.

Special thanks go to Leonie Dransfeld for her guidance with Henretta and not shouting at me too much during my late night muck ups, and to German Medina-Ruiz for teaching me some Spanish (swearwords) - you are sadly missed and I hope you have enough for a round when we meet again. Smoko regards to Tom Speedy, Maeve and Rachel and Rob Potter, who have helped feed my nicotine addiction. Thanks to my mother and Robin, my family, and regards to John Newcombe and Bill Goulding who have added a little something even though they're not here. Special thanks to Babette Hoogakker for keeping me going, reading many a draft and providing a light at the end of the tunnel - Thank you.

## Graduate School of the Southampton Oceanography Centre

This PhD dissertation by

Alex James Poulton

has been produced under the supervision of the following persons;

**Supervisor/s**

Professor Patrick M. Holligan

Dr. Duncan Purdie

Professor Jim Aiken

**Chair of Advisory Panel**

Dr. Kelvin Richards

**Member/s of Advisory Panel**

Dr. Toby Tyrrell

## Declaration

This thesis is the result of work done wholly while under registered postgraduate candidature.

# QUOTATIONS

*"...the poverty of volume is a noteworthy, newly emerged, certain fact."*

Hensen and others (~1890) describing the (then) unexpected results from the subtropical Great Plankton Expedition (1889), which contradicted the widespread belief that the tropical seas were the marine equivalent of the tropical rainforest: verdant and luxuriant.

Quoted and adapted from Mills (1989)

*"The fundamental questions asked by physiologically orientated plankton biologists are: what organisms are present and at what concentrations and biomass, what are their specific growth rates, what regulates their growth rates and how do the organisms interact with one another and with the environment to form the communities or assemblages we encounter in sampling them."*

Quoted from Eppley (1981a)

# THESIS CONTENTS (1)

## THESIS CONTENTS (2)

# LIST OF FIGURES (1)

# LIST OF FIGURES (2)

# LIST OF TABLES

# GLOSSARY OF SELECTED THESIS ABBREVIATIONS

| Abbreviation | Definition |
|---|---|
| | **Phytoplankton Biomarker Pigments** |
| β-Car | β- Carotene |
| ΣPP | Total Photoprotective Pigments |
| ΣPS | Total Photosynthetic Pigments |
| But-Fuco | 19-Butanoyloxyfucoxanthin |
| Hex-Fuco | 19-hexanoyloxyfucoxanthin |
| Allo | Alloxanthin |
| Chl *a* | Chlorophyll *a* (Mono-vinyl Chlorophyll *a*) |
| TChl *b* | Chlorophyll *b* (TChl b = Dv Chl *b* + Chl *b*) |
| TChl *c* | Chlorophyll *c* (TChl *c* = Chlorophyll $c_1c_2$ + Chlorophyll $c_3$) |
| Diadino | Diadinoxanthin |
| Dv chl *a* | Divinyl Chlorophyll *a* |
| Fuco | Fucoxanthin |
| Lut | Lutein |
| Perid | Peridinin |
| Pras | Prasinoxanthin |
| Tcaro | Total Carotenoids |
| TChl *a* | Total Chlorophyll *a* ( = Chl *a* + Dv chl *a*) |
| Viola | Violaxanthin |
| Zea | Zeaxanthin |
| | **Parameters of the chlorophyll *a* profiles and water-column** |
| Flchla | Chlorophyll *a* concentration from discrete acetone extraction measurements. |
| $C_{z0}$ | Chlorophyll *a* concentration in surface (7m) waters from acetone extraction. |
| $F_{z0}$ | Chlorophyll *a* concentration in surface (7m) waters from calibrated *in-situ* fluorescence. |
| CM | Depth of maximum chlorophyll a concentration (*Chlorophyll a Maximum*). |
| FM | Fluorescence maximum detected by *in-situ* fluorescence measurements. |
| $C_{CM}$ | Chlorophyll *a* concentration at the CM from discrete Flchl*a* measurements. |
| $F_{FM}$ | CM Chlorophyll *a* concentration from calibrated *in-situ* fluorescence measurements. |
| $C_{TOT}$ | Total water-column (0 - 200 m) integrated Flchla from discrete measurements. |
| $F_{TOT}$ | Total water-column (0 - 200 m) integrated chlorophyll *a* concentration from calibrated *in-situ* fluorescence measurements. |
| $C_{eu}$ / $F_{eu}$ | Euphotic zone integrated chlorophyll *a* concentration. |
| $C_{60m}$ | Integrated Flchl*a* in the upper 60 m (Upper portion of the water-column). |
| $C_{200m}$ | Integrated Flchl*a* between 60 and 200 m (Deep portion of the water-column). |
| $Z_{CM}$ | Depth of the chlorophyll *a* maximum. |
| $Z_{FM}$ | Depth of the fluorescence maximum. |
| $CM_{WID}$ | Width of the chlorophyll maximum. |
| $Z_{CC}$ | Depth of the centroid of the chlorophyll a distribution. |
| PAR | Photosynthetically Active Radiation (between 400 - 700 nm). |
| $K_d$ | Vertical attenuation coefficient of PAR. |
| $Z_{eu}$ | Pentration depth of 1% surface PAR (*Euphotic zone depth*). |
| MLD | Depth of the upper mixed layer. |
| $Z_{NO3}$ | Estimated depth of the nitracline. |
| $Z_{NO2}$ | Estimated depth of the nitrite maximum. |
| $Z_{PO4}$ | Estimated depth of the phosphocline |
| $Z_{SiO2}$ | Estimated depth of the silicocline. |
| | **Regions and provinces of the Atlantic Ocean** |
| EQU | Equatorial Atlantic Ocean (5°N - 5°S) |
| NASW | North Atlantic Subtropical Waters (20 - 35°N) |
| NATD | North Atlantic Drift (35 - 40°N) |
| SASW | South Atlantic Subtropical Waters (5 - 30°S) |
| SATW | South Atlantic Temperate Waters (30 - 40°S) |
| UPW | Upwelling waters off NW Africa (5 - 20°N) |

# CHAPTER 1: GENERAL INTRODUCTION

## PREFACE

About 40-50% of annual global photosynthesis occurs in aquatic environments, despite the disproportionately small amount of plant biomass within aquatic ecosystems compared with terrestrial ecosystems (Falkowski, 1994; Williams, 1998). In the open ocean primary production is dominated by prokaryotic and eukaryotic photoautotrophs, termed phytoplankton, which exhibit a high degree of taxonomic and morphological diversity (e.g. Tett and Barton, 1995). Seventy percent of the Earth's surface is covered by ocean, and roughly 60 - 70% of the oceans are within the latitudinal boundaries of the subtropics (10 - 40°N/S) and tropics (10°N - 10°N). Although high-latitude temperate waters are often characterised by high seasonal rates of primary productivity (e.g. during the spring bloom), the high surface area of subtropical waters and the often year-round algal blooms in tropical equatorial waters also represent important sources of global productivity (Longhurst, 1993; Karl *et al.,* 1995, 2001a). Variations in the productivity of the subtropical gyres, often termed "biological deserts" (e.g. Ryther, 1969), and tropical waters due to climatically driven fluctuations in the physical forcing of the environment can therefore have important consequences for the global carbon cycle and oceanic productivity (Karl *et al.,* 1995, 2001a).

Phytoplankton metabolism is dependent upon the fixation of carbon through photosynthesis; with both the rate and yield of photosynthesis often limited by the availability of solar irradiance (light) and inorganic nutrients (e.g. nitrogen and phosphorus). In the open-ocean, light availability is regulated by the atmosphere (cloud cover) and the optical properties of the upper ocean determined by the suspended particulate material (i.e. algal cells), by dissolved material and by the water itself. Absorption and scattering of light cause a decrease in light levels with depth, so that for the clearest oceanic waters the percentage of surface irradiance falls below 0.1% within a few hundred meters. Nutrient availability in the open ocean is controlled by the uptake and biologically-mediated regeneration of nutrients in upper light-rich waters, the sinking of particles to depth and their biological and/or chemical remineralisation therein. These factors combine to cause an increasing nutrient gradient with depth; so that upper waters (<100 m) are often nutrient depleted and deep waters are nutrient enriched. However, phytoplankton are not suspended in a static medium; wind-induced mixing and the interaction of currents on the upper oceans (<500 m) cause phytoplankton cells to experience highly variable light and nutrient conditions. Variations in the physical forcing of the environment cause fluctuation between two types of water-column structure; thermal stratification of the water-column in waters experiencing high solar radiation and low turbulence, and vigorous mixing of the water-column in waters experiencing high wind stress and low levels of solar radiation.

The general introduction that follows provides an overview of the major surface currents and hydrographic conditions, light and nutrient availability and algal physiology, and the distribution of phytoplankton biomass and productivity in the subtropical (10 - 40°N/S) and tropical (10°N - 10°S) Atlantic Ocean (section 1.1). This is followed by a brief introduction to the main phytoplankton groups present in the open ocean and their photophysiology (section 1.2), and a description of phytoplankton community dynamics in the open ocean and community composition in the different

regions of the subtropical and tropical Atlantic Ocean (section 1.3). Lastly, a short introduction to the thesis and the major objectives and research questions are described (section 1.4).

## 1.1. Regional Hydrography

### 1.1.1. Surface Currents and Wind Patterns

Surface currents in the subtropical (10 - 40°N/S) and tropical (10°N - 10°S) Atlantic Ocean are driven by the overlying atmospheric wind patterns (i.e. wind forcing). The Westerly winds dominate high latitudes (>50°N), whereas the Trade winds influence lower latitudes (Brown *et al.,* 1989a). Seasonality of atmospheric high and low pressure systems causes changes in wind patterns and the underlying current patterns during the year. Trade winds are strongest in the winter in both hemispheres; February in the northern hemisphere and August in the southern hemisphere (Brown *et al.,* 1989a). The equatorial region between the Trade Winds is characterised by an area of relatively calm winds (Doldrums), high cloud cover and a large amount of rainfall (Tchernia, 1980; Brown *et al.*, 1989a); the Inter-Tropical Convergence Zone (ITCZ).

Figure 1.1 shows the surface current systems in the subtropical and tropical Atlantic Ocean (a), as well as annual mean temperature (b) and salinity (c) at the seasurface. Surface currents in the subtropical and tropical Atlantic Ocean form three inter-related current systems; the North Atlantic Subtropical Gyre (NASG), the Equatorial current system and the South Atlantic Subtropical Gyre (SASG) (Fig 1.1a). Wind and related current flow in the different hemispheres cause the clockwise circulation of the SASG, which represents roughly half of the South Atlantic, and the anti-clockwise circulation of the NASG, which represents just over a third of the North Atlantic (Fig. 1.1a; Boltovskoy, 1999). Surface equatorial currents include four adjacent and counter-flowing currents (Fig. 1.1a); the westward flowing North Equatorial Current (NEqC), the eastward flowing North Equatorial Counter Current (NECC), the westward flowing South Equatorial Current (SEqC) and the eastward flowing South Equatorial Counter Current (SECC). The flow of the NEqC and SEqC build up water on the western side of the equatorial Atlantic, which is balanced by the flow of the counter currents and the coastal Guyana and Brazil Currents (Fig. 1.1a; Tchernia, 1980; Tomczak and Godfrey, 1994).

The two equatorial currents, combined with the effects of the low-latitude Trade winds and the Earth's spin (Coriolis Force), cause the offshore movement of water along the eastern boundary of the Atlantic Ocean. This offshore movement of water is counterbalanced by the upward movement of deep water into the surface layer along the coast of Africa (coastal upwelling) within the Canary and Benguela Currents. Along the equator, the divergence of the Trade winds and the associated high wind stress, cause eddy upwelling and the movement of deep cool water into the surface layer (Longhurst, 1993). Therefore, there are two principal causes of upwelling in the subtropical and tropical Atlantic Ocean; offshore movement of the boundary currents along the coast and wind-driven equatorial divergence. The upward movement of cold, dense and relatively old water into the surface layer has consequences for the nutrient dynamics and phytoplankton communities in these regions of the Atlantic Ocean.

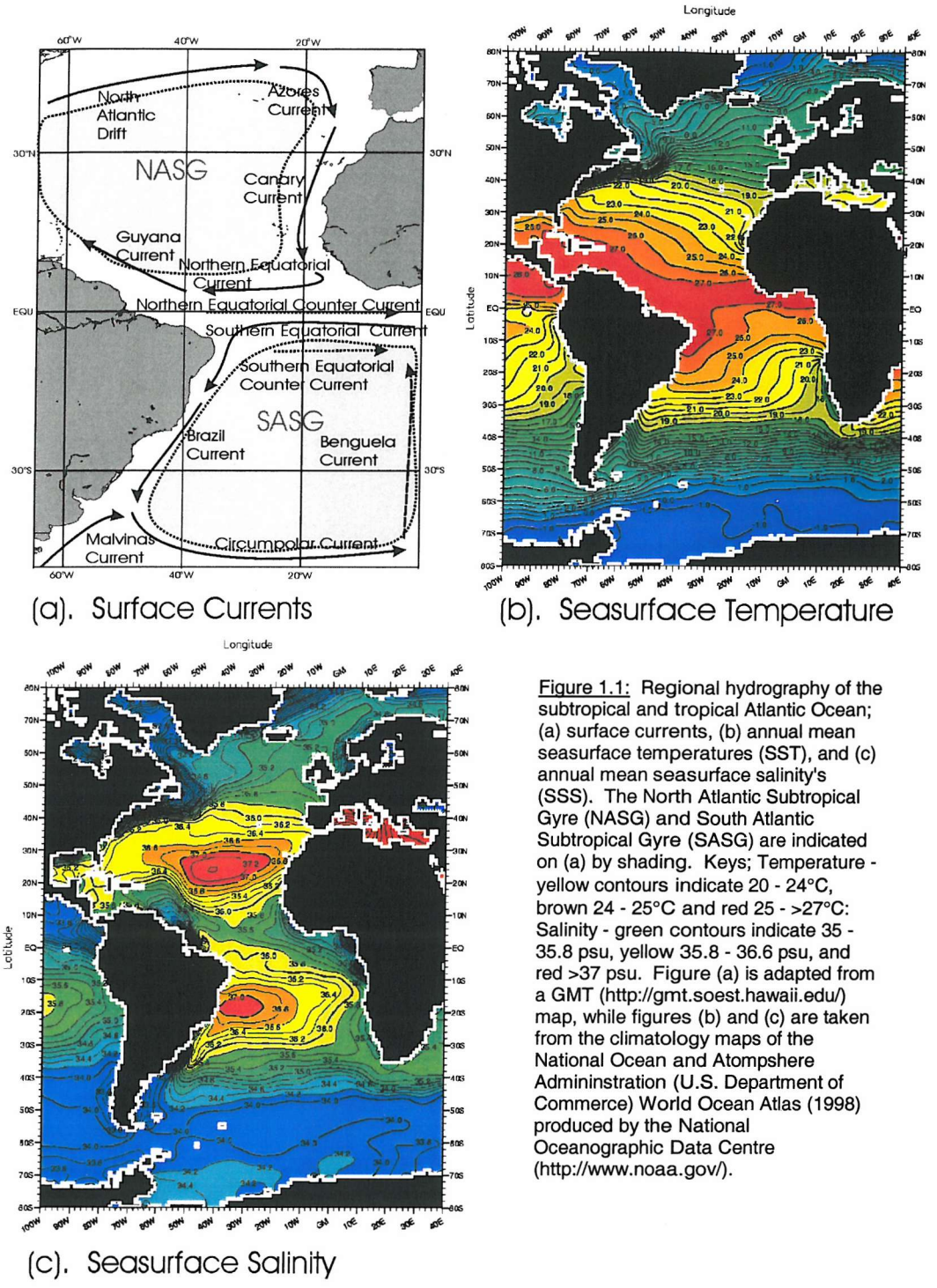


Figure 1.1: Regional hydrography of the subtropical and tropical Atlantic Ocean; (a) surface currents, (b) annual mean seasurface temperatures (SST), and (c) annual mean seasurface salinity's (SSS). The North Atlantic Subtropical Gyre (NASG) and South Atlantic Subtropical Gyre (SASG) are indicated on (a) by shading. Keys; Temperature - yellow contours indicate 20 - 24°C, brown 24 - 25°C and red 25 - >27°C: Salinity - green contours indicate 35 - 35.8 psu, yellow 35.8 - 36.6 psu, and red >37 psu. Figure (a) is adapted from a GMT (http://gmt.soest.hawaii.edu/) map, while figures (b) and (c) are taken from the climatology maps of the National Ocean and Atompshere Admininstration (U.S. Department of Commerce) World Ocean Atlas (1998) produced by the National Oceanographic Data Centre (http://www.noaa.gov/).

### 1.1.2. Temperature, Salinity and Water-column Structure

Temperature in combination with salinity controls the density of seawater, and therefore the physical structure of the upper water-column. Solar radiation absorbed by the upper ocean and atmosphere causes heating of the ocean and atmosphere to produce current and climate patterns (Pond and Pickard, 1983; Brown *et al.,* 1989b; Reddy, 2001). Within the upper ocean, temperature decreases with depth as waters become increasingly isolated from solar warming. The temperature gradient is inversely related to the amount of wind and wave-induced turbulence at the seasurface (Reddy,

2001). The horizon where temperature changes are maximal is termed the thermocline or with reference to related density changes, the pycnocline. Turbulence at the ocean surface cause a layer of uniform characteristics (temperature, salinity) within surface waters, that ranges from tens to hundreds of meters depending upon the magnitude of physical forcing: this homogenous layer is referred to as the upper mixed layer (Reddy, 2001).

The magnitude of solar radiation varies spatially (latitude) and temporally (seasonally) to produce variations in the temperature and stratification of the oceans (Brown *et al.,* 1989b; Reddy, 2001). The pattern of latitudinal variation of surface temperature (Fig. 1.1b) in the Atlantic Ocean follows the pattern of solar heat supply; maximum around the equator and decreasing with increasing latitude (Brown *et al.,* 1989b; Reddy, 2001). Seasonal variation of seasurface temperatures in the oceans depends upon the seasonal variations in solar radiation, that are maximum in summer and minimum in winter (Brown *et al.,* 1989b; Reddy, 2001). However, the magnitude of seasonal changes in solar radiation, and therefore seasurface temperatures, varies with the regional heat budget (Brown *et al.,* 1989b; Reddy, 2001); both are relatively large in high-latitude polar and temperate waters and small in low-latitude tropical and equatorial waters.

The structure of the water-column varies with the amount of solar radiation and turbulence at the seasurface, and much of the regional variation in water-column structure can be described by the structures found during seasonal changes in temperate waters. During winter, solar heating is at a minimum causing low surface temperatures and high turbulence, which together cause well mixed homogenous conditions throughout the top 200 - 300 m of the water-column (Brown *et al.,* 1989b). In summer, in response to increased solar heating and reduced wind stress, the mixed layer shallows and a seasonal thermocline is established, causing isolation of the upper ocean from deeper waters (Brown *et al.,* 1989b; Barber, 2001). Annually high heat budgets around the equator cause permanent stratification of low-latitude tropical waters (Brown *et al.,* 1989b; Reddy, 2001), whereas at high-latitudes the regional heat budgets are seasonally variable (Longhurst, 1993).

Surface waters of the subtropical and tropical Atlantic Ocean are influenced by large amounts of solar heating leading to characteristically high seasurface temperatures (SST), which are maximal around the equator and decrease both to the north and south (Fig. 1.1b). Zonal and meridional displacement of seasurface isotherms are due to the effects of wind driven surface currents (Reddy, 2001); the NEqC and SEqC push warm water to the west which is counterbalanced by the upwelling of relatively cool, dense water in the eastern tropics (Fig. 1.1b). Regional differences between the rates of evaporation and precipitation are the main factors controlling seasurface salinity. In areas with high seasurface salinity (e.g. subtropical gyres), evaporation rates are higher than precipitation rates, whereas the opposite is true in areas with low seasurface salinity (e.g. equatorial waters; Fig. 1.1c). The equatorial Atlantic Ocean is influenced by both the ITCZ with high rates of precipitation compared with evaporation rates, and the annual rainfall in this area is ~2 m $yr^{-1}$ (Tchernia, 1980), and western inputs of low salinity river water from the Amazon River (which represents ~20% of the world's river water; DeMaster, 2001), that cause a general lowering of sea surface salinity (Fig. 1.1c; Muller-Karger, 1988; Brown *et al.,* 1989a; Signorini *et al.,* 1999).

### 1.1.2. Light Availability

The light field in the open ocean varies with depth, time of day and seasonally (Sathyendranath and Platt, 2001). Temporal variations occur on several scales, ranging from seconds (response to clouds and vertical mixing) to seasonal differences in irradiance due to the earth's rotation (Sathyendranath and Platt, 2001). Figure 1.2 shows average downwelling irradiance (a), latitudinal variations in seasonal irradiance (b) and the percentage of cloud cover (c) over the subtropical and tropical Atlantic Ocean. Within surface waters of the subtropical (10 - 40°N/S) and tropical (10°N - 10°S) Atlantic Ocean there is a large amount of incident radiation throughout the year (Fig. 1.2a, b), although only ~50% of this incident light is in wavelengths suitable for photosynthesis (400 - 700 nm); termed Photosynthetically Active Radiation (Kirk, 1992; Kirk, 1994). Highest mean downward fluxes of Photosynthetically Active Radiation (PAR) are observed in the subtropical gyres of the Atlantic Ocean (>275 W $m^{-2}$), whereas tropical waters experience slightly lower (200 - 250 W $m^{-2}$) irradiances (Fig. 1.2a; Bishop and Rossow, 1991; Bishop *et al.,* 1997). There are also differences between the mean downwelling irradiance between northern (200 - 250 W $m^{-2}$) and southern (>250 W $m^{-2}$) subtropical waters (Fig. 1.2a).

These regional differences in solar irradiance are likely to be related to differences in cloud cover; tropical waters annually experience ~70 - 80% cloud cover (partly due to the ITCZ), while the northern subtropical gyre experiences ~50 - 60% and the southern subtropical gyre ~40 - 60% (Fig. 1.2b). Due to the short generation times of phytoplankton, compared with terrestrial systems, temporal variability in the incident light regime is likely to be more influential on oceanic biomass and production (Bishop and Rossow, 1991). Seasonal changes in the incident light regime are minimal near the equator and increase with increasing latitude (Kirk, 1994); in tropical equatorial waters seasonal minima and maxima range from ~32 to 38 MJ $m^{-2}$ $d^{-1}$, whereas at the high-latitude boundaries of the subtropical gyres (30 - 40°N/S) seasonal variations range from ~20 MJ $m^{-2}$ $d^{-1}$ in mid-winter to ~40 MJ $m^{-2}$ $d^{-1}$ during mid-summer (Fig. 1.2c). Therefore, phytoplankton populations in tropical waters are not likely to experience large-scale day-to-day or seasonal variations in incidental light levels and will encounter similar light regimes for extended periods of time (Bishop and Rossow, 1991). Phytoplankton within subtropical waters will experience significant day-to-day and seasonal variability, with its magnitude increasing with increasing latitude, although not as severe as those experienced by temperate high-latitude phytoplankton populations (<10 to >40 MJ $m^{-2}$ $d^{-1}$; Fig. 1.2c).

In oceanic waters roughly 66% of the total solar radiation penetrating the ocean surface is absorbed within the top 10 m, and it is this energy combined with wind-induced turbulence that forms and maintains the upper mixed layer (Kirk, 1992). Light penetration is governed by absorption and scattering, which are controlled by the nature of the particulate material present in the water column and by the optical properties of the water itself (Kirk, 1992). Particulate material in the open ocean is mainly composed of phytoplankton cells, dissolved organic material (DOM) and non-living yellow-brown detrital organic material derived from the breakdown of cells through lysis or grazing (Kirk, 1992; Sathyendranath and Platt, 2001). In oceanic waters with few pigmented particles in surface waters (e.g. subtropical gyres), the light field is mainly derived from the optical properties of water;

water absorbs very strongly in the red end of the spectrum giving subtropical waters a characteristic blue colour (Kirk, 1992).

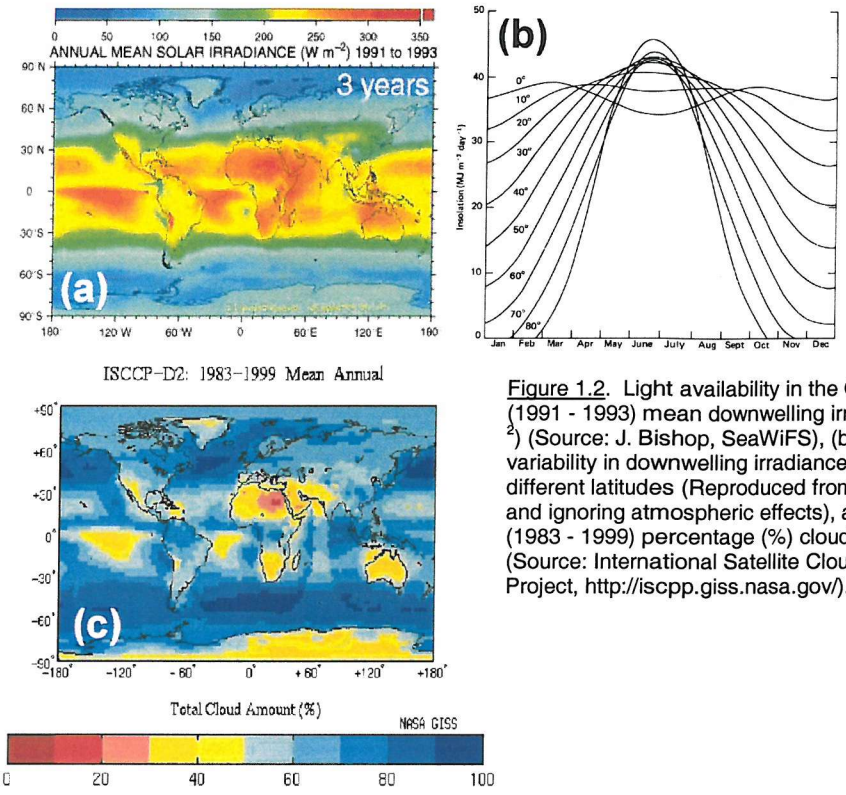


Figure 1.2. Light availability in the Ocean; (a) 3-yr (1991 - 1993) mean downwelling irradiance (W $m^{-2}$) (Source: J. Bishop, SeaWiFS), (b) seasonal variability in downwelling irradiance (MJ $m^{-2}$ $d^{-1}$) at different latitudes (Reproduced from Kirk, 1992, and ignoring atmospheric effects), and (c) 17-yr (1983 - 1999) percentage (%) cloud cover (Source: International Satellite Cloud Climatology Project, http://iscpp.giss.nasa.gov/).

Absorption and scattering in the water-column cause an exponential decrease of light with depth, which can be measured as the vertical attenuation coefficient ($K_d$; Kirk, 1992, 1994) and used to characterise the underwater light field. The vertical attenuation coefficient ($K_d$) is calculated as the negative log (- ln) of the difference in irradiance (E) between two depths (e.g. the surface and 10 m) divided by the depth change (i.e. in this case 10 m); $K_d = -\ln (E_0/E_Z) / \Delta_Z$ (Kirk, 1994). Using $K_d$, the depth distribution of the phytoplankton community can be normalised to irradiance (i.e. 'optical depths') which correspond to percentage PAR depths (Kirk, 1992; Falkowski and Raven, 1997).

With high phytoplankton abundances, high rates of absorption and scattering of the light by algal cells cause a rapid decrease in light levels with depth and a high $K_d$ (Kirk, 1994, 1994). Primary production (photosynthesis) in the ocean occurs within upper light-rich waters that is termed the euphotic zone (Kirk, 1994), and is defined as the portion of the water-column above the depth at which the ambient light (PAR) levels are reduced to 1% of the surface level (Sathyendranath and Platt, 2001). However, it should be noted that this is a relative term whereas photosynthesis is a quantum process and depends on the absolute light availability rather than its relative availability (Sathyendranath and Platt, 2001). The euphotic zone depth and vertical attenuation of light are closely related, such that waters with low $K_d$ have deep euphotic zones (100 - 150 m; e.g. subtropical gyres) and waters with high $K_d$ have shallow euphotic zones (10 - 50 m; e.g. upwelling and tropical waters).

## 1.1.3. Oceanic Nutrient Cycles and Availability

*Oceanic Nutrient Cycles*

Within the open ocean, nitrogen (N) and phosphorus (P) are thought to be the main macro-nutrients limiting photosynthetic organisms (Dugdale, 1967b; Falkowski and Raven, 1997; Tyrrell, 1999), while silica (silicate) limitation is restricted to phytoplankton groups (e.g. diatoms) that require silicate for structural components (DeMaster, 2001). Trace nutrient elements (e.g. iron, zinc, copper) are required in relatively small amounts (<0.1 μM) for the production of metabolic intermediates and are not thought to be limiting to phytoplankton communities in the tropical and subtropical Atlantic Ocean, although concentrations may become limiting in environments rich in the other nutrients (N, P, silica). Nutrient-depleted areas of the ocean where inorganic nutrient concentrations are low (<0.5 μM) and limiting to the autotrophic community are termed oligotrophic. A simple schematic of the N and P cycles in the open ocean is presented in Figure 1.2a, and the main steps are described below;

(1). Nitrogen (N) introduced into the euphotic zone from outside is commonly termed 'new' nutrients (Dugdale and Goering, 1967). Inorganic nitrogen (nitrate, $NO_3^-$) and inorganic phosphorus (phosphate, $PO_4^{3+}$) enter the euphotic zone from deep aphotic waters (Fig. 1.2a) through the prevalent nutrient gradients, vertical mixing and turbulence, including upwelling (Venrick, 1990a, b; Letelier *et al.,* 2000). In oligotrophic waters there is also evidence that vertical migration by large phytoplankton colonies or mats may import new nutrients into the euphotic zone (Fig. 1.2a) in internal cellular reserves (Villareal *et al.,* 1993, 1996, 1999a, b). Physical processes that contribute to new nutrient fluxes include shear-induced turbulence, internal tides, the breaking of internal waves, wind-driven Ekman pumping and cyclonic mesoscale eddies (McGowan and Haywood, 1978; Klein and Coste, 1984; Dandonneau and Lemasson, 1987; McGillicuddy *et al.,* 1997, 1998).

(2). Within the euphotic zone $NO_3^-$ and $PO_4^{3+}$ are taken up by autotrophic cells (Fig. 1.2a) and utilised to form organic metabolic intermediates and cellular structures (e.g. proteins, pigments, adenosine tri-phosphate). Autotrophs (and heterotrophs) are consumed within the marine food chain so that organic nutrients are found in various forms; particulate organic forms (Particulate Organic Nitrogen, PON, and Particulate Organic Phosphorus, POP) in living cells and detrital material formed from dead cells, and dissolved organic forms (Dissolved Organic Nitrogen, DON, and Dissolved Organic Phosphorus, DOP) which are released from cells during growth and lysis. DON and DOP in the euphotic zone are also associated with dissolved organic carbon (DOC), and the three are the major components of dissolved organic matter (DOM) in the ocean. PON and POP are associated with particulate organic carbon (POC) in the open-ocean, of which living cells and detrital organic material are the main components.

DON and DOP may be lost from algal cells through cell leakage (e.g. Karl *et al.,* 1998) or during grazing (e.g. Banse, 1992, 1995), or in association with PON and POP during cell break-up from heterotrophic grazing or viral activity (e.g. Parsons *et al.,* 1984; Metzler *et al.,* 1997). Within the euphotic zone, biologically-produced nutrients are important ($NH_4^+$ and urea) N sources for pelagic communities, and are mainly released from heterotrophic grazing ('sloppy feeding') and excretion (Eppley *et al.,* 1973; Probyn, 1987; Banse, 1992, 1995). Other sources of new nutrients (N and P)

into the euphotic zone (Fig. 1.2a) are from atmospheric deposition in the form of dust storms (dry deposition) or rainfall (wet deposition) (Paerl *et al.*, 1990, 1999; Migon and Sandroni, 1999), and through the activity of N-fixers (Dugdale and Goering, 1967; Capone *et al.*, 1997) which often release a portion of the N-fixed as DON (Capone *et al.*, 1994). Organic nitrogen produced and recycled within the euphotic zone is termed 'regenerated' (Dugdale and Goering, 1967), and in the upper portion of the euphotic zone are the main nutrient sources for autotrophic (regenerated) production (Jackson, 1980). Depending upon the level of DOM release from algal cells, regenerated production in the upper portion of the euphotic zone can be regarded as either controlled mainly by heterotrophs (assuming DOM leakage of <5 - 10%; Banse, 1992, 1995) or by bacteria-phytoplankton-heterotroph interactions (assuming DOM leakage of >50%; Karl *et al.*, 1998).

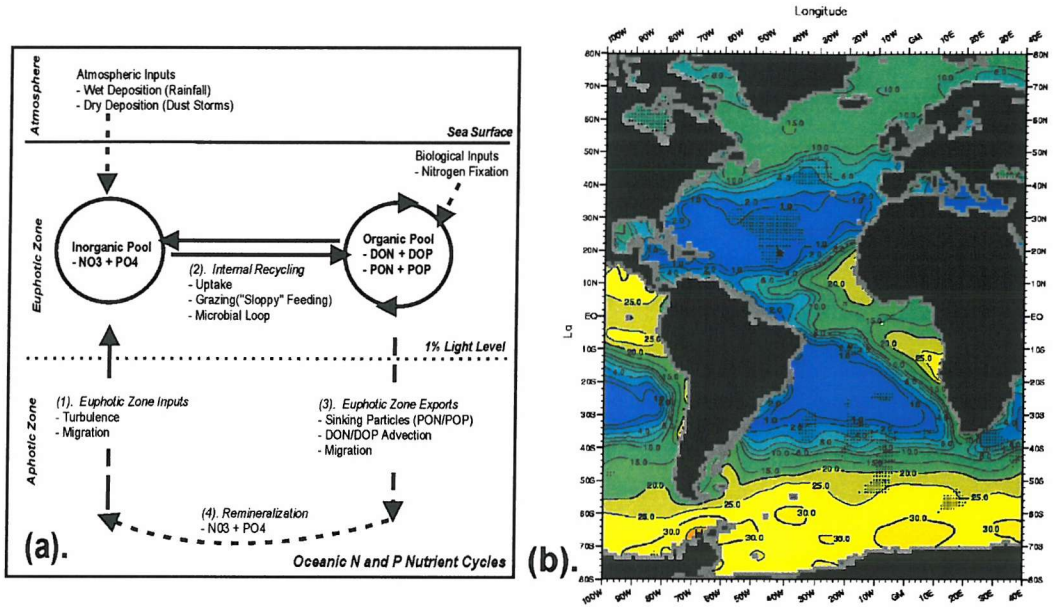


Figure 1.3: Nutrient availability; (a) schematic of nitrogen (N) and phosphorus (P) cycles in the marine environment (see text for abbreviations), and (b) annual mean 100 m nitrate concentrations (μM). Deep blue nitrate contours indicate concentrations ~1 - 2 μM, pale blue to green contours indicate concentrations from ~ 4 - 15 μM and pale green to yellow contours indicate concentrations from ~20 - 30 μM. Plot (a) is adapted from Doney *et al.*, (1996) and plot (b) is taken from the NOAA World Ocean Atlas (1998) produced by the National Oceanographic Data Centre (http://www.noaa.gov/).

(3). N and P are exported out of the euphotic zone (Fig. 1.2a) as PON and POP within migrating or sinking algal cells (e.g. Villarreal *et al.*, 1993, 1996, 1999a, b), vertically migrating zooplankton which may graze in surface waters and excrete at depth (Longhurst and Harrison, 1989), sinking faecal pellets (Jumars *et al.*, 1989), and from DON and DOP advection due to the inverse gradient between high concentrations in the upper euphotic zone and relatively low concentrations in deep aphotic waters (Vidal *et al.*, 1999). However, DON and DOP are rapidly released from faecal pellets, so that the loss of organic nutrients through the sinking of faecal pellets out of the euphotic zone is relatively low (Jumars *et al.*, 1989). A proportion of DON and DOP can also be exported out of the euphotic zone during turbulence and mixing (Keil and Kirchman, 1999), although the net effect may represent a small loss compared with production of DON and DOP in the euphotic zone (T. Tyrrell, pers. comm.).

(4). Within the aphotic zone, N and P are remineralised by bacterial decomposition of organic material into inorganic forms which can be passed back into the euphotic zone through upward flux mechanisms (Fig. 1.2a). N is remineralised from PON through ammonification (PON to $NH_4^+$) and nitrification ($NH_4^+$ to $NO_2^-$, and then $NO_2^-$ to $NO_3^-$) (Karl and Michaels, 2001), while P is remineralised from the decomposition (respiration) of organic material (Ruttenberg, 2001).

The oceanic silica cycle is mainly in inorganic forms and includes the production of opaline silica by uptake of dissolved silica and its dissolution following cell death (DeMaster, 2001). The distribution of silica (silicate) in the open ocean is similar to that of N and P: depleted in surface waters due to biological uptake and enriched in deep aphotic waters due to inorganic dissolution and silicate regeneration (DeMaster, 2001). However, the depth of the silicate maximum is deeper than the maxima for N and P, as regeneration of organic matter (sources of N and P) occurs at shallower depths than significant silica dissolution (DeMaster, 2001). It should be noted that due to the under-saturation of biogenic silica in surface waters, inorganic dissolution of silica also takes place within the water-column as soon as the cell membrane is removed from the cell by either microbial or grazing activities (DeMaster, 2001). Thus, the intra-cellular concentration of silica required to form silicate structural material has a relatively high metabolic cost attributed to it when compared with other structural material (DeMaster, 2001). Limitation of oceanic diatoms and silica requiring algae is usually associated with waters that are already rich in other limiting nutrients (N and P), so that silica limitation is mainly found at high latitudes (>50°N/S) and in upwelling waters (DeMaster, 2001).

*Nutrient Availability in Oceanic Waters*

In the upper ocean, the distribution of inorganic forms of N, P and silica are similar; all three nutrients are utilised and depleted in upper waters, lost from the euphotic zone in sinking particles (living and detrital) and enriched in deep aphotic waters due to remineralisation. In contrast, organic nutrients show a different depth distribution; highest concentrations are found in upper waters associated with autotrophic growth and heterotrophic grazing (Karl and Michaels, 2001b). Inorganic nutrient depletion in upper waters (<100 m) and enriched concentrations at depth, lead to a steep concentration versus depth gradient (Karl and Michaels, 2001b). The depth of significant increase from low concentrations in surface waters is termed the nutricline, or with reference to specific nutrients, the nitracline ($NO_3$), phosphocline ($PO_4$) and silicline (silicate). In upper waters (<200 m), nutricline depths can be used as estimates of the relative availability of nutrients to phytoplankton communities; a shallow nutricline indicates that a smaller portion of the water-column is nutrient depleted, whereas a deep nutricline indicates the reverse.

The distribution of nitrate in the Atlantic Ocean (Fig. 1.2b) illustrates the major features of the distribution of these nutrients in subtropical and tropical waters. Within both subtropical gyres of the Atlantic Ocean, $NO_3$ is depleted (<1 μM) in upper waters (<100 m), while around the equator, in the eastern boundary currents (e.g. off NW Africa) and around the subtropical convergences (30 - 40°N/S) there are relatively high (>>2 μM) nitrate concentrations at 100 m (Fig. 1.2b). Increased nutrient concentrations off NW Africa and around the equator are related to the upwelling of deep

nutrient-rich water into the surface layer, while increased nutrient concentrations in association with the subtropical convergences and high-latitude waters are associated with seasonal (winter) mixing. Although the depth of the nitracline is not illustrated in Figure 1.2b, it is clear that the nitrate concentration at 100 m is proportional to the nitracline depth; where the nitracline is shallow (<100 m) there are high nitrate concentrations in the upper 100 m (e.g. tropical equatorial waters and off NW Africa), whereas where the nitracline is deep (>100 m), upper waters are nitrate depleted (e.g. subtropical gyres). The nitrate gradient in the upper waters of the subtropical and tropical Atlantic Ocean is strongest near the equator and weakens to the north and south in association with deeper and temporally variable mixed layers (Planas *et al.,* 1999). Planas *et al.,* (1999) found that in areas were there was a low nitrate flux (e.g. subtropical gyres), phytoplankton nitrate requirements were higher than the upward diffusive flux, which indicates important roles for other types of nitrogen input into the euphotic zone (e.g. nitrogen fixation, atmospheric inputs; Fig. 1.2a)

Recent research (Wu *et al.,* 2000; Cavender-Bares *et al.,* 2001) has led to the proposal of fundamental differences in the inorganic nutrient dynamics in the North Pacific Subtropical Gyre (NPSG) and western portion of the North Atlantic Subtropical Gyre (Sargasso Sea). Following deep winter mixing in the Sargasso Sea the N:P ratio is much higher than in the NPSG, where the scale of winter mixing is less, and soluble reactive phosphorus concentrations in upper waters (<100 m) in the Sargasso Sea are between 1 - 10 nM during summer which are at least an order of magnitude lower than in the NPSG (Cavender-Bares *et al.,* 2001). Therefore, it has been proposed that phytoplankton communities in the Sargasso Sea are more severely P limited compared with the NPSG (Wu *et al.,* 2000). However, a study by Canellas *et al.,* (2000) found that phosphate uptake rates in the Atlantic Ocean are low, except in surface waters south of 25°S, which suggests that over large areas of the subtropical Atlantic Ocean inorganic P is not limiting community production (Canellas *et al.,* 2000). This finding contradicts the conclusions of Wu *et al.,* (2000) and Cavender-Bares *et al.,* (2001). In view of these apparent inter- and intra-ocean differences in nutrient dynamics, there have been calls for similar comparative studies of the phytoplankton communities found in these different oceans and ocean basins to be carried out (Cavender-Bares *et al.,* 2001).

There is also evidence of differences between the organic nutrient cycles in the NPSG and Sargasso Sea. In the Sargasso Sea, DOC accumulates in the upper water-column during early spring due to increased primary production and is partially consumed in the summer and autumn (Carlson *et al.,* 1994a). DOC that escapes remineralisation is exported from the surface ocean during winter mixing, and this relatively short flux is estimated to be greater than the annual particle flux (Carlson and Ducklow, 1994; Carlson *et al.,* 1994a). For the 1995 spring bloom in the Sargasso Sea, net DOC production was 59 - 70% of the net community production (Hansen and Carlson, 1998). Net DOC production was maximal during the period of deep convective overturn of the water column indicating linkage between the processes (Hansen and Carlson, 1998, 2001). However, in the NPSG there is growing evidence that there has been a change in the dynamics of the DOM pool between 1993 - 1999, which is though to be associated with a *'Domain-Shift'* in phytoplankton communities (Karl *et al.,* 2001a; Church *et al.,* 2002). Between 1993 - 1999 the composition of DOM has changed, with a relative enrichment of DON and DOC while DOP has remained at pre-1993

concentrations (Church *et al.,* 2002). Such a net accumulation of a C- and N-enriched DOM pool implies non-steady state dynamics in primary production and utilisation of organic matter in the NPSG (Church *et al.,* 2002); increases in the size of the DOM pool may indicate that bacterioplankton growth is limited by other factors as their high affinity for DOC uptake should result in a permanently low labile pool of DOC. The utilisation of this N-enriched DOM pool by phytoplankton within the NPSG is theoretically possible (Karl, 1999), although to date there has been no reports within the literature.

### 1.1.4. Distribution of Phytoplankton Biomass (Chlorophyll *a*)

*Basinscale Patterns of Phytoplankton Biomass and Primary Productivity*

Chlorophyll *a* is the main light-harvesting pigment in all phytoplankton taxa and its concentration is generally considered to be proportional to the biomass, or standing stock, of the autotrophic community in the ocean. Recent developments in the methodologies for remotely sensing chlorophyll *a* concentration from high altitude satellites have allowed the basinscale patterns of phytoplankton biomass to be investigated (e.g. Longhurst *et al.,* 1995), although there remain difficulties in data interpretation associated with atmospheric corrections (e.g. aerosols), detection in waters containing large concentrations of non-living detrital material (e.g. coastal waters), and extrapolation of surface measurements to depth. Combination of the data on the distribution of biomass (chlorophyll *a*) with light (PAR) availability has allowed the development of the first series of models for estimating global patterns of carbon fixation (i.e. primary productivity; Sathyendranath and Platt, 2001). Figure 1.4 shows a yearly composite (1998) of the distribution of chlorophyll *a* in surface waters of the global ocean (a) and an estimate of the distribution of primary productivity (b) based on a model developed by Behrenfeld and Falkowski (1997) and surface chlorophyll concentrations from 1997 - 1999 (Behrenfeld *et al.,* 2002).

Within the Atlantic Ocean, the central ranges of the subtropical gyres in both hemispheres are characterised by very low biomass in surface waters, with chlorophyll *a* concentrations <0.2 mg $m^{-3}$ in the gyre centres and slightly elevated at the gyre boundaries (~0.3 mg $m^{-3}$), while the estimated rates of primary production are <200 g C $m^{-2}$ $y^{-1}$ (Fig. 1.4). Areas of increased chlorophyll *a* concentration are associated with the subtropical convergences at the northern and southern boundaries of the subtropical gyres (0.5 - 2.0 mg $m^{-3}$), upwelling waters off NW Africa (1.0 - 10.0 mg $m^{-3}$) and waters along the equator and associated with the equatorial divergence (0.5 - 2.0 mg $m^{-3}$). Elevated biomass measurements are accompanied by increases in the estimated rates of carbon fixation; ~300 g C $m^{-2}$ $y^{-1}$ in the subtropical convergences, 400 - >600 g C $m^{-2}$ $y^{-1}$ off NW Africa, and >200 g C $m^{-2}$ $y^{-1}$ around the equator (Fig. 1.4). Therefore, upwelling of cool, nutrient-rich water off NW Africa and along the equator causes enhanced phytoplankton biomass and primary productivity (e.g. Sathyendranath and Platt, 2001). The annual production in these areas is thought to be higher than the seasonal production in temperature waters due to the much longer activity time (almost year-round) of regional upwelling (Longhurst, 1993).

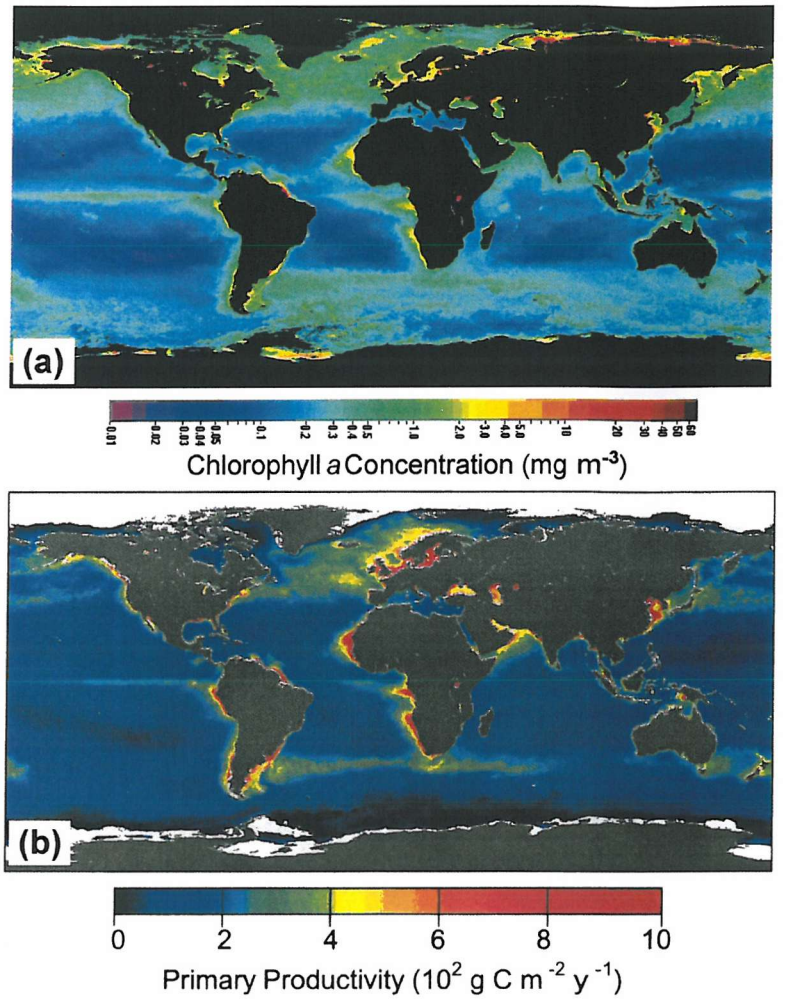


Figure 1.4. Global distribution of biomass (chlorophyll *a*) and primary production in surface waters; (a) SeaWiFS composite of surface chlorophyll *a* concentration for 1998 (Source: http://seawifs.gsfc.nasa.gov/), and (b) estimated annual net primary production for November 1997 to October 1999 calculated using monthly SeaWiFS satellite measurements of near-surface chlorophyll *a* and the Vertically Generalised Production model of Behrenfeld and Falkowski (1997) (reproduced from Behrenfeld *et al.*, 2002).

The contribution of tropical equatorial waters to the total annual carbon fixation of the entire Atlantic Ocean has been estimated to be ~30% (2.5 Gt $yr^{-1}$ of a total of 7.7 Gt $yr^{-1}$; Longhurst, 1993). Seasonal variations in biomass and productivity are averaged out of Figure 1.4, although they are known to occur mainly in temperate high-latitude waters (seasonal variations in heat budget and climate-induced turbulence), and in tropical and subtropical waters which experience seasonal upwelling or mixing. In the majority of tropical and subtropical waters seasonal variations are thought to be minimal and this has led to these areas being termed 'biological deserts' (e.g. Ryther, 1969). However, the subtropical gyres are important in global productivity due to their relatively high surface area and variations in their rates of productivity can have profound effects on calculated rates of global carbon fixation; during a review of estimated annual rates of global carbon fixation, Berger (1989) found a range of 18.6 Gt $yr^{-1}$ and 26.9 Gt $yr^{-1}$ depending on the rates assumed for the oligotrophic areas.

*Vertical Distribution of Phytoplankton Biomass (chlorophyll a)*

Although the development of satellite techniques for remotely sensing chlorophyll *a* has allowed the basinscale distribution of phytoplankton to be studied, these techniques only detect chlorophyll *a* concentrations within near surface waters and cannot describe the vertical chlorophyll *a* profile. The depth to which remote-sensing penetrates the water-column in the open-ocean is dependent upon the vertical attenuation of light; sensed water depths range from ~25 m in clear oligotrophic waters with chlorophyll *a* concentrations ~0.1 mg $m^{-3}$, to <5 m in eutrophic oceanic waters with chlorophyll *a* concentrations ~10 mg $m^{-3}$ (Longhurst, 1998). However, in situations where nutrient concentrations are low and limiting in the upper 50 - 100 m of the water-column, there is an increase in chlorophyll *a* concentration to a maximum in association with the deep nutriclines and lower portion of the euphotic zone. This Chlorophyll *a* Maximum (CM) is now recognised as a ubiquitous feature of tropical and subtropical open oceans (Gould, 1987), as well as coastal and shelf seas (Longhurst and Harrison, 1989).

The depth of the CM varies from 20 - 150 m depending upon the prevalent light and nutrient conditions (Cullen, 1982); for example, Herbland and Voituriez (1979) found the CM between depths of 20 - 80 m in the equatorial Atlantic and off NW Africa; during a review of the literature, Cullen (1982) reported CM depths of 20 m in the Guinea Dome (11°N, 20°W), 150 m in the NPSG, 50 m off the Oregon coast in the Pacific (44°N, 127°W), 20 m in the western English Channel, and 20 - 30 m off Southern California (33°N, 147°W); and, McManus and Dawson (1994) found the CM between 75 - 100 m in the Caribbean Sea and western tropical Atlantic Ocean. From their studies in the eastern Atlantic Ocean, Herbland and Voituriez (1979) described a highly significant inverse relationship between the surface chlorophyll *a* concentration and the CM chlorophyll *a* concentrations, which implies that surface concentrations can be used to predict the vertical chlorophyll *a* profile. However, the mechanisms involved in the formation of the CM are likely to vary regionally (Cullen, 1982), and the relationship between surface chlorophyll *a* and the CM need to be tested on a regional basis. This is especially relevant in tropical and subtropical waters, were the physiology of phytoplankton cells causes non-linearity of the phytoplankton biomass to chlorophyll *a* concentration relationship (Cullen, 1982).

## 1.2. Phytoplankton Taxonomy and Ecophyslology

### 1.2.1. Phytoplankton Taxonomy

*Species, Ecological Niches and Diversity*

A species is the basic unit of biological classification, although several definitions exist which are dependent upon the level of classification used (Lincoln *et al.,* 1998); the biological and genetic concept (based on gene pools and genetic isolation) and the morphological concept (based on appearance). Most of the current research on naturally occurring phytoplankton species is based on the process of species identification according to morphological traits and therefore based around the morphospecies. At present little research has considered the genetics of phytoplankton species (see

review by Medlin *et al.,* 2000), and it has been speculated that some morphospecies are likely to be the same genetic species showing adaptations to environmental conditions (i.e. phenotypic adaptation). Knowledge of such morphological adaptation has considerable ecological value (H. Kinkel, pers. comm.) so that the morphological species concept remains viable. From the few genetic studies of phytoplankton species and populations carried out so far, it has been concluded that considerable genetic diversity exists on both spatial and temporal scales which may give rise to ecophysiologically different populations (Medlin *et al.,* 2000). Further complication of studies based on morphological distinct species is encountered due to the wide diversity of some taxa during their life cycles; where separate stages of the life cycles have distinctly different cell forms (e.g. hetero- and holo-coccolith life-stages within coccolithophores; Cros *et al.,* 2000) .

The ecological niche relates to the physical space an organism occupies and the functional role of the organism in the community, as well as its position within the gradients of the environment (Odum, 1971). In simple terms, a niche describes the 'job description' of a species (Odum, 1971; Falkowski and Raven, 1997) or the 'ecological role of a species in the community' (Lincoln et al., 1998). Within ecological texts two distinctly different niches are recognised; the fundamental niche and the realised niche (e.g. Odum, 1971). The fundamental niche describes the multidimensional space that represents the total range of conditions within which an organism can function and could exist in the absence of other competing organisms, whereas the realised niche is the reduced part of the fundamental niche due to competition (Odum, 1971; Lincoln *et al.,* 1998).

Diversity is the number of species contained within or supported by a given environment, which is related to the competitive dynamics and structure of a community and is composed of two components (Magurran, 1988): the measure of the number of species (species richness) and a measure of the partitioning of the total numbers between individual species (relative abundances). Within a community, diversity is related to the patterns of resource-partitioning, where the relative abundance of a species is relative to the portion of the niche-space it occupies (Magurran, 1988); low diversity indicates that a few species are dominating the resources, whereas high diversity indicates that the resources are more equally divided. Several trends in diversity relative to the ecosystem and environment have been identified, and include a stability-diversity trend where there is a tendency for phytoplankton communities to exhibit increased diversity in highly stable environments due to diversification of the ecosystem niches and the "accumulation of species due to an evolutionary or successional past" (Margalef, 1978). Another trend identified is an inverse relationship between productivity and diversity; highly productive phytoplankton communities have low diversity and are often dominated by one or a few species, whereas communities with low productivity exhibit high diversity (Margalef, 1978; Falkowski and Raven, 1997). However, there is also evidence that highly productive ecosystems may also have high diversity and that the relationship between diversity and productivity is a more complex bell-shape than simply linear (e.g. Clarke and Warwick, 1994).

*Phytoplankton Groups*

Phytoplankton can be classified in terms of size, shape, physiological characteristics, or by taxonomic affiliation (Karl, 1999). The wide diversity of cell shape and form are thought to be

interpretable as adaptations to survival and growth in temporally unstable and often turbulent environments (Margalef, 1978). Sieburth (1979) defined several plankton groups based on cell size; the picoplankton with cell diameters between 0.2 - 2.0 μm, the nanoplankton with cells in the 2.0 - 20.0 μm size range, and the microplankton with cells within the 20 - 200 μm size range. Such size ranges are not exclusive to single phytoplankton taxonomic groups; many different taxa are present in several size groups.

Phytoplankton taxonomy is an ever-changing field with the reclassification of species into different taxa, and there is continuing debate about the 'correct' affiliation of particular genera and species. All phytoplankton reproduce asexually by binary fission as part of complex life cycles which include sexual and resting stages. Most planktonic flagellate groups are known currently only as motile cells, with nonmotile life stages described as other species (Tomas, 1997). Many species are difficult to identify under the light microscope from preserved material and full identification requires the establishment of a culture to study the life cycle as well as electron microscope work (Tomas, 1997). As a result the life cycles of many common species remain unknown and two or more names representing different life stages may be in use for a single species.

Despite these inherent problems, phytoplankton may be separated into 6 major categories or lineages, with one category from the Eubacteria (prokarytotic 'true' bacteria) and 5 from the Eukaryotic lineage (Jeffrey and Vesk, 1997; Tomas, 1997; Tree of Life, 2001, http://tolweb.org/); the Alveolates (dinoflagellates), the Stramenopiles (diatoms, chrysophytes, pyrmnesiophytes, chloromonads), the Green algae (including chlorophytes and prasinophytes), the Red algae (including rhodophytes), the Cryptomonads and the prokaryotic Cyanobacteria (including cyanophytes and prochlorophytes). Apart from cyanobacteria, all the other algal groups are eukaryotic and therefore contain cellular organelles contained within membranes. Several of the algal subgroups are restricted to freshwater environments or are represented in the open ocean by only a few species. Thus, only the ten major phytoplankton groups present in the open ocean will be discussed; the diatoms, dinoflagellates, chrysophytes, chloromonads, prymnesiophytes, cryptomonads, chlorophytes, prasinophytes, cyanophytes and prochlorophytes. The common cell shapes and characteristics of these main groups, apart from the cyanophytes and prochlorophytes, are present in Figure 1.5.

(1). *Diatoms* (Bacillariophyta) - Diatom cells are characteristically surrounded by 2 silica valves (frustules) bounded by an outer organic covering. Diatoms exist as single cells or chains, and exhibit a high diversity of cell and colony shapes and sizes (generally 5 - 200 μm, with some up to 2000 μm in diameter) with the valve symmetry dividing species into pennate or centric diatoms (Fig. 1.3a, b). Diatoms are a widespread phytoplankton group, and their relatively high growth rates under nutrient-rich conditions leads to formation of episodic blooms. However, due to the specific requirement of silica for frustule formation, diatom growth can be limited by silica availability. Although most species are generally regarded as autotrophic some subtropical and tropical species are associated with symbiotic cyanobacteria (Jeffrey and Vesk, 1997; Tomas, 1997) and there is evidence that some small pennate diatoms may act as heterotrophs in benthic enviroments and during post bloom conditions (D. Harbour pers. comm.).

(2). *Dinoflagellates* (Dinophyta) - Dinoflagellates are a diverse group of flagellates of which around half the known species are autotrophic and the others heterotrophic (Tomas, 1997). Some autotrophic dinoflagellates are mixotrophic (i.e. faculative heterotrophs) while others are associated with cyanobacterial symbionts from the genera *Synechocystis* and *Synechococcus* (Jeffrey and Vesk, 1997; Tomas, 1997). Dinoflagellates may be found as single cells or chains with cell sizes ranging from 5 - 2000 μm. Dinoflagellates are characterised by 2 dissimilar flagella: a ribbon-like transverse flagellum in a girdle groove encircling the cell and dividing it into an upper (epitheca) and lower (hypotheca) portion, and a smooth longitudinal flagellum within a longitudinal groove (sulcus) (Fig. 1.3c, d). Dinoflagellates are given their name due to their swimming motion (*dinos* = whirling) where the transverse flagellum causes rotational movement of the cell while the longitudinal flagellum provides the propulsion. Dinoflagellates can be divided into 2 types based on the composition of the cell wall; one group contains cellulose plates within the cell membrane and are termed thecate or armoured (Fig. 1.3c), while the other group has a naked or athecate cell surface (Fig. 1.3d). Many dinoflagellate species are cosmopolitan and probably represent a complex of ecological strains that are currently identified as different species (Tomas, 1997).

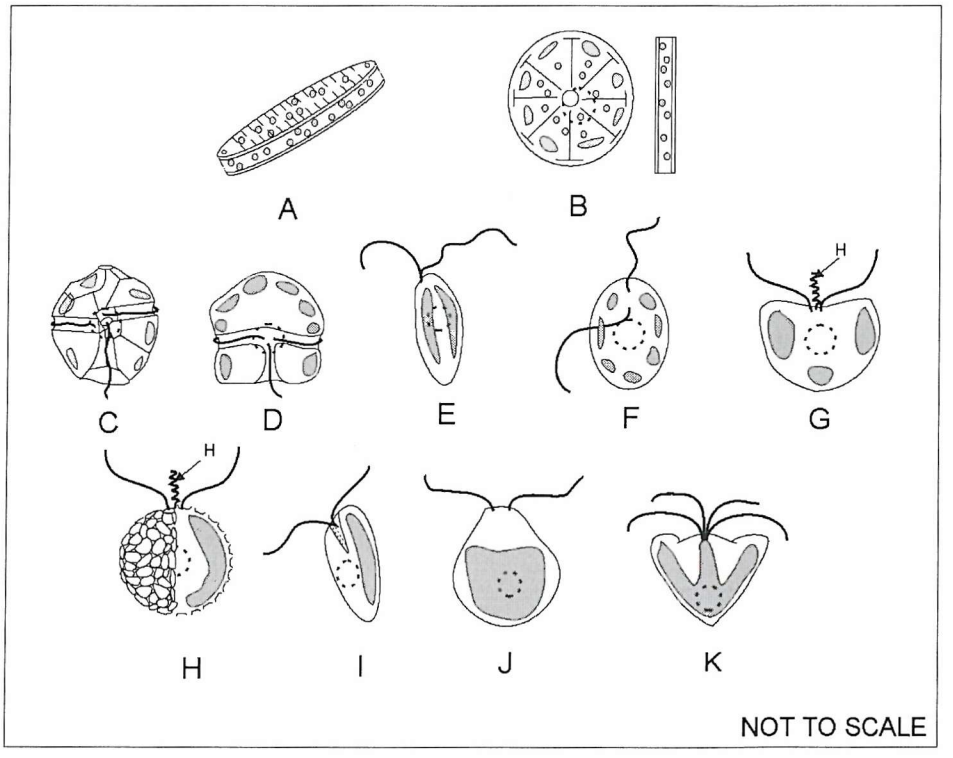


Figure 1.5: Generalised phytoplankton cell types; (A) pennate diatom, (B) centric diatom, (C) thecate dinoflagellate, (D) athecate dinoflagellate, (E) chrysophyte, (F) raphidophyte / chloromonad, (G) naked prymnesiophyte, (H) coccolithophore, (I) cryptophyte, (J) chlorophyte, and (K) prasinophyte. Redrawn and adapted from Tomas (1997). H indicates the haptonema, shaded blocks indicate chloroplasts and dashed structures represent nuclei.

(3). *Chrysophytes* (Chrysophyta, Class Chrysophyceae) - The chrysophytes are a group of pico- and nano-planktonic flagellates which are mostly found in freshwater or inshore waters. The general cell shape is illustrated in Figure 1.3e, although there is a wide diversity of cell morphologies. Nutritional modes include autotrophic, mixotrophic and heterotrophic species. There are 3 types of

marine chrysophyte; the silicoflagellates, picoplanktonic chrysophytes (2 - 3 μm) and the nanoplanktonic chrysophytes (2 - 5 μm). The silicoflagellates are associated with a basket-like siliceous skeleton and cell dimensions are between 20 - 100 μm, while the nanoplanktonic chrysophytes are covered with ornamented siliceous plates and the picoplanktonic chrysophytes have cell surfaces composed of either silicified, cellulose or chitin plates, or are naked. Based on ultrastructural and genetic analysis, the picoplanktonic chrysophytes have been renamed and classified into a separate class, the pelagophytes, which includes the genera *Pelagococcus*, *Aureococcus* and *Pelagomonas* (Anderson *et al.,* 1993). The pelagophytes are now thought to be important components of the picoeukaryotic component of the picoplankton in the open ocean (Anderson *et al.,* 1993, 1996).

(4). *Chloromonads* (Chrysophyta, Class Raphidophyceae) - The chloromonads are also mainly found in freshwater environments, although coastal marine chloromonad blooms are common and the three main marine genera are *Chattonella, Fibrocapsa* and *Heterosigma* (Jeffrey and Vesk, 1997; Tomas, 1997). Chloromonad cells range between 30 - 100 μm in length, and are naked with 2 smooth flagella (often pointing in different directions) and one hairy flagella (Fig. 1.2f).

(5). *Prymnesiophytes* (Haptophyta, Class Prymnesiophyceae) - The prymnesiophytes are nanoplanktonic (2 - 50 μm) biflagellate cells with a third characteristic appendage, the haptonema, located between the flagella (Fig. 1.2g, h). In some prymnesiophyte species and life stages the haptonema is absent and the only evidence of its presence is basal structures within the cell (Tomas, 1997). The prymnesiophytes include species with organic (cellulose and polysaccharides) scales, naked cells and species with calcareous ($CaCO_3$) plates (i.e. the coccolithophores). Coccolithophore species identification is based on the coccolith morphology, and are broadly separated into two groups based on the form of the calcite crystals; the holococcolithophores with regular packed calcite crystals and the heterococcolithophores with modifed calcite crystals. However, recent observations of individual coccolithophore cells with both types of coccoliths has led to the discovery that single species can exhibit different morphologies during different life stages (Cros *et al.,* 2000). As a result, some species are known by two different names (Tomas, 1997; Cros *et al.,* 2000). The function of the coccoliths is not fully understood, although it has been suggested that they may act as ballast, light scatters, antigrazing and as a biproduct of photosynthesis (see review by Young, 1994). The prymnesiophytes are a widespread group with several species known to form extensive blooms in temperate and high-latitude waters (e.g. *Phaeocystis pouchetti, Emiliania huxleyi*). The coccolithophores exhibit the highest diversity in tropical and subtropical waters (Winter *et al.,* 1994).

(6). *Cryptomonads* (Cryptophyta) - The cryptomonads are nanoplanktonic flagellates found in marine, freshwater and estuarine conditions. Cryptomonad cells are asymmetric ovoid cells (6 - 20 μm long) with 2 flagella inserted into an apical or sub-apical furrow (Fig. 1.2i). The cryptomonad cell covering (pellicle) is unique to the group in that it consists of a ridged cell wall superimposed on an inner component made of regular sheets. Phototrophic and heterotrophic cryptomonad species are found, as well as some that are found as endosymbionts in planktonic ciliates (e.g. *Myrionecta rubra*).

(7). *Chlorophytes* (Chlorophyta, Class Chlorophyceae) - Chlorophytes are small nanoplanktonic ovoid cells (<20 μm) which posses 2 or 4 smooth, equal flagella which are inserted apically (Fig. 1.2j). The cell wall in chlorophytes may be naked or with a cellulose component and some species possess an eyespot. Most planktonic species are found in coastal waters and rock pools, although there are a few open ocean species.

(8). *Prasinophytes* (Chlorophyta, Class Prasinophyceae) - The prasinophytes are a heterogeneous collection of primitive green nanoplanktonic flagellates (2 - 30 μm long) with a high diversity of cell shapes. The number of flagella ranges from 1 - 16 with most possessing 4 which are inserted apically into the cell in association with a slight depression (Fig. 1.2k). In some prasinophyte species the flagella and cell are covered in organic scales while other species have naked cells.

(9). *Cyanophytes* (Cyanobacteria) - The cyanophytes are prokaryotic blue-green algae which may be found as single picoplanktonic (~1 μm) cells (e.g. *Synechococcus* spp.), large (>200 μm) filamentous colonies (e.g. *Trichodesmium erythraeum*) or as symbiotic associations within other phytoplankton cells. Cyanophyte cells posses no flagella and their prokaryotic status means that they have no membrane bound organelles (e.g. chloroplasts, nuclei) and the pigments are associated with membranes arranged in flattened vesicles (Falkowski and Raven, 1997). Cyanophytes are important in many marine environments especially in subtropical and tropical waters, where many species have important roles in nitrogen fixation (e.g. *Trichodesmium* spp.; Carpenter, 1983a, b).

(10). *Prochlorophytes* (Cyanobacteria) - The prochlorophytes are small prokaryotic cells and the group contains the genera *Prochloron* (found as marine invertebrate symbionts), *Prochlorothrix* (freeliving filamentous cells) and *Prochlorococcus*. *Prochlorococcus* spp. are found as picoplanktonic (0.6 - 0.8 μm) sheathed single cells and are important in subtropical and tropical marine environments where they represent the dominant component of the biomass (e.g. Campbell *et al.,* 1994; Partensky *et al.,* 1996).

### 1.2.2. Ecophysiology: Photophysiology, Nutrient and Temperature Physiology

*Phytoplankton Pigments*

The photosynthetic apparatus of phytoplankton cells is composed of 2 physically independent systems (Photosystem 1 and Photosystem 2). Each photosystem consists of a light-harvesting complex (LHC) energetically coupled, through the transfer of light energy, to a photochemical component contained within a reaction centre (RC) (Falkowski and Raven, 1997). The LHC is composed of an ensemble of pigment-protein complexes (the pigment bed or antenna) that absorb photons and transfer the associated excitation energy to the reaction centres from higher to lower excitation states and between pigment-protein complexes (Falkowski and Raven, 1997). The LHC proportion of the pigment bed contains accessory pigments (carotenoids and several forms of chlorophyll) that either transfer excitation energy to chlorophyll *a* (i.e. photosynthetic), or dissipate excess excitation energy as heat and/or fluorescence (i.e. photoprotectant). Therefore, accessory

pigments in the pigment bed can be classified according to their role; photosynthetic (PS) or photoprotectant (PP).

Although PS and PP pigments are closely related in terms of their composition, their absorption spectra differ from that of chlorophyll *a* (Falkowski and Raven, 1997), so that different pigment suites are suited to different light environments (Kirk, 1992). Within the pigment bed in some phytoplankton taxa (e.g. diatoms), the PP pigments are associated with 'xanthophyll cycles', where the PP pigments are cycled from a PS form (e.g. violoxanthin) to a closely related PP form (e.g. zeaxanthin) through enzyme-catalysed and light-mediated changes in their molecular structure (Falkowski and Raven, 1997; Porra *et al.*, 1997). However, prochlorophytes and cyanophytes do not posses xanthophyll cycles (Falkowski and Raven, 1997) and the PP pigments (e.g. zeaxanthin) remain in their PP role.

Table 1.1: The distribution of chlorophylls, photosynthetic (PS) and photoprotectant (PP) accessory pigments in marine phytoplankton taxa. Major pigment markers for each phytoplankton group are highlighted in bold. Information has been compiled from Barlow *et al.*, 1993; Millie *et al.*, 1993; Barlow *et al.*, 1997a, b; Jeffrey and Vesk, 1997; Jeffrey *et al.*, 1997; Gibb *et al.*, 2000, 2001, with SCOR-UNESCO abbreviations.

| Taxa | Chlorophyll (s) | PS Pigments | PP Pigments |
|---|---|---|---|
| **Diatoms** | Chlorophyll *a* (Chl a)<br>Chlorophyll *c*[2] (Chl c) | **Fucoxanthin (Fuco)** | β Carotene (β-Car)<br>Diatoxanthin (Diato)<br>**Diadinoxanthin (Diadino)** |
| **Dinoflageliates** | Chlorophyll *a* (Chl *a*)<br>Chlorophyll *c*[4] (Chl *c*) | **Peridinin (Perid)**<br>Fucoxanthin (Fuco)<br>19-Butanoyloxyfucoxanthin (But-fuco) | β Carotene (β-Car)<br>**Diadinoxanthin (Diadino)** |
| **Chrysophytes / Pelagophytes / Chloromonads** | Chlorophyll *a* (Chl *a*)<br>Chlorophyll *c*[3] (Chl *c*) | Violaxanthin (Viola)<br>**Fucoxanthin (Fuco)**<br>**19-Butanoyloxyfucoxanthin (But-fuco)** | β Carotene (β-Car)<br>**Diadinoxanthin (Diadino)** |
| **Prymnesiophytes** | Chlorophyll *a* (Chl *a*)<br>Chlorophyll *c*[1] (Chl *c*) | **19-Hexanoyloxyfucoxanthin (Hex-fuco)**<br>**Fucoxanthin (Fuco)**<br>**19-Butanoyloxyfucoxanthin (But-fuco)** | β Carotene (β-Car)<br>Diatoxanthin (Diato)<br>**Diadinoxanthin (Diadino)** |
| **Cryptomonads** | Chlorophyll *a* (Chl *a*)<br>Chlorophyll *c*[4] (Chl *c*) | **Phycobiliproteins** | β Carotene (β-Car)<br>**Alloxanthin (Allo)** |
| **Chlorophytes** | Chlorophyll *a* (Chl *a*)<br>**Chlorophyll *b* (Chl *b*)** | **Violaxanthin (Viola),**<br>**Neoxanthin (Neo)** | β Carotene (β-Car)<br>**Lutein (Lut)**<br>Zeaxanthin (Zea) |
| **Prasinophytes** | Chlorophyll *a* (Chl *a*)<br>**Chlorophyll *b* (Chl *b*)** | **Violaxanthin (Viola),**<br>**Neoxanthin (Neo),**<br>**Prasinoxanthin (Pras)** | β Carotene (β-Car)<br>Lutein (Lut)<br>Zeaxanthin (Zea) |
| **Cyanophytes** | Chlorophyll *a* (Chl *a*) | **Phycobiliproteins** | β Carotene (β-Car)<br>**Zeaxanthin (Zea)** |
| **Prochlorophytes** | Divinyl chlorophyll *a*<br>(Dv Chl *a*)<br>Divinyl chlorophyll *b*<br>(Dv Chl *b*) | | β Carotene (β-Car)<br>**Zeaxanthin (ZEA)** |

[1] Contains all chlorophyll c derivatives ($c_1$, $c_2$ and $c_3$), [2] contains only $c_1$ and $c_2$, [3] contains $c_2$ and $c_3$ only, and [4] contains $c_2$ only.

The pigment composition of the pigment bed differs between phytoplankton taxa and species, and between cells of the same species in different light environments (Falkowski and Raven, 1997). Therefore, the analysis of the accessory pigments can provide valuable chemotaxonomic and physiological information (Jeffrey *et al.*, 1997). However, due to the complexities of pigment variations with cell status, cross-taxa specific biomarkers and the occurrence

of endosymbionts with their own pigment signatures within other taxa, it has been recommended that pigment analysis should be accompanied by phytoplankton cell counts and community composition data (Jeffrey *et al.,* 1997). Despite these problems various authors have proposed schemes of pigment biomarkers and chemotaxonomic relationships as the basis for using pigment data to describe phytoplankton community composition. Table 1.1 shows the distribution of chlorophylls, photosynthetic and photoprotectant pigments within the different phytoplankton groups described in the previous section, with the pigments used to distinguish particular phytoplankton groups in bold. The major differences between phytoplankton groups include the restriction of chlorophyll c to eukaryotic phytoplankton, the restriction of phycobilins to prokaryotic cyanophytes and cryptomonads, and the restriction of the divinyl forms of chlorophyll *a* and *b* to the prochlorophytes (Table 1.1). Several phytoplankton groups share characteristic pigments, while other are restricted to single taxa; e.g. fucoxanthin is found in diatoms, dinoflagellates, chrysophytes (pelagophytes), and prymnesiophytes, while peridinin is only found in dinoflagellates, and 19'-hexanoyloxyfucoxanthin is restricted to prymnesiophytes (Table 1.1).

*Photophysiology*

An understanding of phytoplankton photophysiology is dependent on information about variations in the size or composition of the pigment bed, the number of RC, and the ratio of RC waiting for a photon to those already busy absorbing one (termed the functional absorption cross-section; Falkowski and Raven, 1997). Cellular responses to irradiance conditions are dependent upon the length of exposure of the algal cell to a particular (mean) light level; photoinhibition is the short term (seconds - minutes) reduction in the ability of the algal cell to utilise light energy (photosynthetic efficiency) during periods of exposure to detrimental (high) light levels, whereas photoacclimation involves the adjustment of the photosynthetic apparatus to prolonged periods (hours - days) in a particular (mean) light regime whether it be high or low light (Falkowski and Raven, 1997).

Photosynthetic excitation energy can be dissipated within the photosynthetic apparatus by either photochemical quenching via the standard photosynthetic route, or by non-photochemical quenching where the excitation energy bypasses the RC and is passed to a quencher (PP pigments) in the pigment bed and the energy is lost as fluorescence and/or heat (Falkowski and Raven, 1997). Both quenching mechanisms reduce the amount of excitation energy delivered to the reaction centres and serve to prevent photo-induced damage to the photosynthetic apparatus. However, with prolonged periods of exposure to high irradiance, non-photochemical quenching is unable to prevent damage to the reaction centre and this leads to a loss in functional reaction centres and a decrease in photosynthetic efficiency. Repair of the reaction centres takes place during the night and involves protein synthesis, which means it is a nutrient dependent process. In low nutrient environments, nutrient availability may be insufficient for repair of photoinduced damage to the photosynthetic apparatus, and thus limit the efficiency with which phytoplankton in oligotrophic waters (dissolved inorganic nitrogen concentrations <0.5 μM) convert solar irradiance to stored chemical energy (Falkowski *et al.,* 1992).

During long exposure times to high or low irradiance, photoacclimation occurs and involves either marked (up to 5 - 10 fold) changes in the cellular concentration of pigments through pigment synthesis in low light and pigment degradation in high light, or changes in the number of reaction centres relative to the pigment bed size (Falkowski and Raven, 1997). Increases of PS pigments increase the functional absorption cross-section, while increases of PP pigments effectively reduce the functional absorption cross-section and increase non-photochemical quenching (Falkowski and Raven, 1997). Changes in the intra-cellular pigment concentrations are not a linear function of light level or pigment (Prezelin, 1987; Falkowski and Raven, 1997). Increases in cellular pigmentation beyond a certain level cause a paradoxical decrease in photosynthetic efficiency, which has been termed the 'package effect' (Falkowski and Raven, 1997). The 'package effect' is due to selfshading of the LHC of the photosynthetic apparatus within the algal cells chloroplasts' thykaloid membranes (Falkowski and Raven, 1997).

The overall effect of photoacclimation is irradiance-determined variations in the cell carbon to chlorophyll ratios, especially in the high light domains of the tropical and subtropical ocean; surface populations have high carbon:chlorophyll ratios, whilst deep populations have low carbon:chlorophyll ratios (Cullen, 1982; Falkowski and Raven, 1997). Therefore, in tropical and subtropical waters chlorophyll *a* concentration is a poor indicator of autotrophic biomass and changes in biomass may occur independently of changes in chlorophyll *a* concentration (Cullen, 1982; Longhurst and Harrison, 1989).

*Nutrient Physiology*

Nutrient uptake by algal cells is dependent upon the movement of nutrient salts through the cell membrane, which is a function of the ambient nutrient concentrations, cellular nutrient levels and cell size (Chisholm, 1992; Kiørbe, 1993; Riebesell and Wolf-Gladrow, 2002). The degree of nutrient limitation is proportional to cell size due to the dependency of diffusion on the cell surface area to cell volume ratio; small cells have a greater ratio than large cells and thus a lower diffusive nutrient uptake threshold (Chisholm, 1992; Kiørbe, 1993; Riebesell and Wolf-Gladrow, 2002). An example given in Riebesell and Wolf-Gladrow (2002) states that an algal cell with a cell radius of ~10 μm growing at a rate of 1 division per day would become diffusion limited at inorganic nutrient concentrations of <1 μM, however, the inorganic nitrogen concentrations in oligotrophic waters are <0.1 μM which would support a maximum growth rate of <0.1 division per day. In comparison, a picoplankton cell with a cell radius of ~1 μm would be able to maintain a growth rate of 1 division per day at inorganic nitrogen concentrations as low as 0.01 μM without suffering diffusion limitation (Riebesell and Wolf-Gladrow, 2002).

Although these examples assume that the algal cells have highly efficient nutrient uptake kinetics for inorganic nitrogen, it suggests that large phytoplankton are poorly adapted for low nutrient environments compared with small picoplanktonic cells (Riebesell and Wolf-Gladrow, 2002). However, large phytoplankton cells (>5 μm) do occur in oligotrophic waters, and are thought to be maintained by a variety of strategies. These adaptive strategies include; exotic shapes to increase the surface area to volume ratio and nutrient flux per unit of cell volume (e.g. Margalef, 1978; Pahlow

*et al.,* 1997; Riebesell and Wolf-Gladrow, 2002); swimming and sinking to reduce the effect of diffusion limitation (e.g. Kiørbe, 1993; Riebesell and Wolf-Gladrow, 2002) and, in the case of some large taxa, buoyancy regulation to commute to the deep nutrient rich waters at the bottom of the euphotic zone and return to the surface layer with increased cellular nutrient pools (e.g. Joseph *et al.,* 1997; Brokhuizen, 1999; Villareal *et al.,* 1993, 1996, 1999a, b); nitrogen fixing abilities or association with nitrogen fixing cyanobacteria (e.g. Venrick, 1974; Carpenter, 1983a, b; Longhurst, 1998); use of large cell vacuoles for inorganic nutrient storage and luxury consumption during periods of increased nutrient concentration (e.g. Riebesell and Wolf-Gladrow, 2002); rapid, pulsed nutrient uptake by nutrient-starved algal cells (e.g. McCarthy and Goldman, 1979; Goldman and Glibert, 1983); utilisation of dissolved organic nutrient pools (e.g. Bonin and Maestrini, 1981; Karl, 1999); and in the case of some coccoid cyanophytes (*Synechococcus* spp.), storage of cellular nitrogen reserves as accessory pigments (phycoerythrin; e.g. Fogg, 1986). However, this latter strategy has been questioned after detailed culture work on several *Synechococcus* strains has found that high-light adapted cells contained <3% of the cellular nitrogen within phycoerythrin, which indicates that such a reserve would be a relatively ineffective nitrogen reserve, and that there were strain specific differences in the regulation and breakdown of phycoerythrin in nitrogen-starved conditions (Kana and Glibert, 1987a). Another advantage of large cell size and low cell abundances in low nutrient waters dominated by small cells, is a relative refuge from grazing due to the comparatively low grazing pressure on large cells in the oligotrophic ocean (Riebesell and Wolf-Gladrow, 2002).

*Temperature Effects*

The physiological responses of phytoplankton to temperature fluctuations are linked to both the light-dependent (photochemical) and light-independent (carboxylation) photosynthetic reactions, although on different scales (Kirk, 1994; Falkowski and Raven, 1997). Temperature changes effect the rates of enzyme-catalysed reactions; increases in temperature cause increases in the rate of enzyme reactions as a result of increased substrate-enzyme molecular interactions (Falkowski and Raven, 1997). Cellular photochemistry is not regulated by enzyme activity and is therefore largely temperature independent, although temperature does affect electron transport through temperature related changes in membrane fluidity and electron carrier diffusion through intracellular membranes (Falkowski and Raven, 1997). In contrast, carboxylation (photosynthetic carbon reduction cycle; Calvin-Benson Cycle) is dependent upon enzyme-mediated reactions and is therefore sensitive to temperature fluctuations (Kirk, 1994; Falkowski and Raven, 1997). At higher temperatures, enzyme activity and the Calvin-Benson Cycle requires more substrates from photochemistry to saturate the cycle. Along with increases in the rate of the Calvin-Benson Cycle are associated increases in respiration rate and the light intensity required for photosynthesis to equal respiration (light compensation point; Kirk, 1994).

In nature, water temperature effects on phytoplankton growth are difficult to decouple from nutrient and light effects; high water temperatures characterise low nutrient and high light environments where algal populations are nutrient stressed and photoinhibited, whereas low water temperatures characterise high nutrient and low light environments (Falkowski and Raven, 1997).

Although laboratory studies have shown that the growth rate of resource-saturated phytoplankton cells is directly related to temperature (e.g. Eppley, 1972), in the open ocean nutrient and light-limitation restrict algal responses to temperature fluctuations.

## 1.3. Phytoplankton Community Structure and Dynamics

### 1.3.1. The 'Classical-foodchain' and the 'Microbial loop'

The availability of new nutrients and the ambient nutrient concentrations in the euphotic zone of the ocean have a direct influence on the type of phytoplankton found and the general community and ecosystem structure (Fig. 1.4). In low new nutrient environments, small phytoplankton cells (picoplankton) generally dominate as their small cell sizes enables more efficient nutrient uptake at low ambient concentrations, as well as efficient light harvesting (Chisholm, 1992; Kiørbe, 1993; Agusti, 1994; Fogg, 1986, 1995; Raven, 1998; Agawin *et al.,* 2000). In contrast, under high new nutrient conditions, larger phytoplankton cells (nano-and micro-phytoplankton) can efficiently outcompete small cells due to their higher maximal growth rates (Chisholm, 1992).

When small cells dominate the autotrophic biomass, close coupling between production and consumption due to similar generation times of the pico- and nano-plankton producers and nano- and microplankton grazers make organic nutrient cycling between components of the community important (Azam *et al.,* 1983; Fogg, 1995); so that large numbers of heterotrophic bacteria and small autotrophs and heterotrophs are present in the community (i.e. the microbial food chain; Fig. 1.4). Within the microbial food chain the dominant cells are too small (<2 μm) to be efficiently grazed by large heterotrophs (e.g. mesozooplankton, gelatinous heterotrophs), and grazing due to small heterotrophic cells (nanoflagellates and microzooplankton) is important (Fig. 1.4). These small grazers are in turn grazed by larger heterotrophs, and thus there is a link between the picoplankton and higher trophic levels via the microzooplankton (Calbert and Landry, 1999; Fig. 1.4). When nutrients are available in higher concentrations, large phytoplankton cells dominate and these in turn are grazed by large grazers and there is a more direct link to higher trophic levels (i.e. the 'classical' food chain; Fig. 1.4).

Separation of the microbial and classical food chain may occur spatially and temporally, although components of both may also coexist (Karl, 1999). An example of the spatial separation of the food chains would be between upwelling and oligotrophic oceanic conditions, while temporal separation of the two food chains can best be described in terms of the annual cycle of primary production in seasonally variable temperate waters; summer conditions are typically nutrient limited (oligotrophic) and dominated by small cells with low overall productivity and the microbial food web dominates, whereas during spring, nutrient conditions are suitable for large cells to dominate and for a brief period of time the classical food chain takes over as the main trophic transfer pathway. Such seasonal changes in phytoplankton communities can also occur in subtropical waters where there is significant winter mixing, and the spring bloom is occasionally diatom dominated (e.g. north-western Sargasso Sea near Bermuda; Durand *et al.,* 2001).

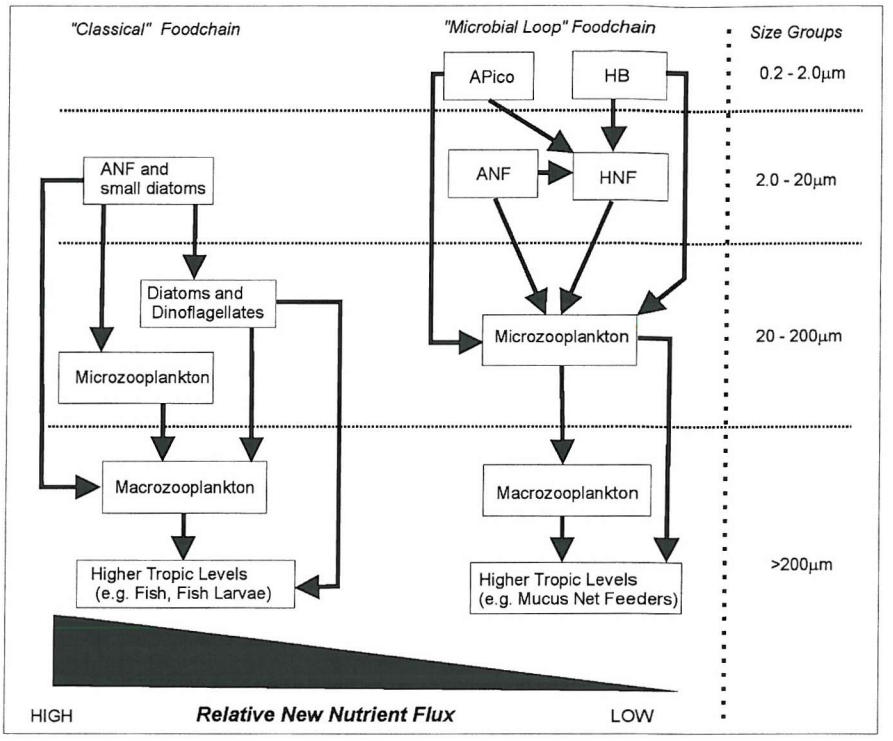


Figure 1.6: Relationship between nutrient supply and types of oceanic phytoplankton communities. The microbial loop foodchain dominates in low new nutrient conditions (right), and the classical food chain dominates in high new nutrient conditions (left). Key: APico indicates autotrophic pico-plankton (prochlorophytes, *Synechococcus* and pico-eukaryotes), HB heterotrophic bacteria (bacterioplankton), ANF autotrophic nanoflagellates, and HNF heterotrophic nano-flagellates.

An important concept for oceanic biogeochemistry and the global carbon cycle is the balance between production and consumption in oceanic food chains. Relatively constant temporal rates of primary production will allow close coupling between production and consumption, whereas sudden bursts of primary production and plant biomass have less probability of being efficiently consumed (e.g. Boltovskoy, 1999). In situations where production and consumption are balanced the amounts of organic matter that is unused and able to sink to the sea floor (export production) will be low, whereas out-of-balance situations will be characterised by higher export of organic matter to the sea floor (e.g. Boltovskoy, 1999). When small autotrophic cells dominate the productivity and biomass, small heterotrophs with similar growth rates are the dominant grazers (microbial loop; Fig. 1.4; Kiørbe, 1993) and export production is minimal with little organic carbon lost from the upper ocean. In contrast, where large phytoplankton dominate and are not readily consumed by large grazers (classical food chain; Fig. 1.4; Kiørbe, 1993), export production is likely to be high due to the ungrazed fraction as well as the characteristically higher sinking rates of larger particles (algal cells, faecal pellets). Therefore, the size distribution of the phytoplankton community and the trophic structure of the consumer population largely determine both the composition and magnitude of the exported particulate material (Michaels and Silver, 1988).

The relative importance of nutrient control (bottom-up) and grazer control (top-down) of the autotrophic population is another important concept within oceanic phytoplankton communities. Within oligotrophic waters the situation can be said to be nutrient and therefore bottom-up controlled,

however the dominance of the microbial community with its actively growing heterotrophic grazer community complicates the argument; small grazers have generation times of the same order as the autotrophs so that close coupling of the two populations is likely (Fogg, 1995), and there is a case for strong top-down control of the picoplankton by nanoheterotrophs (Calbert and Landry, 1999). Resource control includes the availability of inorganic and organic nutrients whereas predation includes the activity of phagotrophic protozoans, predatory bacteria, viral infections and possibly mixotrophic autotrophs (Karl, 1999).

### 1.3.2. Phytoplankton community structure in subtropical waters

Although there have been several recent studies of the phytoplankton in the subtropical waters of the northern Atlantic Ocean (e.g. Bermuda Atlantic Timeseries (BATS) programme; Steinberg, 2001), the subtropical waters of the North Pacific Subtropical Gyre around Hawaii have been intensively studied for the last four decades (the Hawaiian Oceanographic Timeseries (HOTS) programme; Karl, 1999). Thus, much of the information on phytoplankton community structure in subtropical waters originates from the NPSG. The ecosystem of the South Atlantic subtropical waters are largely under-sampled and poorly known, although it is reasonable to propose that there is a high degree of similarity with the northern subtropical gyre of the Atlantic and Pacific (Longhurst, 1998).

Until relatively recently (1988), phytoplankton communities in the subtropical gyres were considered to be dominated by eukaryotic micro-autotrophs (e.g. monads, flagellates and diatoms; Beers *et al.,* 1982) and mesozooplankton (Karl, 1999). McGowan (1977) hypothesised, after studying the distribution and biomass of the mesozooplankton community in the NPSG, that low temporal or spatial heterogeneity of biomass indicated that the NPSG community was a "climax community" (Venrick, 1982). A climax community is an old ecosystem at the final stage of succession, where the components of the food web have evolved in unison internally and within the habitat characteristics and climate, so that species have evolved their physiology, behaviour and population dynamics to maximise fitness within the physical and biological variations of the environment, and that such species are unable to survive in a situation where the habitat variables were different or constantly fluctuating (Odum, 1971; McGowan, 1977; Karl, 1999). In this view of the NPSG ecosystem, McGowan (1977) also made the point that in such a system *in-situ* processes predominate the regulation of the community due to the lack of dynamic physical processes.

With the advent of new flowcytometric and pigment analysis techniques, it has became apparent that these communities are in fact dominated by much smaller picoplanktonic cells (Waterbury *et al.,* 1979; Chisholm *et al.,* 1988), although these were noticed previously but poorly understood (see the "*little green cells*" described by Beers *et al.,* 1982). Similarly, the physical environment is now known to vary significantly on seasonal, interannual and decadal scales (Polovina *et al.,* 1995), which counters previous conclusions about the lack of dynamic physical processes. In many ways our understanding of the structure of subtropical gyre phytoplankton communities is still evolving, and the present view is one of a dominant photoautotrophic picoplankton-supported microbial food web, which is occasionally overshadowed by a larger

eukaryotic-grazer food chain during episodic new nutrient injections and causes significantly increased export production (Platt and Harrison, 1985; Karl, 1999). Typically, prochlorophytes contribute up to 50% of total chlorophyll *a* (Campbell *et al.,* 1994), while *Synechococcus*, and a diverse assemblage of autotrophic pico- and small nano-eukaryotes (<5 μm) account for the majority of the remaining standing stock (Anderson *et al.,* 1996), with smaller contributions from large (>5 μm) phytoplankton cells such as diatoms and dinoflagellates (Goldman, 1993; Karl, 1999). The pico- and nano-eukaryotic portion of the community often includes poorly-known and studied species, genera, and even classes (e.g. the pelagophytes; Anderson *et al.,* 1993; 1996), as well as representatives from most marine phytoplankton classes; dinoflagellates, chrysophytes, and prymnesiophytes (including coccolithophores) (Venrick, 1982; Bidigare *et al.,* 1990; Letelier *et al.,* 1993).

Studies of the vertical and horizontal distribution of large (>5m) phytoplankton cells in subtropical waters has led to the recognition of the presence of highly specialised communities (e.g. Venrick, 1982). Through the use of multivariate statistics, these phytoplankton communities have been found to form depth-specific layers, which has led to the proposal of the existence of taxonomically distinct and physiologically specialised floras within the water-column; a 'sun' flora within the upper light-rich, nutrient-poor waters (e.g. Venrick, 1982; Longhurst and Harrison, 1989) and a 'shade' flora within the deep light-poor, nutrient-rich waters (e.g. Sournia, 1982; Venrick, 1982). Members of the proposed 'sun' flora include the diatom species *Haslea wawrikae* and *Hemiaulus hauckii* (Furuya and Marumo, 1983; Venrick, 1999), the cyanophyte *Trichodesmium* spp. (Longhurst and Harrison, 1989), and the coccolithophores *Acanthoica quattrospina*, *Anoplosolenia brasiliensis*, *Calcidiscus leptoporus*, *Discosphaera tubifer*, *Helicosphaera carteri* and *H. hyalina*, *Rhabdosphaera claviger*, *Umbellosphaera irregularis* and *U. tenuis* (Winter *et al.,* 1994; Furuya and Marumo, 1983; Venrick, 1999; Haider and Thierstein, 2001). Due to the low new nutrient concentrations in surface waters, the sun flora are likely to have developed various strategies to overcome severe nutrient starvation; for example, two of the species proposed as members of the 'sun' flora are also associated with nitrogen fixation (*Trichodesmium* spp. and *Hemiaulus hauckii*).

Members of the proposed 'shade' flora include the diatoms *Planktoniella sol*, *Thalassionema nitzschioides*, *Gossleriella tropica*, *Rhizosolenia castracanei* and *R. temperei* (Sournia, 1982; Furuya and Marumo, 1983; Venrick, 1999), the dinoflagellates *Ceratium gravidum*, *C. incisum*, *C. longissimum*, *C. platycorne*, *C. ranipes*, *C. vultur*, *Heterodinium scrippsii*, *Pyrocystis pseudonoctiluca*, *Triposolenia truncata* and *Oxytoxum laticeps* (Sournia, 1982; Venrick, 1999), the prasinophyte *Halosphaera viridis* (Sournia, 1982), and the coccolithophores *Florisphaera profunda*, *Oolithotus fragilis*, *Thorosphaera flabellata*, *Calciosolenia murrayi*, *Halopappus* spp., and *Ophiaster hydroideus* (Sournia, 1982; Furuya and Marumo, 1983; Winter *et al.,* 1994; Venrick, 1999; Haider and Thierstein, 2001). Adaptations to survival in the deep nutrient-rich, but light-limited waters of the subtropical gyres are likely to include the development of suitable pigment suites for maximum light harvesting at low light levels, and possibly motility or buoyancy reversals to migrate into more optimal light conditions that are found shallower in the water-column.

### 1.3.3. Phytoplankton Community Structure in tropical (Upwelling) waters

Upwelling is a circulation pattern that overrides both the nutrient limitation of permanently stratified low- and mid-latitude waters and the light limitation of deep nutrient-rich waters (Barber and Smith, 1981; Barber, 2001). Upwelling ecosystems are those that occupy regions of the ocean where there is temporally persistent upward motion of sea water that transports subsurface water with increased inorganic nutrients into the sunlit surface layer (Barber and Smith, 1981; Barber, 2001). The combination of increased nutrient supply and a favourable light regime characterise upwelling systems as high biomass and productivity ecosystems (see Fig. 1.4) and support highly productive fisheries (Ryther, 1969; Barber and Smith, 1981; Barber, 2001). Two contrasting views of coastal upwelling ecosystems exist, one views such ecosystems as analogous to temperate ecosystems during the spring bloom (e.g. Cushing, 1971) while the other maintains that such ecosystems are very different (e.g. Ryther, 1969); however, as pointed out by Barber and Smith (1981) few truly comparative studies exist in view of large-scale interannual and spatial variations in ecosystem structure and function.

Within the Atlantic Ocean, two spatially separate types of upwelling ecosystem are found; the coastal upwelling off NW Africa and the mid-ocean upwelling along the equator (equatorial divergence). The causes of the upward movement of deep nutrient-rich water in these two types of upwelling differ; so that in coastal upwelling, the surface layer diverges away from the coastline and flows offshore as subsurface water flows inshore towards the coast, while oceanic upwelling is largely due to the divergence of one surface layer away from another under the effects of the wind patterns (Barber and Smith, 1981; Barber, 2001). The divergence and pelagic upwelling along the equator in the Atlantic Ocean is due to the interaction of thermocline and nutricline tiling (due to remote physical forcing), high positive wind stress curl on the upper ocean and the resultant eddy upwelling as the ocean responds to intensified basin-scale winds during the boreal summer (Longhurst, 1993).

In coastal and equatorial upwelling ecosystems, optimal nutrient and light conditions (i.e. nutrient concentrations and light conditions well above those required to saturate cellular requirements) for high rates of primary production are maintained for several months, or longer, each year, and in low-latitude Trade wind regions they may persist for the entire year (Barber and Smith, 1981; Longhurst, 1993; Barber, 2001). Thus, the annual production in upwelling regions is much higher than those in permanently or seasonally nutrient- or light-limited regions (Longhurst, 1993; Barber, 2001). Although upwelling supplies large amounts of new nutrients, high production fuels a large and diverse heterotrophic grazing community which, along with heterotrophic bacteria, cause increased regeneration of organic nutrients which support the microbial portion of the community (Barber, 2001). The sinking of particulate material from surface high nutrient waters (export production) and its regeneration at depth causes nutrient 'trapping' in upwelling systems that maintain elevated nutrient concentrations in bottom waters moving inshore and benthic sediments (Barber, 2001).

The phytoplankton community in coastal upwelling waters is often dominated by large-celled, chain-forming or colonial diatoms with individual cell diameters of >10 - 100 μm and cell colony/chain sizes up to 2000 μm (Herbland *et al.,* 1987; Barber, 2001). Such phytoplankton are readily available to planktivorous fish and other large grazers, which means that in coastal upwelling ecosystem the food chain is very short and energy transfer within the ecosystem is highly efficient (Barber, 2001). Large diatoms are well adapted to upwelling conditions due to their high nutrient uptake rates in high nutrient concentrations, and therefore can outcompete other phytoplankton groups as long as silica concentrations do not become limiting. Another advantage to large cell size in upwelling waters may be that the rapid sinking rates associated with large cells allows these cells to sink out of surface waters being advected offshore and into deep waters that are being advected inshore; thus, large diatoms may be able to remain in the central nutrient-rich waters of the upwelling system (Barber, 2001). This strategy may also be employed by large motile dinoflagellate cells, and is known to occur in some upwelling zooplankton species that migrate downwards when they are saturated with food (Barber, 2001). In contrast, smaller cells will sink slower and are more likely to be advected offshore into lower nutrient conditions (Barber, 2001).

In coastal upwelling waters with depleted silica concentrations other phytoplankton groups become dominant (e.g. large dinoflagellates) and with increasing nutrient depletion as the upwelled water is advected offshore there is a succession of the community towards small cells and the characteristic picoplankton dominated community of more oligotrophic waters (Barber and Smith, 1981). The picoplankton proportion of the phytoplankton community is also elevated compared with subtropical waters, although it remains a minor contributor compared to the larger phytoplankton proportion (Barber, 2001). There is also a shift in the picoplankton from dominance by prochlorophytes to dominance by *Synechococcus* spp. and picoeukaryotes (Agawin *et al.,* 2000). This shift in dominance is thought to be due to the nutrient preferences of these two groups; *Synechococcus* prefers nitrate while prochlorophytes prefer ammonia and urea (Rippka *et al.,* 2000; Karl and Michaels, 2001). In fact, it has been proposed that prochlorophytes are unable to utilise nitrate and may lack the necessary intra-cellular pathways and enzyme systems to use nitrate for growth (Karl and Michaels, 2001; Karl *et al.,* 2002b).

In the equatorial Atlantic, upwelling is permanent east of 20 - 30°W, from 6 - 7°N to 7 - 8°S, although it merges with coastal upwelling off NW Africa seasonally (Vinogradov, 1981; Longhurst, 1993). The narrow bands of upwelling along the equator, alternating with narrow zones of downwelling, cause a banded pattern to the distribution of plankton communities and biomass (Vinogradov, 1981). The community structure in the upwelling waters of the Atlantic Ocean appears to be different to those found in coastal upwelling conditions (Longhurst and Pauly, 1987). Although there are increases in chlorophyll *a* the majority of the biomass remains in the pico- and nano-sized cell ranges; 85 - 95% of the chlorophyll *a* is contained in particles <10 μm and 75 - 90% of the particulate carbon and nitrogen pass through a 3 μm filter, while the >10 μm chlorophyll *a* concentrations remain less than 15% of the total (Herbland and LeBouteiller, 1981; Herbland *et al.,* 1985, 1987). This contrasts coastal upwelling waters in the Atlantic Ocean where <60% of the total chlorophyll *a* is contained in particles <10 μm (Herbland *et al.,* 1985, 1987). Due to the small cell

sizes characteristic of the equatorial divergence, and therefore dominance of the microbial loop food chain, there is likely to be a close link between production and consumption, with micro-heterotrophic grazers regulating the abundance of small autotrophic cells (Longhurst and Pauly, 1987).

## 1.4. Thesis Introduction and Objectives

### 1.4.1. Atlantic Meridional Transect Programme

Due to the spatial remoteness of much of the tropical and subtropical oceans, little attention has been placed on the dynamics of the phytoplankton communities and several recent discoveries have shown the importance of understanding these large and complex "biological deserts"; (1) time series measurements in the North Pacific Subtropical Gyre have shown that previous assumptions that the community was at a '*climax*' stage of biological succession is false, and there is evidence that there has been a rapid '*domain shift*' process occurring over the last 30 years (Karl, 1999; Karl *et al.,* 2001a); (2) in the subtropical Atlantic Ocean, there is debate as to whether the plankton community respires more organic carbon than it produces and the subtropical oceans are in fact carbon sources and not sinks (e.g. Del Giorgio *et al.,* 1997; Duarte *et al.,* 2001), or if respiration is equal to photosynthesis in the oligotrophic oceans due to external DOC (DOM) sources and/or temporal balance of the two processes (e.g. Geider, 1997; Williams, 1998); (3) recent research from the Atlantic Ocean has shown that there are large scale interannual variations in the rates of primary production in subtropical ocean regions, which do not appear to be linked to changes in photosynthetic biomass and may be due to physiological and/or community structural changes (Maranon and Holligan, 1999; Maranon *et al.,* 2000).

This study is concerned with investigating the spatial and temporal variability of phytoplankton community structure in the Atlantic Ocean between 40°N and 40°S, and linking hydrographic structure and variability to changes in community composition. From September 1995 to May 2000 the Atlantic Meridional Transect (AMT) programme of cruises has biannually resampled along a meridional latitudinal line in the subtropical and tropical Atlantic Ocean. The measurement of phytoplankton community structure derived from pigments and large (>5 μm) phytoplankton species identification from the AMT cruises forms the basis for this study. Therefore, the species analysis within this study does not include the abundant picoplankton proportion of the phytoplankton community of the subtropical and tropical waters of the Atlantic Ocean.

### 1.4.2. Objectives and Outline of the Thesis

The main objective of the AMT programme is the "improvement of our knowledge of marine biogeochemical processes, ecosystem dynamics, food webs and fisheries and to characterise physical and biogeochemical provinces" (Aiken *et al.,* 2000). This study fits within this objective in terms of improving knowledge of the basinscale changes in phytoplankton community structure and providing insight into the spatial and temporal changes in dynamics of oceanic ecosystems. Thus,

the overall aim of this thesis is to "investigate the spatial and temporal variability of phytoplankton community composition in the subtropical and tropical Atlantic Ocean" in terms of biomass measurements (pigments) and species identification (light microscopy for species >5μm in diameter).

The main research themes of this thesis are to;

(1) Characterise the composition of the phytoplankton communities, and describe its variability on (i) spatial (latitudinal and vertical) and (ii) temporal (intercruise, interannual) scales.
(2) Determine the components of the phytoplankton community which are responsible for spatial / temporal variability and gain insight into their respective ecology.
(3) Provide a regional approach to the classification of the hydrographic conditions and phytoplankton communities present in the tropical and subtropical Atlantic Ocean.
(4) Investigate relationships between hydrographic variability and changes in the structure of the phytoplankton community.
(5) Gain insight into the ecology of different phytoplankton communities within different environments of the subtropical and tropical Atlantic Ocean.
(6) Compare the phytoplankton communities of the subtropical Atlantic Ocean with relevent processes in other subtropical environments (e.g. North Pacific Subtropical Gyre) and put the AMT project into the context of current understanding of subtropical ecosystems.

Key to the analysis of spatial and temporal variability of the phytoplankton communities in the subtropical and tropical Atlantic Ocean is an understanding of the variability characteristic of the hydrographic environment. Several hydrographic parameters sutitable to characterise the hydrographic environment are introduced in **Chapter 3**, and are analysed in terms of latitudinal and vertical (spatial) variability, and intercruise (seasonal / interannual) variability. Basinscale (40°N to 40°S) changes in the structure of the phytoplankton communities are investigated in **Chapter 4** through the application of multivariate statistics to identify different assemblages and communities, and investigate the important components (species / taxa) driving such changes. Temporal (1995 - 2000) changes in the structure of the phytoplankton community within the subtropical South Atlantic are investigated in **Chapter 5** in view of the hydrographic variability identified in Chapter 3. Multivariate statistics are again used in Chapter 5 to determine interannual variability in the phytoplankton community composition and identify the important components causing such variability. The ubiquitous chlorophyll *a* maximum found throughout the subtropical and tropical Atlantic Ocean is investigated in **Chapter 6** with the aim of examining regional processes of formation, ecosystem structure and relationships to hydrographic parameters. Finally, **Chapter 7** presents a synthesis of the results of this study in view of other subtropical and tropical studies and aims to provide a summary of the spatial and temporal variability observed in terms of succession of phytoplankton community components.

# CHAPTER 2: METHODOLOGY

## 2.1. The Atlantic Meridional Transect (AMT) Programme

The Atlantic Meridional Transect (AMT) programme is based on a time-series of measurements taken during the biannual passage of the *RRS James Clark Ross* which routinely sails from the U.K. (~50°N) to Montevideo (Uruguay, ~ 35°S), and the Falkland Islands (~50°S). During September the *RRS James Clark Ross* sails south to the Falklands and returns to the U.K. the following April - May. The general cruise transect follows the 20°W meridian in the northern hemisphere, crosses the equator and passes down the coast of South America (Fig. 2.1). However, AMT-6 (April, 1998) and AMT-8 (April, 1999) involved changes in the cruise track. On AMT-6 the *RRS James Clark Ross* left from Cape Town (South Africa) and travelled up the western coast of S. Africa until past the equator where it rejoined the standard AMT cruise track. Due to this difference in the cruises track, data from AMT-6 it is not included in this study (details of this cruise can be found in Barlow *et al.,* 2002). AMT-8 involved a port call at Ascension Island (ca. 10°S) causing a cruise track further east into southern subtropical waters than previous AMT cruises (Fig. 2.1). Biological, chemical and physical measurements are made during daily CTD stations (0 - 200 m or 0 - 250 m) approximately 270 nm apart at between 25 - 30 locations.

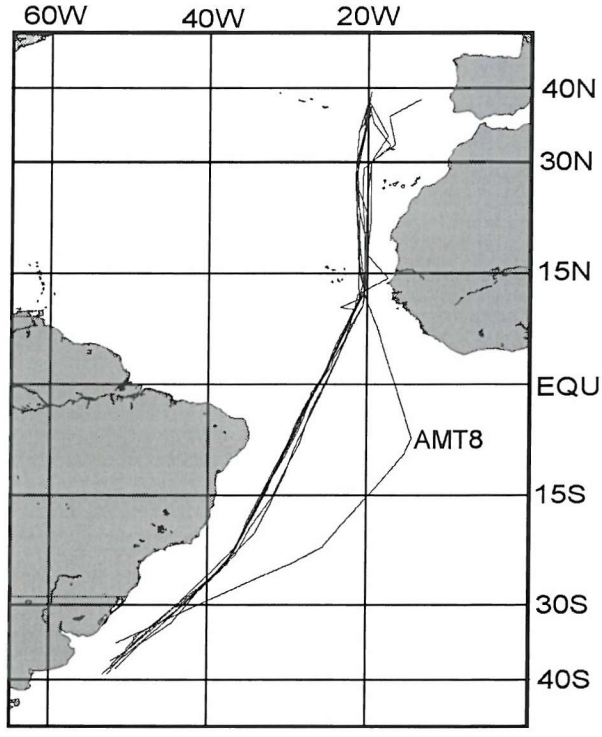


Figure 2.1: Cruise track in tropical and subtropical waters (40°N - 40°S) of the Atlantic Ocean of the Atlantic Meridional Transect (AMT) programme between 1995 - 2000 (AMT cruises 1 - 5, 7 - 10). Cruise dates, directions and details are provided in Table 2.1. Note the difference in cruise track for AMT-8.

The data presented in this thesis include AMT-1-5 and AMT-7-10 (September, 1995 - April, 2000) from a latitudinal range of 40°N to 40°S (Fig. 2.1). Cruise dates and details are found in Table 2.1, while Table 2.2 gives a summary of the measurements and personnel involved in their collection.

Table 2.1: Dates, directions and Principal Scientific Officers (PSO) for AMT cruises 1 - 5, 7 -10.

| AMT | Depart | Date | Arrive | Date | PSO | Notes |
|---|---|---|---|---|---|---|
| 1 | U.K. | 21/09/95 | Falklands Is. | 24/10/95 | D. Robins | |
| 2 | Falkland Is. | 22/04/96 | U.K. | 28/05/96 | D. Robins | |
| 3 | U.K. | 20/09/96 | Falkland Is. | 25/10/96 | T. Bale | |
| 4 | Falkland Is. | 21/04/97 | U.K. | 27/05/97 | T. Bale | |
| 5 | U.K. | 14/09/97 | Falkland Is. | 17/10/97 | J. Aiken | |
| 7 | U.K. | 14/09/98 | Falkland Is. | 25/10/98 | J. Aiken | Port call at Dakar (NW Africa) |
| 8 | Falkland Is. | 25/04/99 | U.K. | 07/06/99 | N. Rees | Port call at Ascension Island |
| 9 | U.K. | 15/09/99 | Montevideo | 13/10/99 | N. Rees | |
| 10 | Montevideo | 12/04/00 | U.K. | 07/05/00 | C. Gallienne | |

Table 2.2: Summary table of personnel responsible for the collection of phytoplankton data during the AMT cruises. Key: Fchl*a* is acetone extracted chlorophyll *a* measurements, pigment concentrations determined by High Performance Liquid Chromatography (HPLC), species identification and abundance determined by light microscope, nutrient concentrations determined by colourimetric methods and PAR measurements made by a WetLabs sensor. NA indicates that these measurements were not available for the present study (see notes below).

| AMT | Fchl*a* | Pigments (HPLC) | Species | Nutrients | PAR |
|---|---|---|---|---|---|
| 1 | G. Westbrook | C. Trees, G. Westbrook | D. Harbour | M. Woodward | NA[c] |
| 2 | P. Holligan, E. Maranon | C. Trees | D. Harbour | M. Woodward | NA[c] |
| 3 | R. Barlow, E. Maranon | R. Barlow | D. Harbour | M. Woodward | NA[c] |
| 4 | D. Suggett | S. Gibb | D. Harbour | M. Woodward | NA[c] |
| 5 | D. Suggett | S. Gibb | D. Harbour | M. Woodward | NA[c] |
| 7 | A. Poulton | L. Dransfeld | D. Harbour | N. Lefevre, J. Aiken, M. Lucas | D. Suggett N. Rees |
| 8 | A. Poulton | A. Poulton, L. Dransfeld | A. Poulton | NA[b] | N. Rees G. Westbrook |
| 9 | H. Willson | NA[a] | NA[a] | NA[b] | NA[c] |
| 10 | T. O'Hlggins, A. Poulton | V. Hill | A. Poulton | NA[b] | M. Moore |

Note: [a] Pigment and species samples were collected during AMT-9 and await analysis, [b] Nutrient measurements were made during AMT-8, 9 and 10, however the data is not currently available, and [c] PAR data was collected from AMT-1 to 5 but was not available for the present study.

## 2.2. Water Sampling

Water samples were collected from 0 - 250m during daily 10.00 - 12.00 am (local time) deployments of either a Neil Brown MK IIIB or Seabird SB911plus CTD Rossette bottle-sampler, equipped with 12 x 10L (Neil Brown) or 12 x 30L (Seabird) Go-Flow Niskin bottles. Selection of sampling depths was based on down-cast profiles of Temperature and Salinity (CTD Sensor package), Fluorescence (Wet Labs Inc.) and Transmittance (Wet Labs Inc), and bottles fired at 10 - 12 depths during the upcast. During some cruises (Table 2.1) vertical light (PAR) profiles were determined from a PAR sensor (Chelsea Instruments) attached to a Fast Repetition Rate Fluorometer. The precision of the CTD salinity and temperature sensors were checked periodically during each cruise through onboard salinity determination using a Guideline AUTOSAL precision salinometer, and comparison with ISO precision digital thermometers and Expendable Bathythermograph (XBT) casts (Aiken *et al.*, 1998).

Water samples were decanted into either black bag-shaded 10L carboys or directly into sample bottles from Niskin bottles ondeck using non-toxic silicon tubing. Chlorophyll *a* (by

fluorescence; section 2.4.1) and pigment (by HPLC: section 2.4.2) samples were collected from a minimum of eight depths depending upon water budget constraints. Duplicate 100 ml samples for the enumeration and identification of phytoplankton species were routinely collected from 2 - 3 depths from the surface (7m) layer, an intermediate depth (e.g. base of the upper mixed layer) and from the *in-situ* fluorescence maximum (i.e. Chlorophyll *a* Maximum). During AMT-8 samples for phytoplankton species identification were collected from up to 3 additional intermediate depths including the top of the *in-situ* fluorescence maximum.

## 2.3. Analysis of CTD Data

### 2.3.1. Density Calculations

Depending upon the CTD package used and the processing of the CTD data, density ($\sigma t$) was either supplied with the CTD data files, or has been calculated for each depth using the temperature and salinity data and the following equations;

$$\text{Density } (\sigma t) = \text{Density (kg m}^{-3}) - 1000$$

where;

$$\text{Density (kg m}^{-3}) = (a^0+(a^1+(a^2+(a^3+(a^4+(a^5*T)*T)*T)*T)*T)*T) + (b^0+(b^1+(b^2+(b^3+(b^4*T)*T)*T)*T)*T) * S + (c^0+(c^1+c^2*T)*T) * S * (\sqrt{(S)}) + ((d^0*S)^2)$$

where; T = temperature, S = salinity, $a^0 = 999.843$, $a^1 = 6.794e^{-2}$, $a^2 = 9.095e^{-3}$, $a^3 = 1.001e^{-4}$, $a^4 = 1.120e^{-6}$, $a^5 = 6.536e^{-9}$, $b^0 = 8.245e^{-1}$, $b^1 = 4.090e^{-3}$, $b^2 = 7.644e^{-5}$, $b^3 = 8.247e^{-7}$, $b^4 = 5.388e^{-9}$, $c^0 = -5.725e^{-3}$, $c^1 = 1.023e^{-4}$, $c^2 = -1.655e^{-6}$ and $d^0 = 4.381e^{-4}$ (International Equation of State of Sea Water, 1980).

### 2.3.2. Calculation of the Depth of the Mixed Layer (MLD)

Determination of the Upper Mixed Layer Depth (MLD) from both temperature and density profiles followed the method employed by Hooker *et al.,* (2000) with the CTD data converted into 5m depth bins; the rate of change in temperature and density is calculated for all depth pairs and the beginning of the thermocline or pycnocline is defined where the rate is >0.1°C $m^{-1}$ or >0.035 $m^{-1}$, respectively. Where the rate of temperature or density change was below these levels the MLD was defined by an increase of 0.5°C or 0.1$\sigma t$ from surface (7m) values (Hooker *et al.,* 2000). Individual cruise comparisons of MLD from temperature and density profiles show that some cruises include stations where there are more than one upper mixed layer present ($p < 0.001$ or non-significant, NS); AMT-1 $r = 0.997$, $n = 18$; AMT-2 $r = 0.959$, $n = 19$; AMT-3 $r = 0.287$, NS $n = 20$ or $r = 0.929$, $n = 15$; AMT-4 $r = 0.968$, $n = 32$: AMT-5 $r = 0.745$, $n = 18$; AMT-7 $r = 0.988$, $n = 26$; AMT-8 $r = 0.982$, $n = 24$; AMT-9 $r = 0.972$, $n = 34$; AMT-10 $r = -0.047$, NS $n = 17$ or $r = 0.983$, $n = 13$. Comparison between the MLD from density and temperature showed good agreement for the full dataset (AMT-1 - 10 $r = 0.865$, $p<0.001$, $n = 209$) and the MLD presented in this study are those from density profiles.

### 2.3.3. Brunt - Väisälä Buoyancy Frequency: Depth and Value of the Maximum

The Brunt - Väisälä buoyancy frequency ($N^2$) is a stability index where the depth of the maximum value is proportional to the pycnocline depth and the value of this maximum is proportional to the amount of energy required to mix the water-column (e.g. Knauss, 1996). $N^2$ has been calculated from the CTD density profiles into 5m bins following the equation;

$$N^2 = (-9.81/ \text{average } \sigma t) * (\Delta \sigma t / \Delta zm) \qquad \text{(e.g. Knauss, 1996)}$$

where -9.81 is the acceleration of gravity, average $\sigma t$ within this study has been taken as 1026 kg $m^{-3}$, $\Delta \sigma t$ is the difference in density between depth pairs and $\Delta zm$ is the difference in depth.

## 2.4. Phytoplankton Pigments and Fluorescence

### 2.4.1. Fluorometric Chlorophyll a Measurements (Flchla)

Measurements of chlorophyll *a* concentration from acetone extraction and subsequent fluorometry (Flchl*a*) have been routinely made on all AMT cruises, although there have been slight variations in the methods employed (Table 2.3). Generally, between 100 ml - 500 ml of seawater was filtered through Whatman GF/F (pore size 0.7μm) filters and extracted in 10 ml 90% acetone (HPLC grade) in the dark at -20°C. After 12 - 24 hrs the samples were brought to room temperature in the dark and the chlorophyll *a* fluorescence (F) measured. Flchl*a* concentration is then calculated using the following equation;

$$\text{Flchl}a\ (\mu g\ l^{-1} \text{ or } mg\ m^{-3}) = (V1 / V2) * (F)$$

where V1 is the volume of acetone used (ml), V2 is the volume filtered (ml), and F is the raw fluorescence reading. During AMT-1 and 2 Flchla and phaeopigment measurements were taken following the acidification method of Holm-Hansen *et al.,* (1965) on a PML built fluorometer (Table 2.3). The Turner Designs AU-10 fluorometer used during later cruises (Table 2.3) was set up with excitation and emission light-filters following Welschmeyer (1994) to allow for accurate chlorophyll *a* (Chl-*a*) measurements without interference from phaeopigments or chlorophyll *b*. Pre-cruise and post-cruise calibration of both fluorometers used Chl-*a* standards where the Chl-*a* concentration was first determined spectrophotometrically (Cecil 292 Digital Ultraviolet Spectrophotometer) on a Chl-*a* standard solution (Sigma UK) made up in 90% acetone (HPLC grade) following Jeffrey and Humphrey (1975); absorption values at 630nm ($E_{630}$), 647nm ($E_{647}$) and 664nm ($E_{664}$) were measured and corrected for turbidity by subtracting the 750nm reading. Chl*a* concentration was calculated following the formula;

$$\text{Chl}a\ (mg\ l^{-1}) = 11.85E_{664} - 1.54E_{647} - 0.08E_{630} \qquad \text{(Jeffrey and Humphrey, 1975)}$$

The Chl-*a* standard solution was then diluted to a suitable concentration for the fluorometer (typically 100-fold dilution). Between AMT-8 and 9 the Turner A10-AU Fluorometer was not recalibrated and so the calibration used for AMT-8 was applied to the AMT-9 fluorescence data.

Table 2.3: Methodological specifics for measurements of acetone extracted chlorophyll *a* concentration (Fchl*a*) from all AMT cruises. Note the use of the Holm-Hansen *et al.*, (1965) method during the first three AMT cruises and application of the Welschmeyer (1994) light-filters during the remaining cruises. During several AMT cruises more than one set of Fchl*a* measurements were taken: during AMT-2 one set was collected for standard measurements and one for primary production studies (size-fractionated); during AMT-3 one set was collected for standard measurements, one for primary production and one for comparison of the Holm-Hansen *et al.*, (1965) and Welschmeyer (1994) measurements; during AMT-8 and AMT-10 one set was collected for standard measurements and one for size-fractionated Fchl*a*.

| AMT | Method | Filtering details; 1 - Volume (ml) 2 - Filter type | Extraction Method | Fluorometer Used |
|---|---|---|---|---|
| 1 | Holm-Hansen *et al.*, (1965) | 1 - 500 ml<br>2 - 0.7 μm Whatman GF/F | 10ml 90% acetone<br>15 - 18hrs -20°C | PML built Fluorometer |
| 2a | Holm-Hansen *et al.*, (1965) | 1 - 250 ml<br>2 - 0.7 μm Whatman GF/F | 10ml 90% acetone<br>12hrs -20°C | PML built Fluorometer |
| 2b | Holm-Hansen *et al.*, (1965) | 1 - 250 ml<br>2 - 0.2 μm Polycarbonate | 10ml 90% acetone<br>12hrs -20°C | PML built Fluorometer |
| 3a | Welschmeyer, (1994) | 1 - 250 ml<br>2 - 0.7 μm Whatman GF/F | 10ml 90% acetone<br>12-18 hrs -20°C | Turner Designs AU-10 (SOC) |
| 3b | Welschmeyer, (1994) | 1 - 250 ml<br>2 - 0.2 μm Polycarbonate | 10ml 90% acetone<br>12hrs -20°C | Turner Designs AU-10 (SOC) |
| 3c | Holm-Hansen *et al.*, (1965) | 1 - 250 ml<br>2 - 0.2 μm Polycarbonate | 10ml 90% acetone<br>12hrs - 20°C | PML built Fluorometer |
| 4 | Welschmeyer, (1994) | 1 - 1000 ml<br>2 - 0.7 μm Whatman GF/F | 10ml 90% acetone<br>18-24hrs -60°C | Turner Designs AU-10 (SOC) |
| 5 | Welschmeyer, (1994) | 1 - 250 ml<br>2 - 0.7 μm Whatman GF/F | 10ml 90% acetone<br>12hrs - 20°C | Turner Designs AU-10 (SOC) |
| 7 | Welschmeyer, (1994) | 1 - 100 - 250 ml<br>2 - 0.7 μm Whatman GF/F | 10ml 90% acetone<br>12-24hrs -20°C | Turner Designs AU-10 (SOC) |
| 8a | Welschmeyer, (1994) | 1 - 250 - 500 ml<br>2 - 0.7 μm Whatman GF/F | 10ml 90% acetone<br>12-24hrs -20°C | Turner Designs AU-10 (SOC) |
| 8b | Welschmeyer, (1994) | 1 - 250 - 500 ml<br>2 - 0.2 μm Polycarbonate | 10ml 90% acetone<br>12 - 24hrs - 20C | Turner Designs AU-10 (SOC) |
| 9 | Welschmeyer, (1994) | 1 - 100 - 250 ml<br>2 - 0.7 μm Whatman GF/F | 10ml 90% acetone<br>12-24hrs -20°C | Turner Designs AU-10 (SOC) |
| 10a | Welschmeyer, (1994) | 1 - 500 ml<br>2 - 0.7 μm Whatman GF/F | 10ml 90% acetone<br>12-24hrs -20°C | Turner Designs AU-10 (SOC) |
| 10b | Welschmeyer, (1994) | 1 - 500 ml<br>2 - 0.2 μm Polycarbonate | 10ml 90% acetone<br>Sonication and Centrifugation | Turner Designs AU-10 (SOC) |

During AMT-8 and AMT-10 measurements were also taken of size-fractionated chl*a* following the size categories of Sieburth (1979), by progressively filtering 250 - 500 ml water samples through 47mm diameter 20μm, 2μm and 0.2μm polycarbonate (Poretics U.K.) filters. Filters were placed in plastic test tubes with 10ml 90% acetone (HPLC grade) and either extracted overnight or processed immediately by sonication (30 seconds) and centrifugation (2000 rpm for 10 mins). Fluorescence was measured with the Turner Designs AU-10 fluorometer set up following Welschmeyer (1994) as described above.

Chl*a* measurements from 25mm Whatman GF/F (extracted overnight) and 47mm polycarbonate filters (AMT-8 extracted overnight, AMT-10 sonicated) were in good agreement for both AMT-8 ($r = 0.956$, $p<0.001$, $n = 119$) and AMT-10 ($r = 0.887$, $p<0.001$, $n = 61$) with the slope of the Model II regression line close to one for both cruises (AMT-8: 0.98, AMT-10: 1.15). Good agreement between the Whatman GF/F measurements and size-fractionated measurements indicate that most of the chl*a* containing particles in the subtropical and tropical Atlantic Ocean are retained by Whatman GF/F filters. Previous comparisons of the efficiency of particle retention by Whatman GF/F filters and 0.2μm polycarbonate filters have led to conflicting reports; Vaulot *et al.*, (1990) have reported >98% efficiency, whereas Campbell *et al.*, (1994) have reported an average of 15% loss. The most recent

study by Chavez *et al.,* (1995) indicated that there is no significant difference between the two filter types which is consistent with the results presented here.

There two potential sources of error in the measurement of chl*a* from fluorescence (Flchl*a*); operator error (i.e. sample preparation, fluorometer calibration) and differences between the acidification technique of Holm-Hansen *et al.,* (1965), and the light-filter set up of Welschmeyer (1994). Operator errors are considered to be minimal due to simplicity and relative consistency of the methods used. Measurements of Flchl*a* made during AMT-2 by two different operators showed good agreement ($r = 0.866$, $p<0.001$, $n = 50$) with the slope of the regression line close to 1 (0.98) (E. Maranon pers. comm.). The standard deviation of the Flchl*a* measurements, estimated from triplicate measurements from two depths (7m and 90m), was found to be <10% of the mean during AMT-10; the standard deviation for the surface sample (average Flchl*a* = 0.084 mg $m^{-3}$) was 0.004 mg $m^{-3}$ (4.8%) and 0.017 mg $m^{-3}$ (6.3%) for the deep sample (average Flchl*a* = 0.270 mg $m^{-3}$). Errors associated with differences in the volume filtered were also estimated during AMT-10 from triplicate Flchl*a* measurements (overall average = 0.10 mg $m^{-3}$) for 6 different volumes (50, 100, 150, 200, 250, 350 and 500 ml) from one depth (7m). A 1-way ANOVA found no significant differences between Flchl*a* measurements for all the volumes ($F = 0.18$, NS, $n = 21$), although the standard deviation decreased from ~13% for 50 and 100 ml to <5% for volumes over 150 ml.

Differences between the acidification and Welschmeyer (1994) techniques can be significant; Welschmeyer's (1994) selection of excitation and emission light-filters was specifically aimed at correcting the errors in the acidification technique due to fluorometric interference of the chl*a* signal by divinyl chlorophyll *a*, chlorophyll *b*, chlorophyll *c* and phaeopigments (Trees *et al.,* 1985; Welschmeyer, 1994). In situations where there are large amounts of chlorophyll *b* the acidification technique underestimates chl*a* concentration, whereas the reverse is true where large concentrations of chlorophyll *c* and/or divinyl chlorophyll *a* are present (Trees *et al.,* 1985). Following Welschmeyer (1994), the difference is decreased but reversed in high chlorophyll *b* situations, with an overestimation of ~10% for chlorophyll *a* measurements made when chlorophyll *b* to chlorophyll *a* ratios are 1. Although the Welschmeyer (1994) light-filters are not affected by phaeopigments and chlorophyll *c*, it does not differentiate between chlorophyll *a* and chlorophyllide *a* (a breakdown product from grazing or cell senescence; Jeffrey *et al.,* 1997) due to their identical spectral properties (Welschmeyer, 1994). On AMT-3 a comparison of Flchl*a* measurements from the acidification technique and using the Welschmeyer (1994) light-filters showed good agreement ($r = 0.933$, $p<0.001$, $n = 20$), with the slope of the regression line not significantly different from 1 (E. Maranon pers. comm.; Bale and Mantoura, 1996). This comparison has been taken to indicate that Flchl*a* data from AMT-1, 2 and 3 are comparable (Bale and Mantoura, 1996).

### 2.4.2. Chemotaxonomic Pigment Measurements (High Performance Liquid Chromatography)

*General Methodology* - Duplicate samples for the determination of pigment concentration were taken with 1.0 - 4.2L filtered onto Whatman GF/F (pore-size 0.7μm) filters under positive pressure. Pigment samples were either analysed onboard or on return to the laboratory (Table 2.4), with at least one set of filters flash frozen and stored in liquid nitrogen (-196°C) until further analysis, while others were

flash frozen with liquid nitrogen and stored at -80°C until they were transferred to liquid nitrogen on return to the U.K. During AMT-8 the majority of pigment samples were analysed onboard, however a small number were returned to the U.K. in liquid nitrogen and analysed within 2 months of the end of the cruise. The methods, techniques and equipment for the determination of pigment concentrations by High Performance Liquid Chromatography (HPLC) varied between cruises (Table 2.4). Significant differences in AMT methodology were changes from the Wright et al. (1991) to Barlow et al. (1997a,b) methods after AMT-2 and the use of a UV/Visible detector and fluorometer on some cruises and a Photo-Diode Array on others (Table 2.4). Detection of divinyl chlorophyll *a* was by use of a chromatic equation (following Latasa *et al.,* 1996) during AMT-2 and 3, whereas chromatographic separation was possible following the methods of Barlow *et al.,* (1997a, b) during later cruises (Table 2.4).

Table 2.4: Methodological specifics for the HPLC determination of phytoplankton pigment concentrations from all AMT cruises (adapted partly from Gibb *et al.*, 2000).

| AMT | Investigator(s) | Method (s) | Detectors | Dv Chl a Separation | Analysis | Pigment Quantification |
|---|---|---|---|---|---|---|
| 1 | C. Trees<br>G. Westbrook | Wright *et al.,* (1991) | UV/visible detector + Fluorometer | Dichromatic equation | Lab. | Internal Standard |
| 2 | C. Trees | Wright *et al.,* (1991) | UV/visible detector + Fluorometer | Dichromatic equation | Lab. | Internal Standard |
| 3 | R. Barlow | Wright *et al.,* (1991) / Barlow *et al.,* (1997a,b) | UV/visible detector + Fluorometer | Dichromatic equation / Chromatography | Lab. | Individual response factors |
| 4 | S. Gibb | Barlow *et al.,* (1997a,b) | Photodiode Array | Chromatography | Lab. | Internal Standard |
| 5 | S. Gibb | Barlow *et al.,* (1997a,b) | Photodiode Array | Chromatography | Shipboard | Internal Standard |
| 7 | L. Dransfeld | Barlow *et al.,* (1997a,b) | Photodiode Array | Chromatography | Shipboard | Internal Standard |
| 8 | A. Poulton<br>L. Dransfeld | Barlow *et al.,* (1997a,b) | UV/visible detector + Fluorometer | Chromatography | Shipboard and Lab. | Internal Standard |
| 10 | V. Hill | Barlow *et al.,* (1997a,b) | Photodiode Array | Chromatography | Lab. | Individual response factors |

Differences between the methods of Barlow *et al.,* (1997a, b) and Wright *et al.,* (1991) include the sample extraction process and the conditions of the mobile phase. Following Wright *et al.,* (1991) pigment extraction is in 100% acetone (HPLC grade) over a period of 15 hrs at -20°C in the dark and followed by centrifugation, whereas the Barlow *et al.,* (1997a, b) method involves extraction in 90% acetone (HPLC grade) with almost immediate sonication and subsequent centrifugation. However, during the processing of AMT-10 pigment samples extraction was in 90% acetone (HPLC grade) over a period of 12hrs at -20°C in the dark, followed by sonication in a sonic bath and centrifugation (V. Hill pers. comm.). The mobile phase for Wright *et al.,* (1991) includes three solvents (A - 80:20 methanol:0.5 M ammonium acetate, B - 90:10 acetonitrile:water, C - ethyl acetate) whereas the Barlow *et al.,* (1997a, b) method includes only 2 solvents (A - 70:30 methanol: 1M ammonium acetate, B - 100% methanol). Further details of the methods should be sought in the original papers; the Barlow *et al.,* (1997a, b) method is outlined below in the AMT-8 methodology.

An internal standard was used to quantify pigment concentrations during all AMT cruises apart from AMT-3 and 10 (Table 2.4), where quantification was based on individual response factors calculated from injection of pigment standards (Gibb *et al.,* 2000). The internal standard used was the non-fluorescing carotenoid canthoxanthin, which is found rarely in the marine environment (Gibb *et*

*al.,* 2000). Pigment standards were obtained from Sigma U.K. (chlorophyll *a*, chlorophyll *b*), VKI Denmark (all carotenoids, chlorophyll *c*) and University of Hawaii (divinyl chlorophyll *a* and divinyl chlorophyll *b*).

*HPLC Methodology for AMT8* - Phytoplankton pigment concentrations were analysed by reverse-phase HPLC on a C8 column (Alltech Hypersil 3-mm MOS2) following the methodology of Barlow *et al.,* (1997a, b) which allows the separation of divinyl chlorophyll *a* and monovinyl chlorophyll *a*, but does not separate divinyl chlorophyll *b* and chlorophyll *b* (Barlow *et al.,* 1997a, b). Frozen filters were extracted in 2 ml 90% acetone (HPLC Grade) containing a known concentration of canthoxanthin, which acted as an internal standard (Gibb *et al.,* 2000), sonicated (~20 secs), and centrifuged to settle out filter debris. An aliquot (~1 - 1.5 ml) of the centrifuged extract was placed in vials and mixed with an equal volume of 1 M ammonium acetate prior to injection. Samples were injected into a Thermoseparation Products HPLC system, fitted with an autosampler, a P2000 solvent pump, SN4000 integrator and a UV6000 variable UV/visible detector. Pigments were separated by a solvent gradient changing from 75 - 0% solvent A and 25 - 100% solvent B over 25 minutes at a flow rate of 1 ml $min^{-1}$, after which the column was reconditioned for 7 minutes. Solvent A consisted of 70:30 Methanol:1 M ammonium acetate (v/v), while solvent B consisted of 100% Methanol. Chlorophylls and accessory pigments were detected by absorbance at 440nm. Data collection and integration were carried out using the Thermoproducts PC1000 software.

Pigments were identified by the comparison of retention times with authentic standards in acetone; chlorophyll *a* and chlorophyll *b* (Sigma Chemical Company), chlorophyll *c* and carotenoids (VKI Water Quality Institute, Denmark) and divinyl chlorophyll *a* (R. Bidigare, Hawaii). Pigment concentrations were calculated by the response factors of each pigment standard with respect to the internal standard (canthoxanthin). Pigment concentrations were determined from one set of replicates throughout AMT-8, and the results checked on a small subset following an identical protocol with the added use of a Photodiode Array at Plymouth Marine Laboratory (Rees and Gibb pers.comm.).

*Internal Comparisons of Total Chlorophyll a and Total Accessory Pigments* - A ubiquitous relationship has been found between HPLC measurements of total chlorophyll *a* and total accessory pigments (chlorophylls *c*, *b* and carotenoids) from a wide range of environments, with an average correlation coefficient (r) of 0.889 and an overall slope of the log accessory pigments to log total chlorophyll *a* of 0.93 (Trees *et al.,* 2000). Such a relationship indicates that, despite taxonomic and physiological variations, chlorophyll *a* concentrations are related to the total amount of accessory pigments, and can be used as an internal qualitative comparison of HPLC datasets. The AMT pigment dataset gives a similar relationship to that found by Trees *et al.,* (2000); AMT correlation coefficients (r) range from 0.840 to 0.981 (Fig. 2.2). The gradient of the Model II regression line varies slightly from 1.02 - 1.35 (Fig. 2.2), which may be due to the fact that Trees *et al.,* (2000) included chlorophyll *a* allomer, chlorophyll *a* epimer and chlorophyllide *a* in their total chlorophyll *a* measurements whereas these were not measured during most AMT cruises, as well as the fact that several accessory pigments were not fully quantified throughout the AMT programme (diadinoxanthin, diatoxanthin, dinoxanthin,

prasinoxanthin, violaxanthin, β-carotene). Another possible reason for the differences in the regression equations is that the range of chlorophyll *a* and carotenoid concentrations experienced on each cruise are variable (Fig. 2.2). Variability in the relationships between total chlorophyll *a* and total carotenoids may be taken as an indication that the absolute pigment measurements should be treated with caution, whereas pigment ratios (e.g. Hex-fuco:Chl *a*) represent a better basis for inter-cruise comparisons.

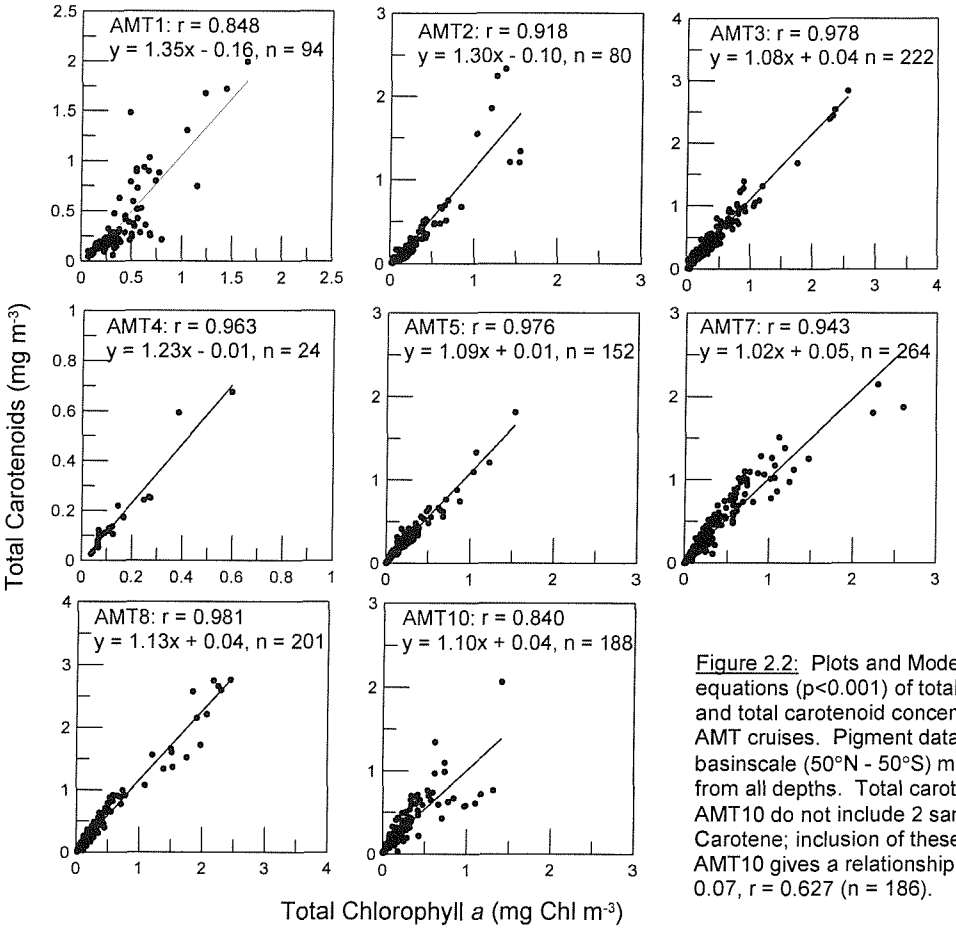


Figure 2.2: Plots and Model II regression equations ($p<0.001$) of total chlorophyll *a* and total carotenoid concentrations for the AMT cruises. Pigment data includes basinscale (50°N - 50°S) measurements from all depths. Total carotenoids from AMT10 do not include 2 samples and β-Carotene; inclusion of these results for AMT10 gives a relationship of $y = 1.51x + 0.07$, $r = 0.627$ ($n = 186$).

*Comparison of Chlorophyll a Measurements from Fluorometry and HPLC* - Fundamental differences exist between fluorescence and HPLC measurements of chlorophyll *a*; HPLC minimises interference due to overlapping fluorescence and absorbance bands of the different pigments as the pigments are physically separated and individually quantified by absorption and/or fluorescence detectors, whereas fluorometers measure chlorophyll *a* fluorescence within a variable background mixture of pigments (Trees *et al.*, 1985). Fluorometric techniques tend to underestimate or overestimate the chlorophyll *a* concentration due to the interference of other pigments and chlorophylls depending upon the method applied (Trees *et al.*, 1985; Welschmeyer, 1994). Comparisons of total chlorophyll *a* from HPLC (TChl *a* = divinyl chlorophyll *a* + chlorophyll *a*) and acetone extraction (Fchl*a*) techniques for the AMT dataset show that although there is good agreement between methods ($r = 0.818$ - $0.945$), the slope of the regression lines are variable between cruises (Table 2.5). Thus, during most cruises chlorophyll *a* concentrations from HPLC are 14 - 33% lower than Fchl*a*, whereas during some cruises (AMT-3, 4) HPLC gives on average 18 - 22% higher chlorophyll *a* concentrations (Table 2.5).

Table 2.5: Summary table of the results from analysis of the relationship between fluorometric chlorophyll *a* (Flchl*a*) and total chlorophyll *a* from HPLC (TChl *a*). Measurements for this analysis are limited to those collected in the subtropical and tropical Atlantic Ocean (40°N - 40°S). Table includes the Pearson's moment correlation coefficient (r) and Model II regression equations, as well as the average and range of percentage error of the HPLC TChl *a* compared with the Flchl*a*. [Percentage difference calculated as (Flchl*a* - TChl *a* / Flchl*a*)*100).] The number of samples included in the analysis are indicated by n.

| AMT Cruise Number | r | All Data 40°N - 40°S Model II Regression Equations | [n] | Average % Difference |
|---|---|---|---|---|
| 1 | 0.941 | y = 0.67 x chl*a* + 0.01 | [n = 82] | +22.4 |
| 2 | 0.888 | y = 0.93 x chl*a* - 0.02 | [n = 55] | +14.7 |
| 3 | 0.875 | y = 1.21 x chl*a* - 0.02 | [n = 131] | -17.9 |
| 4 | 0.933 | y = 1.02 x chl*a* + 0.02 | [n = 24] | -21.9 |
| 5 | 0.978 | y = 0.90 x chl*a* + 0.01 | [n = 186] | +7.66 |
| 7 | 0.941 | y = 0.74 x chl*a* - 0.03 | [n = 227] | +33.3 |
| 8 | 0.928 | y = 0.75 x chl*a* - 0.01 | [n = 151] | +25.9 |
| 10 | 0.699 | y = 0.70 x chl*a* - 0.01 | [n = 134] | +23.8 |
| Total (Excluding AMT-10) | 0.914 | y = 0.81 x chl*a* - 0.002 | [n = 846] | +12.6 |

Poor correlation and regression results for TChl *a* and Flchl*a* from AMT-10, as well as the variable relationship observed between TChl *a* and total carotenoids (Fig. 2.2), combined with the good agreement between size-fractionated and standard Flchl*a* measurements, indicate problems with the pigment data from AMT-10. Variability in the relationship between TChl *a* and Flchl*a* measurements for the different cruises support the earlier conclusion from the TChl *a* and total carotenoid relationships; for inter-cruise comparisons pigment ratios are a better measurement than absolute pigment concentrations.

Table 2.6: Pigment lists from all AMT cruises, indicating pigments that have been identified during all AMTs and those which have not (shaded rows). SCOR-UNESCO abbreviations are taken from Jeffrey *et al.*, (1997).

| Pigment / Pigment Group | SCOR-UNESCO Abbreviation | AMT Cruise 1 | 2 | 3 | 5 | 7 | 8 | 10 |
|---|---|---|---|---|---|---|---|---|
| Chlorophyll *c* ($c_1c_2$ + $c_3$) | Chl *c* | Y | Y | Y | Y | Y | Y | Y |
| Peridinin, Fucoxanthin and Alloxanthin | Perid + Fuco + Allo | Y | Y | Y | Y | Y | Y | Y |
| 19'-Hex- and 19'-Butanoyloxyfucoxanthin | Hex-fuco + But-fuco | Y | Y | Y | Y | Y | Y | Y |
| Diatoxanthin | Diato | Y | Y | Y | Y | Y | N | N |
| Diadinoxanthin | Diadino | N | Y | Y | Y | Y | Y | N |
| Dinoxanthin | Dino | Y | Y | N | N | N | N | N |
| Prasinoxanthin | Pras | Y | Y | N | Y | N | N | N |
| Violaxanthin | Viola | N | N | Y | Y | Y | N | Y |
| Zeaxanthin and Lutein | Zea + Lut | Y | Y | Y | Y | Y | Y | Y |
| Chlorophyll *b* (+Divinyl chlorophyll *b*) | Chl *b* | Y | Y | Y | Y | Y | Y | Y |
| Divinyl chlorophyll *a* | Dv Chl *a* | Y | Y | Y | Y | Y | Y | Y |
| Monovinyl chlorophyll *a* | Chl *a* | Y | Y | Y | Y | Y | Y | Y |
| β-Carotene | β-Car | N | Y | N | Y | Y | Y | Y |

*The AMT Pigment Database* - Although samples have been routinely collected from all AMT cruises, HPLC pigment measurements are not currently available for all cruises; pigment data is missing from 20°S to 26°N from AMT-2, there are no pigment data from depths other than the surface (7 m) for AMT-4 (J. Aiken pers. comm.) and AMT-9 pigment samples have not been analysed. Of the pigments analysed only 10 have been separated and measured from all AMT cruises (Table 2.6) and these will form the basis of inter-cruise comparisons of the pigment database. (Note: zeaxanthin and lutein were not always resolved and therefore these two pigments have been added together for inter-cruise comparison).

### 2.4.4. *In-situ* Fluorescence and Chlorophyll *a* Concentration

*In-situ* fluorescence is the standard technique for measuring chlorophyll *a* continuously both vertically (CTD) and horizontally. Although the relationship between chlorophyll *a* concentration and fluorescence can vary depending upon the type of fluorometer, the physiological state of the algal population or types of phytoplankton present (Falkowski and Raven, 1997), fluorescence is generally a good indicator of the large scale distribution of phytoplankton biomass.

In order to calibrate and convert the raw fluorescence data from CTD casts during AMT-7, 8 and 10, raw fluorescence data was binned into 1 - 2m bins that corresponded to discrete sampling depths. Samples from the upper 40 m were excluded from the analysis to minimise the effects of fluorescence quenching due to high ambient light levels in upper waters with high incident irradiances (Falkowski and Raven, 1997). The relationships between *in-situ* fluorescence (F) and Flchla concentration (Fig. 2.3) for the 3 cruises are described by the following Model II regression equations;

AMT-7 chl *a* = (4.33 x F) - 0.22 ($r = 0.860$, $p<0.001$, $n = 169$)

AMT-8 chl *a* = (3.45 x F) - 0.10 ($r = 0.809$, $p<0.001$, $n = 111$)

AMT-10 chl *a* = (20.08 x F) - 0.46 ($r = 0.794$, $p<0.001$, $n = 101$)

Inter-cruise differences in the regression equations are probably due to the use of different *in-situ* fluorometers; AMT-7 and 8 used a WetLabs fluorometer while AMT-10 used a PML fluorometer.

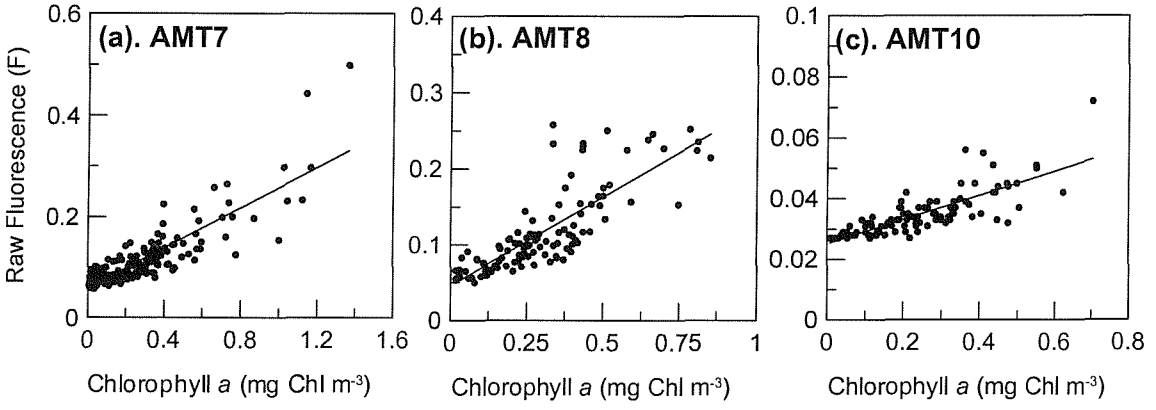


Figure 2.3: Plots of the relationships between raw *in-situ* fluorescence from the fluorometer and discretely measured chlorophyll *a* concentration (mg Chl $m^{-3}$) from acetone extractions (grey line is regression equation, see text for equations); (a) AMT-7, (b) AMT-8, and (c) AMT-10.

## 2.5. Phytoplankton Enumeration and Species Identification

### 2.5.1. Enumeration

Duplicate 100 ml water samples were preserved separately with 1 - 2% acidic Lugols solution and 0.4% borax buffered Formaldehyde in 100 ml glass bottles (Throndsen, 1978). Enumeration followed the Utermöhl inverted light microscope technique (Hasle, 1978) and the recommendations of Sournia (1978), with chlorophyll *a* measurements (i.e. Flchl*a*) used to determine settling volumes; <0.5 mg $m^{-3}$ - 100 ml; 0.5 - 1.0 mg $m^{-3}$ - 50 ml; >1.0 mg $m^{-3}$ - 10 or 25 ml (D. Harbour, pers.comm.). All samples were gently mixed for between 1 - 2 minutes before settling of either the entire volume or a

subsample. Samples were settled in 100 ml or 50 ml HydroBios tower and slide combinations and 25 ml Duncan and Associates chambers with settling times ranging from 80 hours (100 ml) to 24 hours (25 ml).

Samples were examined under either a Leica DMIRB, Leitz Fluovet or a Nikon Eclipse TS100 inverted microscope. Lugol's preserved samples were enumerated for diatoms, autotrophic dinoflagellates, small flagellates and other autrophic taxa with cell counts from the whole area of the settling area (x 200) for large cells (>5 μm in diameter) and discrete transects or fields or view (x 400) for small cells (<5 μm in diameter). Formaldehyde samples were enumerated for coccolithophores and the whole area of the settling chamber was examined under high magnification (x 400) with the use of oil immersion (x 1000) and phase contrast techniques for identification of small species. Cell numbers (cells $l^{-1}$) were calculated from the settled volume for all species, with abundances calculated from transects and fields of view by applying the ratio of sample counted (transect area or eye-piece area, respectively) to the total settling chamber area, with adjustments based on the magnification used. The number of transects or fields of view examined was determined by the total cell numbers experienced; the counts were continued until >200 cells were counted in total (for all small taxa) (Venrick, 1978) which usually resulted in the minimum examination of 2 transects and 10 fields of view. Such considerations were not possible with large cells, although the dependency of settling volume on chlorophyll *a* concentration meant that when cell numbers were low the whole preserved volume was examined. Where colonial phytoplankton species were encountered all individual cells were counted, however for colonies of *Trichodesmium* spp. with very small cell sizes (~10 μm in diameter) measurements were taken of the length of the individual trichomes in the colonies and the total length divided by the average cell size to give cell numbers (D. Harbour pers. comm.).

Genus and species identification followed Dodge (1982) for dinoflagellates, Kleijne (1993) and Winter and Siesser (1994) for coccolithophores, and Tomas (1997) for diatoms, dinoflagellates and coccolithophores. Autotrophic dinoflagellate species were distinguished from heterotrophic dinoflagellate species following the species list of Lessard and Swift (1986) and the comments of Tomas (1997). When phytoplankton cells could not be identified to genus or species level they were grouped into size-specific morphotypes which were internally compatible for the AMT database. Species identification and cell count data from all the AMT cruises were revised following recommendations by Tomas (1997) and logical restrictions to the microscope method and operator experience. For the statistical analysis of variability in the species composition and data presentation each species was assigned a species code and the full species name and corresponding code is presented in a table for each chapter (see Tables 4.2 and 5.1). Species or morphotypes were also grouped into taxonomic groups for analysis and presentation; diatoms (D), coccolithophores (CC), autotrophic dinoflagellates (AD) and a mixed taxa group including several endosymbiotic species (ED). The endosymbiotic group included species which are associated with symbiotic cyanobacteria or flagellates, as well as species with the ability to fix nitrogen; *Trichodesmium* spp., *Myrionecta rubra*, *Hemiaulus hauckii*, *Hemiaulus membranaceus*, *Hemiaulus sinensis*, *Histioneis* spp., *Ornithocercus* spp., *Rhizosolenia hebetata*, *Leptocylindrus mediterraneus*, *Amphisolenia globifera*, *Citharistes* spp., *Guinardia cylindrus*.

As discussed in depth by Venrick (1978, 1982), there are several sources of error associated with the settling and counting of phytoplankton samples under the light microscope; e.g. preservation problems, subsampling errors, enumeration errors, identification difficulties with small cells (e.g. nanoflagellates) with unknown nutritional or taxonomic affiliations, inaccuracies with estimating large rare cell abundances, and the dependency of the observations on the experience of the observer. As a measure of the precision of single counts (no replication), Venrick (1978) proposed that the standard error of the counts was proportional to the square-root of the total cell numbers, assuming normal (Poisson) distribution of the data. Applying this formula to the counts of phytoplankton (>5 μm) species used in multivariate analysis for AMT-8 gives a range of standard error between 0.4 - 5.4% of the mean and the relationship between the standard error and the total count is characterised by an inverse exponential relationship; i.e. the errors associated with counting decrease as the number of cells increase. However, this is not likely to represent a true measurement of the errors associated with enumeration of the phytoplankton community and there may be arguments against assuming normal (Poisson) distribution of phytoplankton cells. Although no direct measure of the variance due to the sampling and enumeration methods have been made within this study several precautions have been made to limit the effects of these biases; (1) statistical analysis and presentation of the phytoplankton community from light microscope counts has been limited to large (>5 μm) identifiable cells and none of the counts of small cells of unknown taxonomic and nutritional affiliation are used, (2) as recommended by Venrick (1978) several data transformations (see section 2.6.1) have been applied to either downplay the influence of large rare species or their removal from the data through application of a numerical definition of 'rare' and 'common', and (3) 'normalisation' of the species data to the experience of the investigator through the combining of certain species or genera and the creation of several size-specific morphotypes.

### 2.5.2. Biovolume and Biomass Calculations

Due to the high diversity of cell size in phytoplankton communities, absolute species abundances do not fully represent the inter-species relationships and biomass is a better measure of phytoplankton standing stock (Smayda, 1978). However, the conversion of cell numbers into cell biomass is problematic due to cell shrinkage with preservation, the unknown cellular components (i.e. vacuole size) and intra-species variations in cell size (e.g. decrease in diatom cell size with binary fission). Therefore, measurements of phytoplankton biomass must be considered as semi-quantitative estimates and within this study are only used to identify trends in biomass distribution and relationships to other phytoplankton variables (e.g. chlorophyll *a*). Cell abundances were converted into biovolume and biomass based on individual species cell carbon content (pg C per cell $ml^{-1}$). Cell carbon values are based on the formulae of Kovala and Larrence (1966) where simple geometric shapes with cell dimension measurements are converted to cell biovolume and carbon content using an Excel spreadsheet (written by L. Maddock, 1995). Cell dimensions were determined by D. Harbour (PML) or taken from the literature (Tomas, 1997) with conversion to relevant cell dimensions.

## 2.6. Statistical Analysis: Community and Species Composition Analysis

Various statistical methods and techniques have been used in this study, including standard statistical techniques to investigate relationships between variables and multivariate techniques to analysis changes in the phytoplankton community composition. Non-multivariate standard statistics (correlation, 1-way ANOVA and Turkey tests) have been carried out the using the statistics package Minitab (v.12), following the recommendations of Fowler and Cohen (1993). Model II regression equations have been calculated following the equations of Ricker (1973). Where mutiple correlations have been carried out the p values have been Bonferroni corrected following the recommendations of Curtin and Schulz (1998). Multivariate analysis of the phytoplankton community data and hydrographic data have been carried out using the ecological statistical program Plymouth Routines In Marine Ecological Research (PRIMER v 5.2.2) and the recommendations of Clarke and Warwick (1994). Full details, including the choice of the relevant techniques are discussed in the following sections.

### 2.6.1. Background to Multivariate Techniques: Choice of Techniques

Biological community composition data is inherently multivariate; i.e. made up of a high number of variables (species) relative to a slightly lower number of samples (Clarke and Warwick, 1994). Multivariate statistical techniques provide a powerful statistical basis for investigating and describing multiple dependent relationships between numerous variables (species) that are characterised by interrelations (James and McCulloch, 1990). The starting point for multivariate analysis is the data matrix (species vs. samples) and, depending upon the biological questions and nature of the data collection, several transformations of the data may be applied. The basis for the multivariate techniques used in this study is the calculation of a similarity (or dissimilarity) matrix, which describes the relationships between the variables and samples. The pattern of the relationships between variables can either be described by ordination (reduction of a matrix of similarities among variables to one or a few dimensions) or by cluster analysis (classification of the variables into hierarchical categories on the basis of a similarity matrix) (James and McCulloch, 1990). Ordination (multi-dimensional scaling) techniques include Principal Component Analysis (PCA) and non-metric Multi-Dimensional Scaling (MDS), which differ in that PCA uses the dissimilarity distances between variables while MDS uses the ranks of the dissimilarity distances (James and McCulloch, 1990).

Although PCA analysis has been used for the analysis of species composition data in the literature (e.g. Eynaud *et al.,* 1999), there are several important limitations of the technique relative to its application to species data; (a) its definition of dissimilarity (Euclidean Distance) is inflexible and unsuitable for species abundance data, and (b) it is sensitive to outliers and requires the removal of rare species so that the number of species is comparable to the number of samples (James and McCulloch, 1990; Clarke and Warwick, 1994). As an alternative technique, non-metric MDS analysis is more flexible due it simple approach of constructing a map where the inter-point distances have the same rank order as the corresponding dissimilarities between samples (Clarke and Warwick, 1994). Advantages of non-metric MDS analysis also include a lack of assumptions, easy to use different

definitions of similarity and there is no implicit need to remove rare species, while the critical limitation of the non-metric MDS technique is that interpretations must be qualitative and subjective as the axes are not functions of the original variables (James and McCulloch, 1990; Clarke and Warwick, 1994). Agglomerate hierarchical cluster analysis (cluster analysis) provides a descriptive analysis (a dendrogram) of the (dis-) similarity matrix through the joining of variables; the two most similar variables are joined into a group and the similarity of this group to all other units is calculated so that repeatedly the two most similar groups are joined until only a single group remains (James and McCulloch, 1990).

### 2.6.2. Data transformation

Depending upon the ecological question being addressed and the nature of the species data, several transformations may be applied to the raw cell counts to downplay the influence of rare or dominant species (Clarke and Warwick, 1994). Two transformation methods have been used in this study; reduction to a simple presence / absence (PA) matrix and square-root transformation (SQRT). PA transformation results in appointing all community components an equal role in the statistics and drastically downplaying the role of rare and dominant species, while SQRT transformation retains the influence of the dominant components in the community. However, SQRT transformation in this study has been accompanied by removal of rare components following the recommendations of Clarke and Warwick (1994); in the case of species data, rare species were defined as ones that consistently accounted for either <3% (Chapter 4) or <10% (Chapter 5) of the total cell numbers in all samples, while in the case of pigment data, rare pigments were defined as ones that consistently represented <3% of the total pigment concentration. Analysis of pigment or species assemblages does not involve any transformation of the data but rather the data has been standardised (converted to percentages) following the recommendations of Clarke and Warwick (1994).

### 2.6.3. Similarity Indices

Within studies of phytoplankton community composition in the literature, several different similarity indices have been used; e.g. Whittaker Similarity Index used by Furuya and Marumo (1983), Kendal's non-parametric ($\tau$) Correlation Coefficient or Spearman's ($\rho$) correlation coefficients used by Venrick (1971 - 1999). However, within this study the Bray-Curtis Similarity Index has been used for (transformed) community data and the dissimilarity Normalised Euclidean Distance Index has been used for hydrographic data. The Bray-Curtis Similarity Index, like other similarity indices, compares the species composition of different communities or community subsets, so that the theoretical range of the percent similarity index is from 0% for samples with no species in common to 100% for identical associations (Venrick, 1982; Clarke and Warwick, 1994). A value of 100% similarity is unlikely to be observed even between replicate samples of the same association because species abundance fluctuations in the field and sampling errors in the laboratory reduce the index (Venrick, 1982). Such errors have been termed 'bias' and several equations to estimate its magnitude have been developed by Venrick (1982). However, within this study an alternative approach has been applied:

transformation of the species data to downplay the influence of abundance changes on measurement of the similarity between samples (Clarke and Warwick, 1994). It should be noted that any measure of community similarity is victim to similar bias and that the selection of a similarity index is less important than an understanding of how the index works under various conditions (Venrick, 1982).

Multivariate analysis of hydrographic parameters involves finding similarities between samples based on parameters that have different intervals and scales. The Bray-Curtis Similarity Index is unsuitable for this purpose and Normalised Euclidean Distance is recommended for this purpose (Clarke and Warwick, 1994).

### 2.6.4. Cluster Analysis

The purpose of cluster analysis is to identify groups of samples which are more similar in their composition to other groups and cluster these groups at decreasing levels of similarity and provide a plot (i.e. dendrogram) of these relationships (Clarke and Warwick, 1994). Alternatively, variables (species) may be clustered to indicate similarities in their distribution and occurrence (i.e. identification of assemblages; termed Recurrent Species Analysis by Venrick, 1999). Clusters (or groups) of variables can then be identified from the dendrogram by taking a standard level of similarity (or Euclidean Distance in the case of clustering of hydrographic parameters) and identifying the samples contained in each cluster. For the cluster analysis in this study the default settings of the PRIMER program have been used (i.e. group averaged cluster analysis) following Clarke and Warwick (1994).

Further analysis of the clusters to determine the role of each variable (species) in the formation of each cluster can also be carried out. Within this study, the PRIMER subroutine SIMPER ('Similarity Percentages') has been used to calculate the average dissimilarity ($\delta$) between all pairs of inter-group samples (i.e. every sample in group 1 paired with every sample in group 2), and breaks this average down into separate contributions from each species ($\delta i$) to the total average dissimilarity (Clarke and Warwick, 1994). Breakdown of the total dissimilarity ($\delta$) between groups into the contribution of each variable ($\delta i$), shows that the majority of components have a role in the separation of groups and the full results are too numerous to be easily presented or interpreted. An easier interpretation may be carried out if the components responsible for a fixed percentage of the total dissimilarity between groups are identified, along with the average dissimilarity between groups ($\delta$), the average abundances these components represent in each group and the average contribution of each component to the overall dissimilarity ($\delta i$). The ratio of average contribution from each variable ($\delta i$) to its standard deviation is indicative of how consistently within each group of samples an individual component contributes to the overall dissimilarity and therefore high values are indicative of variables that are good at discriminating between clusters (Clarke and Warwick, 1994).

### 2.6.5. Non-metric Multi-Dimensional Scaling (Kruskal's non-metric Procedure)

Non-metric MDS (also referred to as Kruskal's non-metric procedure) displays inter-sample relationships on a continuous scale, producing a map or ordination plot where the inter-sample

distances are proportional to the (dis-) similarities between samples or groups of samples (Clarke and Warwick, 1994). An MDS plot is validated by its stress value, which is a measure of the difficulty of compressing the inter-sample relationships into 2-dimensional space (i.e. a measure of fit; Clarke and Warwick, 1994). The MDS algorithm reanalyses the inter-sample distances until a suitably low stress value is achieved, in this study the default number of restarts (10) was used. Critical stress values for the interpretation of MDS analysis are; <0.05, excellent representation with no prospect of misinterpretation; <0.10, good ordination, little prospect of misinterpretation, <0.20, potentially useful although interpretation needs checking, >0.30, samples too close to being arbitrarily placed in 2-dimensions (Clarke and Warwick, 1994). One method of checking an MDS ordination is to superimpose the groups from the Cluster analysis on the MDS and look for distortion or overlap (Clarke and Warwick, 1994). Thus, Cluster and MDS analysis can be used in conjunction with one another to support and give added weight to the interpretation when the interpretation is questionable as indicated by high stress.

### 2.6.2. Univariate Methods in Community Analysis: Diversity

Community diversity is composed of two inter-related measures; the measure of the number of species (i.e. richness) and the measure of the partitioning of the total numbers between individual species (i.e. dominance or evenness). Several diversity indices exist (see Magurran, 1988) which either measure richness (e.g. Margalef's Index) or dominance (e.g. Pielou's Evenness), or in the case of Shannon's Diversity Index (H'), both. Diversity was calculated after elimination of rare species or pigments as defined above. H' was calculated by the PRIMER subprogram DIVERSE (see Clarke and Warwick, 1994) following the equation;

$$H' (Ln) = \Sigma pi \, Ln \, pi \qquad \text{(Magurran, 1988)}$$

where pi is the proportion of species found in the ith species. The true value of pi is unknown but is estimated from ni/N, where ni is the number of individuals of the ith species and N is the total number of individuals. High values of H' indicate high diversity, whereas low values of H' indicate low diversity and dominance of the community by one or a few species. Also calculated by DIVERSE was Pielou's Evenness (J') measure, following the equation;

$$J' = H' / Hmax \qquad \text{(Magurran, 1988)}$$

where Hmax is the maximum diversity possible if all the species were equally abundant and is calculated as;

$$Hmax = H' / Ln \, S \qquad \text{(Magurran, 1988)}$$

where S is the number of species present in the sample. J' is restricted to a value between 0 - 1, where 1 represents a situation where all species are equally abundant. In certain cases the total number of species was also used a measure of the species richness.

## 2.7. Ancillary Measurements

### 2.7.1. Macronutrients (Nitrate, Nitrite, Phosphate and Silicate) and Estimated Nutricline Depths

Nutrient samples were collected from all depths sampled by the CTD Niskin bottles following clean handling techniques (Bale and Mantoura, 1996, 1997; Aiken *et al.,* 1998, 2000); samples were decanted from Niskin bottles into clean Nalgene bottles via non-toxic silica tubing whilst wearing sterile plastic gloves. Nutrient concentrations were determined colourimetrically using a 4-channel Technicon Autoanalyser and standard methodologies (see Aiken *et al.,* 1998) either immediately onboard or on return to the UK. Samples for analysis in the UK were frozen at -20°C onboard the *RRS James Clark Ross*. Frozen nutrient samples have been shown to preserve nitrate and silicate concentrations, but to give higher phosphate concentrations than in those analysed immediately (Chapman and Mostert, 1990). Generally, the nutrient concentrations found in the upper water-column of the tropical and subtropical Atlantic Ocean are close to, or below, the detection limits of the micromolar techniques (0.2 μM) used (Aiken *et al.,* 1998). The depth of the nutriclines for each nutrient have been estimated from the vertical nutrient profiles and are taken as a proxy for nutrient availability; the nutricline is assumed to occur at an intermediate depth above the first depth of an increased nutrient concentration relative to the low surface and subsurface concentrations. However, these estimates do not give a quantitative measure of the vertical gradient in nutrient concentrations, which is difficult to estimate due to the discrete collection of samples, a lack of a reference depth and the majority of measurements being under the detection limits of the methods used.

### 2.7.2. Photosynthetically Active Radiation (PAR) Measurements

Measurements of the vertical PAR distribution were made with a calibrated PAR sensor (Chelsea Instruments) attached to the Fast Repetition Rate Fluorometer deployed on the CTD. The underwater light field was characterised by calculating the vertical attenuation coefficient ($K_d$) following the quation;

$$K_d\ (m^{-1}) = -\text{Ln}\ (E_o / E_z) / \Delta_{zm} \qquad \text{(Kirk, 1994)}$$

where $E_o$ is the irradiance at depth 1, $E_z$ is the irradiance at depth 2 and $\Delta_{zm}$ is the difference between depths. The slope of the line from regression analysis of the natural log PAR data against depth for the upper water-column above the fluorescence maximum gives the water-column $K_d$. $K_d$ was calculated for waters above the fluorescence maximum due to the influence of the fluorescence maximum on the underwater field (Kirk, 1994). Fixed depths or the depth of certain features were converted to irradiance-normalised depths, or optical depths (ξ), following the equation;

$$\xi = K_d * zm \qquad \text{(Falkowski and Raven, 1997)}$$

Optical depths correspond to percentage PAR depths (Kirk, 1994; Falkowski and Raven, 1997) as follows; ξ 1.4 is equivalent to 25% PAR, ξ 2.3 is 10% PAR, ξ 4.6 is 1% PAR and ξ 6.9 is 0.1% PAR. The depths of these reference isolumes can be calculated by rearranging the optical depth equation; e.g.

$$\text{Depth of 10\% PAR (m)} = \xi\ 2.3 / K_d. \qquad \text{(Falkowski and Raven, 1997)}$$

# CHAPTER 3: HYDROGRAPHIC ENVIRONMENT: SPATIAL AND TEMPORAL VARIABILITY

## 3.1. Introduction and Data Presentation

The hydrographic environment in the tropical and subtropical Atlantic Ocean controls the availability of nutrients and light to phytoplankton communities, and thus the community structure. The overall aim of this chapter is to provide a background to the hydrographic environment sampled by the AMT programme in terms of regional (latitudinal), vertical and temporal changes in the structure of the water-column. The spatial (latitudinal / vertical) and temporal (seasonal / intercruise) variability of several hydrographic parameters are presented with particular reference to AMT-7 (September, 1998). These characteristics are presented for all AMT cruises with the aim of identifying temporally stable or variable parameters. Most parameters are available for all the AMT cruises; however, a few are only available for a limited number of cruises (see methods). Hydrographic parameters which are available for all AMT cruises are; temperature (°C), salinity (psu), density ($\sigma t$), upper mixed layer depth (MLD), the depth and value of the maximum Brunt - Väisälä Frequency ($ZN^2max$ and $N^2max$, respectively), whereas estimated euphotic zone depths ($Z_{eu}$ are only available from AMT-7, 8 and 10 and the estimated depth of the macro-nutriclines (e.g. nitracline; $Z_{NO3}$) are only available from AMT-1 - 4 and 7. Therefore, AMT-7 represents the only cruise where both nutrients and light data are currently available and the spatial distribution of all parameters will be presented before analysis of all the AMT hydrographic data.

## 3.2. Spatial Patterns of the Hydrographic Environment during AMT-7 (September, 1998)

### 3.2.1. Physical Parameters

The spatial distribution of all hydrographic parameters discussed in this chapter are presented for AMT-7 in Figure 3.1. Seasurface water temperatures (SST) in the subtropical and tropical Atlantic Ocean during AMT-7 show a latitudinal gradient, with highest SST values found at the equator (Fig. 3.1a). The subtropical gyres in both hemispheres exhibit high salinity 'cores' with relatively low salinity surface values off NW Africa and the along the equator (Fig. 3.1b). High SST and salinity's characterise the central subtropical gyres and are indicative of strong heating and high evaporation rates (Brown *et al.,* 1989a). By contrast the lower salinity of the equatorial Atlantic Ocean is influenced by the overlying Inter-Tropical Convergence Zone (e.g. Tchernia, 1980; Brown *et al.,* 1989a; Aiken *et al.,* 2000) and entrainment of Amazon River outflow in the North Equatorial Counter Current (Muller-Karger *et al.,* 1988).

The relationship between temperature and salinity in the subtropical and tropical Atlantic Ocean shows regional variations (Hooker *et al.,* 2000; Fig. 3.1a, b); in the subtropical gyres both temperature and salinity increase, while in equatorial waters temperature increases are accompanied by decreases in salinity. Density changes are related to the relationship between temperature and

salinity, with a latitudinal gradient from low equatorial surface water densities to relatively higher densities in the subtropical gyres (Fig. 3.1c; Hooker *et al.,* 2000).

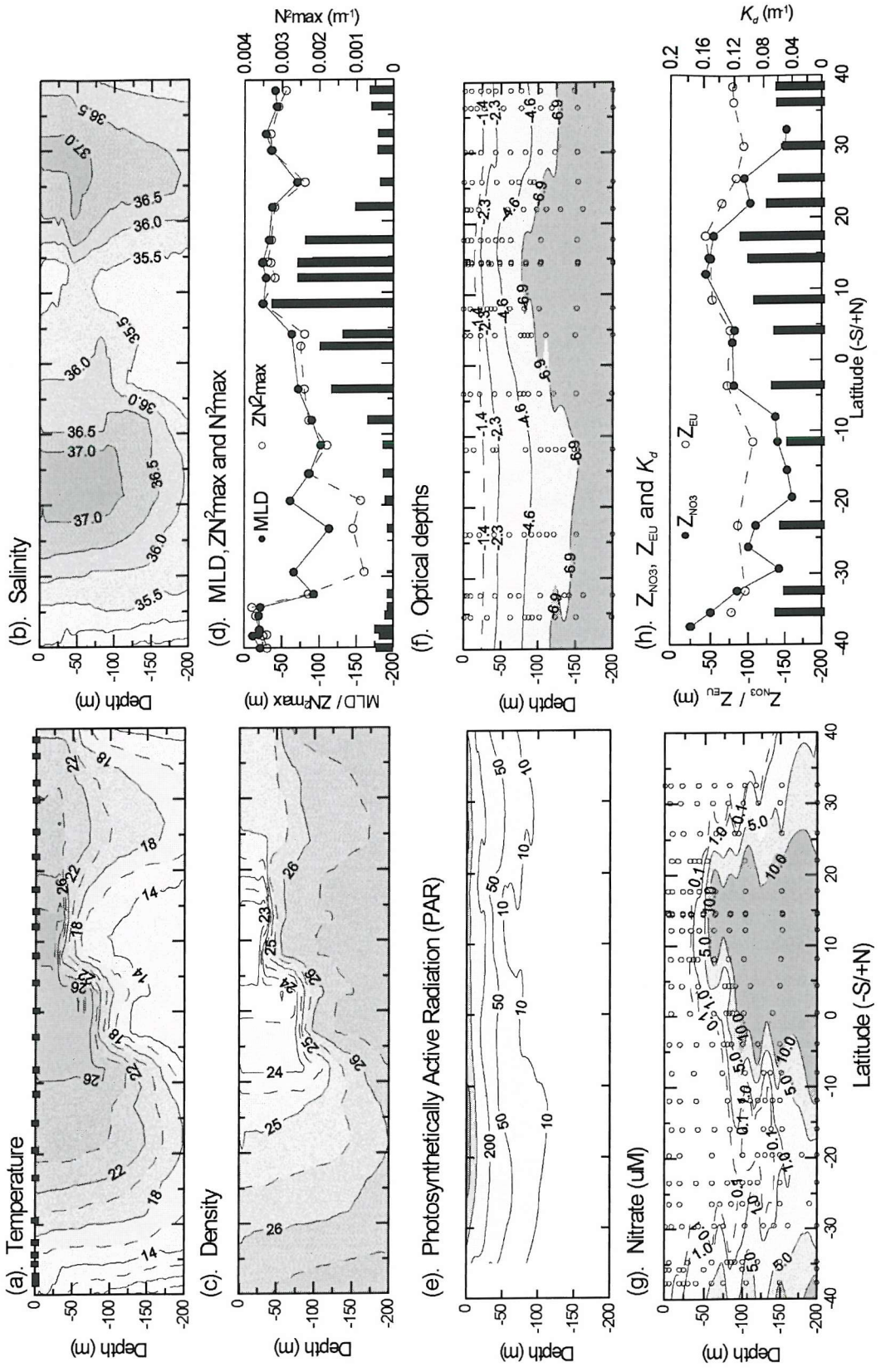


Fig. 3.1: Hydrographic characteristics from AMT7 (September, 1998); (a) Temperature (°C), (b) Salinity (psu), (c) Density (σt), (d) Mixed layer depth (MLD, closed circles), Depth of the Brunt-Vaisala frequency maximum ($ZN^2max$, open circles) and its value ($N^2max$, blocks), (e) Photosynthetically Active Radiation (PAR), (f) Optical depths (ξ; - 4.6 indicates 1% PAR isolume), (g) Nitrate concentration (μM), (h) Estimated depth the nitracline ($Z_{NO3}$ , closed circles), Euphotic Zone ($Z_{eu}$, open circles) and vertical attenuation coefficient for PAR ($K_d$, blocks; $m^{-1}$). Profiles for temperature, salinity, density and PAR were undertaken between 0 – 200 m at station positions indicated by black blocks on (a). Open circles indicate sampling depths for optical depth and nitrate concentration.

Around the equator and off NW Africa the isopycnals shallow (Fig. 3.1c) which indicates the upward movement of cold, high-density water from depth (i.e. upwelling). Upper mixed layer depths (MLD) and the depth of the Brunt - Väisälä frequency maximum ($ZN^2max$; thermocline) are also shallow around the equator (~75 m) and off NW Africa (~25 m), while the value of the Brunt - Väisälä frequency maximum ($N^2max$; water-column stability) is higher than in other areas of the Atlantic (Fig. 3.1d). A shallow MLD and thermocline are also observed at the northern and southern ends of the transect (~40°N/S), although the value of the $N^2max$ is lower than seen off NW Africa (Fig. 3.1d), indicative of a generally less stratified water-column (mixed).

Isopycnals, MLD and thermocline depths are shallow and at constant depths in northern subtropical waters, whereas in southern subtropical waters they are much deeper (Fig. 3.1c and d). These differences are partly due to the AMT cruise track; in the northern hemisphere the AMT cruise track passes through the edge of the subtropical gyre, whereas in the southern hemisphere the cruise track passes through the central gyre (see Fig. 2.1 in methods). In southern subtropical waters there are also pronounced differences in MLD and $ZN^2max$, which indicates that the depth of the maximum density gradient is deeper than the MLD (Fig. 3.1d).

### 3.2.2. Light and Nutrients

The vertical distribution of isolumes is based on calculations of the downwelling vertical light attenuation coefficient ($K_d$; see methods 2.7.2) which is relative to the exponential decrease of light with depth (Kirk, 1992; 1994). The depth of the euphotic zone ($Z_{eu}$) is commonly defined as the depth of 1% of surface irradiace (e.g. Falkowski and Raven, 1997). Latitudinal variations in $K_d$ and $Z_{eu}$ are presented for AMT-7 in Figure 3.1. The underwater light field of the subtropical and tropical Atlantic Ocean is characterised by a deep $Z_{eu}$ in the subtropical gyres (~100 m) and shallowing (50 - <75 m) of the $Z_{eu}$ around the equator and off NW Africa (Fig. 3.1e - h). Surface and subsurface waters (0 – 25 m) experience extremely high light levels (1000 - 2000 μM photons $m^{-2}$ $s^{-1}$, Fig. 3.1e; >25% PAR or >ξ -1.4; Fig. 3.1f). Such high irradiance levels may be photoinhibitory, although the absolute irradiance at which photoinhibition occurs is dependent upon the phytoplankton taxa present, nutrient conditions, the spectral qualities of the incidental irradiance and the degree of cloud cover (Falkowski and Raven, 1997).

The physical structure of the upper water-column (MLD, thermocline depth and water-column stability) is related to the availability of nitrate; shallow MLD and thermoclines coinside where there is a shallowing of the nitrate contours off NW Africa and around the equator (Fig. 3.1d, g and h). The relative distance between nutrient contours is roughly proportional to the gradient of nitrate flux into the upper water-column; where nitrate contours are relatively close (off NW Africa) nitrate fluxes are high, whereas when they are relatively distant (subtropical gyres) lower nitrate fluxes are experienced (Fig. 3.1g). The concentration of nitrate in upper waters (<100 m) of the subtropical gyres are very close to the detection limits of the micromolar techniques used in the AMT programme (i.e. 0.2 μM; Aiken *et al.*, 2000), which is another indication of the depleted nitrate status of these waters (i.e. oligotrophic). Shallowing of the nutrient contours is also observed at the southern end of the transect (Fig. 3.1g),

and is associated with the South American continental shelf, River Plate and southern subtropical convergence. A comparison of the estimated depth of the nitracline ($Z_{NO3}$) and the distribution of nitrate contours shows the distribution of the two is related (Fig. 3.1g and h); shallow off NW Africa (~50 m) and around the equator (~75 m), and deep in the northern and southern subtropical gyres (~150 m). However, it should be noted that the depth of the nitracline does not indicate the absolute nitrate concentrations or give an indication of the nitrate gradient.

### 3.3. Regionality of the Hydrographic Environment: Cluster Analysis of AMT-7 Data

Regional variability of the hydrographic environment during AMT-7 is clear from the previous section, and this section investigates the existence of statistically distinct regions through multivariate analysis of several hydrographic parameters. Cluster and non-metric Multidimensional Scaling (MDS) analysis of environmental data are based on a Normalised Euclidean Distance with no transformation of the data, default options in the PRIMER program (see methods 2.6.1) and following the recommendations of Clarke and Warwick (1994). Two types of analysis have been carried out; (1) MDS1: Basic analysis of water-column parameters (UMD, ZEUP, $ZNO_3$), and (2) MDS2: Analysis of four hydrographic parameters (temperature, salinity, optical depth and nitrate concentration) at 6 depths (7, 20, 50, 100, 150 and 200 m). The MDS ordinations for the two analyses with the sample clusters from the cluster dendrogram (not presented for clarity) are shown in Figure 3.2.

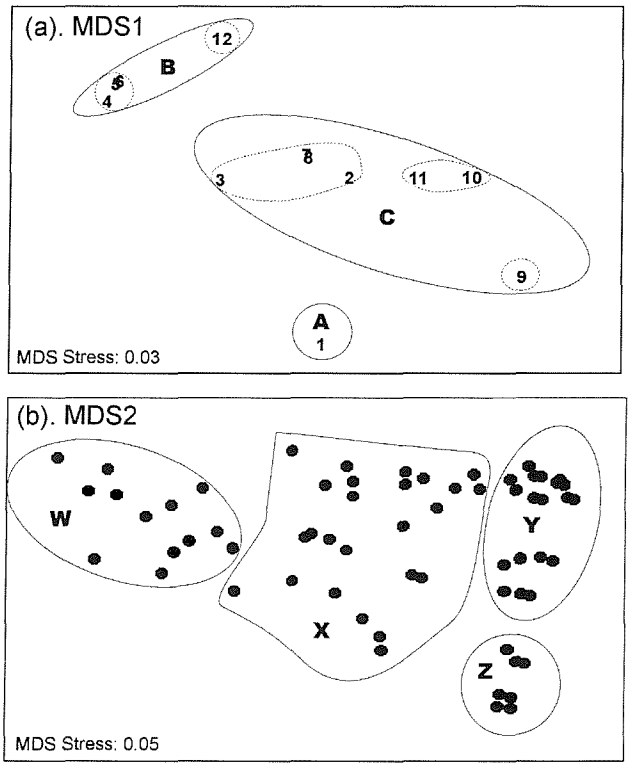


Fig. 3.2: MDS ordinations from analysis of AMT7 hydrographic parameters; (a) MDS1, and (b) MDS2. Superimposed on plots are groups identified from Cluster analysis at a Normalised Euclidean Distance of 2 (solid lines) and 1.5 (dashed lines). Station numbers are identified on (a), however the data points on (b) are not presented.

### 3.3.1. Analysis of Water-Column Parameters (MDS1)

The MDS ordination and Cluster diagram for MDS1 show separation at a Normalised Euclidean Distance of 2.0 into three major station groups (Fig. 3.2; Table 3.1). The MDS stress is low (<0.1) indicating good representation of the data and is likely to be due to the low level of the dimensional picture (3 variables). Further separation into sub-groups occurs at a Normalised Euclidean Distance of 1.5 and leads to six groups (Table 3.1). These results indicate dissimilarity between environments in several regions of the tropical and subtropical Atlantic Ocean (Table 3.1, Fig. 3.3); high dissimilarity of station 1 (30.0°N) from all other stations, high similarity between stations off NW Africa (4, 5 and 6) and station 12 (-35.5°S), and high similarity between stations in the northern (2 and 3) and southern subtropical waters (7 - 11). Further separation of stations into six groups is limited to subtropical waters (Table 3.1, Fig. 3.3), with high similarity between stations in the northern subtropical gyre (2 and 3) and stations around the equator (7 and 8), and separation of the other southern subtropical stations into a central group (9) and a southern subtropical group (10 and 11).

Table 3.1: Cluster and MDS results from analysis of AMT-7 station hydrographic parameters (MLD, $Z_{eu}$ and $Z_{NO3}$) at two different levels of dissimilarity; Normalised Euclidean Distance (NED) of 2 and 1.5.

| Station Number | Latitude (N / S) | MLD (m) | $Z_{eu}$ (m) | $Z_{NO3}$ (m) | Groups (NED: 2) | Groups (NED: 1.5) |
|---|---|---|---|---|---|---|
| 1 | 30.0°N | 36.6 | 93.1 | 150.0 | A | A |
| 2 | 25.5°N | 70.4 | 82.9 | 94.0 | B | B1 |
| 3 | 22.0°N | 36.9 | 63.7 | 102.0 | B | B1 |
| 4 | 17.4°N | 32.7 | 42.6 | 53.0 | C | C2 |
| 5 | 14.4°N | 24.4 | 47.0 | 48.0 | C | C2 |
| 6 | 14.2°N | 23.6 | 49.1 | 48.0 | C | C2 |
| 7 | 4.2°N | 63.1 | 74.9 | 81.0 | B | B1 |
| 8 | -3.6°S | 72.0 | 71.3 | 80.0 | B | B1 |
| 9 | -11.6°S | 101.9 | 106.0 | 140.0 | B | B2 |
| 10 | -23.3°S | 113.2 | 85.7 | 110.0 | B | B3 |
| 11 | -32.4°S | 92.9 | 96 | 85.0 | B | B3 |
| 12 | -35.5°S | 19.4 | 77.3 | 50.0 | C | C1 |

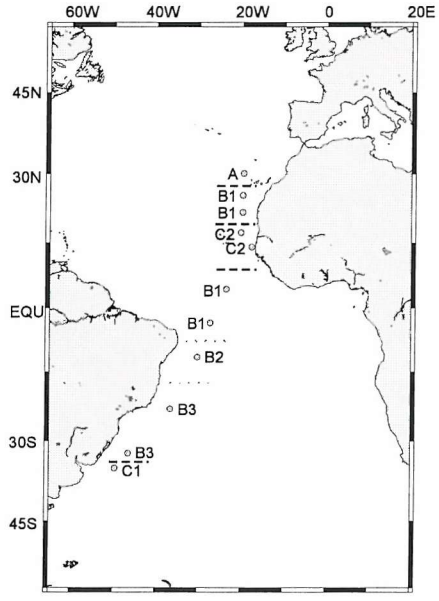


Fig. 3.3: Positions of the station clusters idenfied through cluster and non-metric MDS (Fig. 3.2a) of station mixed layer depths (MLD), euphotic depths ($Z_{eu}$) and nitracline depths ($Z_{NO3}$). See Table 3.1 for further details. Map produced using Online Map Creation (GMT) software (http://www.aquarius.geomar.de/omc/omc_intro.html).

### 3.3.2. Analysis of Parameters at Several Depths (MDS2)

Table 3.2: Cluster and MDS results from analysis of AMT-7 hydrographic parameters (temperature, salinity, optical depth and nitrate concentration) from six depths. Shading is used to highlight the distribution of group Y and W.

| Station Number | Latitude | 7m | 20m | 50m | 100m | 150m | 200m |
|---|---|---|---|---|---|---|---|
| 1 | 30.0°N | Y | Y | Y | X | X | X |
| 2 | 25.5°N | Y | Y | Y | X | X | X |
| 3 | 22.0°N | Y | Y | Y | X | X | X |
| 4 | 17.4°N | Y | Y | X | W | W | W |
| 5 | 14.4°N | Z | Z | X | W | W | W |
| 6 | 14.2°N | Z | Z | X | W | W | W |
| 7 | 4.2°N | Z | Z | Z | X | W | W |
| 8 | -3.6°S | Y | Y | Y | X | W | W |
| 9 | -11.6°S | Y | Y | Y | Y | X | X |
| 10 | -23.3°S | Y | Y | Y | X | X | X |
| 11 | -35.5°S | X | X | X | X | X | X |

The MDS ordination and Cluster diagram for MDS2 shows separation at a Normalised Euclidean Distance of 2.0 (Fig. 3.2), which corresponds to a classification of the AMT-7 depths into 4 groups (Table 3.2). MDS stress is low (<0.1) which indicates that a good representation of the data is available and is likely to be due to the low level of the dimensional picture (6 variables). If the groupings are superimposed on a depth matrix (Table 3.2) hydrographic conditions are seen as a layered system. This layering relates to all the variables (see Fig. 3.1); group W represents the upwelling of cold, saline, nutrient-rich waters with low light levels, group Z represents high temperature and low salinity water with intermediate light and nutrient conditions, group Y represents high temperature and hypersaline waters of the subtropical gyres with high light and low nutrients, and group X represents 'warm' saline deeper waters with intermediate nutrient and light conditions.

## 3.4. Seasonal and Interannual Variability of the Hydrographic Environment: AMT-1 - 10

### 3.4.1. Seasurface Temperature, Salinity and Density

Surface (15 m) values of temperature, salinity and density are presented from all the AMT cruises in seasonal cruise groupings in Figure 3.4. Intercruise differences in seasurface temperature (SST) are related to seasonal changes; SST during September cruises are higher in the northern hemisphere and lower in the southern hemisphere than during May cruises (Fig. 3.4a). Seasonal differences in SST are ~2.5°C in the tropics and up to 5°C in mid-latitudes (Fig. 3.4a; Aiken *et al.*, 2000). Intercruise SST differences within seasonal cruise groups are higher during May cruises than September cruises; May cruise SSTs vary by as much as 1°C in northern and southern hemisphere waters (Fig. 3.4a).

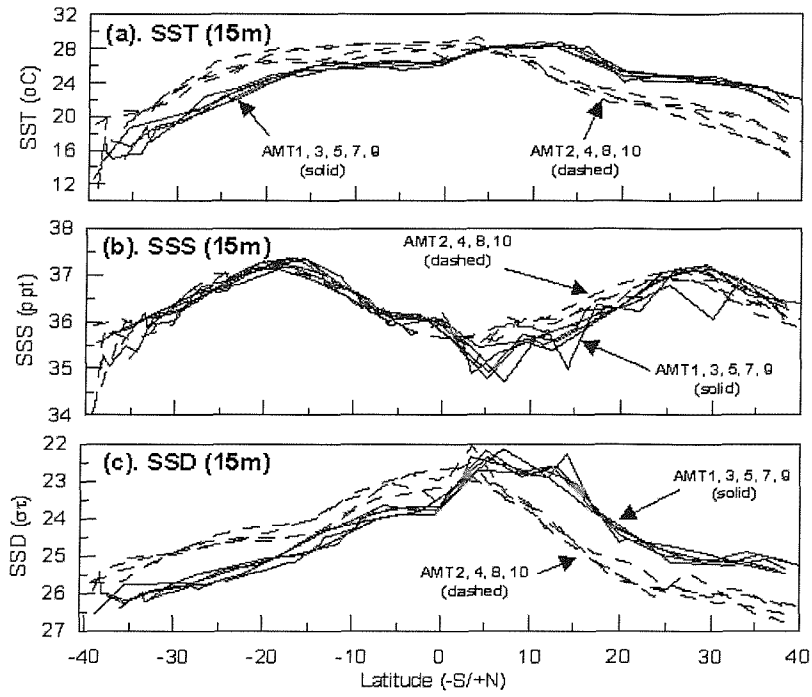


Fig. 3.4: Seasurface (15 m) temperature (SST; a), salinity (SSS; b) and density (SSD; c) for all the AMT cruises. September cruises (AMT-1, 3, 5, 7 and 9) indicated by solid line and May cruises (AMT-2, 4, 8, and 10) indicated by dashed line.

Intercruise differences in seasurface salinity's (SSS) in subtropical waters are small, with evidence of seasonal differences restricted to waters off NW Africa (5 - 20°N; Fig. 3.4b). Seasonal differences in SSS are likely to be related to the movement of the Inter-Tropical Convergence Zone between 6°N (November - April) and 15°N (August) (Longhurst, 1998), although the AMT cruises are likely to find the Inter-Tropical Convergence Zone in transition. Intercruise differences in SSS were found on AMT-9 at ~30°N, AMT-7 at ~14°N, during several September and May cruises ~5°N, and ~35 - 40°S (Fig. 3.4b). Variations during AMT-7 are related to a deviation of the cruise track into inshore waters off Dakar (NW Africa) and are therefore likely to be due to increased riverine input. Variations ~5°N are likely to be due to Amazon River input from the western Equatorial Atlantic that has been entrained in the Northern Equatorial Counter Current and is usually observed during September (Muller-Karger *et al.,* 1988). Differences ~35 - 40°S are likely to be due to the influence of the River Plate riverine inputs from Uruguay and the subtropical convergence (Aiken *et al.,* 2000). Patterns of seasurface density (SSD; Fig. 3.4c) are related to regional changes in the importance of SST and SSS in determining density; around the equator and off NW Africa seasonal and annual changes in SST and SSS cause changes in SSD, while in the subtropical gyres fluctuations of SST are more important in determining changes in SSD.

### 3.4.2. Depth of the 26.0σt Isopycnal

Intercruise and seasonal variations in the water-column structure are investigated in this section by seasonal and intercruise comparison of the depth of the 26.0 σt density isopycnal. Figure 3.5 presents the depth of the 26.0 σt isopycnals during all the AMT cruises, and shows a regular pattern; shallow in

the northern hemisphere and deeper around the equator and southern subtropical gyre, and shallow again at the southern end of the transect (Fig. 3.5). Throughout most of the subtropical and tropical Atlantic Ocean there is little evidence of either seasonal or interannual variability apart from at the latitudinal ends of the transect (Fig. 3.5); during September cruises the 26.0 σt isopycnal is at, or near, the surface at the southern end of the transect and at a depth of around 50 m in northern waters (Fig. 3.5a), whereas during May cruises the 26.0 σt isopycnal is at, or near, the surface from 20 - 40°N in the northern hemisphere and subsurface or around a depth of 100 - 150 m from 35 - 40°S in the southern hemisphere (Fig. 3.5b). During the AMT-10 cruise the depth of the 26.0 σt isopycnal south of 5°S was slightly shallower (10 - 50 m) than during previous cruises (Fig. 3.5b).

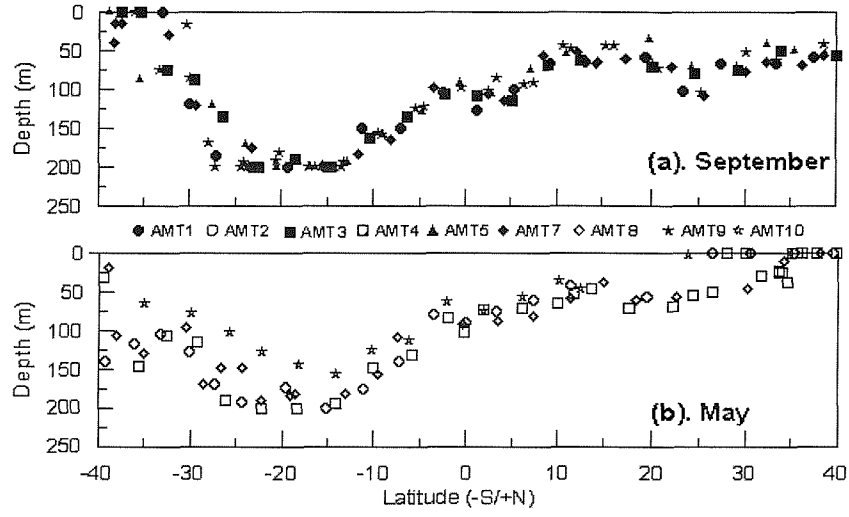


Fig. 3.5: Depth of 26.0 σt isopycnal; (a) September cruises, and (b) May cruises. Figure contains key to the individual cruise data points.

### 3.4.3. Upper Mixed Layer Depths (MLD) and the Brunt - Väisälä Frequency ($N^2$max)

Further seasonal and interannual variations in the water-column structure are analysed with regard to the depth of the upper mixed layer (MLD) and thermocline (indicated by the depth of the Brunt-Väisälä frequency maximum). MLD, depth of the Brunt-Väisälä frequency maximum and the value of the maximum are presented for all AMT cruises, with seasonal cruise groupings, in Figure 3.6 and 3.7. MLD are around 25 - 50 m in the northern hemisphere, with slight decreases off NW Africa (~25 m) and deepening around the equator (~50 - 100 m) and in the southern subtropical gyre (50 - >150 m; Fig. 3.6). MLD in the South Atlantic Ocean (10 - 30°S) and around the equator (5°N - 10°S) show seasonal and interannual variations, with interannual variability observed during September cruises (Fig. 3.5). MLD in the South Atlantic Ocean and around the equator are generally higher during September cruises, although there is a large amount of interannual variability (50 - >150 m), whereas UMD in the South Atlantic during May cruises are typically 50 - 75 m throughout the tropical and subtropical Atlantic Ocean (Fig. 3.6). Shallow September MLD (<50 m) are seen in the South Atlantic Ocean during AMT-3, 5 and at a few stations during AMT-7, whereas MLD during other AMT cruises are much deeper (>75 m; Fig. 3.6a).

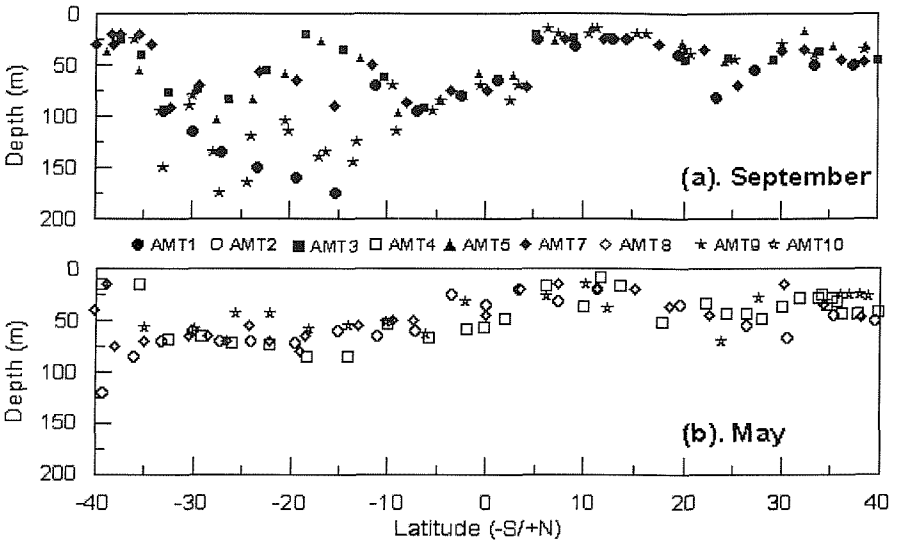


Fig. 3.6: Depth of the upper mixed layer from density measurements (MLD); (a) September cruises, and (b) May cruises. Figure contains key to the individual cruise data points.

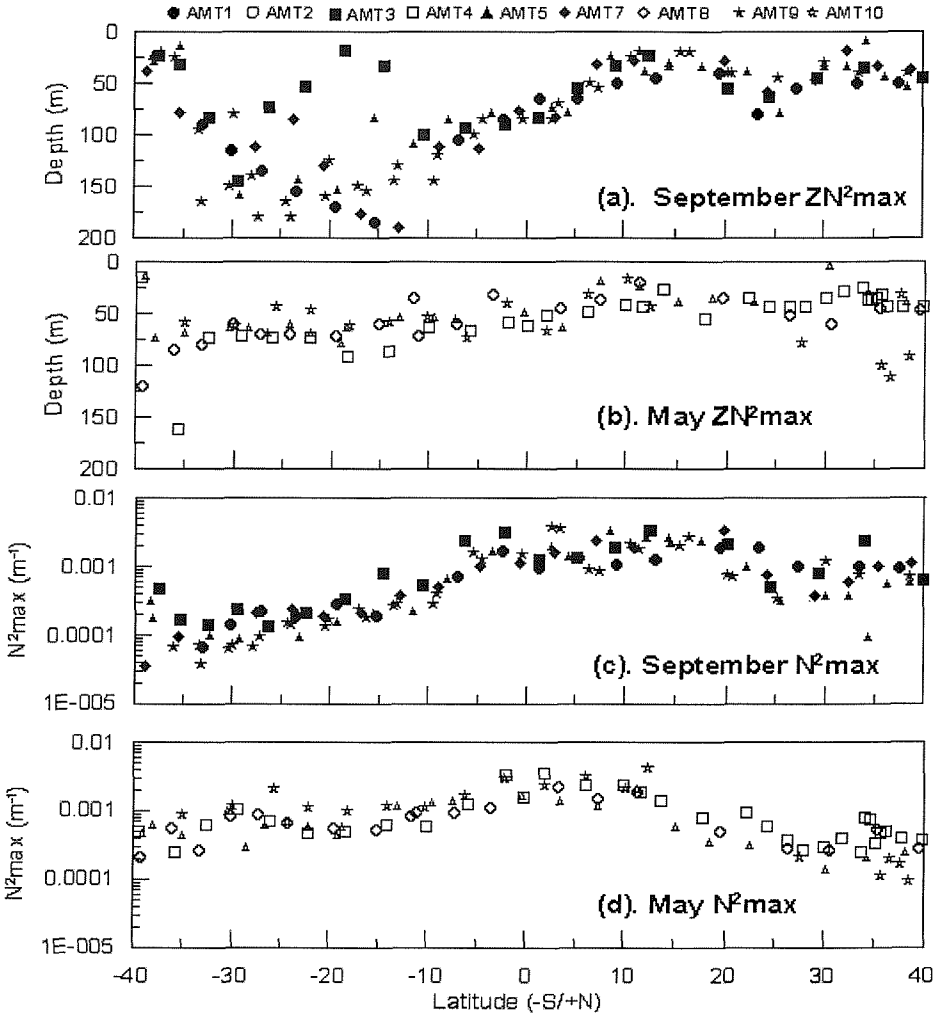


Fig 3.7: Depth of the Brunt - Väisälä frequency maximum ($ZN^2max$) and its value ($N^2max$); (a) September $ZN^2max$, (b) May $N^2max$, (c) September $N^2max$ values, and (d) May $N^2max$ values. Figure contains key to the individual cruise data points and are identical to Fig. 3.5.

The distributions of MLD and depth of the Brunt - Väisälä frequency maximum ($ZN^2max$) are very similar both spatially and temporally (Fig. 3.6 and 3.7); $ZN^2max$ for AMT-3, 5 and 7 are shallower than those for other AMT cruises during September in the South Atlantic Ocean (Fig. 3.6a). Maximum values for the density gradient ($N^2max$) were found off NW Africa and around the equator, whereas relatively low values were observed in the subtropical gyres and in association with waters at either end of the transect (Fig. 3.7c and d). Seasonal variability of the $N^2max$ values show that September cruises have lower values in the southern hemisphere and higher values in the northern hemisphere, while May cruises represent the reverse (Fig. 3.7c and d). Seasonal variations in $N^2max$ are also found in the equatorial Atlantic and off NW Africa, with high values from 0 - 20°N during September cruises and restricted to 0 - 10°N during May cruises (Fig. 3.7c and d). There is no evidence of large-scale interannual variations of the $N^2max$ value during any of the September or May cruises, although some of the AMT-3 and 10 values are slightly higher (Fig. 3.7c and d).

### 3.4.5. Vertical Attenuation Coefficient ($K_d$) and Euphotic Zone Depth ($Z_{eu}$)

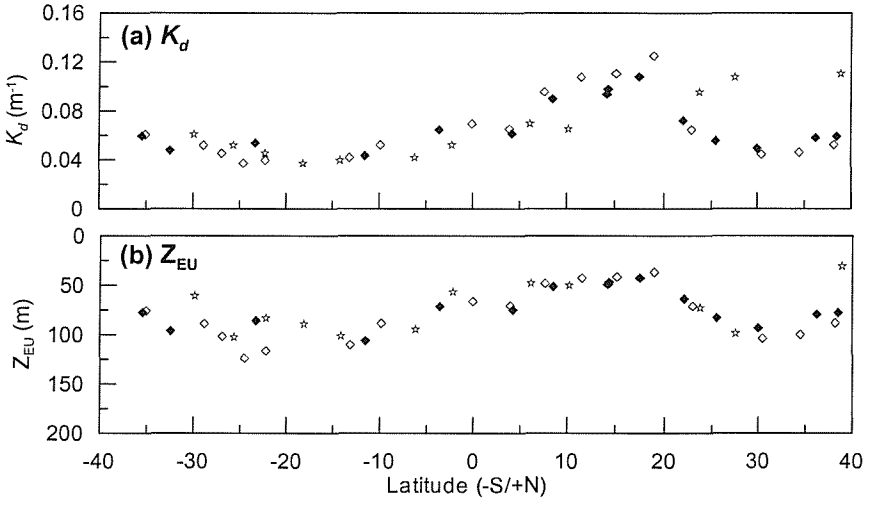


Fig. 3.8: Characteristics of the underwater light field during AMT-7, 8 and 10; (a) Vertical attenuation coefficient ($K_d$), and (b) Euphotic zone depth ($Z_{eu}$). Note parameters not separated for season, although key for individual cruises is identical to previous figures (closed diamonds are AMT-7, open diamonds are AMT-8 and open stars are AMT-10).

The analysis of intercruise and seasonal variations in the light environment in the subtropical and tropical Atlantic Ocean are limited to three cruises; AMT-7 (September, 1998), 8 (May, 1999) and 10 (May, 2000). Measurements of $K_d$ and $Z_{eu}$ (depth of 1% surface irradiance) are presented from these three cruise in Figure 3.8. $K_d$ and $Z_{eu}$ show similar trends for all three cruises; low $K_d$ and deep $Z_{eu}$ in the subtropical gyres and high $K_d$ and shallow $Z_{eu}$ around the equator and off NW Africa (Fig. 3.8). There is no evidence of any significant seasonal or interannual differences in either $K_d$ or $Z_{eu}$ during AMT-7, 8 and 10. Intercruise similarities in $K_d$ indicate that surface waters experience extremely high irradiances; around the equator and off NW Africa surface irradiances are typically 47 - 55% PAR, and 70 - 85% PAR in the subtropical gyres (Fig. 3.1 and 3.8).

### 3.4.6. Nitracline Depth ($Z_{NO3}$) and Relationship to the other Nutriclines

Analysis of seasonal and interannual variations in the nutrient environment of the tropical and subtropical Atlantic Ocean are limited to five cruises; AMT-1 (September, 1995), 2 (May, 1996), 3 (September, 1996), 4 (May, 1997) and 7 (September, 1998). The estimated depth of the nitracline ($Z_{NO3}$) from these cruises and the relationships between the nitracline and the other nutriclines are presented in Figure 3.9. $Z_{NO3}$ for AMT-1, 2, 3, 4 and 7 show similar trends; deep $Z_{NO3}$ in the subtropical gyres (~100 - 200 m) and shallow around the equator (~75 m) and off NW Africa (~50 m; Fig. 3.9a). There is little evidence for major seasonal or interannual variability of the $Z_{NO3}$ (Fig. 3.9a), although the nitracline in the subtropical waters of both the South (~20 - 25°S) and North (~25 - 35°N) Atlantic Ocean vary by between 50 - 100 m during several cruises (Fig. 3.9). However, such intercruise variability is more likely to be related to differences in sampling depths rather than real differences (see methods 2.7.1 for details of the estimation of the $Z_{NO3}$ and other nutriclines). Significant relationships exist between the estimated depth of the nutriclines from AMT-1 - 4, with the phosphocline ($Z_{PO4}$) and siliocline ($Z_{SiO2}$) generally found at the same depth as the nitracline (Fig. 3.9c, d). The relationships between different nutriclines and the nitracline are described by the following Model II regression equations;

$$Z_{NO2} = 0.73 * Z_{NO3} + 18.1 \; (r = 0.853, p<0.005, n = 74)$$

$$Z_{PO4} = 0.95 * Z_{NO3} + 6.0 \; (r = 0.943, p<0.005, n = 74)$$

$$Z_{SiO2} = 0.94 * Z_{NO3} + 1.9 \; (r = 0.887, p<0.005, n = 74)$$

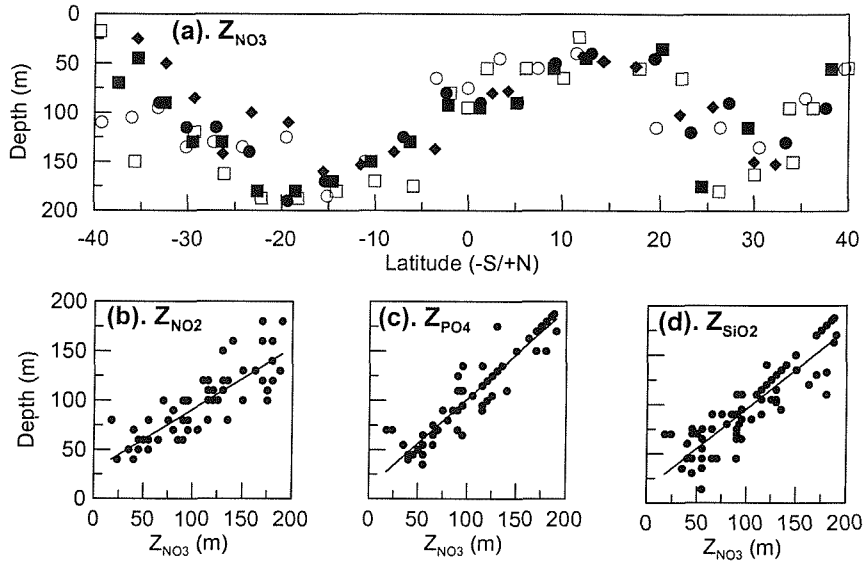


Fig. 3.9: Estimated nitracline depth and relationship to other nutriclines; (a) latitudinal depth distribution of nitracline depth ($Z_{NO3}$), (b) relationship between $Z_{NO3}$ and nitrite maximum depth ($Z_{NO2}$), (c) relationship between $Z_{NO3}$ and phosphocline depth ($Z_{PO4}$), and (d) relationship between $Z_{NO3}$ and siliocline depth ($z_{SiO2}$). Note: on (a) $Z_{NO3}$ is not separated by season, although key for individual cruises identical to previous figures; AMT-1 data are closed circles, AMT-2 are open circles, AMT3 are closed squares, AMT-4 are open squares and AMT-7 are closed diamonds.

The slope of the regression line is less for the relationship between the nitrite maximum depth ($Z_{NO2}$) and $Z_{NO3}$ (i.e. 0.73) which indicates that there is a different relationship between these two than

the other nutriclines; shallow $Z_{NO3}$ and $Z_{NO2}$ are near the same depth whereas with increasing $Z_{NO3}$ the $Z_{NO2}$ is found at shallower depths, with the relative depth difference increasing with increasing $Z_{NO3}$ depth (Fig. 3.9b). Significant relationships between the depths of the nitracline and other nutriclines indicate that the depth of the nitracline can be used as a proxy for the depth of the other nutriclines, although there are periods when the relationship is not as linear.

## 3.5. Discussion

### 3.5.1. Regionality of the Hydrographic Environment

The hydrographic environment in the open ocean regulates the growth and survival of phytoplankton, by controlling the availability of light and nutrients. Spatial variability of the hydrographic conditions are not restricted to latitudinal (regional) differences as there are also important vertical differences; conditions found throughout the water-column in one region may be replicated elsewhere within a smaller and deeper portion of the water-column (Table 3.2). Separation of the water-column into different environmental layers with different hydrographic parameters is shown by multivariate statistical analysis (Table 3.2) and will have important consequences for phytoplankton communities in tropical and subtropical waters. In subtropical waters, such layering can be simplified into a 2-layer model (first proposed by Dugdale and Goering, 1976); an upper nutrient-poor and light-rich layer and a deeper nutrient-rich and light-poor layer. At the basinscale the upward nutrient fluxes will control the vertical extent of these two layers. In tropical waters experiencing upwelling of nutrients into the euphotic zone, the 2-layered system will be modified into an upper nutrient-rich and light-rich layer and a deep nutrient-poor and light-poor layer. In equatorial waters, the multivariate analysis (Table 3.2) indicates a third (middle) layer; so that this 3-layer system is likely to include an upper nutrient-poor and light-rich layer, a middle layer of intermediate conditions (relatively nutrient- and light-rich) and a deep layer of nutrient-rich and light-poor waters. Surface waters throughout the subtropical and tropical Atlantic Ocean are likely to be characterised by photoinhibition due to the excessive incidental irradiances experienced (>1000 μM photons $m^{-2}$ $s^{-1}$; Fig. 3.1e; Bishop and Rossow, 1991). The depth to which photoinhibition occurs is likely to increase in subtropical waters due to lower vertical attenuation coefficients and higher light penetration (Figs. 3.1 and 3.7).

The spatial variability of the hydrographic conditions can be basically described by six regions that relate to the dominant physical processes and previous hydrological analysis of AMT hydrographic data by Hooker et al. (2000), although they are not identical (Fig. 3.10). The six regions are (Fig. 3.10b) (1) North Atlantic Drift (35 - 40°N; NATD), (2) North Atlantic Subtropical Waters (20 - 35°N; NASW), (3) Upwelling waters off NW Africa (5 - 20°N; UPW), (4) Equatorial Atlantic (5°N - 5°S; EQU), (5) South Atlantic Subtropical Waters (5 - 30°S; SASW) and (6) South Atlantic Temperate Waters (30 - 40°S; SATW). Mixing processes in these regions will differ between seasonally mixed and stratified areas (NATD, SATW) and permanently stratified areas (NASW, EQU and SASW). Episodic upwelling events in UPW will cause temporally variable mixed and stratified periods that are similar to the conditions found in seasonally variable regions (Cullen, 1982). NATD, SATW and UPW

will experience mixed conditions due to wind mixing and in the case of UPW, upwelling and the onset of stratification from solar heating. Areas of permanent stratification are maintained due to the low amplitude of seasonal differences in heating which prevents winter turnover (Hooker *et al.,* 2000). In such regions the upper mixed layer is formed and maintained by diurnal differences in temperature, which causes convectional mixing, as well as episodic wind events such as storms (Longhurst, 1988; Hooker *et al.,* 2000).

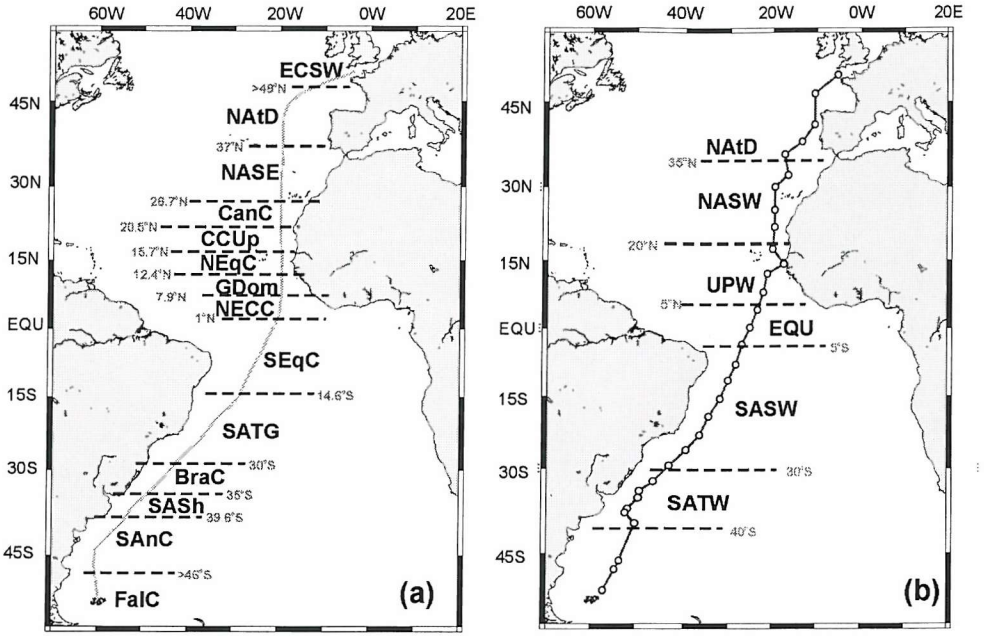


Fig.3.10: Hydrographic provinces in the subtropical and tropical Atlantic Ocean; (a) Hydrographic provinces proposed by Hooker *et al.,* (2000) after analysis of density characteristics, and (b) provinces used for the analysis of spatial variability within this study. The latitudinal boundaries of each province are indicated with dashed lines and text. A generic AMT cruise track is superimposed on (a) while (b) presents the AMT cruise track and station positions (open circles). Maps produced using Online Map Creation (GMT) software (http://www.aquarius.geomar.de/omc/omc_intro.html).

Light and nutrient conditions also vary between the regions identified (Figs. 3.1, 3.8 and 3.9) with high light and nutrient conditions found year-round in UPW and seasonally during alternative times in NATD and SATW. Within the NASW and SASW nutrients are at very low concentrations in upper waters (<100 m) while nutrient rich waters and low light conditions are found at depth (Fig. 3.1). The EQU is an intermediate situation with high light levels and relatively high nutrient concentrations compared to the subtropical gyres (Figs. 3.1, 3.8 and 3.9). Nutrient conditions in EQU are also likely to fluctuate due to seasonal upwelling of deep nutrient rich water as a result of the divergence of the Trade winds on the upper ocean (Longhurst, 1993) and seasonal changes in the strength of the Equatorial Undercurrent and South Equatorial Current (Monger *et al.,* 1997 and references therein). Enhancement of the high nutrient conditions in EQU could also come from western Amazon plume inputs and from the east by the advection of nutrient-rich Benguela upwelling waters (Boltovskoy, 1999). Seasonality of the source water for upwelling in the vicinity of the equator also determines the nutrient concentrations available (Kinkel *et al.,* 2000 and references therein).

The upwelling signals seen during AMT cruises are likely to be caused by filaments of upwelled water being advected offshore from the upwelling cells close to the NW Africa coast, rather

than independent upwelling cells (Hooker *et al.,* 2000; Maranon *et al.,* 2001). The full extent and magnitude of upwelling is dependent upon regional factors, including upwelled source water and bottom topography (Longhurst and Pauly, 1987; Longhurst, 1998). Regional bottom topography can cause localised upwelling (Metzler *et al.,* 1997) or can limit the magnitude of the algal community response; strong inshore mixing off the coast of NW Africa often extends to the continental shelf and restricts the productivity of the onshelf phytoplankton community (Wooster *et al.,* 1976; Barton *et al.,* 1977; Longhurst, 1998). The UPW includes upwelling off Mauritania (termed Canary Current Upwelling by Hooker *et al.,* 2000; Fig. 3.10) and the seasonal uplift of the thermocline around the Guinea Dome (~12°N, ~22°W; Signorini *et al.,* 1999).

Within the NASW and SASW, inorganic nutrient concentrations are extremely low with the nutriclines deep in the water- column (>100 m) and often well below the depth of the euphotic zone (1% PAR; Figs. 3.1, 3.8 and 3.9). There is also evidence that riverine inputs of phosphate from the Amazon and Orinoco rivers in Central America have a high degree of influence on the seasonal cycle of phosphate in the tropical equatorial Atlantic and the western part of the Sargasso Sea (Conkright *et al.,* 2000). In the subtropical gyres of the Atlantic Ocean there is a deficit between the upward flux of nitrate and the phytoplankton community nitrate requirements which indicates important roles for alternative methods of nitrate input; e.g. pulsed nutrient fluxes due to wind field variations, internal waves and inputs from the atmosphere (Planas *et al.,* 1999). Low concentrations of new nutrients (<0.1 μM) in upper waters also indicates the importance of regenerated nutrients and regenerated production, with estimates of ammonia based primary productivity up to 90% of the total productivity in the upper water-column (Probyn, 1987). Likely sources of regenerated nutrients include nano- and micro-zooplankton (Probyn, 1987), although larger zooplankton may also be important (Biggs, 1977).

### 3.5.2. Regional Interannual and Seasonal Variability

The AMT cruises have sampled both the boreal (northern) and austral (southern) hemispheres in alternative states of late winter and late summer. May cruises sampled during the boreal spring and austral fall, whereas September cruises sampled the boreal fall and the austral spring. Intercruise periods include the South Atlantic winter/North Atlantic summer (June - August) and the South Atlantic summer/North Atlantic winter (October - March). Thus, there is very little seasonal resolution in the AMT sampling program (Aiken *et al.,* 2000), however the regular timing of the cruises roughly coincide with the seasonal equinoxes, which means that sampling has been carried out regularly at two distinct seasons in each hemisphere at almost identical times of the year.

Most of the temporal variability in the hydrographic parameters can be explained in terms of the seasonal changes in the regional heat budget with boreal spring cruises experiencing higher seasurface temperatures and densities in the northern hemisphere and post-winter conditions in the southern hemisphere. Seasonal variations in the heat budget and wind patterns cause variations in the degree of stratification and the vertical water-column structure with MLD stable during post-summer conditions in southern subtropical waters and the pycnocline representing a stronger density gradient. However, in the SASW (5 - 30°S), the post winter MLD are highly variable and examination of the individual density profiles (Fig. 3.11) shows that this variability is most pronounced in the central

area of the SASW (15 - 20°S). Such variability may be due to differences in the onset of seasonal heating although no large-scale differences in the absolute values of SST or SSD, or in the values of the density profiles are evident (Fig. 3.11; c.f. Fig. 3.4). Another possibility is that the degree and length of winter mixing in the South Atlantic Ocean may vary interannually or there may have been increased frequency of storm events preceding AMT-1 and AMT-9. A preliminary examination of variations in the wind speeds at two latitudes in the South Atlantic Ocean (20°W, 10°S and 20°W, 20°W; Fig. 3.10) from reprocessed NOAA satellite data indicates a lack of increased wind speeds associated with November 1997 - February 1998 that are present during other years (Fig. 3.12). These observations coincide with a strong El-Nino-Southern-Oscillation event in the Pacific Ocean, which through climatic linkage ("teleconnections") influences the climatic conditions in the South Atlantic Ocean (Elliott *et al.*, 2001). Further discussion of the temporal variability in the SASW is provided in Chapter 5 with reference to temporal trends in the phytoplankton community.

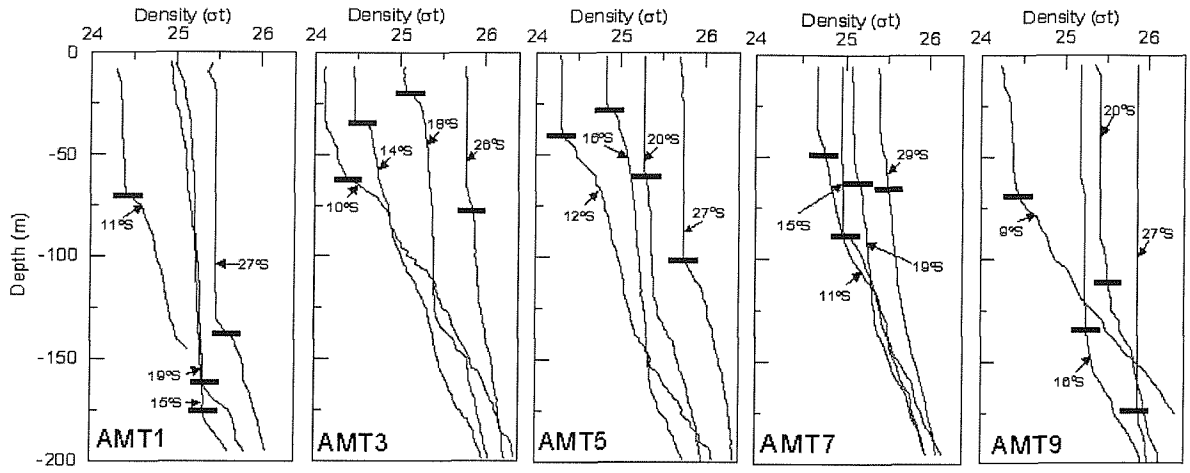


Fig. 3.11: Density (σt) profiles for anomalous MLD (see text) for selected stations from AMT-1, 3, 5, 7 and 9. Thick solid bars indicate calculated MLD, with latitudes of individual profiles indicated by solid arrows and text.

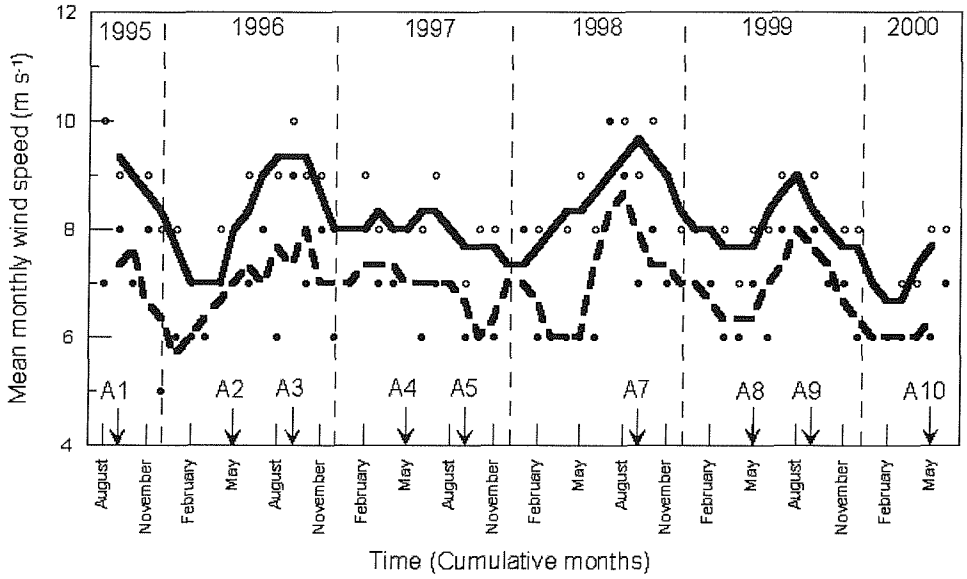


Fig. 3.12: Three-point running average (thick lines) of mean monthly wind speeds (m/s) from 1995 - 2000 at two latitudes in the South Atlantic Ocean; open circles (solid line) from 20°W 10°S and closed circles (dashed line) from 20°W 20°S. Data provided by the NOAA-CIRES Climate Diagnostic Centre, Boulder, Colorado (http://www.cdc.noaa.gov/).

There is little evidence of temporal variability of nutrient and light conditions in the tropical and subtropical Atlantic Ocean (Figs. 3.8 and 3.9), although the dataset is much smaller compared to the

other hydrographic parameters. The UPW and EQU have shallow nitraclines during both September and May cruises (Figs. 3.8 and 3.9) that indicates that along the AMT transect these areas have elevated nutrient inputs during both austral spring and boreal fall. Nutriclines in the SASW and NASW are typically deep during both sets of cruises with slight variations in depth (Figs. 3.8 and 3.9) probably more indicative of different sampling regimes than real differences. Within the NATD and SATW there are indications of seasonal changes in nitracline depth (Figs. 3.8 and 3.9) with the onset of stratification and winter mixing although the nutrient data is inadequate to fully investigate such trends.

Seasonal changes in the incidental light regime of the Atlantic Ocean are minimal near the equator and increase with increasing latitude (Kirk, 1992). Inter-seasonal differences in daily irradiance are likely to be highest between 30 - 40°N/S and lowest around the equator (Kirk, 1992), although the movement of the cloud belt associated with the Inter-Tropical Convergence Zone may also effect this relationship. Therefore, within tropical systems short day-to-day variability is unlikely and phytoplankton communities will experience similar incidental light regimes (Bishop and Rossow, 1991), whereas communities in subtropical waters will experience slight seasonal differences in irradiance. The timing of the AMT cruises around the summer maximum insolation periods for both hemispheres (June in north, December in south) leads to a lack of any strong evidence of seasonal or interannual variations in the underwater light field (see Kirk, 1992); Maranon *et al.,* (2000) tested for seasonal and interannual differences in the surface incidental irradiance during AMT-1-3 and found no significant differences between years or seasons.

## 3.6. Summary and Conclusions

1. Multivariate statistical (Cluster) analysis of the statistical similarities (Bray-Curtis similarity index) of station hydrographic parameters for AMT-7 (September, 1998) reveals clustering of station into several distinct hydrographic regions (Fig. 3.3). These regions are related to, although not identical with, the hydrographic provinces proposed by Hooker *et al.,* (2000) based on analysis of surface hydrographic measurements from earlier AMT cruises (Fig. 3.10a). The station clusters include (Fig. 3.3); (i) (new) nutrient depleted subtropical gyres of the north (2 stations at 22.0°N and 25.5°N) and south (5 stations between 4.2°N and 32.4°S) Atlantic Ocean, (ii) (new) nutrient rich waters off NW Africa (3 stations between 14.2°N - 17.4°N) and (iii) waters at the latitudinal extremes of the AMT transect (1 station at 30.0°N and 1 station at 35.5°S). Re-analysis of the station clusters at a higher level of dissimilarity leads to the separation of equatorial waters (2 stations at 4.2°N and 3.6°N), and of the southern subtropical gyre edge (2 stations at 23.3 and 32.4°S) and the central southern gyre range (1 station at 11.6°S). Formalising spatial and temporal variations in the hydrographic environment leads to the provinsional identification of 6 major hydrographic regions (Fig. 3.10b) which will be used in further analysis of the spatial variability of the phytoplankton community. These regions include the (i) North Atlantic Drift (35°N - 40°N), (ii) North Atlantic Subtropical Waters (20°N - 35°N), (iii) tropical upwelling waters off NW Africa (5°N - 20°N), (iv) tropical equatorial waters (5°S - 5°S), (v) South Atlantic Subtropical Waters (5°S - 30°S), and (vi) South Atlantic Temperate Waters (30°S - 40°S). Regional

(latitudinal) differences in the physical and hydrological conditions of the water-column in the subtropical and tropical Atlantic Ocean provide a regional (spatial) basis for the investigation of variability of the algal communities.

2. Multivariate statistical analysis of vertical differences in hydrographic parameters leads to the clustering of depths with statistically similar properties, with the depth range of the clusters varying with latitude (Fig. 3.2b, Table 3.2). This represents a background to further investigation of vertical differences in phytoplankton community strucutre. In the subtropical gyres of the Atlantic Ocean, the surface (0 - 50 m) high temperature and salinity, light-rich and nutrient-poor waters are resolved from deep (100 - 200 m) warm, saline, light-poor and nutrient-rich waters (Table 3.2). In the waters off NW Africa and around the equator the water-column is separated into 3-layers (Table 3.2); (i) a high temperature and low salinity upper layer with low-nutrient and high-light levels (0 - 20 m off NW Africa, 0 - 50 m around the equator), (ii) intermediate nutrient and light layer (~50 m off NW Africa and ~100 m around the equator), and (iii) a cold, nutrient-rich and light-poor layer (100 - 200 m off NW Africa and 150 - 200 m around the equator). Vertical separation of the nutrient and light conditions in upper and deeper waters in the subtropical and tropical Atlantic Ocean has implications for the growth and survival strategies required by the algal communities.

3. Through examination of the intercruise (seasonal) variability of hydrographic parameters seasonal trends have been identified in both the northern (0 - 40°N) and southern (0 - 40°S) hemispheres of the Atlantic Ocean; in late summer (September in northern hemisphere and May in southern hemisphere), seasurface temperatures and densities are higher (Fig. 3.4), MLD depths are generally shallower (Fig. 3.6) and the density gradient of the seasonal thermocline is steeper (Fig. 3.7). There is no evidence for intercruise (seasonal) variability in nutricline depths (Fig. 3.9) or vertical attenuation coefficients (Fig. 3.8) in the tropical and subtropical Atlantic Ocean. However, the absolute light levels are required to fully investigate interannual differences in irradiance. Seasonal differences in the physical water-column structure will have consequences for the algal communities in terms of nutrient and light availability.

4. Interannual variations in the depth of Mixed Layer (MLD) are identified within the South Atlantic Subtropical Waters for post-winter AMT cruises in the southern hemisphere (Fig. 3.11). The MLD for AMT-3, 5 and 7 are shallower (<75 m) than those during AMT-1 and 9 (> 100 m) and a preliminary examination of the wind speeds during this time of year shows a decrease during AMT-3 and 5 which partly coincide with the 1997 - 1998 El-Nino-Southern-Oscillation event in the Southern Pacific Ocean (Fig. 3.12). Possible interannual differences in the physical structure of the water-column in the South Atlantic Ocean are likely to have interannual consequences for the algal community and may result in temporal variability of the community composition.

# CHAPTER 4: SPATIAL VARIABILITY OF THE PHYTOPLANKTON COMMUNITY COMPOSITION DURING MAY, 1999 (AMT-8): PIGMENT SIGNATURES AND PHYTOPLANKTON SPECIES

## 4.1. Introduction and Outline

### 4.1.1. Chapter Structure and Outline

The main aim of this chapter is to characterise the composition of the phytoplankton communities present in the subtropical and tropical Atlantic Ocean, and identify spatial patterns of compositional change in terms of latitudinal and veritcal differences. Multivariate (Cluster) statistics are used to identify (species and taxa) assembalges and investigate the community components important in causing these patterns. Analysis of the community in terms of phytoplankton chemotaxonomic pigments (section 4.2) and species identification data (section 4.3) is investigated both horizontally (latitude) and vertically (0 - 200 m) during AMT-8 (May, 1999), with the aim of identifying dominant patterns of community composition.

### 4.1.2. Atlantic Meridional Transect (AMT) Cruise 8 (May, 1999)

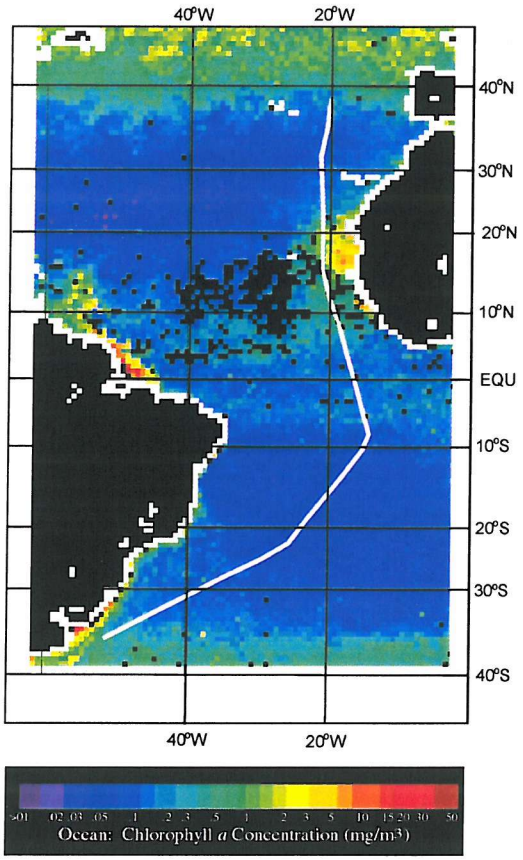


Fig. 4.1: AMT-8 (25/04/99 - 07/06/99) cruise track (white line) in the tropical and subtropical Atlantic Ocean between the subtropical convergences (40°N and 40°S). Cruise track is superimposed on a SeaWiFS composite (April - May, 1999) of surface chlorophyll *a* concentration (see colour bar below). SeaWiFS image courtesy of NASA/ORBIMAGE. Black pixels indicate clouds and are likely to correspond to the position of the ITCZ. Low surface chlorophyll *a* concentrations (<0.1 mg $m^{-3}$) characterise the subtropical gyres in both the northern and southern hemisphere, whereas increases in surface chlorophyll *a* concentration are found off NW Africa (0.5 - 3 mg $m^{-3}$) and at the subtropical convergences (>0.5 mg $m^{-3}$). Surface chlorophyll *a* concentrations in the equatorial Atlantic (10°N - 10°S) show patchy increases of 0.3 - 0.4 mg $m^{-3}$.

Sampling was carried out during AMT-8 (May, 1999). The cruise track for AMT-8 (Fig. 4.1) was slightly different than other AMT cruises (see Fig. 2.1) due to a portcall at Ascension Island (10°S), and thus the southern leg travelled further east (<30°W) in the south Atlantic Ocean than previous

AMT cruises (>30°W). Hydrographic conditions during AMT-8 were similar to other AMT cruises and are discussed in Chapter 3. Unlike other AMT cruises samples for phytoplankton identification during AMT-8 were collected from Niskin bottles closed at up to 6 depths during the downcast of the CTD. Sampling depths were selected based on temperature and fluorescence profiles to include the surface, mixed later and fluorescence maximum. Counting and identification of cells followed the Uttermöhl inverted microscope technique (Hasle, 1978; see methods 2.5).

### 4.1.3. Chemotaxonomic Pigments

Pigments identified by HPLC during AMT-8, along with their function and phytoplankton group affiliations, are presented in Table 4.1. Also included in Table 4.1 are the SCOR-UNESCO abbreviations (Jeffrey et al., 1997) that will be used throughout this chapter.

Table 4.1: Diagnostic pigments identified during AMT-8; indicating pigment function (photoprotectant [PP] or photosynthetic [PS]), major taxonomic affiliations (in bold) and SCOR-UNESCO abbreviations (Jeffrey *et al.*, 1997). Adapted from Millie *et al.*, (1993), Andersen *et al.*, (1996), Barlow *et al.*, (1997a, b), and Gibb *et al.*, (2000, 2001).

| *Pigment* | *SCOR-UNESCO* | *Role* | *Affiliation(s)* |
|---|---|---|---|
| Alloxanthin | Allo | PP | **Cryptophytes** |
| β-Carotene | β-Car | PP | All Groups |
| 19'-Butanoyloxyfucoxanthin | But-fuco | PS | Dinophytes, **Chrysophytes, Pelagophytes**, Prymnesiophytes |
| Chlorophyll *a* | Chl *a* | PS | All eukaryotic Groups |
| Chlorophyll *b*[a] | Chl *b* | PS | **[Prochlorophytes]**, Chlorophytes, Prasinophytes |
| Chlorophyll $c_1c_2$ | Chl $c_1c_2$ | PS | Bacillariophytes, Dinophytes, Chrysophytes, Prymnesiophytes, Cryptophytes |
| Chlorophyll $c_3$ | Chl $c_3$ | PS | Bacillariophytes, Dinophytes, Chrysophytes, Prymnesiophytes, |
| Diadinoxanthin | Diadino | PP | Bacillariophytes, Dinophytes, Chrysophytes, Prymnesiophytes, Prasinophytes |
| Divinyl chlorophyll *a* | Dv Chla *a* | PS | **Prochlorophytes** |
| Fucoxanthin | Fuco | PS | **Bacillariophytes**, **Dinophytes**, Chrysophytes, Prymnesiophytes, |
| 19'-Hexanoyloxyfucoxanthin | Hex-fuco | PS | Dinophytes, **Prymnesiophytes** |
| Peridinin | Perid | PS | **Dinophytes** |
| Zeaxanthin | Zea | PP | **Prochlorophytes, Cyanophytes**, Prasinophytes, Chlorophytes, Cryptophytes |

[a] includes both Divinyl chlorophyll *b* and chlorophyll *b*.

### 4.1.4. Nano- and Microphytoplankton Species

Where nano- and microphytoplankton species are identified in the statistical analysis of this chapter they are referred to by an AMT-specific species code (e.g. D52, ED1), with the full species names given in Table 4.2 and in the text. Therefore, Table 4.1 does not present all the species and morphotypes identified from the light microscope counts; 105 species and morphotypes were identified from AMT-8, including 35 diatoms, 39 autotrophic dinoflagellates, 20 coccolithophores, 7 species associated with endosymbiotic cyanophytes and 3 miscellaneous taxa. Numerous naked and athecate flagellates (<5 μm in diameter), including some small dinoflagellates, were also observed and counted. However, due to their unknown trophic status and taxonomic affiliations they were removed from statistical analysis and presentation. Species and morphotype names, taxonomic affiliations and published distributions of selected species are also given in Table 4.2. Species distribution data is taken from; [1] Sournia, (1982), [2] Thomas, (1997), [3] Winter et al., (1994), [4] Furuya and Marumo, (1983), [5] Venrick, (1988; 1990a; 1999), [6] Haider and Thierstein, (2001), or this study [7].

Table 4.2: Nano- and microphytoplankton species names, codes and reported geographic and vertical distribution (see text for references). [Note: Genus *Chaetoceros* spit into species with chloroplasts in setae (*Phaeoceros*) and species without chloroplasts in setae (*Hyalochaetae*).]

| Spp. Code | Species / Genus Names (common or type species in brackets) | Distribution [Source - see text] |
|---|---|---|
| | 1. Diatoms (D) | |
| D8 | *Bacteriastrum* spp. | Tropical / Temperate [2] |
| D10 | Centric 10μm diameter | |
| D12 | Centric 20μm diameter | |
| D18 | *Cerataulina pelagica* | Cosmopolitan [2] |
| D21 | *Chaetoceros* spp. - *Phaeoceros* | |
| D29 | *Dactyliosolen* spp. (e.g. *D. phuketensis*) | Tropical / Temperate [2] |
| D41 | *Haslea* spp. (e.g. *H. wawrikae*) | Tropical sun flora [2], [4] |
| D45 | *Leptocylindrus danicus* and *minimus* | Cosmopolitan [2] |
| D52 | *Nitzschia longissima* (cf. *Cylindrotheca closterium*) | Cosmopolitan / Coastal [2] |
| D56 | Small Unidentified Pennates (10-30 μm) | |
| D57 | Pennate spp. 'C' (50 μm) | |
| D59 | *Planktoniella sol* | Tropical shade flora [1], [2], [4] |
| D62 | *Proboscia alata* | Cosmopolitan (?) [2] |
| D64 | *Pseudo-nitzschia* spp. complex | Cosmopolitan (?) [2] |
| D81 | *Thalassionema* spp. (e.g. *T. nitzschioides*) | Cosmopolitan, Tropical shade flora (?) [2], [4], [5] |
| D84 | *Mastogloia rostrata* | |
| | 2. Autotrophic Dinoflagellates (Ad) | |
| AD10 | *Ceratium fusus* | Cosmopolitan / Coastal [2] |
| AD26 | *Ceratium teres* | Cosmopolitan / Rare [2] |
| AD30 | *Ceratocorys* spp. (e.g. *C. armata*) | Tropical [2] |
| AD37 | *Gonyaulax polygramma* | Cosmopolitan [2] |
| AD39 | *Gonyaulax* spp. | |
| AD40 | *Gymnodinium / Gyrodinium aureolum*-complex | |
| AD43 | *Microcanthodinium* spp. | |
| AD45 | *Oxytoxum scolopax* | Tropical [2] |
| AD46 | *Oxytoxum sphaeroideum* | |
| AD47 | *Oxytoxum* spp. (e.g. *O. laticeps*) | Tropical shade flora (?) [5] |
| AD49 | *Phalacroma rotundatum* | Cosmopolitan [2] |
| AD50 | *Prorocentrum dentatum* | Cosmopolitan [2] |
| AD53 | *Prorocentrum* spp. Small (e.g. *P. balticum*) | |
| AD54 | *Prorocentrum* spp. Medium (e.g. *P. compressum*) | |
| AD59 | *Scrippsiella / Alexandrium* spp. | |
| AD60 | *Torodinium* spp. (e.g. *T. teredo*) | Cosmopolitan [2] |
| | 3. Coccolithophores (CC) | |
| CC1 | 10-25μm Coccospheres | |
| CC2 | *Acanthoica* sp. (e.g. *A. quattrospina*) | Cosmopolitan, Tropical sun flora [2], [3], [5] |
| CC3 | *Anoplosolenia* sp. (e.g. *A. brasiliensis*) | Cosmopolitan, Tropical sun flora [2], [5] |
| CC5 | *Calcidiscus leptoporus* (inc. *Coccolithus pelagicus*[a]) | Cosmopolitan, Tropical sun flora [2], [6] |
| CC6 | *Calciosolenia* sp. (e.g. *C. murrayi*) | Cosmopolitan, Tropical shade flora [2], [4], [5] |
| CC7 | *Discosphaera tubifer* (inc. *Papposphaera lepida*) | Tropical sun flora [3], [4], [5], [6], [7] |
| CC8 | *Emiliania huxleyi*, *Gephyrocapsa* spp. and 5μm Coccospheres | Cosmopolitan (?) [3] |
| CC9 | *Halopappus* spp. (inc. *Calciopappus* spp. + *Michaelsarsia* spp.) | Tropical shade flora [5], [7] |
| CC10 | *Helicosphaera* spp. (*H. carteri* and *H. hyalina*) | Cosmopolitan, Tropical sun flora [2], [6] |
| CC11 | *Oolithotus* spp. (e.g. *O. fragilis*) | Tropical shade flora [1], [2], [4], [5] |
| CC12 | *Ophiaster* spp. (e.g. *O. hydroideus*) | Tropical shade flora [4], [5], [6], [7] |
| CC13 | *Ponotosphaera* spp. (e.g. *P. syracusana*) | Cosmopolitan [2], [5] |
| CC14 | *Rhabdosphaera* sp. cf. *claviger* (inc. var. *stylifera*) | Tropical sun flora [3], [5], [6] |
| CC16 | *Syracosphaera* sp. cf. *prolongata* (and *S. pirus*) | Tropical [3], [5], [7] |
| CC17 | *Umbellosphaera* spp. (*U. irregularis* and *U. tenuis*) | Tropical sun flora [3], [4], [5], [7] |
| CC19 | Unidentified coccolithophore sp. (a.k.a. "Heart") | |
| CC20 | *Gephyrocapsa ornata* (a.k.a. "Spike") | Rare *Gephyrocapsa* sp. |
| | 4. 'Endosymbiotic' species | |
| ED1 | *Leptocylindrus mediterraneus* (D) | Cosmopolitan / Tropical [2] |
| ED5 | *Hemiaulus hauckii* (D) | Tropical sun flora [2], [4], [5] |
| ED9 | *Myrionecta rubra* (planktonic autotrophic ciliate) | |
| ED12 | *Trichodesmium* spp. (Cyanophyte) | Tropical sun flora [4], [7] |
| | 5. Miscellaneous autotrophic taxa | |
| MSC3 | Cryptomonads (Cryptophyte) | |
| MSC16 | Pyramimonas spp. (Chlorophyte) | |
| MSC18 | Siiicoflagellates (Chrysophytes) | Cosmopolitan, Tropical shade flora (?) [2], [4], [5] |

[a] due to identification experience *C. leptoporus* and *C. pelagicus* were grouped for analysis; the majority of the numbers are likely to be *C. leptoporus* as *C. pelagicus* is commonly though of as a subarctic species (Brand, 1994).

## 4.1.5. Total Chlorophyll *a* and Size-fractionated Chlorophyll a

The distribution of contributions to the total chlorophyll a (Tchl*a*) from picoplankton (0.2 - 2.0 μm), nanoplankton (2.0 - 20 μm) and microplankton (>20 μm) are presented in Figure 4.2, as an introduction to the distribution of the phytoplankton community (Tchl*a*) and its components. Measurements of Tchl*a* and chlorophyll *a* concentration in the size-fractions are from acetone extraction (Flchl*a*). Tchl*a* concentration (Fig. 4.2a) shows an increase with depth to produce a pronounced Chlorophyll *a* Maximum (CM). The distribution of Tchl*a* (Fig. 4.2a) is similar to the total chlorophyll *a* (TChl *a* = Chl *a* + Dv Chl *a*) distribution shown by HPLC pigment analysis (Fig. 4.3a), although the Flchl*a* concentrations are slightly higher than HPLC measurements of chlorophyll *a*. Stations in the subtropical gyres with deep CM (>80m) are characterised by low surface and CM Flchl*a* concentrations (<0.1 mg $m^{-3}$ and 0.2 - 0.3 mg $m^{-3}$, respectively), whereas waters around the equator and off NW Africa are characterised by shallower CM (<75 m and ~30 m, respectively) and increases in both surface and CM Flchl*a* concentrations (0.2 - 0.3 mg $m^{-3}$ and 0.4 - >0.6 mg $m^{-3}$, respectively) (Fig. 4.2a).

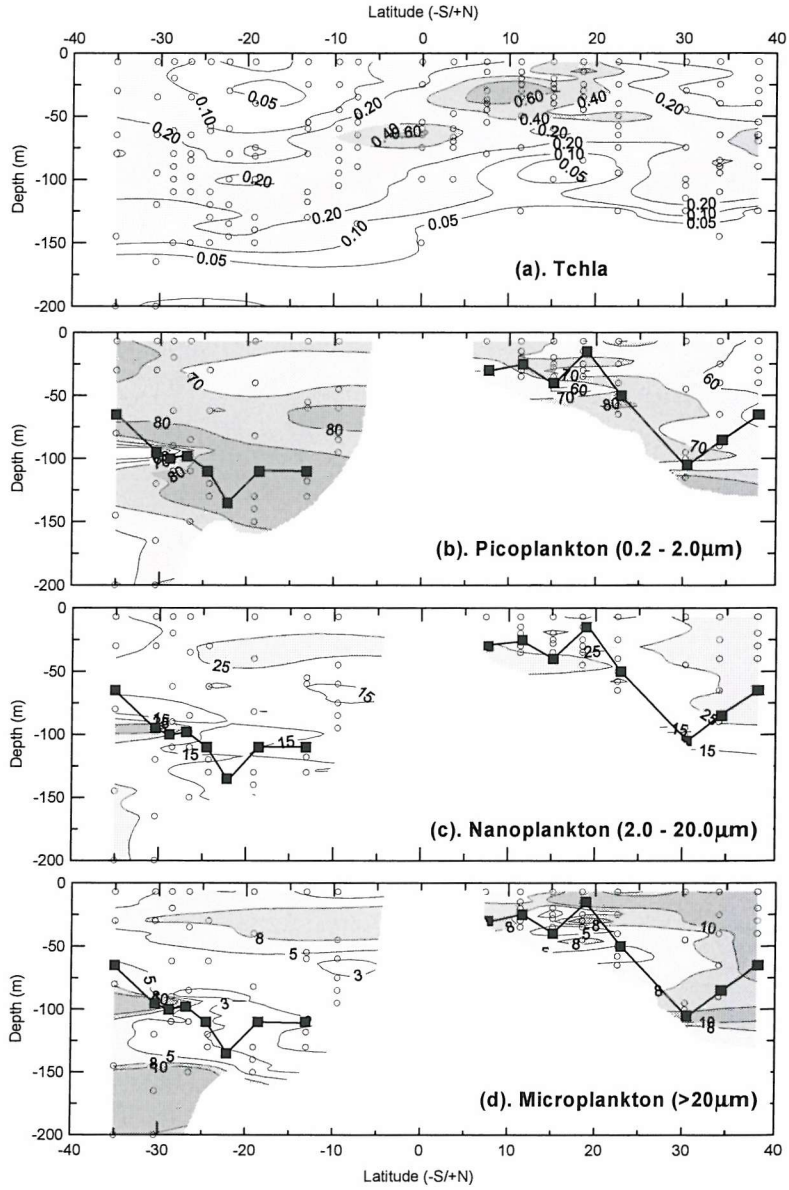


Figure 4.2: Chlorophyll *a* depth distribution and community size structure; (a) total chlorophyll *a* concentration (mg $m^{-3}$), (b) percentage (%) in picoplankton (0.2 - 2 μm) fraction, (c) percentage (%) in nanoplankton (2 - 20 μm) fraction, and (d) percentage (%) in microplankton (>20 μm) fraction. Open circles indicate sampling depths, filled squares and thick lines indicate depth of the CM as determined from acetone extraction. Due to sampling constraints size-fractionated chlorophyll *a* measurements were not taken around the equator. Therefore, (a) is based on un-fractionated chlorophyll *a* measurements taken in conjunction with the size-fractionated measurements.

Picoplankton generally represent 60 - 80% of Tchl*a*, although there are decreases in picoplankton contributions around the northern and southern ends of the transect and in surface waters off NW Africa (Fig. 4.2b). Decreases in picoplankton contributions are accompanied by increased nanoplankton contributions and increases of Tchl*a* concentration (Fig. 4.2); e.g. off NW Africa and at the northern end of the transect. Within the subtropical gyres, picoplankton are the dominant contributors to Tchla (~70 - 80%), especially within the CM (>80% Tchl *a*), although there is a slight reduction in picoplankton contributions in surface waters (<70%) where the nano- and micro-plankton make up around 30% of Tchl*a* (Fig. 4.2).

## 4.2. Basinscale Changes in Phytoplankton Community Structure from Chemotaxonomic Pigment Composition

### 4.2.1. Pigment Distribution

Total chlorophyll *a* (TChl *a*) from HPLC pigment analysis, increases in concentration with depth to produce a CM, which is present throughout the subtropical and tropical Atlantic, although its depth varies from <25 m off NW Africa to >100 m in the southern subtropical gyre (Fig. 4.3a). Within the northern and southern subtropical gyres, deep (~100-150 m) CM are associated with relatively low TChl *a* concentrations (~0.1 - 0.2 mg $m^{-3}$). Shallowing and strengthening of the CM is observed around the equator (Fig. 4.3a) where the CM is ~60 m and TChl *a* concentrations are 0.2 - 0.4 mg $m^{-3}$, and off NW Africa where the CM is generally <40 m and contains >0.4 mg $m^{-3}$ (Fig. 4.3a). Apart from where the CM shallows, or is sub-surface, surface TChl *a* concentrations are typically 0.05 - 0.1 mg $m^{-3}$ with lowest surface TChl *a* concentrations in the upper waters of the southern subtropical gyre (Fig. 4.3a).

The contribution of divinyl chlorophyll *a* (Dv Chl *a*) to TChl *a* is typically between 10 - 50% within the CM (Fig. 4.3b). Dv Chl *a* is present in high concentrations in both the northern and southern subtropical gyres but is almost absent around NW Africa between 10 - 20°N. Dv Chl *a* contributions (Fig. 4.3b) are higher in the southern subtropical gyre (>30 - 50% of TChl *a*) than in the northern gyre (~20% of TChl *a*). The distribution of chlorophyll *b* (TChl *b* = Dv Chl *b* + Chl *b*) is also related to the CM (Fig. 4.3c). Maximum TChl *b* concentrations (>0.1 mg $m^{-3}$) are found in the CM off NW Africa, around the equator and in the southern subtropical gyre (Fig. 4.3c). However, TChl *b* is not observed at stations in northern subtropical waters (~22°N and ~30°N; Fig. 4.3c).

Separation of the accessory pigments into photosynthetic (PS) and photoprotectant (PP) pigments (see Table 4.1) shows that the distribution of total PS closely follows the CM (Fig. 4.3d), whereas the distribution of total PP is typically higher in surface waters (>0.05 mg $m^{-3}$) than in the CM (<0.05 mg $m^{-3}$). However, PP concentrations are relatively high (0.1 - 0.15 mg $m^{-3}$) at depth around the equator (Fig. 4.3e). 19'-hexanoyloxyfucoxanthin (Hex-fuco) is commonly the dominant PS pigment, and is found in relatively low concentrations in surface waters (<0.05 mg $m^{-3}$; <30% of total carotenoids) and increases with depth to a maximum (>0.05 - 0.2 mg $m^{-3}$; >30 - 50% of total carotenoids), which is closely associated with the CM (cf. Fig. 4.3d). Zeaxanthin (Zea) is the dominant PP pigment in the subtropical Atlantic (40 - 70% of total carotenoids in upper 50m) and

often shows a surface maximum and a decrease with depth where the CM is deep (<100m). Shallowing of the CM is associated with increased concentrations of Zea in surface and subsurface waters, as well as higher concentrations in association with the CM (cf. Fig. 4.3e). The ratio between the dominant PS and PP pigments (i.e. Hex-fuco: Zea) varies (Fig. 4.3f); Zea dominates surface waters, while deeper waters are dominated by Hex-fuco (Fig. 4.3f). The depth of cross-over from Zea to Hex-fuco dominance occurs slightly above the CM, with the difference in the depths of the crossover and the CM varying with CM depth; where the CM is deep the boundary is displaced above, while when the CM shallows the boundary occurs at, or near, the CM (Fig. 4.3f).

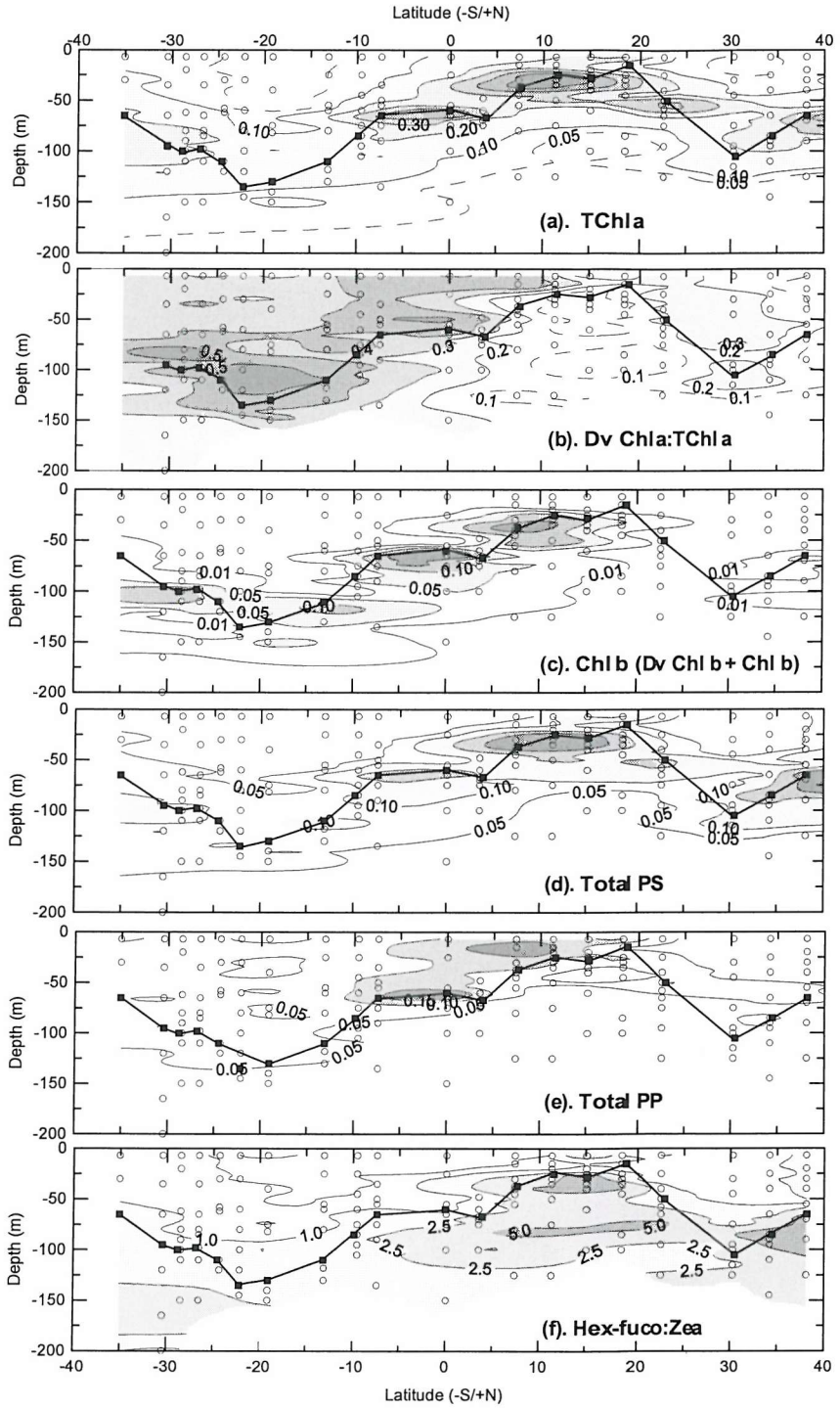


Figure 4.3: Phytoplankton pigment distribution (mg $m^{-3}$); (a) TChl *a*, (b) ratio of Dv Chl *a*:TChl *a*, (c) TChl *b*, (d) total PS, (e) total PP, and (f) ratio of Hex-fuco:Zea. Open circles indicate sampling depths and filled squares with joining line indicate the depth of the CM as determined from pigment analysis.

### 4.2.2. Accessory Pigment Diversity

Accessory pigment Shannon (H') diversity ranges from 1.5 - 2.0 in the subtropical and tropical Atlantic Ocean, with highest diversity found in association with the CM (Fig. 4.4). Surface and subsurface waters typically have lower H' than the CM, especially in the northern and southern subtropical gyres, which confirms Zea dominance in upper waters. High H' in association with the CM (Fig. 4.4) indicates that although the CM is characterised by an increase in pigment concentrations, such an increase is shared between all the accessory pigments and there is little dominance of the CM by one accessory pigment. Although Hex-fuco is dominant within the CM, other pigments are also present in high and almost equal concentrations (e.g. 19'-butanoyloxyfucoxanthin). Where the CM shallows around the equator and off NW Africa diversity increases in surface and subsurface waters, and the dominance of Zea is reduced (Fig. 4.4).

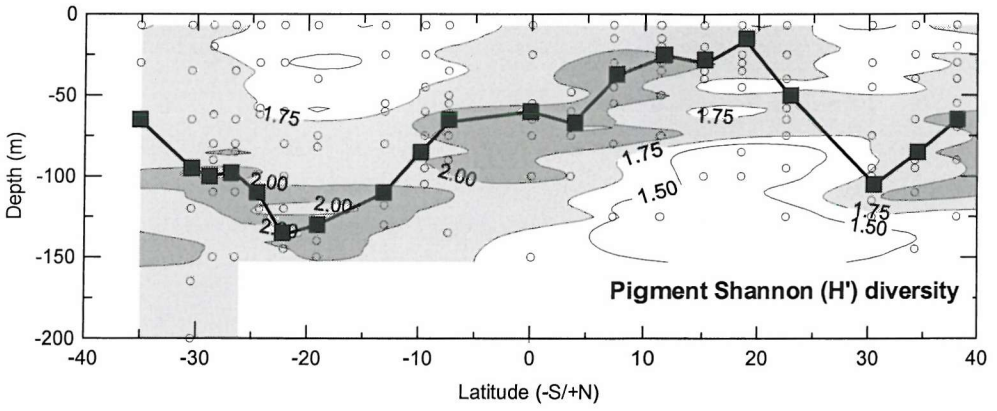


Figure 4.4: Shannon (H') diversity of accessory pigments. Open circles indicate sampling depths, closed squares indicate depth of the CM from pigment analysis. CM depths are joined by thick black line.

### 4.2.3. Basinscale Analysis of Community Pigment Composition

The concentration and distribution of pigments change with both latitude and depth (Fig. 4.3). In order to investigate changes in phytoplankton community composition, the similarity of pigment composition of all samples was compared by cluster analysis of Bray-Curtis percentage similarities on square-root (SQRT) transformed pigment concentrations. The dendrogram for cluster analysis of all pigment samples is presented in Figure 4.5, and shows separation of the samples into five major clusters (labelled A - E; Fig. 4.5); cluster E separates first (~25% Bray-Curtis similarity) which indicates that the composition of the samples in this cluster is highly dissimilar (i.e. ~75%) to the other pigment samples. Separation of further pigment sample clusters (A - D) occurs at ~60% Bray-Curtis similarity (Fig. 4.5), indicating a higher level of similarity between the remaining samples. Clusters A and B separate ~70% similarity, whereas clusters C and D separate ~62% similarity (Fig. 4.5). Each pigment sample is classified by its cluster and plotted on a latitudinal section in Figure 4.6, with sample groups identified. The presentation of the cluster samples in this way (Fig. 4.6) shows that the pigment clusters identified in the analysis of individual stations form discrete layers. The depth of these layers varies with latitude and forms an overlaying pattern, with outcropping at the surface and depth changes with latitude (Fig. 4.6). (Note: clusters are numbered sequentially according to the cluster diagram and not according to their distribution).

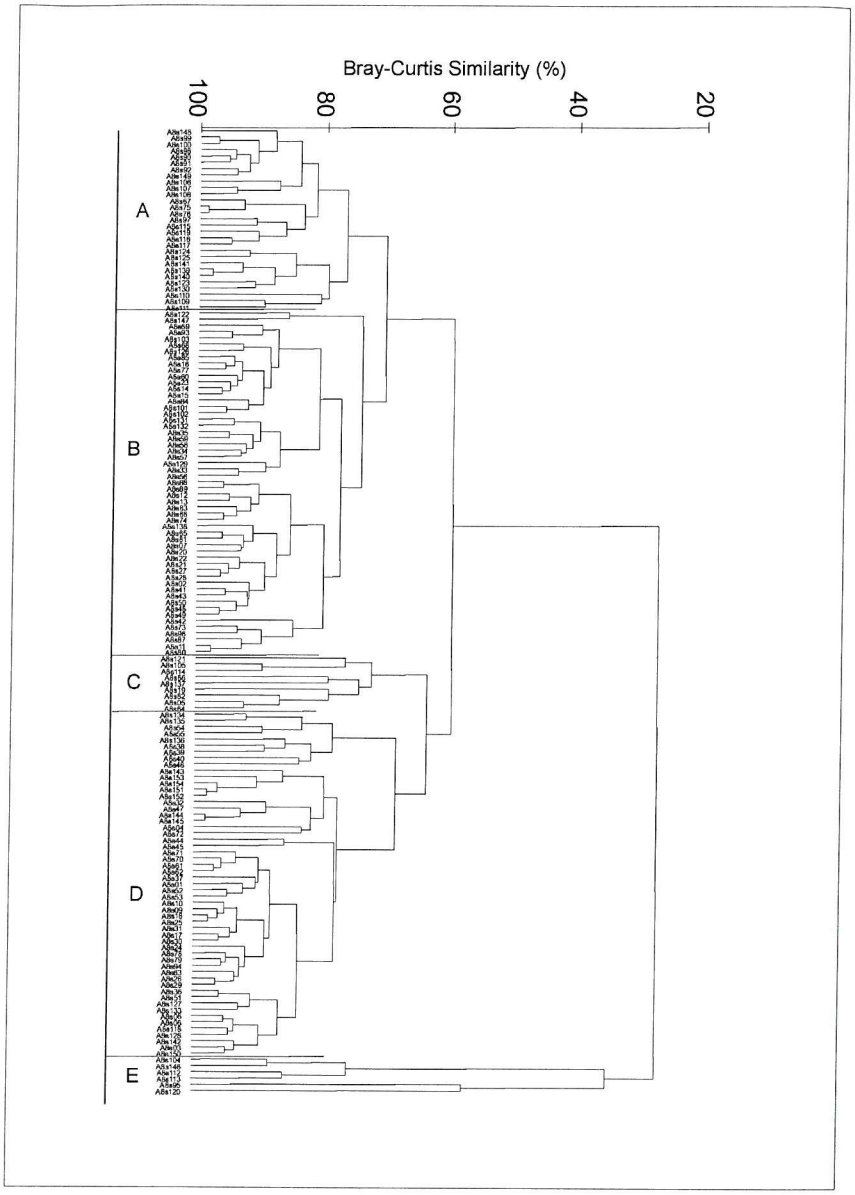


Figure 4.5: Cluster dendrogram for the analysis of all pigment samples taken during AMT-8. Note: separation of 5 major sample clusters (A-E). Each pigment sample is identified with an AMT cruise number ID (A8) and then sequentially with depth and latitude.

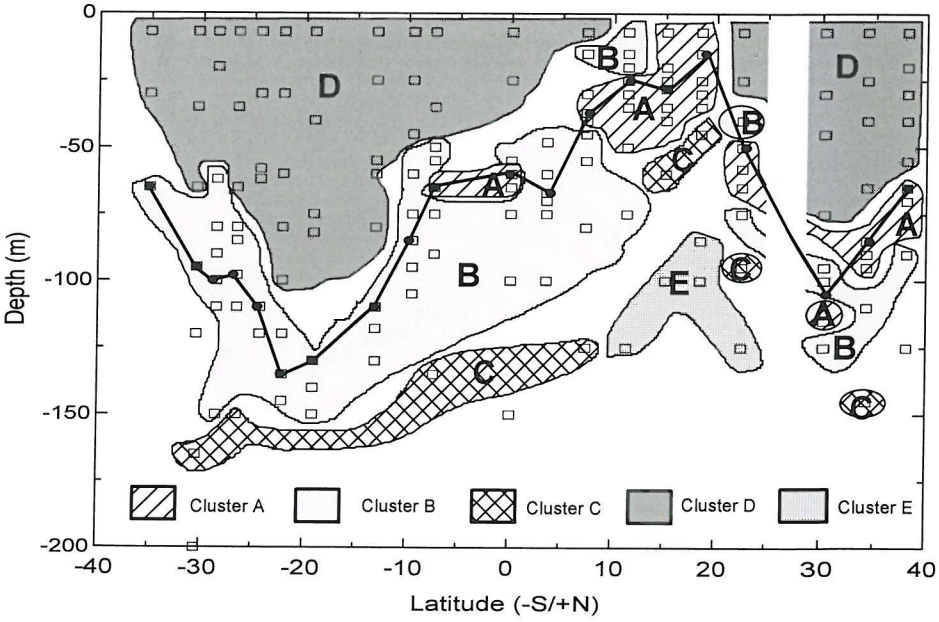


Figure 4.6: Sample clusters A - E superimposed onto a plot of the pigment sample positions (open squares; depth and latitude). The CM depth is indicated by filled circles and joining thick black line. Note: three samples are not placed within clusters and represent samples which were not included in the cluster analysis due to poor pigment quantification (identified during quality control of the pigment data).

Most of the surface waters of the subtropical Atlantic Ocean are characterised as cluster D, which is replaced around NW Africa by clusters A and B (~10 - 20°N; Fig. 4.6). Cluster D is commonly found in the upper 50 m, apart from 10 - 20°N were it is replaced by group B (~12°N) and A (15 - 20°N), and reaches a maximum depth of 100m in the centre of the southern subtropical gyre and ~75m in the northern subtropical gyre (Fig. 4.6). Cluster A is found at the surface off NW Africa and below cluster B from 8 - 12°N, below cluster D between 0 - 8°S and between 30 - 40°N (Fig. 4.6). Cluster B is also found at the surface off NW Africa (~10-12°N), as well as under cluster D in the southern hemisphere and under cluster A in the northern hemisphere (Fig. 4.6). Cluster C represents a deeper stratum, found below cluster B throughout the subtropical Atlantic, although its depth does change off NW Africa where it is found directly under cluster A (Fig. 4.6). Cluster E is a smaller group and is restricted to deeper waters off NW Africa where it underlies clusters C and A, although one sample at 38°N is also from cluster E (Fig. 4.6). The CM (filled circles) is not restricted to one layer and its composition changes with latitude; the CM between 35°S - ~ 5°N is found in cluster B, although it also includes cluster A between ~8°S - 0°; between 5 - 38°N the CM is found in cluster A, although it does appear once in cluster B at 30°N (Fig. 4.5).

Table 4.3: Breakdown of the dissimilarity between pigment sample clusters (SIMPER analysis) separated based on cluster analysis of pigment composition from all samples. Table includes pigment abbreviations (see Table 4.1), average dissimilarity between clusters (δ), average individual pigment concentrations (ng $l^{-1}$) in each cluster, average contribution of individual pigments to the total dissimilarity (δi), the ratio of δi to SD(δi) and the cumulative percentage contribution of each pigment to total dissimilarity between clusters.

| *Pigment* | *Average concentration (ng $l^{-1}$)* | *Average concentration (ng $l^{-1}$)* | *Average Contribution to Dissimilarity* (δi) | *Ratio of δi/SD (δi)* | *Cumulative percentage of total dissimilarity* |
|---|---|---|---|---|---|
| | Cluster A | Cluster B | Average δ = 29.5 | | |
| Chl *a* | 342.9 | 118.3 | 5.0 | 2.3 | 16.8 |
| TChl *b* | 78.1 | 46.5 | 3.9 | 1.3 | 30.0 |
| Fuco | 51.6 | 8.5 | 3.1 | 1.7 | 40.5 |
| Dv Chl *a* | 63.5 | 73.6 | 2.6 | 1.2 | 49.3 |
| Hex-fuco | 132.2 | 57.7 | 2.5 | 1.9 | 57.9 |
| But-fuco | 77.2 | 36.5 | 1.9 | 1.7 | 64.3 |
| Zea | 51.6 | 44.2 | 1.9 | 1.3 | 70.8 |
| Chl $c_1c_2$ | 69.5 | 29.1 | 1.9 | 2.2 | 77.3 |
| Perid | 12.6 | 1.3 | 1.6 | 1.3 | 82.8 |
| Diadino | 15.6 | 4.4 | 1.6 | 1.4 | 88.2 |
| Chl $c_3$ | 37.3 | 14.8 | 1.5 | 2.1 | **93.3%** |
| | Cluster A | Cluster D | Average δ = 49.1 | | |
| Chl *a* | 342.9 | 52.2 | 8.8 | 3.7 | 17.9 |
| Hex-fuco | 132.2 | 22.5 | 5.3 | 3.1 | 28.7 |
| But-fuco | 77.2 | 7.7 | 5.0 | 2.7 | 38.8 |
| TChl *b* | 78.1 | 0.0 | 4.9 | 1.3 | 48.8 |
| Chl $c_1c_2$ | 69.5 | 9.1 | 4.3 | 3.2 | 57.6 |
| Chl $c_3$ | 37.3 | 1.5 | 4.3 | 3.8 | 66.4 |
| Fuco | 51.6 | 4.4 | 4.1 | 2.0 | 74.8 |
| Dv Chl *a* | 63.5 | 25.7 | 3.2 | 1.6 | 81.3 |
| Perid | 12.6 | 0.4 | 2.0 | 1.3 | 85.4 |
| Zea | 51.6 | 44.1 | 2.0 | 1.3 | 89.5 |
| β-Car | 26.2 | 7.3 | 2.0 | 1.6 | **93.5%** |
| | Cluster B | Cluster D | Average δ = 34.5 | | |
| TChl *b* | 46.5 | 0.0 | 4.8 | 1.0 | 13.9 |
| Dv Chl *a* | 73.6 | 25.7 | 4.0 | 1.6 | 25.5 |
| Chl *a* | 118.3 | 52.2 | 3.9 | 1.7 | 36.9 |
| But-fuco | 36.5 | 7.7 | 3.7 | 1.7 | 47.6 |
| Chl $c_3$ | 14.8 | 1.5 | 3.4 | 2.4 | 57.4 |
| Hex-fuco | 57.7 | 22.5 | 3.1 | 1.9 | 66.4 |
| Chl $c_1c_2$ | 29.1 | 9.1 | 2.8 | 1.6 | 74.3 |
| Zea | 44.2 | 44.1 | 2.5 | 1.3 | 81.7 |
| β-Car | 20.8 | 7.3 | 2.2 | 1.5 | 88.1 |
| Fuco | 8.5 | 4.4 | 2.0 | 1.2 | **93.9%** |

Breakdown of the dissimilarity between the main pigment sample clusters into contributions from each pigment (SIMPER analysis; methods 2.6.4) was carried out on all the clusters (A - E) and the results are presented in Table 4.3. Clusters C and E differ from the other clusters due to significantly lower concentrations of all pigments, and therefore represent low-pigmented waters below the CM. Group A differs from group B and D due to higher concentrations of all pigments, with good discriminating pigments between groups A and B + D (Table 4.3) being the concentration of chlorophyll *a* (Chl *a*), Hex-fuco, chlorophyll $c_1c_2$ (Chl $c_1c_2$) and chlorophyll $c_3$ (Chl $c_3$). Group B and D differ in that group B has much higher concentrations of all the pigments, apart from Zea concentrations which are quite similar between the two (~0.04 mg $m^{-3}$), with good discriminating pigments being Chl $c_3$ and Hex-fuco (Table 4.3).

## 4.2.4. Pigment Assemblages

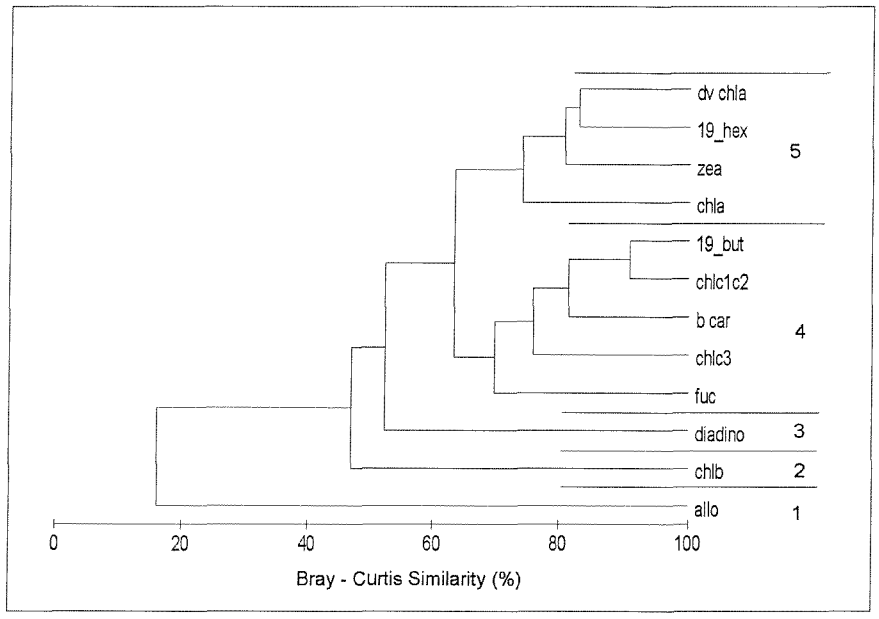


Figure 4.7: Cluster dendrogram of pigment assemblages (1 - 5).

An alternative approach to investigating changes in community pigment composition is to perform cluster analysis on the individual pigments and define 'pigment assemblages': i.e. groups of pigments which tend to co-occur in similar concentrations in different samples. Cluster analysis of the pigment assemblages is based on square-root (SQRT) transformed data, with removal of rare (consistently <3% of the total) pigments, in this case peridinin (Perid) and lutein (Lut). The cluster dendrogram is presented in Figure 4.7, and shows separation of the pigments into five assemblages; 1 (Alloxanthin; Allo), 2 (TChl *b*), 3 (Diadinoxanthin; Diadino), 4 (Fuco + Chl $c_3$ + β-Car + Chl $c_1c_2$ + But-fuco) and 5 (Chl *a* + Zea + Hex-fuco + Dv Chl *a*). Separation of groups 1, 2 and 3 occurs above the 60% Bray-Curtis similarity level, whereas separation of groups 4 and 5 occurs just after the 60% Bray-Curtis similarity level (Fig. 4.7). Group 5 is the dominant assemblage throughout the subtropical and tropical Atlantic (Fig. 4.8), although there is an absence of Dv Chl *a* off NW Africa (Fig. 4.3b). (Note: pigment concentrations were converted from mg $m^{-3}$ to ng $l^{-1}$ to comply with the PRIMER programme.)

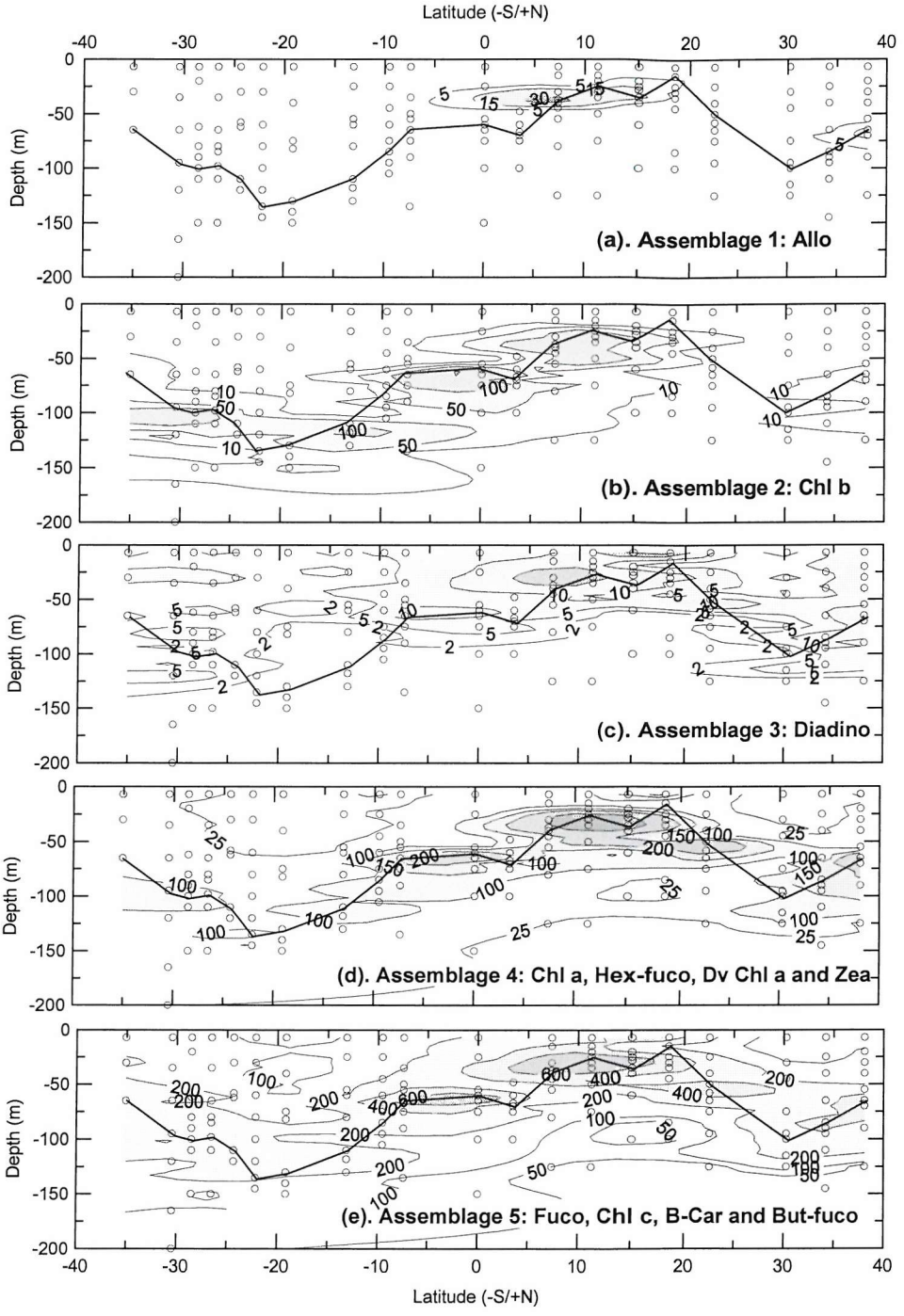


Figure 4.8: Pigment assemblage distribution and concentration (ng $l^{-1}$); (a) Assemblage 1 (Allo), (b) Assemblage 2 (TChl *b*), (c) Assemblage 3 (Diadino), (d) Assemblage 4 (Fuco, Chl $c_3$, β-Car, Chl $c_1c_2$, But-fuco), and (e) Assemblage 5 (Chl *a*, Zea, Hex-fuco and Dv Chl *a*). Open circles indicate sampling depths and black line joins CM depth.

Assemblage 1 (Allo) occurs only around NW Africa and at depth at the northern extreme of the AMT-8 transect (Fig. 4.8a). The relatively rare pigments (Perid + Lut), eliminated from the analysis also occur off NW Africa, although only episodically and in low concentrations (Perid mean 15.3 ng $l^{-1}$, 3.0 - 44.3 ng $l^{-1}$, n = 29; Lut 3.9 - 9.4 ng $l^{-1}$, n = 2). TChl *b* (assemblage 2) shows a maximum at depth, associated with the CM (cf. Fig. 4.3c), throughout the subtropical and tropical Atlantic Ocean, apart from between 20 - 30°N (Fig. 4.8b). Diadino (Assemblage 3) is found in high concentrations in surface and subsurface waters above the CM, and shows a marked maximum in concentration off NW Africa and towards the northern end of the transect (Fig. 4.8c). Assemblage 4

(Chl *a* + Hex-fuco + Dv Chl *a* + Zea) and 5 (Fuco + Chl $c_1c_2$ + Chl $c_3$ + β-Car + But-fuco) are closely associated with the CM, and indicate that the CM is not just a chlorophyll *a* maximum but also a pigment maximum (Fig. 4.8d and e). Assemblage 4 is associated with the CM throughout the subtropical and tropical Atlantic Ocean with a maximum around the equator and off NW Africa (Fig. 4.8d). Assemblage 5 is present throughout the subtropical Atlantic Ocean, with notable concentration maxima in deep waters around the equator (Fig. 4.8e; ~60 m, 5°S - 0°) and in shallow subsurface waters off NW Africa (Fig. 4.8e; ~30 m, ~10°N).

## 4.3. Nano- and Microphytoplankton Species Biogeography and Vertical Distribution

### 4.3.1. Nano- and Microphytoplankton Cell Densities

The distribution and abundance of 'common' (consistently >3% of total numbers; see methods 2.6.1) nano- and microphytoplankton species is presented in Figure 4.9. A comparison with the distribution of chlorophyll *a* (Tchla, Fig. 4.2a, and HPLC TChl a, Fig. 4.3a) indicates that apart from off NW Africa and at the northern end of the transect there is no clear relationship between chlorophyll *a* concentration and cell numbers; the CM is not an abundance maxima for large cells in most of the subtropical and tropical Atlantic Ocean.

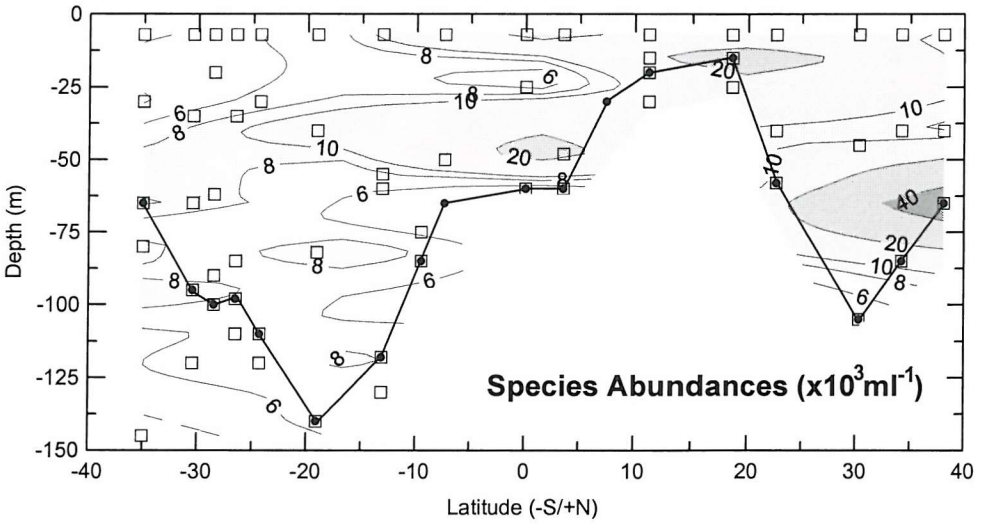


Figure 4.9: The distribution and abundance (x$10^3$ cells $l^{-1}$) of nano- and microphytoplankton species identified from light microscopy. Open squares indicate sampling depths and filled squares indicate CM depth with joining line as determined from acetone extraction.

Relatively high cells numbers are found in subsurface waters (Fig. 4.9) of the southern subtropical gyre (~50 m, >10 x $10^3$ cells $l^{-1}$), around the equator (~50 m, 10 - 20 x $10^3$ cells $l^{-1}$), off NW Africa (<25 m, 10 - >20 x $10^3$ cells $l^{-1}$) and at depth at the northern end of the transect (50 - 75 m, 20 - >40 x $10^3$ cells $l^{-1}$). High cell numbers (>10 x $10^3$ cells $l^{-1}$) in the southern subtropical gyre (~19°S) are associated with an increase in the abundance of the coccolithophores *Umbellosphaera irregularis* and *U. tenuis*. High cell densities off NW Africa (>10 x $10^3$ cells $l^{-1}$) and in the surface waters of the equator (~20 x $10^3$ cells $l^{-1}$) are associated with the colonial cyanophyte *Trichodesmium* spp., although the highest cell numbers in the CM off NW Africa are associated with increases of several taxa, including the diatoms *Leptocylindrus danicus* and *L. minimus*, a small 50 μm pennate spp. (termed Pennate sp. 'C'), *Pseudo-nitzschia* spp. (most likely *P. delicatissima* and *P. seriata*) and the

autotrophic dinoflagellate *Prorocentrum dentatum*. High cell densities in the CM at the northern end of the AMT-8 transect (~38°N) are also associated with increases in all taxa, especially *Pseudo-nitzschia* spp. and small (5 - 10 μm) coccolithophore taxa (i.e. *Emiliania huxley*, *Gephyrocapsa* spp. and 5 μm coccolithophores).

### 4.3.2. Nano- and Microphytoplankton Species Diversity

Calculations of autotrophic community diversity are based only on the abundance of large (~5 - 200 μm) identifiable, common (consistently >3% total numbers) phytoplankton species. Shannon (H') diversity and Pielou's evenness (J') are presented in Figure 4.10. In the subtropical and tropical Atlantic Ocean community H' and J' range from <1.5 - >2.0 and <0.4 - >0.7, respectively (Fig. 4.10). Regions of high diversity generally correspond to regions of relatively high evenness (Fig. 4.10), indicating that there is little dominance of the large (>5 μm) phytoplankton community by one or several species; cell numbers are evenly spread between all the species present. Low diversity (<1.5) and high dominance (<0.5) are found in surface and subsurface waters around the equator and are related to the high cell densities (0.6 - 23.8 x $10^3$ cells $l^{-1}$) of *Trichodesmium* spp. There is no clear relationship between diversity (or dominance) and chlorophyll *a* concentration (compare Fig. 4.2 and 4.10), although in some areas there does appear to be lower diversity (and increased dominance) in surface waters relatively to deeper waters associated with the CM (Fig. 4.10). Generally, areas with increased cell densities (Fig. 4.9) are also associated with lower diversity and evenness (Fig. 4.10).

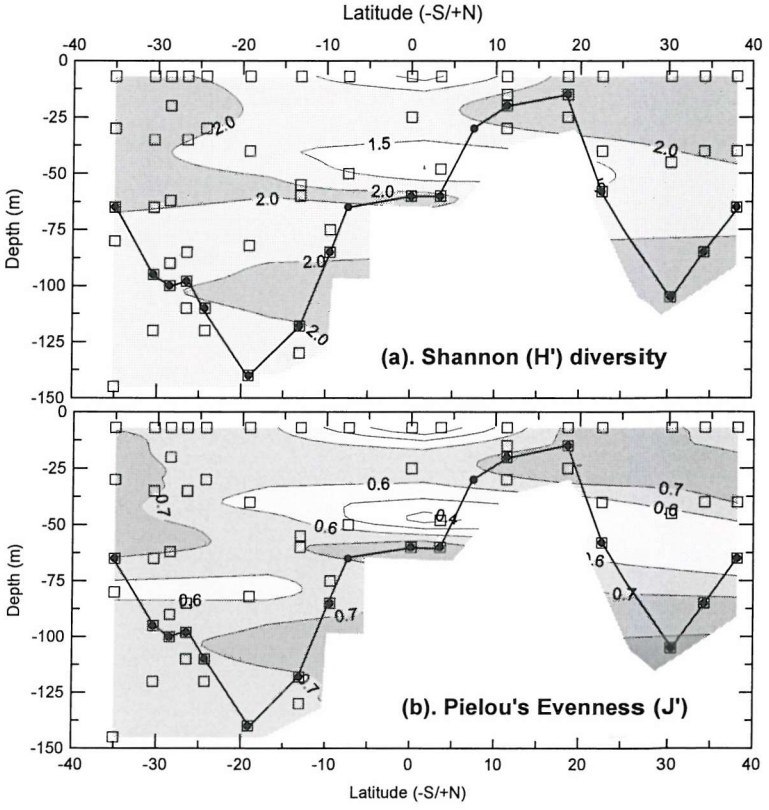


Figure 4.10: Diversity of the nano- and microphytoplankton community; (a) Shannon (H') diversity, and (b) Pielou's evenness (J'). Diversity calculations are only based on common (>3% of total numbers) species. Open squares indicate sampling depths and closed circles and thick line indicate depth of the CM as determined from acetone extraction.

### 4.3.3. Basin-scale Species Composition Analysis

The analysis of species composition is based on determining the similarity of species occurrences and cell densities in all samples. Two related, but independent, approaches have been used: (a) composition analysis of all species observed with a reduction of the data to a simple presence / absence (PA) index, and (b) composition analysis of only the common species, with elimination of rare species (consistently <3% of total numbers) and a square-root (SQRT) transformation of the data. Reduction of species cell numbers to a simple PA format allows all species, whether they are found in all samples or only in a few, to influence the statistics. In this way, large rare species that are indicative of environmental conditions are not eliminated. (It should be noted that the PA transformation and subsequent cluster analysis is carried out on averages of the PA analysis and not absolute values). Elimination of rare species and SQRT transformation means that only the numerically dominant species will influence the statistics, and rare episodic species will be ignored. The cluster dendrograms for both PA and SQRT analysis are presented in Figure 4.11.

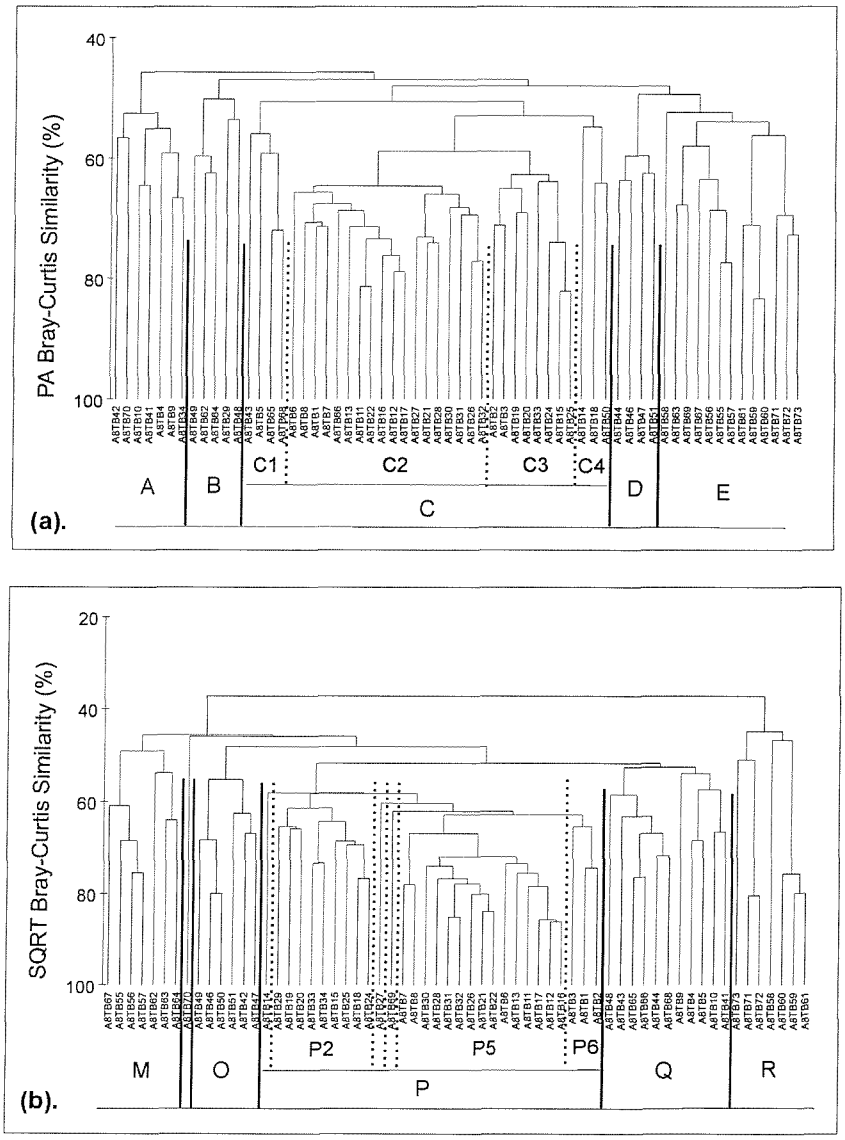


Figure 4.11: Cluster dendrograms for analysis of species composition; (a) all species PA transformation, and (b) elimination of rare species and SQRT transformation. Major sample clusters are identified with letters A - E for PA treatment and M - R for SQRT treatment. Sub-clusters are identified with numbers.

*(a). Reduction of all species cell densities to a PA matrix:* - Cluster analysis of the PA matrix shows separation of samples at several levels of similarity (Fig. 4.11a); five clusters (A - E) can be separated at ~50% Bray-Curtis similarity. Further separation of group C into four sub-groups can be seen to occur at ~55 - 60% Bray-Curtis similarity (Fig. 4.11a). The positions of the five main clusters and the four subsequent subgroups are presented in the tropical and subtropical Atlantic Ocean in Figure 4.12a, and indicate layering of the large phytoplankton community. Cluster C occurs in the upper waters of the southern hemisphere and in association with the surface waters of the northern subtropical gyre (Fig. 4.12a). In the southern hemisphere, clusters A and B occur below C, whereas cluster B occurs below D at the equator (and at the surface), and clusters A and B occur below E in the northern hemisphere (Fig. 4.12a). Cluster D is restricted in its occurrence to the surface at the equator and at depth ~9°S (Fig. 4.12a). Cluster E is found in the waters off NW Africa and at the northern end of the transect, and is found below clusters B and C from ~20 - 35°N (Fig. 4.12a). The CM varies in its composition and is found in several different clusters throughout the subtropical and tropical Atlantic (Fig. 4.12a); 35 - 10°S clusters C3 and C4 (with the notable exception of B at 19°S), 9°S cluster A, 0.05°N cluster B, 3.5°N cluster D, and 10 - 40°N cluster E (with the notable exception of clusters B and A at ~22 °N and 34°N, respectively).

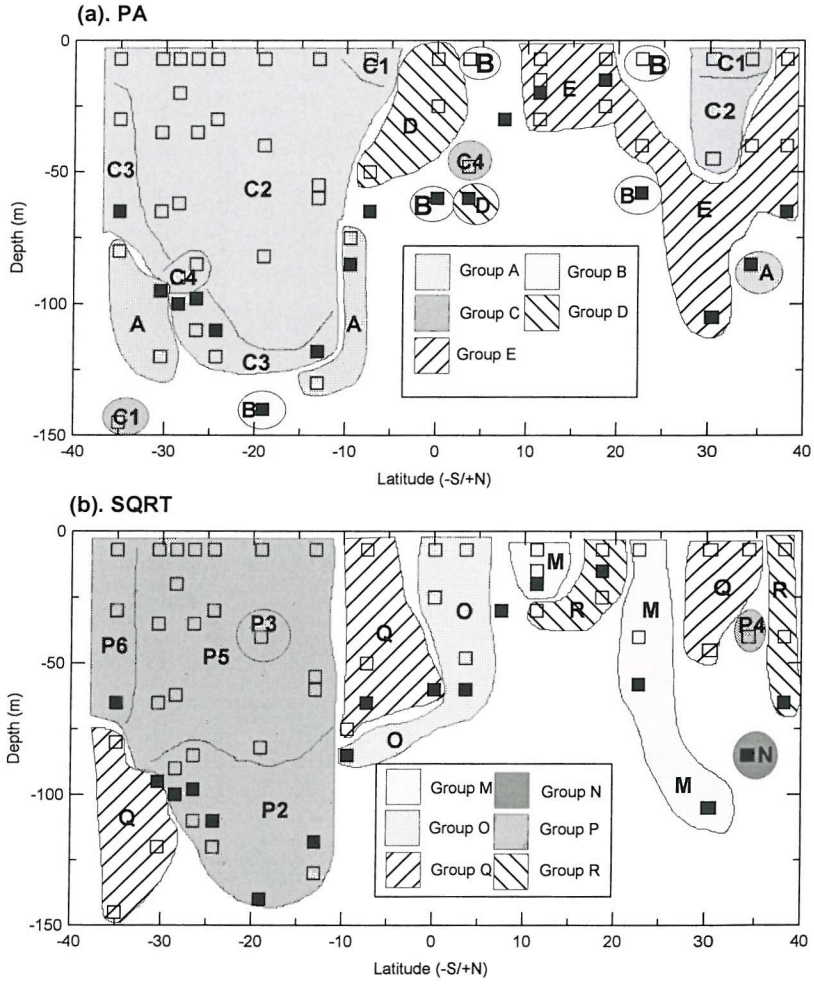


Figure 4.12: Sample clusters from species composition analysis; (a) PA treatment, and (b) SQRT treatment (see text). Open squares indicate sampling depths and filled squares indicate CM depth from acetone extraction. Groups are enclosed in shaded contours, although the contours are unlikely to fully represent the extent of the group's ranges and should be regarded as a 'best fit'. Note: Group C (a) and P (b) are subdivided into sub-clusters based on the cluster dendrograms and are keyed with numbers (see text).

Table 4.4: Summary table of the results from the breakdown of dissimilarity between sample clusters A - E into contributions from individual species (SIMPER analysis). Only the top 5 species and the total percentage dissimilarity explained by these species are presented. Table includes species codes (see Table 4.2), average dissimilarity between clusters (δ), average species' contribution to total dissimilarity (δi), average cell abundances of individual species in each cluster, ratio of δi to SD(δi), and cumulative percentage of individual species contributions to total dissimilarity.

| *Species Code* | *Average cell no. (cells $l^{-1}$)* | *Average cell no. (cells $l^{-1}$)* | *Average Species Contribution to Dissimilarity (δi)* | *Ratio of δi/SD (δi)* | *Cumulative percentage of total dissimilarity* |
|---|---|---|---|---|---|
| | Cluster A | Cluster B | Average δ = 57.2 | | |
| Ad40 | 11.4 | 76.0 | 2.0 | 2.3 | |
| Ad46 | 0.0 | 22.0 | 1.9 | 1.9 | |
| Ad47 | 17.1 | 80.0 | 1.7 | 1.5 | |
| CC11 | 37.1 | 4.0 | 1.7 | 1.5 | |
| CC13 | 20.0 | 0.0 | 1.6 | 1.5 | 15.6% |
| | Cluster A | Cluster C | Average δ = 52.4 | | |
| CC14 | 0.0 | 73.1 | 1.5 | 1.6 | |
| CC13 | 20.0 | 1.1 | 1.4 | 1.4 | |
| CC19 | 21.4 | 78.3 | 1.4 | 1.4 | |
| CC7 | 8.6 | 159.7 | 1.4 | 1.4 | |
| Ad47 | 17.1 | 53.1 | 1.3 | 1.3 | 13.2% |
| | Cluster A | Cluster D | Average δ = 56.5 | | |
| CC10 | 91.4 | 0.0 | 2.5 | 6.3 | |
| CC12 | 154.3 | 0.0 | 2.5 | 6.3 | |
| CC11 | 37.1 | 0.0 | 2.2 | 2.2 | |
| Ad49 | 1.4 | 45.0 | 2.2 | 2.2 | |
| D21 | 42.9 | 20.0 | 1.9 | 1.5 | 19.9% |
| | Cluster A | Cluster E | Average δ = 57.7 | | |
| D62 | 5.7 | 195.4 | 1.7 | 2.2 | |
| Ed9 | 14.3 | 66.1 | 1.6 | 1.9 | |
| Ad47 | 17.1 | 124.6 | 1.5 | 1.5 | |
| CC11 | 37.1 | 20.8 | 1.4 | 1.4 | |
| CC13 | 20.0 | 0.0 | 1.4 | 1.5 | 13.2% |
| | Cluster B | Cluster C | Average δ = 52.8 | | |
| CC7 | 0.0 | 159.7 | 1.8 | 2.6 | |
| CC19 | 0.0 | 78.3 | 1.4 | 1.6 | |
| CC14 | 0.0 | 73.1 | 1.4 | 1.7 | |
| CC20 | 0.0 | 47.7 | 1.4 | 1.5 | |
| Ad40 | 76.0 | 14.0 | 1.2 | 1.2 | 13.8% |
| | Cluster B | Cluster D | Average δ = 53.6 | | |
| Ad40 | 76.0 | 0.0 | 2.4 | 7.5 | |
| D81 | 0.0 | 55.0 | 2.4 | 7.5 | |
| D21 | 0.0 | 20.0 | 2.4 | 7.5 | |
| CC12 | 134.0 | 0.0 | 1.9 | 1.8 | |
| Ed1 | 26.0 | 250.0 | 1.5 | 1.1 | 20.0% |
| | Cluster B | Cluster E | Average δ = 53.5 | | |
| D62 | 0.0 | 195.4 | 1.9 | 6.0 | |
| Ad26 | 22.0 | 0.0 | 1.5 | 1.9 | |
| Ed9 | 8.0 | 66.1 | 1.5 | 1.6 | |
| D64 | 0.0 | 1986.1 | 1.4 | 1.7 | |
| Ed1 | 26.0 | 323.1 | 1.1 | 1.1 | 14.0% |
| | Cluster C | Cluster D | Average δ = 52.1 | | |
| CC7 | 159.7 | 0.0 | 1.9 | 2.6 | |
| D81 | 34.0 | 55.0 | 1.6 | 1.8 | |
| CC19 | 78.3 | 0.0 | 1.5 | 1.6 | |
| CC14 | 73.1 | 0.0 | 1.5 | 1.6 | |
| CC20 | 47.7 | 0.0 | 1.5 | 1.5 | 15.5% |
| | Cluster C | Cluster E | Average δ = 52.0 | | |
| Ed9 | 0.6 | 66.1 | 1.5 | 2.7 | |
| D62 | 4.9 | 195.4 | 1.5 | 2.2 | |
| D64 | 2.6 | 1986.1 | 1.2 | 1.6 | |
| CC19 | 78.3 | 54.6 | 1.1 | 1.4 | |
| CC20 | 47.7 | 18.5 | 1.1 | 1.2 | 12.3% |
| | Cluster D | Cluster E | Average δ = 49.1 | | |
| Ed9 | 0.0 | 66.1 | 1.9 | 2.9 | |
| Ad49 | 45.0 | 11.5 | 1.6 | 1.7 | |
| D64 | 0.0 | 1986.1 | 1.5 | 1.7 | |
| Ad40 | 0.0 | 451.5 | 1.4 | 1.4 | |
| D21 | 20.0 | 106.1 | 1.2 | 1.0 | 15.3% |

Breakdown of the dissimilarity between the main clusters into contributions from each species (SIMPER analysis) leads to statistical results that indicate the relative importance of all species (~105) present in the samples to the overall inter-sample differences. To aid interpretation of the SIMPER results only the top 5 species (representing 12.3 - 20% of the total dissimilarity) that are

important in determining the differences are presented and discussed (Table 4.4). Of interest are the differences between the major clusters A, C, D, E (Table 4.4); 15.6% of the dissimilarity between A and C (δA:C) is due to the absence of *Rhabdosphaera claviger* in A, higher numbers of *Pontosphaera* spp. in A and higher numbers of the 'Heart' coccolithophore, *Discosphaera tubifer* and *Oxytoxum* spp. in C; 15.5% of δC:D is due to the absence of *D. tubifer*, 'Heart', *R. claviger*, and *Gephyrocapsa ornata* and the higher abundance of *Thalassionema* spp. in D; 19.9% of δA:D is due to the absence of *Helicosphaera* spp., *Ophiaster* spp., *Oolithotus* spp., higher abundance of *Phalacroma rotundatum* and the lower abundance of *Phaeoceros Chaetoceros* spp. in D; 13.9% of δB:E is due to the absence or low numbers of *Proboscia alata*, *Myrionecta rubra*, *Pseudo-nitzschia* spp., and *Leptocylindrus mediterraneus* in B and the absence of *Ceratium teres* in E; 12.3% of δC:E is due to the low abundance of *M. rubra*, *P. alata*, and *Pseudo-nitzschia* spp. in C, and the relatively lower cell densities of 'Heart' and *Gephyrocapsa ornata* in E (Table 4.4). It appears from these results that D is separate from other clusters due to its lack of several species common in other groups, whereas E seems to have much lower numbers and species of coccolithophores than other clusters (Table 4.4).

Table 4.5: Summary table of the results from the breakdown of dissimilarity between sample clusters C1 - C4 into contributions from individual species (SIMPER analysis). Only the top 5 species and the total percentage dissimilarity explained by these species are presented. Table includes species codes (see Table 4.2), average dissimilarity between clusters (δ), average species' contribution to total dissimilarity (δi), average cell abundances of individual species in each cluster, ratio of δi to SD(δi), and cumulative percentage of individual species contributions to total dissimilarity.

| *Species Code* | *Average cell no. (cells l$^{-1}$)* | *Average cell no. (cells l$^{-1}$)* | *Average Species Contribution to Dissimilarity (δi)* | *Ratio of δi/SD (δi)* | *Cumulative percentage of total dissimilarity* |
|---|---|---|---|---|---|
| | Group C1 | Group C2 | Average δ = 46.1 | | |
| CC14 | 0.0 | 116.1 | 1.9 | 8.4 | |
| CC16 | 0.0 | 105.6 | 1.7 | 2.7 | |
| CC10 | 0.0 | 52.8 | 1.7 | 2.6 | |
| CC17 | 2.5 | 1285.6 | 1.4 | 1.7 | |
| Ad53 | 17.5 | 64.4 | 1.4 | 1.6 | 16.7% |
| | Group C2 | Group C3 | Average δ = 41.1 | | |
| D41 | 15.6 | 195.0 | 1.4 | 1.8 | |
| CC2 | 26.7 | 8.7 | 1.2 | 1.4 | |
| D52 | 6.7 | 695.0 | 1.1 | 1.3 | |
| CC3 | 1.1 | 41.2 | 1.1 | 1.2 | |
| CC6 | 0.6 | 25.0 | 1.1 | 1.2 | 14.1% |
| | Group C2 | Group C4 | Average δ = 48.1 | | |
| CC19 | 136.1 | 0.0 | 1.8 | 9.5 | |
| CC20 | 70.6 | 0.0 | 1.6 | 2.7 | |
| CC16 | 105.6 | 0.0 | 1.6 | 2.7 | |
| Msc16 | 89.4 | 0.0 | 1.5 | 2.2 | |
| D52 | 6.7 | 56.7 | 1.4 | 1.8 | 16.5% |
| | Group C3 | Group C4 | Average δ = 44.4 | | |
| CC11 | 55.0 | 0.0 | 1.7 | 2.5 | |
| Ad30 | 0.0 | 10.0 | 1.3 | 1.4 | |
| D29 | 0.0 | 46.7 | 1.3 | 1.4 | |
| D41 | 195.0 | 13.3 | 1.3 | 1.4 | |
| Ed5 | 0.0 | 16.7 | 1.2 | 1.4 | 15.5% |

Subdivision of cluster C shows that in the southern hemisphere cluster C2 is widespread at the surface and extends to a depth of ~120m in the central southern subtropical gyre (Fig. 4.12a). Below C2, clusters C3 and C4 are found in the southern hemisphere as an almost continuous layer ranging from ~35 - 10°S (Fig. 4.12a). In the northern hemisphere cluster C divides into C1 at the surface (C1 is also found at the surface at 9°S), and C2 slightly below, although the range and depth of cluster C is much reduced relative to the southern hemisphere (Fig. 4.12a). Breakdown of the dissimilarity between these subgroups of cluster C into the contribution from each species shows that

14.0 - 16.7% of the dissimilarity can be explained by just five species (Table 4.5); 16.7% of δC1:C2 is due to the absence of *R. claviger*, *Syracosphaera* spp., and *Helicosphaera* spp. from C2 and the much higher numbers of *Umbellosphaera irregularis* (and *U. tenuis*) and small *Prorocentrum* spp. in C1; 14.0% of δC2:C3 is due to the higher cell densities of *Haslea* spp., *Nitzschia longissima*, *Anoplosolenia brasiliensis* and *Calciosolenia murrayi* in C3 and the relatively lower numbers of *Acanthoica* spp. in C3; 16.5% of δC2:C4 is due to the absence of 'Heart', *Gephyrocapsa ornata*, *Syracosphaera* spp. and *Pyramimonas* spp. in C4 and the high numbers of *N. longissima* in C4; 15.5% of δC3:C4 is due to the absence of *Oolithotus* spp. in C4, the absence of *Ceratocorys* spp., *Dactyliosolen* spp. and *Hemiaulus hauckii* and higher cell densities of *Haslea* spp. in C3 (Table 4.5).

*(b). SQRT transformation of common species:* - Cluster analysis of the SQRT transformed species abundances shows separation into six clusters ~50% Bray-Curtis similarity level, with further separation of cluster P into six sub-groups at ~ 60% Bray-Curtis similarity (Fig. 4.11b). Superimposing the positions of the five main clusters and the four subgroups again reveals layering of the phytoplankton community in the subtropical and tropical Atlantic Ocean (Fig. 4.12b). Cluster M is found in upper waters at ~10°N and ~22°N and is also found at depth (100 m) at 30°N (Fig. 4.12b). Cluster N is only found once, at depth, in the northern subtropical gyre (Fig. 4.12b; 80 m, ~34°N), and thus will be ignored in further analysis. Cluster O is limited in its distribution to upper waters at the equator and at depth to the south (Fig. 4.12b; 85 m, ~9°S). Clusters P and Q are the most widespread of the groups identified from this analysis. Cluster P occupies the upper waters (<150 m) of the southern hemisphere from 35 - 10°S, and is also found at 40 m around ~ 34°N. Cluster Q occurs at depth from 35 - 30°S, from the surface to 80 m at ~9°S, at 60 m at ~0.05°N, and in the upper waters (<50 m) of the northern subtropical gyre (Fig. 4.12b). Cluster R is also limited in its range and only occurs in the upper waters at ~18°N, at 30 m at ~11°N, and at the northern extreme of the AMT-8 transect (Fig. 4.12b).

Breakdown of the dissimilarity between the main groups into contributions from each species shows that between 31.5 - 53.5% of the dissimilarity can be explained by just five species (Table 4.6); 34.1% of δP:Q is due to higher numbers of *U. irregularis* (and *U. tenuis*), 50 μm pennate diatoms (Pennate sp. 'C'), small coccolithophore species (*E. huxleyi*, *Gephyrocapsa* spp. and small 5 μm coccospheres) and *D. tubifer* in P and the higher abundance of small unidentified Pennate diatoms in Q; 53.5% of δQ:O is due to the absence of *Trichodesmium* spp. in Q, the higher numbers of Pennate sp. 'C' and *L. mediterraneus* in O and the higher cell densities of small (10 - 30 μm) unidentified pennates and small coccolithophore species in Q; 52.1% of δM:O is due to the absence of *Trichodesmium* spp. in M, the higher numbers of small (10 - 30 μm) unidentified pennates, small coccolithophores and Pennate sp. 'C' in P and the lower numbers of *U. irregularis* (and *U. tenuis*) in P; 34.7% of δM:R is due to the lower cell densities of *Pseudo-nitzschia* spp., small coccolithophores, *L. danicus* (and *L. minimus*), Pennate sp. 'C' and small (10 - 30 μm) unidentified pennates in M; 35.2% of δM:Q is due to the higher numbers of small (10 - 30 μm) unidentified pennates, small coccolithophores, *Cryptomonad* spp. and medium sized coccolithophore species (10-25μm) in Q and the lower numbers of *U. irregularis* (and *U. tenuis*) in Q; 34.6% of δQ:R is due to the low numbers of *Pseudo-nitzschia* spp., small coccolithophores, *L. danicus* (and *L. minimus*), Pennate sp. 'C' and

*Prorocentrum dentatum* in Q (Table 4.6). The phytoplankton composition of the CM changes with latitude (Fig. 4.12b); 35 - 10°S cluster P (subgroups P6 and P2, and notably cluster Q at ~28°S), 9°S - 3.5°N cluster O (with the exception of cluster Q at 0.05°N), 11°N and 22 - 30°N cluster M, 18°N and 38°N cluster R, and 34°N cluster N.

Table 4.6: Summary table of the results from the breakdown of dissimilarity between sample clusters M - R into contributions from individual species (SIMPER analysis). Only the top 5 species and the total % dissimilarity explained by these species are presented. Table includes species codes (see Table 4.2), average dissimilarity between clusters (δ), average species' contribution to total dissimilarity (δi), average cell abundances of individual species in each cluster, ratio of δi to SD(δi), and cumulative percentage of individual species contributions to total dissimilarity.

| *Species Code* | *Average cell no. (cells $l^{-1}$)* | *Average cell no. (cells $l^{-1}$)* | *Average Species Contribution to Dissimilarity (δi)* | *Ratio of δi/SD (δi)* | *Cumulative percentage of total dissimilarity* |
|---|---|---|---|---|---|
| | Cluster M | Cluster O | Average δ = 55.4 | | |
| Ed12 | 0.0 | 10462.3 | 16.0 | 1.7 | |
| D56 | 111.4 | 913.3 | 4.4 | 2.0 | |
| CC17 | 610.0 | 155.0 | 3.2 | 1.0 | |
| CC8 | 1074.3 | 1288.3 | 2.8 | 1.4 | |
| D57 | 85.7 | 300.0 | 2.4 | 1.5 | 52.1% |
| | Cluster M | Cluster P | Average δ = 54.0 | | |
| CC17 | 610.0 | 949.3 | 5.1 | 1.7 | |
| CC8 | 1074.3 | 1779.3 | 3.5 | 1.8 | |
| D56 | 111.4 | 526.3 | 3.3 | 1.6 | |
| CC1 | 314.3 | 1164.7 | 3.3 | 1.4 | |
| D57 | 85.7 | 315.0 | 2.3 | 0.9 | 32.5% |
| | Cluster M | Cluster Q | Average δ = 54.4 | | |
| D56 | 111.4 | 1057.8 | 5.7 | 1.4 | |
| CC8 | 1074.3 | 1662.7 | 4.1 | 1.3 | |
| CC17 | 610.0 | 27.3 | 3.7 | 0.8 | |
| Msc3 | 237.1 | 270.9 | 2.9 | 1.0 | |
| CC1 | 314.3 | 735.4 | 2.8 | 2.0 | 35.2% |
| | Cluster M | Cluster R | Average δ = 61.8 | | |
| D64 | 57.1 | 3631.4 | 7.2 | 3.7 | |
| CC8 | 1074.3 | 5807.1 | 4.2 | 0.9 | |
| D45 | 31.4 | 1600.0 | 3.6 | 1.2 | |
| D57 | 85.7 | 1842.9 | 3.3 | 1.1 | |
| D56 | 111.4 | 1014.3 | 3.1 | 1.6 | 34.7% |
| | Cluster O | Cluster P | Average δ = 51.6 | | |
| Ed12 | 10462.3 | 67.0 | 13.9 | 1.6 | |
| CC17 | 155.0 | 949.3 | 3.4 | 1.4 | |
| D57 | 300.0 | 315.0 | 2.4 | 1.4 | |
| D56 | 913.3 | 526.3 | 2.3 | 1.4 | |
| CC8 | 1288.3 | 1779.3 | 2.0 | 1.5 | 46.5% |
| | Cluster O | Cluster Q | Average δ = 52.4 | | |
| Ed12 | 10462.3 | 0.0 | 16.9 | 1.7 | |
| D56 | 913.3 | 1057.3 | 3.3 | 1.4 | |
| D57 | 300.0 | 15.4 | 3.1 | 1.9 | |
| CC8 | 1288.3 | 1662.7 | 2.9 | 1.3 | |
| Ed1 | 195.0 | 26.4 | 1.9 | 1.4 | 53.5% |
| | Cluster O | Cluster R | Average δ = 63.0 | | |
| Ed12 | 10462.3 | 0.0 | 10.2 | 1.5 | |
| D64 | 16.7 | 3631.4 | 6.8 | 4.3 | |
| D45 | 0.0 | 1600.0 | 3.2 | 1.1 | |
| CC8 | 1288.3 | 5807.1 | 3.2 | 0.7 | |
| D57 | 300.0 | 1842.9 | 2.6 | 1.1 | 41.3% |
| | Cluster P | Cluster Q | Average δ = 48.2 | | |
| CC17 | 949.3 | 27.3 | 5.1 | 1.6 | |
| D56 | 526.3 | 1057.3 | 3.6 | 1.4 | |
| CC8 | 1779.3 | 1662.7 | 3.2 | 1.5 | |
| D57 | 315.0 | 15.4 | 2.4 | 0.8 | |
| CC7 | 190.0 | 12.7 | 2.1 | 1.3 | 34.1% |
| | Cluster P | Cluster R | Average δ = 62.4 | | |
| D64 | 1.7 | 3631.4 | 7.2 | 4.7 | |
| D45 | 0.7 | 1600.0 | 3.3 | 1.1 | |
| CC8 | 1779.3 | 5707.1 | 3.1 | 0.7 | |
| D57 | 315.0 | 1842.9 | 3.1 | 1.1 | |
| CC17 | 949.3 | 45.7 | 2.9 | 1.4 | 31.5% |
| | Cluster Q | Cluster R | Average δ = 64.7 | | |
| D64 | 3.6 | 3631.4 | 8.1 | 4.7 | |
| CC8 | 1662.7 | 5807.1 | 4.0 | 0.8 | |
| D45 | 0.0 | 1600.0 | 3.7 | 1.1 | |
| D57 | 15.4 | 1842.9 | 3.6 | 1.1 | |
| Ad50 | 4.5 | 1070.0 | 2.9 | 0.9 | 34.6% |

Subdivision of cluster P shows a similar pattern to that of the P/A analysis (Fig. 4.12a), with P1 and P2 occurring at depth in the southern hemisphere and P3 and P5 occurring in surface and subsurface waters. Cluster P4 occurs only once, at depth in the northern hemisphere (Fig. 4.12b; 40 m, 34°N) and will therefore, along with P1, be largely disregarded from further analysis. Cluster P6 is seen to occur in surface waters at the southern end of the AMT-8 transect (~35°S) from the surface to 65 m (Fig. 4.12b). Breakdown of the dissimilarity between these subgroups of cluster P into the contribution of each species shows that 33.7 - 50.2% of the dissimilarity can be explained by just five species (Table 4.7); 33.7% of δP2:P5 is due to higher numbers of Pennate sp. 'C', *Ophiaster* spp. and *Haslea* spp. in P2 and lower numbers of *U. irregularis* (and *U. tenuis*) and small (10 - 30 μm) unidentified pennates in P2; 50.2% of the δP3:P5 is due to higher numbers of *U. irregularis* (and *U. tenuis*), medium sized (10-25 μm) coccolithophores and small (10 - 30 μm) unidentified pennates in P3, lower cell densities of small coccolithophores and the absence of *Thalassionema* spp. in P5; 34.8% of δP5:P6 is due to higher numbers of *N. longissima*, *Haslea* spp. and *D. tubifer* in P6 and lower abundances of medium sized coccolithophores and small (10 - 30 μm) unidentified pennates in P6 (Table 4.7).

Table 4.7: Summary table of the results from the breakdown of dissimilarity between sample clusters P2 - P6 into contributions from individual species (SIMPER analysis). Only the top 5 species and the total dissimilarity explained by these species are presented. Table includes species codes (see Table 4.2), average dissimilarity between clusters (δ), average species' contribution to total dissimilarity (δi), average cell abundances of individual species in each cluster, ratio of δi to SD(δi), and cumulative percentage of individual species contributions to total dissimilarity.

| Species Code | Average cell no. (cells l-1) | Average cell no. (cells l-1) | Average Species Contribution to Dissimilarity (δi) | Ratio of δi/SD(δi) | Cumulative percentage of total dissimilarity |
|---|---|---|---|---|---|
| | Group P2 | Group P5 | Average δ = 41.4 | | |
| D57 | 844.4 | 99.3 | 3.4 | 1.1 | |
| CC17 | 394.4 | 1101.3 | 3.0 | 1.5 | |
| D56 | 354.4 | 724.7 | 2.7 | 1.7 | |
| CC12 | 430.0 | 27.3 | 2.6 | 1.7 | |
| D41 | 209.0 | 7.3 | 2.1 | 1.5 | 33.7% |
| | Group P3 | Group P5 | Average δ = 37.8 | | |
| CC17 | 6270.0 | 1101.3 | 7.6 | 4.9 | |
| CC1 | 3580.0 | 1071.3 | 4.6 | 3.3 | |
| CC8 | 3560.0 | 2012.7 | 2.6 | 2.9 | |
| D81 | 240.0 | 0.00 | 2.5 | 16.8 | |
| D56 | 240.0 | 724.7 | 1.7 | 1.5 | 50.3% |
| | Group P5 | Group P6 | Average δ = 37.1 | | |
| D52 | 2.0 | 1256.7 | 3.7 | 0.9 | |
| CC1 | 1071.3 | 270.0 | 2.8 | 1.5 | |
| D41 | 7.3 | 230.0 | 2.3 | 2.5 | |
| D56 | 724.7 | 226.7 | 2.1 | 1.5 | |
| CC7 | 224.7 | 556.7 | 2.0 | 1.7 | 34.8% |

### 4.3.4. Basin-scale Recurrent Species Analysis: Species Assemblages

Further analysis of the spatial changes in the species composition of the phytoplankton community is carried out using a slightly different approach to the cluster analysis of sample species composition; cluster analysis of species distributions to identify species assemblages, or recurrent species analysis (Venrick, 1999). Recurrent species analysis is based on determining the similarity of species occurrences in all samples; i.e. the similarity in the distribution of species. In this analysis rare species (consistently <3% of total numbers) have been removed and a square-root transformation (SQRT) has been applied to downplay the influence of the dominant species. The cluster dendrogram for recurrent species analysis is presented in Figure 4.13, and shows separation

of species clusters at several levels. Five species clusters can be identified ~20 - 30% Bray-Curtis similarity level (Fig. 4.13). Cluster 1 includes only one species (*Trichodesmium* spp.), cluster 2 includes 23 species (all the coccolithophores are included in this group), cluster 3 includes 3 species, cluster 4 includes 4 species and cluster 5 includes 9 species (Table 4.8). Subdivision of cluster 2 is also possible at ~38% Bray-Curtis similarity level (Fig. 4.13), with cluster 2a containing 2 diatoms and 2 coccolithophore species, and cluster 2b containing the remaining 19 species (see Table 4.6).

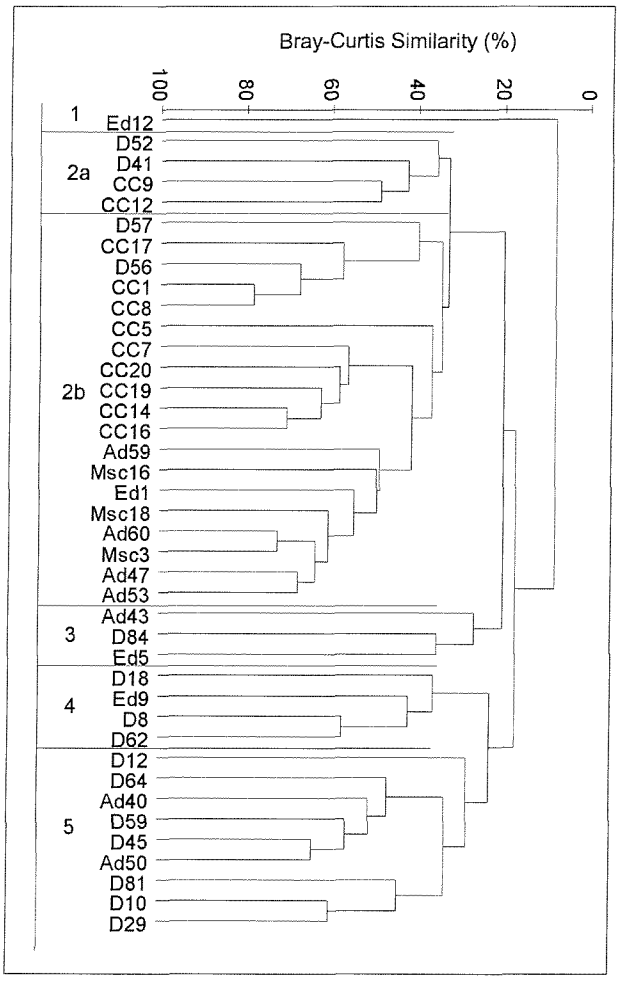


Figure 4.13: Cluster dendrogram for the recurrent species analysis showing the separation of five assemblages (identified with numbers 1 - 5).

Table 4.8: Results table of the recurrent species analysis, indicating the species included in each assemblage (see Table 4.2 for species names) and the abundance of each assemblage.

| Assemblage | Species Codes | Abundance Range |
|---|---|---|
| Assemblage 1 | ED12 | 0 - 23.8 cells x $10^{-3}$ $l^{-1}$ |
| Assemblage 2a | CC9, CC12, D41, D52 | 0 - 4.4 cells x $10^{-3}$ $l^{-1}$ |
| Assemblage 2b | D56, D57, AD47, AD53, AD59, AD60, CC1, CC14, CC16, CC17, CC19, CC20, CC5, CC7, CC8, MSC3, MSC16, MSC18 | 2.0 - 40.8 cells x $10^{-3}$ $l^{-1}$ |
| Assemblage 3 | D84, AD43, ED5 | 0 - 1.1 cells x $10^{-3}$ $l^{-1}$ |
| Assemblage 4 | D8, D18, D62, ED9 | 0 - 2.1 cells x $10^{-3}$ $l^{-1}$ |
| Assemblage 5 | D10, D12, D29, D45, D59, D64, D81, AD40, AD50 | 0 - 13.9 cells x $10^{-3}$ $l^{-1}$ |

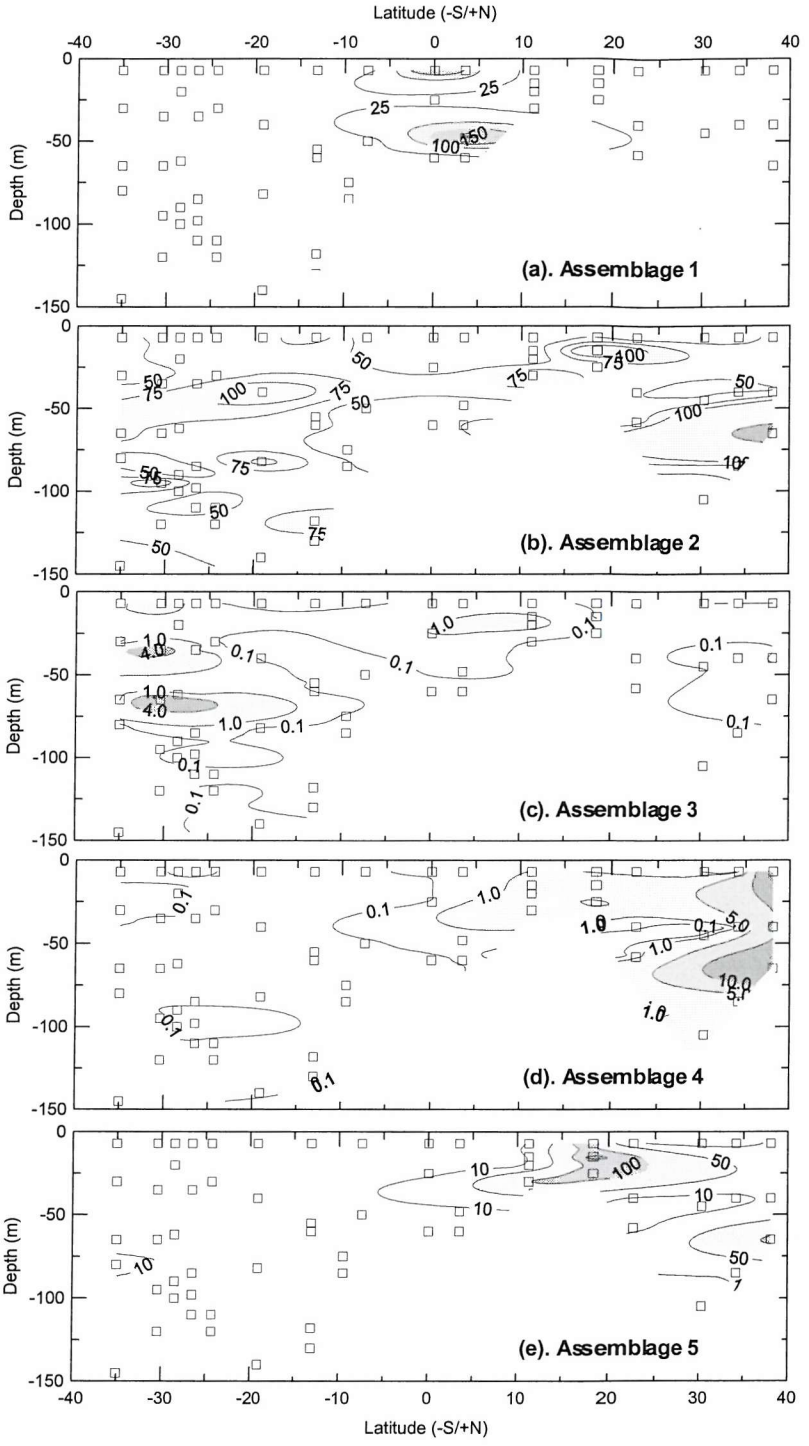


Figure 4.14: The abundance (cells x $10^2$ $l^{-1}$) and distribution of the five species assemblages identified from recurrent species analysis; (a) assemblage 1, (b) assemblage 2, (c) assemblage 3, (d) assemblage 4, and (e) assemblage 5. Open squares indicate the sampling depths. The species in each assemblage are identified in Table 4.8.

The abundance and distribution of the five species assemblages in the tropical and subtropical Atlantic Ocean are presented in Figure 4.14. *Trichodesmium* spp. is present in low abundance's in several regions of the Atlantic Ocean, although its numerical maximum in this study is found in surface waters and at depth (50 m) around the equator (Fig. 4.14a). Assemblage 2 is also found throughout the subtropical and tropical Atlantic Ocean, with abundance maxima located at 40 m at 19°S, 95 m at 30°S, 15 m at 20°N and 65 m at 38°N (Fig. 4.14b). The assemlage 2 maximum at 19°S is due to the high abundance of the coccolithophores *Umbellosphaera irregularis* and *U.*

*tenuis*. The other assemblage 2 maximum at 38°S is mainly composed of small coccolithophore species; *Emiliania huxleyi*, *Gephyrocapsa* spp. and small 5 μm unidentified coccospheres. Assemblage 3 has its numerical maximum at between ~28 - 30°S (high cell densities of the diatoms *Mastogloia rostrata* and *Hemiaulus hauckii*), although the abundance range of this group is much lower than those of groups 1, 2, and 5 (Fig. 4.14c; Table 4.8). Assemblage 4 has a relatively lower abundance range (Table 4.8) and is limited in its distribution to waters at the northern end of the transect (Fig. 4.14d); with high numbers of the diatom species *Bacteriastrum* spp. and *Proboscia alata*, and to a lesser extent the diatom *Cerataulina pelagica* and the planktonic ciliate *Myrionecta rubra*. Assemblage 5 is restricted in its range to the northern hemisphere, with highest cell densities ~20°N and at depth (65 m) at ~38°N. The maximum of assemblage 5 off NW Africa (Fig. 4.14e) is due to an increase in all species of this group, especially the diatoms *L. danicus*, *L. minimus*, *Pseudo-nitzschia* spp., and the autotrophic dinoflagellate *Prorocentrum dentatum*, whereas the maximum at 38°N (Fig. 4.14e) is mainly of the diatom *Pseudo-nitzschia* spp. and to a lesser extent the diatoms *L. danicus*, *L. minimus*, and *Dactyliosolen* spp.

## 4.4. Discussion

### 4.4.1. Community Composition: Pigments

Phytoplankton pigment concentrations in the marine environment are primarily dependent upon the species (community) composition and photo-adaptive state of the community (Bidigare *et al.*, 1990). Along the AMT-8 transect there are several changes in the hydrographic conditions, which have consequences for the phytoplankton community; from strongly stratified oligotrophic conditions in the northern and southern subtropical gyres to mesotrophic and eutrophic semi-turbulent conditions around the equator, off NW Africa and at the northern end of the transect (Chapter 3). Total chlorophyll *a* concentration (Tchl*a* and HPLC TChl *a*), as an expression of phytoplankton biomass, ranges from low concentrations in the gyres (<0.1 - 0.2 mg Chl $m^{-3}$) to high concentrations around the equator (>0.4 mg Chl $m^{-3}$), off NW Africa (>0.4 - 0.6 mg Chl $m^{-3}$) and at the northern end of the transect (0.2 - >0.4 mg Chl $m^{-3}$; Fig. 4.2a, 4.3a). Changes in the phytoplankton community standing stock (chlorophyll *a*) are seen to coincide with changes in the depth of the CM (Fig. 4.2a, 4.3a).

Changes in the phytoplankton community composition occur along the increasing chlorophyll *a* gradient from subtropical waters to equatorial and NW Africa waters. Low TChl *a* waters (0.05 - 0.2 mg $m^{-3}$) are dominated by prochlorophyte and cyanophyte pigments (Dv Chl *a*, Zea, TChl *b*, Chl *a*), with contributions from prymnesiophyte and chrysophyte/pelagophyte pigments (Hex-fuco and But-fuco). High TChl *a* waters (>0.2 mg Chl $m^{-3}$) are dominated by cyanophyte pigments (Zea and Chl *a*), with increased contributions of prymnesiophytes, chrysophytes/pelagophytes and diatoms (Fuco), and minor contributions from dinoflagellates (Peridin), cryptophytes (Allo) and chlorophytes (Lut and TChl *b*). Equatorial waters are characterised by elevated concentrations relative to the subtropical gyres of pigments that typify more oligotrophic waters; Dv Chl *a*, Zea, TChl *b*, Chl *a*, Hex-fuco and But-fuco. Northern temperate waters (35 - 40°N) are separated from northern gyral waters, with waters at depth around 38°N characterised by communities with pigment signatures statistically similar to waters off NW Africa (Fig. 4.6).

Community composition changes follow the observed phytoplankton and hydrographic relationships seen by Bustillosguzman *et al.,* (1995) in the Mediterranean Sea; cyanophytes and prochlorophytes seem to prefer highly stratified conditions, prymnesiophytes and chrysophytes /pelagophytes are found in a wide variety of conditions, and diatoms and chlorophytes are more abundant under semi-mixed or mixed conditions. Based solely on the distribution of peridinin, dinoflagellates would appear to be distributed similar to diatoms and chlorophytes, however, the species data show that dinoflagellates fit into the scheme at several levels; species are found in both oligotrophic and highly eutrophic conditions. Hydrographic relationships are based on nutrient and light availability, with stratified conditions causing nutrient limitation (upper waters) and light limitation (deeper waters), and increased turbulence reducing the limitation of both. Within the tropical and subtropical Atlantic Ocean, the subtropical gyres are characteristically oligotrophic with a deep euphotic zone, whereas around the equator upwelling of cold nutrient rich water causes elevated nutrient concentrations (Chapter 3). Dominance of low nutrient waters by pico- and nano-plankton (prochlorophytes, cyanophytes, prymnesiophytes and chrysophytes/pelagophytes) is thought to be due to nutrient, photophysiological and metabolic advantages inherent of small cell sizes and their low surface area to volume ratios (Raven, 1998); small cells have been shown to absorb more light relative to their volume (Agusti, 1994) and have lower nutrient limitation thresholds (Chisholm, 1992; Agawin *et al.,* 2000). With increased nutrient availability, picoplankton are likely to reach their maximum potential biomass and large cells (diatoms and dinoflagellates), with higher maximum growth rates, can outcompete smaller cells for resources (Chisholm, 1992).

Throughout the subtropical and tropical Atlantic Ocean a significant portion of TChl *a* is associated with the prochlorophyte biomarker pigment divinyl chlorophyll *a;* with contributions to TChl *a* within this study between 20 to 50% (Fig. 4.3b). High contributions of divinyl chlorophyll *a* have been found in many low nutrient environments by several other authors; subtropical Northeast Atlantic up to 50% (Veldhuis and Kraay, 1990), Southern Sargasso 25 - 40% (Goericke and Repeta, 1993), eastern Sargasso Sea 60 - 64% (Partensky *et al.,* 1996), Caribbean consistently 38% (McManus and Dawson, 1994), Western Mediterranean 11 - 40% (Barlow *et al.,* 1997a), Northeast Atlantic 48% in surface waters and 21 - 26% at depth in the CM (Gibb *et al.,* 2001). Previous reports from the AMT program have also found high contributions (up to 66.6%) in surface waters of the subtropical Atlantic (Gibb *et al.,* 2000). It is clear from this study that in the CM of central areas of the subtropical south Atlantic Ocean prochlorophytes (Dv Chl *a*) represent around 50% of the photosynthetic biomass, and are an important component of the phytoplankton community not fully accounted for in the species analysis of this chapter.

High concentrations of chlorophyll *b* (TChl *b*) are also found in association with the CM throughout the subtropical and tropical Atlantic Ocean (Fig. 4.3c), although there are several phytoplankton groups which may have contributed to this maxima; prochlorophytes (Dv Chl *b*), chlorophytes (Chl *b*) and prasinophytes (Chl *b*). Prochlorophytes and chlorophytes have been found to photoacclimate to decreasing light conditions and increasing amounts of blue-green light by increasing cellular concentrations of Chl *b* (Iriarte and Purdie, 1993; Partensky *et al.,* 1993; Bricaud *et al.,* 1999). Such light conditions are found at the bottom of the euphotic zone in the tropical and subtropical ocean, which means that both these groups are adapted to living deep in the euphotic

zone and Chl *b* containing phytoplankton are selected for in this environment (McManus and Dawson, 1994; Ohki and Honjho, 1997).

Many studies have concluded that large concentrations of Chl *b* at depth in association with the CM are indicative of large chlorophyte populations living at depth (e.g. Gieskes and Kraay, 1986; Gibb *et al.,* 2000). However, observations by Goericke and Repeta (1993) have led to the rejection of such conclusions and these authors provide evidence that the majority of Chl *b* found in the subtropical open-ocean is derived from prochlorophytes photoacclimated to the low light conditions deep in the photic zone. Recent results from the North Pacific Subtropical Gyre (NPSG) have shown significant relationships between Chl *b* and the prochlorophyte-derived red fluorescence signal, indicating that prochlorophytes are the major source of Chl *b* in subtropical waters (Karl *et al.,* 2001a). Within this study prasinoxanthin (prasinophytes) and violaxanthin (some chlorophytes) were undetected throughout the tropical and subtropical Atlantic Ocean, whereas lutein (some chlorophytes) was only present in very small concentrations off NW Africa It seems reasonable to conclude, therefore, that the Chl *b* found throughout the Atlantic Ocean, apart from off NW Africa, was mainly derived from photoacclimated prochlorophyte populations, and that an increased contribution may have been made off NW Africa by chlorophytes and possibly prasinophytes. Pigment measurements from the NPSG have also shown an absence of detectable concentrations of violaxanthin and lutein, which suggests that chlorophytes are also relatively rare in the water-column of the NPSG (Bidigare *et al.,* 1990; Letelier *et al.,* 1993). However, it should be noted that the situation could be more complicated than this due to the known occurrence of some chlorophyte species completely lacking in prasinoxanthin (Foss *et al.,* 1986), observations from coastal waters of a *Gymnodinium* spp. containing endosymbiotic Chl *b* (Sournia *et al.,* 1992) and the possibility of previously unknown prasinophytes as components of the picoeukaryotic community.

The widespread distribution of Hex-fuco and But-fuco indicate the importance of prymnesiophytes and pelagophytes (chrysophytes) in the subtropical and tropical Atlantic Ocean. There is also a possibility that autotrophic dinoflagellates may contribute to the distribution of these pigments despite the lack of significant peridinin concentrations. A study from subtropical waters of the Atlantic and Pacific Oceans utilising high resolution Electron Microscope images of algal cells and HPLC measurements of phytoplankton pigment signatures found a discrepancy between the relative abundance of identifiable dinoflagellate cells and peridinin concentrations (Anderson *et al.,* 1996). Anderson *et al.,* (1996) found significantly higher dinoflagellate cell abundances than would be expected solely from peridinin concentrations and noted that many dinoflagellate species may contain other pigments (e.g. But-fuco). Temporal studies in the NPSG have only ever found detectable peridinin concentrations during spring (Bidigare *et al.,* 1990; Letelier *et al.,* 1993). Although, peridinin is thought to be the major photosynthetic carotenoid for most autotrophic dinoflagellates, some *Gymnodinium* spp. have been found to lack peridinin and contain either Fuco, Hex-fuco and/or But-fuco, or a combination, as the major photosynthetic pigments (Millie *et al.,* 1993). Microscopic counts of algal cells during AMT-8 found a number of autotrophic dinoflagellate species present in subtropical and tropical waters, as well as large concentrations of small dinoflagellates that could not be fully identified or classified as autotrophic or heterotrophic and have not been included in the statistical analysis. Thus, small naked dinoflagellates may contribute more

to the phytoplankton communities in subtropical waters than previously thought and there is a need for adequate sampling procedures (e.g. epifluorescence microscopy).

One major problem of this study is the lack of measurements of phycobilin pigments. Although phycobilins are mostly absent from prochlorophytes (Goericke and Repeta, 1993; cf. Penno *et al.,* 2000), they constitute the major light harvesting pigments for other cyanobacteria (Falkowski and Raven, 1997). At present there is no easily employed HPLC method for the measurement of phycobilins as well as other phytoplankton pigments (Jeffrey, 1997), and thus there are few coupled measurements of both phycobilin and carotenoid distribution in the open ocean. Measurements of picoplankton community structure from previous AMT cruises (AMT-3 and 4) have shown that within the southern and northern subtropical gyres prochlorophytes dominate the community in terms of numbers, whereas *Synechococcus* and other picoplankton (picoeukaryotes) are found at relatively lower abundances; prochlorophytes 100,000 - 280,000 $x10^3$ cells $l^{-1}$, *Synechococcus* spp. 4,000 $x10^3$ cells $l^{-1}$ and picoeukaryotes <1,000 $x10^3$ cells $l^{-1}$ (Zubkov *et al.,* 1998). Sharp changes in picoplankton abundance are observed around the equator where prochlorophytes increase dramatically (up to 280,000 $x10^3$ cells $l^{-1}$), and *Synechococcus* spp. and picoeukaryotes have been shown to form deep abundance maxima (23,000 $x10^3$ cells $l^{-1}$ and 10,000 $x10^3$ cells $l^{-1}$, respectively; Zubkov *et al.,* 1998). Changes in the picoplanktonic community were also observed in waters off NW Africa (Zubkov *et al.,* 1998), where prochlorophytes decreased dramatically (40,000 $x10^3$ cells $l^{-1}$) and were replaced by higher abundances of *Synechococcus* (100,000 $x10^3$ cells $l^{-1}$) and to a lesser extent picoeukaryotes (~9,000 $x10^3$ cells $l^{-1}$). Thus, phycobilins are likely to be important in terms of the pigment budget throughout the subtropical and tropical Atlantic Ocean, especially off NW Africa and around the equator.

### 4.4.2. Pigment layering

It is clear from the results presented in this chapter that there is a degree of vertical separation of the pigment signatures of the phytoplankton community in the subtropical and tropical Atlantic Ocean (section 4.2.3). Pigment layering is driven by related pigment concentration and depth changes; low pigment concentrations are associated with surface and deep waters and high pigment concentrations are associated with the CM. Changes in the depth of the CM influence the degree of layering of the community in terms of pigments with largest differences in composition where the CM is deep and higher similarity between layers where the CM is shallow. Accessory pigment diversity also changes relative to the CM depth, with high diversity in the CM and low diversity in surface waters and where the CM is subsurface (Fig. 4.3).

*Subtropical waters* - Within the subtropical southern and northern gyres, surface waters contain low concentrations of all pigments with slightly higher Zea and Diadino concentrations. Due to its role as a photoprotective pigment Zea concentrations would be expected to decrease significantly with depth, and although in some areas they do, Zea concentrations are generally stable with depth. Culturing work with *Prochlorococcus marinus* and *Synechococcus* spp. have shown that Zea concentrations can remain relatively constant despite large changes in irradiance (Kana et al., 1988; Partensky *et al.,* 1993; Bricaud *et al.,* 1999), which would explain inconsistencies in the Zea depth distribution. It is also clear from these results that Zea is the dominant accessory pigment in

surface waters and this indicates the dominance of cyanophytes and prochlorophytes which are photoadapted to the high irradiances experienced in surface waters (Chapter 3), which would otherwise lead to large rates of photoinduced damage to the photosynthetic apparatus (Falkowski and Raven, 1997).

With increasing depth there is an increase in pigment concentrations in association with the CM, showing that the CM in subtropical waters is not just a chlorophyll *a* maxima but is also a significant pigment maxima. The CM layer is associated with increases in all pigments, especially accessory pigments associated with light harvesting (photosynthetic pigments) such as Hex-fuco and But-fuco. There is a swap in dominant accessory pigment with depth; Zea dominates surface waters, whereas deep CM waters are dominated by Hex-fuco (Fig. 4.3f). Such a change in dominance has implications for the community photophysiology, with surface waters being primarily concerned with photoprotection and deep layers more concerned with light harvesting. Other authors have reported similar vertical structuring of pigment signatures, with upper waters dominated by Chl *a* and Zea and a transition of the community associated with the CM where Chl *b* and Hex-fuco are abundant (Gieskes and Kraay, 1986; Ondrusek *et al.,* 1991). Gieskes and Kraay (1986) also reported that another unknown fucoxanthin-derivative was abundant at depth, and with hindsight this pigment was probably But-fuco. High concentrations of Hex-fuco and But-fuco within the CM are thought to support the idea that eukaryotic pico- and nanophytoplankton compromise higher proportions of the community at depth (McManus and Dawson, 1994).

The CM layer is also associated with much higher concentrations of Dv Chl *a* and Chl *b*, which would indicate that there is also a large prochlorophyte contribution to the community in the CM. However, cell densities of prochlorophytes and other picoplankton have been found previously to have similar cell densities throughout the water column and an absence of any detectable maximum (Zubkov *et al.,* 1998). Thus, the CM in subtropical waters is not a biomass maximum, but a pigment maximum associated with increased cellular concentrations of photosynthetic pigments and not with an increase in cell densities (Cullen, 1982; Maranon *et al.,* 2000). Light conditions deep in the euphotic zone of the subtropical oceans are characterised by very low photon fluxes and spectral shifts in the light from green to blue with increasing depth (Bidigare *et al.,* 1990). These changes in the underwater light field favour a change in pigments suited to these light conditions from Fuco (blue to green) to Hex-fuco and Chl *c* (blue-green) to Chl *b* (blue) (Bidigare *et al.,* 1990). Phytoplankton respond to decreases in light and spectral shifts by increasing total cellular pigment concentrations and different phytoplankton groups are best suited to different depths (Falkowski and Raven, 1997). Deeper layers in the subtropical Atlantic Ocean are characterised by an absence of photoprotectant pigments, and a decrease in all photosynthetic pigments, although there are higher concentrations of But-fuco than in the surface that may indicate the importance of low-light adapted pelagophytes/chrysophytes. A similar layered structure from the Sargasso Sea was described by Claustre and Marty (1995) which included cyanophytes dominant in surface waters with 100-10% of surface irradiance, prochlorophytes at intermediate depths (10-0.1%) and flagellates below the euphotic zone (0.1-0.01%).

*Equatorial, semi-temperate and NW Africa* - CM formation in waters with elevated nutrient concentrations is not linked to cellular increases in pigment levels (photoacclimation), but is thought to be due to *in-situ* growth and/or sinking of algal cells to a density discontinuity (Cullen, 1982). The

results presented in this chapter indicate that the CM pigmental composition and layering structure around the equator is similar to that found in southern subtropical waters (Fig. 4.6). Other studies of the community composition in the equatorial Atlantic Ocean have shown similar results (Zubkov *et al.,* 1998; Maranon et al., 2001), leading to the conclusion that increased equatorial nutrient availability lead to an increase in the characteristically oligotrophic community with no change in community composition or succession to alternative communities (cf. Herbland *et al.,* 1987). High concentrations of Zea around the equator (Fig. 4.2e) are likely to be due to higher abundances of cyanophytes, which is supported by reports of higher *Synechococcus* (Zubkov *et al.,* 1998) and *Trichodesmium* cell densities in this area (Tyrrell *et al.,* submit.).

Off NW Africa the CM is shallow and there is a high degree of similarity between the pigments present in surface waters and in the CM (Fig. 4.5). Elevated nutrient concentrations in this area (Chapter 3) cause higher pigment concentrations and increased contributions from diatoms (Fuco), dinoflagellates (Peridin) and chlorophytes (Chl *b*) to the community composition. Shallowing and strengthening of the CM causes deeper waters to be almost completely devoid of most pigments and algal cells found at these depths are likely to be unhealthy or in the form of cysts.

Elevated pigment concentrations are also found as a thin stratum in the northern hemisphere and at the northern end of the AMT-8 transect (Fig. 4.6). This is indicative of higher nutrient availability in northern subtropical waters than southern subtropical waters, which is probably due to the AMT-8 cruise track; during the northern leg of AMT-8 the cruise track passes along the 20°W meridional (Fig. 4.1), and the waters sampled in this region will represent the edge of the northern gyre rather than the gyre centre which is sampled during the southern leg. However, ~30°N the AMT-8 cruise transect crosses more central gyre waters (seen as blue/purple in Fig. 4.1), and the pigmental composition experienced here is very similar to the waters of the southern central gyre (Fig. 4.6) due to very low pigment concentrations, especially Fuco, Chl $c_3$, Diadino and an absence of Peridin (Table 4.3).

### 4.4.3. Community Composition and Species Biogeography

Increase nutrient inputs are accompanied by structural changes in the community composition with increased contributions to total chlorophyll *a* from nano - and microphytoplankton (Fig. 4.2). Despite these trends, nano- and microphytoplankton also contribute to total chlorophyll *a* within the subtropical gyres (Fig. 4.2), and several large phytoplankton species are observed in oligotrophic waters, although at much lower cell densities than the dominant picophytoplankton. Other studies have also observed nano- and microphytoplankton species and communities in low nutrient waters; e.g. Durand *et al.,* (2001) found that the eukaryotic phytoplankton in the Sargasso Sea were dominated by small pico- and nanoplankton (mostly 2 - 4 μm), although populations of coccolithophores and sometimes small pennate diatoms were also observed. Such nano- and microphytoplankton tend to account for significantly higher proportions of total productivity than their contributions to chlorophyll *a* biomass (Maranon *et al.,* 2001). The success and survival of large phytoplankton taxa in such hostile environments is thought to be due to the development of specialised adaptations to the environmental conditions, such as internal nutrient pools (McCarthy and Goldman, 1979; Riebesell and Wolf-Gladrow, 2002), synthesis of specialised light harvesting or

photoprotectant pigments, low 'K-selective' growth rates deep in the thermocline (Kemp *et al.,* 2000) or in surface waters (e.g. *Trichodesmium* spp.; Capone *et al.,* 1997), association with nitrogen-fixing endosymbionts (e.g. occurrence of *Richella intracellularis* in the diatom *Hemiaulus hauckii*; Venrick, 1974), associations with motile taxa (e.g. association of the diatoms *Chaetoceros dadayi* and *C. tetrastichon* with loricate planktonic ciliate species, or the association between *Leptocylindrus mediterraneus* and the motile epiphytic flagellate *Rhizomonas setigera*; Tomas, 1997), and migration between upper nutrient depleted waters and deep nutrient-rich waters (Villareal *et al.,* 1993, 1996, 1999a, b).

High Fuco concentrations off NW Africa and around 38°N are associated with increases in the abundance and diversity of diatoms and dinoflagellates; e.g. off NW Africa high abundances of *Pseudo-nitzschia* spp. and *Leptocylindrus danicus* (and *L. minimus*) were observed and in northern waters higher abundances of *Bacteriastrum* spp. and *Cerataulina pelagica* were found. High concentrations of Zea in surface and subsurface waters around the equator were associated with high numbers of the colonial cyanophyte *Trichodesmium* spp. which dominates the large phytoplankton community, and has previously been reported to contribute to Zea concentrations in the CM as the colonies sink (McManus and Dawson, 1994).

Multivariate analysis of the species abundances reveals several levels of spatial heterogeneity including depth-specific and latitudinal-specific ranges. Within such multivariate analysis all species will make contributions to the patterns observed (Clarke and Warwick, 1994), although only a small proportion of the community and species can be discussed. The distribution of *Trichodesmium* spp. during AMT-8 matches well with the distribution of this species found during previous AMT cruises, showing that these species are most abundant around the equator where the CM and Upper Mixed Layer are shallow and where there is an increased availability of nitrate and other nutrients (Chapter 3; Tyrrell *et al.,* submit.). Numerical dominance of phytoplankton communities by *Trichodesmium* spp. leads to semi-monospecific communities with low diversity (Furuya and Marumo, 1983), and is due to the colonial and filamentous lifestyle of this cyanophyte species where large colony size is accompanied by small cell sizes (~10 μm). *Trichodesmium* spp. are known to show several adaptations to its environment, including nitrogen fixation, neutral buoyancy, low growth rates and large cellular concentrations of the photoprotectant pigment Zea (Carpenter, 1983a; Capone *et al.,* 1997). The global importance of *Trichodesmium* spp. due to its role in nitrogen fixation is becoming increasingly recognised, and it has been termed a 'some-what enigmatic species due to its large size and prominent appearance in environments dominated by small inconspicuous algal cells' (Capone *et al.,* 1997).

The waters off NW Africa are characterised by an increase in cell numbers but a decrease in species richness and diversity and the absence of many species characteristic of southern subtropical waters (e.g. *Ceratium teres*: Table 4.4). Species found in high numbers around the equator and off NW Africa include *Dactyliosolen* spp., *Leptocylindrus danicus*, *L. minimus*, *Planktoniella sol*, *Pseudo-nitzschia* spp. (most likely *P. delicatissima* and *P. seriata*), *Thalassionema* spp., *Gymnodinium / Gyrodinium aureolum*-complex and *Prorocentrum dentatum* (section 4.3.3; Assemblage 5). The eight species of assemblage 5 are also found at the northern end of the transect, along with *Bacteriastrum* spp., *Cerataulina pelagica*, *Proboscia alata* and *Myrionecta rubra* (Assemblage 4). Many of these diatom species (e.g. *L. danicus*, *C. pelagica*, *P. delicatissima*) are

cosmopolitan species found in coastal waters and during temperate spring blooms, and it seems that these species are indicative of increased nutrient loading in the waters off NW Africa. *Planktoniella sol* is a tropical diatom species and these results indicate that it too is able to respond to increased nutrient availability. Thus, there seems to be a link between the conditions favouring these species during temperate spring blooms and in upwelling environments.

Both *Pseudo-nitzschia* spp. and *Gymnodinium / Gyrodinium aureolum*-complex are thought to produce toxins in bloom situations (Tomas, 1997; Pan *et al.,* 2001). High cell densities of these taxa off NW Africa are likely to result in a high amount of toxin concentration in these waters. Current theories on the role of phytoplankton toxins propose that toxin production by diatoms is an anti-grazer strategy, whereas dinoflagellates produce toxins as pheromones for enhanced cell contact during sexual reproduction (Wyatt and Jenkinson, 1997). The impact of toxins produced by these taxa on the phytoplankton community is unknown, and remains an interesting research topic. Species of the genus *Pseudo-nitzschia* are usually associated with temperate waters during spring, although the results presented here show its widespread distribution in tropical and subtropical waters which is supported by Venrick, (1999) and Scharek *et al.,* (1999a, b).

Around the equator there is a change in species composition with a decrease or absence of some coccolithophore species (e.g. *Helicosphaera* spp., *Ophiaster* spp., *Umbellosphaera irregularis*) and several other species (e.g. *Phaeoceros* - *Chaetoceros* spp.). Equatorial phytoplankton communities are dominated by *Trichodesmium* spp. with increased cell densities of several other species (e.g. *Leptocylindrus mediterraneus*, Pennate sp. 'C') and taxa (small unidentified pennates and small coccolithophore species), which are also found in waters to the south of the equator. The equator is thought to be an area of increased nutrient availability, due to thermocline tilting, divergence of surface winds and Ekman pumping (Longhurst, 1993, 1998).

Subtropical phytoplankton communities of the northern and southern gyres have quite similar compositions, with highest similarity between gyres occurring in 'central' gyre communities; 35 - 10°S and 30 - 34°N. Northern gyre edge communities (20 - 30°N) appear to be similar in dominant species composition to southern gyre edge communities (0 - 10°S), however, there are differences in the total species compositions between the two. Central gyre communities are characterised by the presence of subtropical species such as *Discosphaera tubifer*, *Umbellosphaera irregularis*, *Rhabdosphaera claviger*, small *Prorocentrum* spp. and *Ophiaster* spp. Gyre edge communities are characterised by decreased abundances of these species and a mixture of subtropical species and species characterising the surrounding areas; e.g. *Trichodesmium* spp. and *Gymnodinium / Gyrodinium aureolum*-complex.

*Umbellosphaera irregularis*, *U. tenuis*, *Rhabdosphaera claviger* and *Discosphaera tubifer* are known to characterise nitrate-depleted waters and have high temperature and light preferences (Brand, 1994; Cortes *et al.,* 2001; Haider and Thierstein, 2001). Several of the species found in subtropical waters have been found to be impossible to culture with standard nutrient enriched media and do not increase in numbers in waters experiencing increased nutrient concentrations (Karl, 1999); i.e. *D. tubifer*, *Oolithotus fragilis*, *R. claviger* and *U. irregularis* (Brand, 1994). Such resistance to increased nutrient availability, as well as the observation that many coccolithophore species have been found to survive a wide range of environmental conditions but at very low cell densities (Haider and Thierstein, 2001), are thought to indicate that such species are extremely K-selected (Brand,

1994). As well as experiencing low nutrient concentrations, central gyre species are also likely to encounter large amounts of damaging irradiance, including Ultraviolet (UV) light. Several species of *Prorocentrum* spp. have been shown from cultures to contain high cellular concentrations of UV absorbing compounds, making these species suitable for existence in high-light damaging environments (Jeffrey *et al.,* 1999), however other tropical and subtropical species remain to be tested.

### 4.4.4. Sun and Shade Flora

In addition to the layering of the phytoplankton community in terms of biomarker pigments, there is evidence that several species are more abundant within upper waters than deep waters, and several species show the opposite pattern. Several authors have observed this phenomenon (e.g. Venrick, 1982, 1999; Furuya and Marumo, 1983) and it has led to the proposal of depth-specific species assemblages, or floras, which include an upper water flora (sun flora) and a deep-water flora (shade flora) (Sournia, 1982; Semina, 1993, 1997; Longhurst and Harrison, 1989). The separation of such assemblages is related to the separation of the water-column in such environments into an upper light-rich and new nutrient-poor upper layer and a deeper nutrient-rich and light-poor layer (Dugdale and Goering, 1967; Eppley *et al.,* 1973). Separation of the environment into such layers would select for different species that are more suited for growth and survival in either layer (Venrick, 1982). However, current knowledge of the ecology and life cycle strategies of subtropical species prevents conclusions about adaptations to the environment from being drawn.

Separation of the sun and shade flora in this study appears as distinct layers in terms of the phytoplankton species composition, as well as the pigment layering. Separation of these layers is based on both the species composition (in terms of both rare and dominant species) and on the formation of recognisable species assemblages. Simply plotting the abundance of several proposed sun and shade flora species shows that there are differences in the composition of surface and deeper waters (Fig. 4.15). Several authors have already proposed *Discosphaera tubifer, Umbellosphaera irregularis and U. tenuis* as belonging to a sun flora (Table 4.1). This study confirms the affiliation of these species to an upper flora but also proposes that *Syracosphaera prolongata*, and *Acanthoica* spp. should be added. *Rhabdosphaera claviger* appears to be absent from upper waters in the southern hemisphere, however it is proposed here to belong to the sun flora in the northern gyre and around the equator. Another addition to the sun flora are small unidentified pennate diatoms which occur in higher numbers in surface waters than at depth (average = 725 cells $l^{-1}$ in upper waters, 354 cells $l^{-1}$ in deeper waters). *Ophiaster* spp. (most likely *O. hydroideus*) has already been proposed as belonging to the shade flora (Table 4.1), and this study confirms this but also proposes the addition of *Halopappus* spp. (including *Calciopappus* spp. and *Michaelsarsia elegans*), *Haslea* spp., *Nitzschia longissima*, *Anoplosolenia brasiliensis* and *Calciosolenia murrayi.* Also Pennate sp. 'C' was found in higher concentrations in deep waters than in upper waters (upper average = 99.3 cells $l^{-1}$, deeper average = 844.4 cells $l^{-1}$), although there is a large amount of variability in the distribution of this group. There is also evidence from several authors that the prochlorophyte community can be split into depth specific layers based on pigment, molecular and cellular characteristics (Goericke and Repeta, 1993; Letelier *et al.,* 1993; McManus and Dawson,

1994; Scanlan *et al.,* 1996; Zubkov *et al.,* 1998; West and Scanlan, 1999). Generally, upper prochlorophyte populations show higher cell densities, smaller cell sizes with a lower chlorophyll content, hence high ratios of Dv Chl *a*:Dv Chl *b*, whereas deeper populations have lower densities, larger cells with a higher chlorophyll content and hence a low Dv Chl *a*:Dv Chl *b* ratio (Moore and Chisholm, 1999).

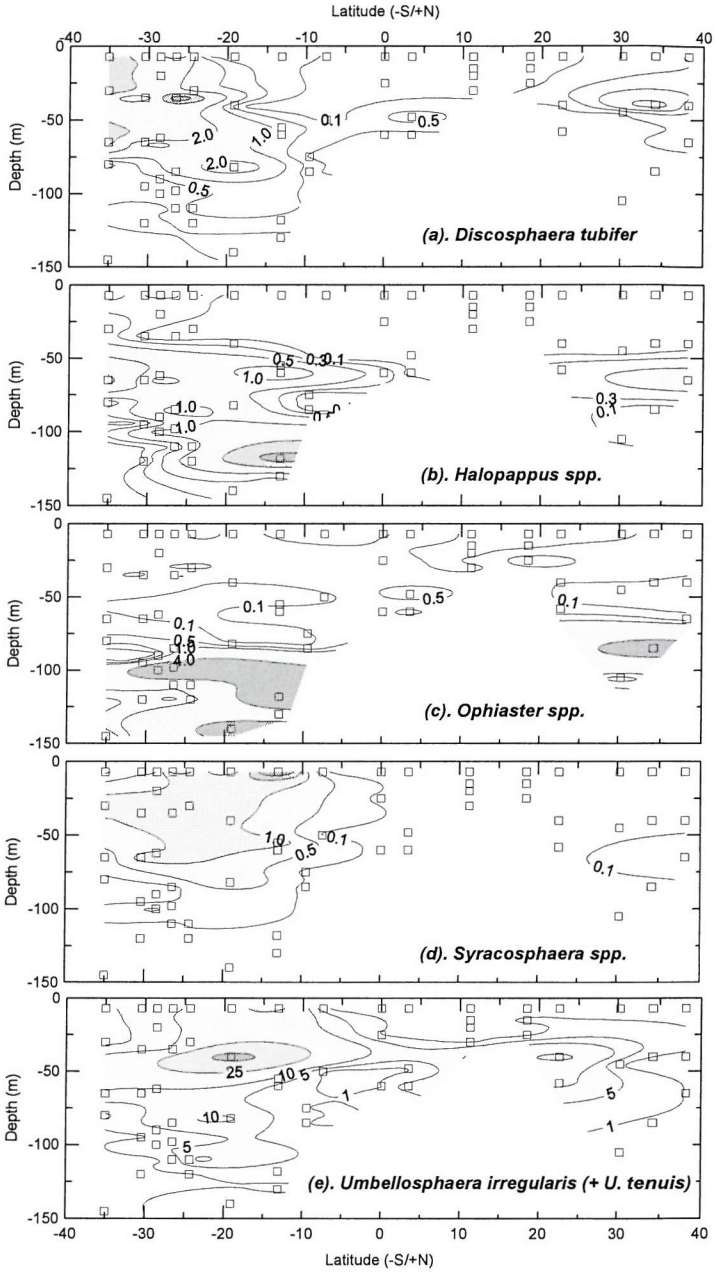


Figure 4.15: Sun and shade coccolithophore species abundances (x$10^2$ cells $l^{-1}$); (a) *Discosphaera tubifer*, (b) *Halopappus* spp., (c) *Ophiaster* spp., (d) *Syracosphaera* spp., and (e) *Umbellosphaera irregularis* and *U. tenuis*. Open squares indicate sampling depths.

## 4.5. Summary and Conclusions

1. Multivariate statistical (cluster) analysis of phytoplankton pigment signatures in the subtropical and tropical Atlantic Ocean show that the composition of the community varies with latitude and depth (Fig. 4.6, 4.8), and leads to the identification of three major communities, that are related to latitudinal differences in the hydrographic environment; (i) Subtropical gyres: An upper (0 - 60 m) community composed of high-light adapted prochlorophytes (divinyl chlorophyll *a*, zeaxanthin), cyanophytes (chlorophyll *a*, zeaxanthin) and possibly some prymnesiophytes (19'-hexanoyloxy-

fucoxanthin). A deep (>60 m and within the Chlorophyll *a* Maximum) community composed of low-light adapted prochlorophytes (divinyl chlorophyll *a*, chlorophyll *b*), cyanophytes (zeaxanthin, chlorophyll *a*), prymnesiophytes (19'-hexanoyloxy-fucoxanthin) and pelagophytes/chrysophytes (19'-butanoyloxy-fucoxanthin). (ii) Equatorial waters: Similar to the composition found in the subtropical gyres, although elevated concentrations of all community pigments, especially increased zeaxanthin concentrations at depth which may be interpreted as increased prochlorophyte and cyanophyte numbers. (iii) NW Africa: Relatively greater abundance of cyanophytes (chlorophyll *a*, zeaxanthin), prymnesiophytes (19'-hexanoyloxy-fucoxanthin), pelagophytes/chrysophytes (19'-butanoyloxy-fucoxanthin), and diatoms (fucoxanthin) and a decrease of prochlorophytes (low divinyl chlorophyll *a*). Community also includes some dinoflagellates (peridinin), prasinophytes and chlorophytes (chlorophyll *b*, lutein).

2. Multivariate statistical (cluster) analysis of the distribution of phytoplankton species (>5 μm in diameter), identified by light microscopy, shows patterns consistent with those identified from the pigment signatures (Fig. 4.12 and 4.14). The results suggest that a significant portion of the prymnesiophyte population in subtropical waters is composed of coccolithophore species; coccolithophores represent the majority of species (total of 20 species identified) and large (>5 μm) phytoplankton cells found in the subtropical gyres (Tables 4.4 - 4.7).

3. Also several assemblages of large (>5 μm) phytoplankton species were identified from the multivariate statistical (cluster) analysis (Figs. 4.12 and 4.14); (i) Subtropical gyres: An upper assemblage including the coccolithophores *Umbellosphaera irregularis* and *U. tenuis*, *Discosphaera tubifer*, and small (10 - 30 μm) pennate diatoms, and a deep assemblage including the coccolithophores *Ophiaster* spp., *Calciosolenia murrayi* and *Anoplosolenia brasiliensis*. (ii) Equatorial waters: The cyanophyte *Trichodesmium* spp. and the diatom *Leptocylindrus mediterraneus*. (iii) NW Africa: Several 'temperate' diatom species such as *Pseudo-nitzschia* spp., *Leptocylindrus danicus* and *L. minimus*, as well as 'tropical' species such as *Planktoniella sol*. (iv) Northern temperate waters: Several 'temperate' species common from the spring blooms in North Atlantic Waters, such as the diatoms *Bacteriastrum* spp., *Proboscia alata*, *Dactyliosolen* spp., *Corataulina pelagica*, and the autotrophic ciliate *Myrionecta rubra*.

4. Although there is agreement between the spatial (latitudinal and vertical) patterns identified from the pigment signatures and large (>5 μm) phytoplankton species there are several inconsistencies; the cell counts indicate that autotrophic dinoflagellates and diatoms are widespread throughout the tropical and subtropical Atlantic Ocean, however their biomarker pigments (peridinin and fucoxanthin) are relatively rare. These differences indicate that diatoms and autotrophic dinoflagellates either contain other accessory pigments (e.g. dinoflagellates may contain 19'-butanoyloxy-fucoxanthin instead or peridinin), or are reliant on other non-photosynthetic nutritional strategies (e.g. mixotrophy or phagotrophy).

# CHAPTER 5: TEMPORAL VARIABILITY OF THE PHYTOPLANKTON COMMUNITY IN SOUTH ATLANTIC SUBTROPICAL WATERS: 1995 - 2000 (AMT-1 - 10)

## 5.1. Introduction and Outline

Results presented previously have indicated intercruise variation in the upper mixed layer depths (MLD; Chapter 3) in the South Atlantic Subtropical Waters (0 - 30°S; SASW), which are likely to relate to changes in the phytoplankton community. The aim of this chapter is to investigate whether the variability in the hydrographic enviroment identified in Chapter 3 is accompanied by variability of the phytoplankton community composition. Univariate and mutlivariate statistical analysis compare intercruise differences (1995 - 2000) in several parameters of the phytoplankton community, including chlorophyll a concentration (as a proxy of biomass; section 5.2.1), pigment ratios (community composition; section 5.2.2), large (>5 μm) phytoplankton taxa biomass and taxa composition (section 5.3), and large phytoplankton species composition (section 5.4). The SASW is the most extensively sampled area along the AMT cruise track, with measurements typically taken from between 8 and 10 stations along the eastern section of the SASW, apart from AMT-8 (May, 1999), which sampled further east in the SASW (Fig. 5.1). Odd AMT cruises (1, 3, 5, 9) sample during the post-winter (spring) period in the South Atlantic, while even AMT cruises (2, 4, 8, 10) sample post-summer (autumn).

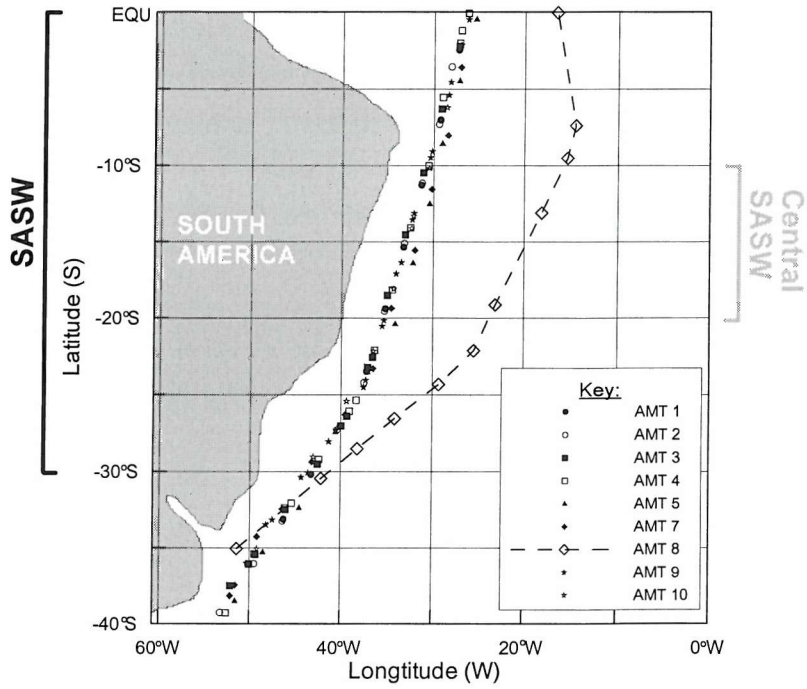


Figure 5.1: AMT cruise tracks in the South Atlantic Ocean indicating the latitudinal range of South Atlantic Subtropical Waters (SASW; 0 - 30°S) and the central SASW (10 - 20°S).

Multivariate analysis of the phytoplankton community in SASW during AMT-8 showed a basic 2-layered system (Chapter 4); an upper community dominated by prochlorophytes and cyanophytes, and a deep diverse community of prochlorophytes, cyanophytes, prymnesiophytes and pelagophytes (chrysophytes), with both communities also composed of characteristic large (>5 μm) phytoplankton

species assemblages. This finding, coupled with the limited depth resolution (2 depths) of typical AMT cruises, leads to the examination of temporal changes of phytoplankton community composition for two portions of the water-column; upper (0 - 60 m) and deep (60 - 200 m) waters. Comparisons are also made between the entire SASW (0 - 30°S) and a central region of the SASW (10 - 20°S) with the intention of minimising the effects of equatorial (0 - 10°S) and southern temperate (>30°S) waters. Spatial and temporal variability of the phytoplankton community is investigated through the examination of photosynthetic standing stock (chlorophyll *a* and large phytoplankton species biomass) and biomarker pigment ratios (section 5.2), and the composition of the nano- and micro phytoplankton community in terms of major phytoplankton groups (section 5.3) and species composition (section 5.4).

A total of 141 species/morphotypes have been identified from the SASW, which includes 61 diatoms, 49 autotrophic dinoflagellates, 19 coccolithophores and 12 endosymbiotic taxa. This total represents ~ 80% of the total species in the entire AMT species database; the SASW flora is not exclusive and includes many species found in other environments. Table 5.1 presents the species codes and full species names that are identified in the multivariate analysis for this chapter.

Table 5.1: Nano- and microphytoplankton species names and codes. Note that the genus *Chaetoceros* has been split into species with chloroplasts within the setae (Phaeceros) and species without chloroplasts in setae (Hyalochaete).

| Species Codes | Species / Genus names (Common species) | Species Codes | Species / Genus names (Common species) |
|---|---|---|---|
| | 1. Diatoms | | 3. Coccolithophores |
| D8 | *Bacteriastrum* spp. | CC1 | 10 - 25μm Coccolithophores |
| D20 | *Chaetoceros* spp. - Hyalochaete | CC2 | *Acanthoica* sp. (cf. *A. quattrospina*) |
| D21 | *Chaetoceros* sp. - Phaeceros | CC7 | *Discosphaera tubifer* (cf. *Pappospaera lepida*) |
| D26 | *Corethron criophilum* (cf. *C. inerme*) | CC8 | *Emiliania huxleyi*, *Gephyrocapsa* & small 5μm Coccolithophores |
| D41 | *Haslea* spp. (cf. *H. wawrikae*) | | |
| D45 | *Leptocylindrus danicus* & *L. minimus* | CC9 | *Halopappus* spp. (including *Calciopappus* and *Michaelsarsia* spp.) |
| D52 | *Nitzschia longissima* (cf. *C. closterium*) | | |
| D56 | Small Unidentified Pennates (10 - 30μm) | CC10 | *Helicosphaera* spp. (*H. carteri* & *H. hyalina*) |
| D57 | Pennate sp. 'C' (50 μm long) | CC12 | *Ophiaster* spp. (cf. *O. hydroideus*) |
| D64 | *Pseudo-nitzschia* complex | CC16 | *Syracosphaera* spp. cf *prolongata* (& *S. pirus*) |
| | | CC17 | *Umbellosphaera* spp. (*U. irregularis* & *U. tenuis*) |
| | 2. Autotrophic Dinoflagellates | CC18 | *Umbilicosphaera sibogae* |
| AD47 | *Oxytoxum* spp. (cf. *O. laticeps*) | CC19 | Unidentified Heart Coccolithophore |
| AD53 | *Prorocentrum* spp. small (cf. *P. balticum*) | CC20 | *Gephyrocapsa ornata* ("Spike") |
| AD59 | *Scrippsiella* / *Alexandrium* spp. | | |
| AD60 | *Torodinium* spp. (cf. *T. teredo*) | | 4. Endosymbiotic Taxa |
| | | ED1 | *Leptocylindrus mediterraneus* |
| | | ED9 | *Myrionecta rubra* |

## 5.2. Photosynthetic Biomass and Community Composition

### 5.2.1. Chlorophyll *a*

Chlorophyll *a* concentrations (from acetone extractions; FIchl*a*), as a proxy of photosynthetic standing stock, are presented as SASW sections in Figure 5.2 and from discrete depths and integrated portions of the water-column from the whole SASW (0 - 30°S) and central (10 - 20°S) SASW in Table 5.2. Vertical (0 - 200m) sections of FIchl*a* from the SASW are similar for all AMT cruises (Fig. 5.2); low FIchl*a* concentrations (<0.1 - 0.2 mg Chl*a* $m^{-3}$) in surface and upper waters (0 - 60 m) and an increase (>0.2 - 0.4 mg Chl*a* $m^{-3}$) to form a Chlorophyll *a* Maximum (CM) at depths ranging from 50 m (SASW edges) to 150 m (central SASW). There is some evidence of intercruise variability from

the SASW FIchl*a* sections; e.g. the 0.3 mg Chl*a* $m^{-3}$ interpolated FIchl*a* contour appears absent from the central SASW during AMT-3, 5, 8 and 10 (Fig. 5.2). Significant differences in FIchl*a* concentrations are tested for by 1-way ANOVA on all measurements and Tukey tests on cruise-pairs (Table 5.3). Significant differences ($p<0.05$) in surface FIchl*a* concentrations ($C_{z0}$) are found in the SASW with AMT-1 higher than AMT3,4,5,7,8 and 10 and AMT-9 higher than AMT-3,4,5,8 and 10, whereas significant differences in $C_{z0}$ are only found between AMT-1 and AMT-3,4,5,7,8 and 9 in the central SASW (Tables 5.2 and 5.3). No significant differences ($p<0.05$) are found in the CM FIchl*a* concentration ($C_{CM}$) or depth of the CM ($Z_{CM}$) for either the whole SASW or central region (Tables 5.2 and 5.3).

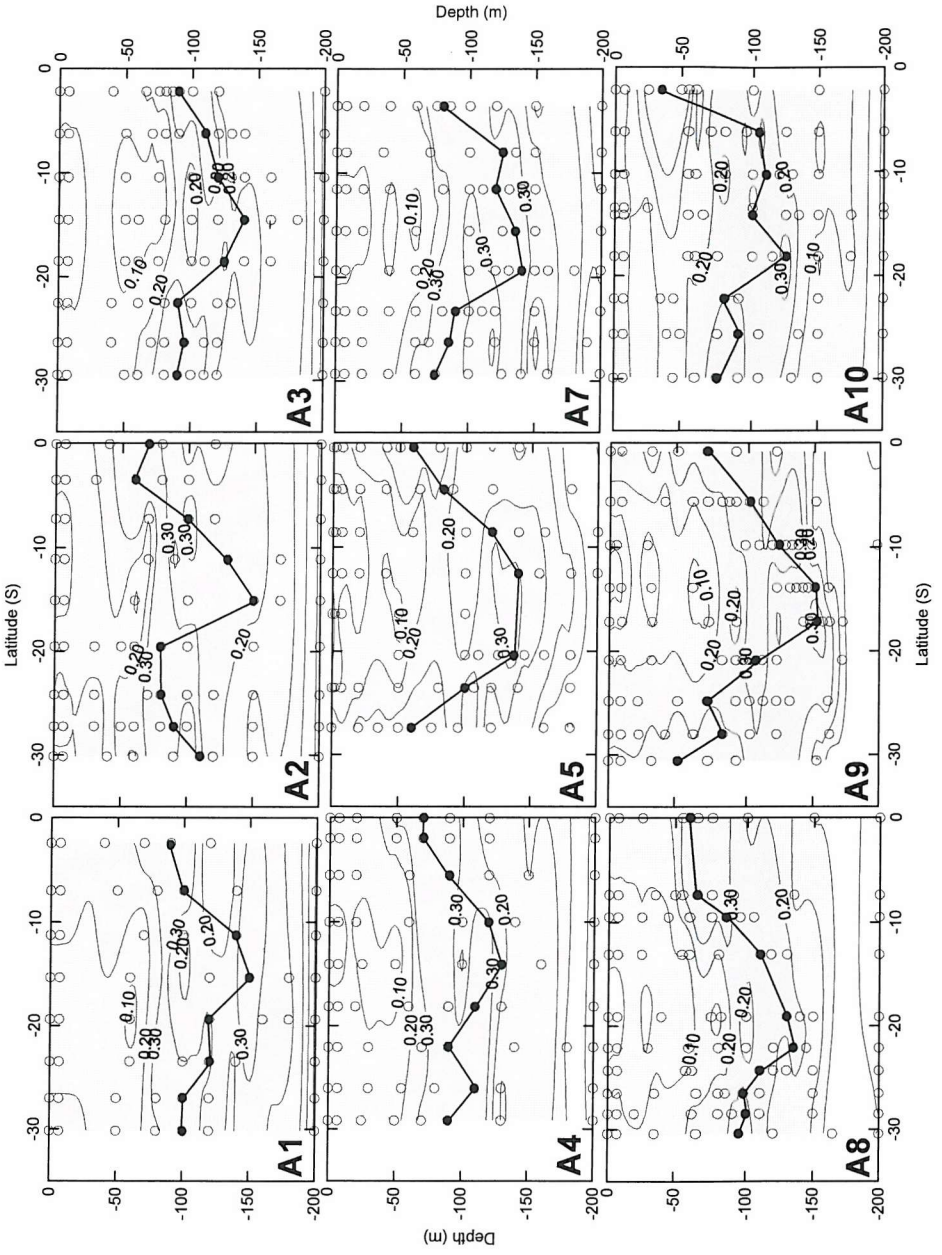


Figure 5.2: SASW (0 - 30°S) sections of chlorophyll *a* concentration (mg $m^{-3}$) for AMT-1 - 5, 7 - 10. Chlorophyll *a* concentrations are those measured from acetone extractions. Sampling depths are indicated by open circles and CM depth are given by filled circles and joining thick black line.

Differences between the SASW and central SASW (Table 5.2) include slightly higher water-column (0 - 200 m) integrated chl*a* concentrations in the SASW (33.9 ± 7.5 mg Chl*a* $m^{-2}$) compared with the central SASW (30.3 ± 6.8 mg Chl*a* $m^{-2}$) and higher integrated FIchl*a* concentrations in the upper portion of the water-column (0 - 60 m) for the SASW (9.4 ± 4.9 mg Chl*a* $m^{-2}$ and 6.0 ± 2.8 mg Chl*a* $m^{-2}$, respectively). However, the FIchl*a* concentration in the lower portion of the water-column

(60 - 200 m) is very similar for both regions (Table 5.2; SASW: 24.7 ± 6.0 mg Chl*a* $m^{-2}$; central SASW; 24.5 ± 5.7 mg Chl*a* $m^{-2}$); the difference in total water-column (0 - 200 m) integrated Flchl*a* concentration is due to changes in the upper portion of the water-column only, despite differences in the $Z_{CM}$ (Table 5.2; SASW: 101.3 ± 26.8 m; central SASW: 123.3 ± 22.4 m).

Table 5.2: Average (± standard deviations) chlorophyll *a* measurements from the SASW (0 - 30°S) and central SASW (10 - 20°S) over the 5 yrs of the AMT cruises (cruise dates as month and year included with cruise number). The number of measurements or stations included in the analysis is shown in brackets; (n). The overall 5-year average of all chlorophyll *a* parameters are provided in final column.

| Parameter (Units) | AMT-1 (9/95) | AMT-2 (5/96) | AMT-3 (9/96) | AMT-4 (5/97) | AMT-5 (9/97) | AMT-7 (9/98) | AMT-8 (5/99) | AMT-9 (9/99) | AMT-10 (5/00) | All |
|---|---|---|---|---|---|---|---|---|---|---|
| SASW (0 - 30°S) | | | | | | | | | | |
| $C_{z0}$ (mg $m^{-3}$) | 0.20 ± 0.06 | 0.14 ± 0.07 | 0.09 ± 0.03 | 0.12 ± 0.03 | 0.12 ± 0.09 | 0.13 ± 0.05 | 0.09 ± 0.04 | 0.19 ± 0.09 | 0.10 ± 0.01 | 0.13 ± 0.07 |
| $C_{CM}$ (mg $m^{-3}$) | 0.42 ± 0.11 | 0.44 ± 0.16 | 0.39 ± 0.07 | 0.42 ± 0.13 | 0.33 ± 0.09 | 0.46 ± 0.12 | 0.35 ± 0.14 | 0.39 ± 0.14 | 0.33 ± 0.07 | 0.39 ± 0.12 |
| $Z_{CM}$ (m) | 115.0 ± 21.4 | 94.4 ± 30.5 | 107.5 ± 19.3 | 97.8 ± 21.1 | 103.3 ± 37.3 | 105.0 ± 25.1 | 98.8 ± 24.5 | 101.6 ± 35.8 | 90.0 ± 27.5 | 101.3 ± 26.8 |
| $C_{TOT}$ (mg $m^{-2}$) | 39.5 ± 7.2 | 36.2 ± 6.4 | 30.2 ± 5.2 | 34.6 ± 6.4 | 29.0 ± 5.1 | 39.8 ± 5.7 | 28.0 ± 4.7 | 38.2 ± 10.3 | 30.0 ± 3.0 | 33.9 ± 7.5 |
| $C_{60m}$ (mg $m^{-2}$) | 10.7 ± 3.8 | 12.3 ± 5.8 | 6.9 ± 6.9 | 8.0 ± 2.3 | 9.3 ± 6.73 | 9.3 ± 3.0 | 7.3 ± 3.3 | 11.4 ± 8.4 | 9.0 ± 4.3 | 9.4 ± 4.9 |
| $C_{200m}$ (mg $m^{-2}$) | 28.7 ± 7.5 | 23.9 ± 5.6 | 23.2 ± 3.6 | 26.6 ± 5.5 | 19.7 ± 3.6 | 30.5 ± 5.2 | 20.7 ± 2.9 | 25.8 ± 7.0 | 21.0 ± 3.7 | 24.5 ± 6.0 |
| $C_{ZCM}$ (mg $m^{-2}$) | 17.8 ± 2.5 | 11.1 ± 4.8 | 11.7 ± 2.9 | 11.7 ± 3.4 | 18.0 ± 3.1 | 15.9 ± 3.0 | 10.5 ± 3.3 | 22.8 ± 5.0 | 11.3 ± 6.4 | 14.4 ± 5.6 |
| [n] | [n = 8] | [n = 9] | [n = 8] | [n = 9] | [n = 7] | [n = 8] | [n = 10] | [n = 9] | [n = 8] | [n = 76] |
| Central (10 - 20°S) | | | | | | | | | | |
| $C_{z0}$ (mg $m^{-3}$) | 0.16 ± 0.05 | 0.10 ± 0.07 | 0.06 ± 0.01 | 0.10 ± 0.05 | 0.06 ± 0.01 | 0.08 ± 0.00 | 0.07 ± 0.03 | 0.05 ± 0.01 | 0.11 ± 0.01 | 0.09 ± 0.04 |
| $C_{CM}$ (mg $m^{-3}$) | 0.39 ± 0.18 | 0.39 ± 0.21 | 0.33 ± 0.03 | 0.35 ± 0.13 | 0.25 ± 0.01 | 0.40 ± 0.04 | 0.36 ± 0.14 | 0.35 ± 0.07 | 0.28 ± 0.02 | 0.35 ± 0.11 |
| $Z_{CM}$ (m) | 136.7 ± 15.3 | 120.0 ± 36.1 | 128.3 ± 10.4 | 120.0 ± 10.0 | 138.0 ± 25.6 | 128.3 ± 10.4 | 97.5 ± 28.4 | 142.6 ± 16.9 | 111.7 ± 12.6 | 123.3 ± 22.4 |
| $C_{TOT}$ (mg $m^{-2}$) | 36.6 ± 6.8 | 33.8 ± 11.6 | 25.5 ± 3.9 | 31.3 ± 8.4 | 25.2 ± 0.6 | 35.7 ± 2.3 | 27.1 ± 4.7 | 26.8 ± 7.1 | 30.1 ± 4.8 | 30.3 ± 6.8 |
| $C_{60m}$ (mg $m^{-2}$) | 8.4 ± 3.8 | 7.1 ± 3.6 | 4.1 ± 0.5 | 6.2 ± 3.3 | 3.3 ± 1.2 | 6.3 ± 2.0 | 6.4 ± 3.1 | 3.3 ± 1.8 | 7.6 ± 1.6 | 6.0 ± 2.8 |
| $C_{200m}$ (mg $m^{-2}$) | 28.2 ± 8.7 | 26.8 ± 8.4 | 21.4 ± 4.1 | 25.1 ± 5.3 | 21.9 ± 0.6 | 29.4 ± 0.7 | 20.7 ± 4.2 | 23.5 ± 8.2 | 22.4 ± 3.3 | 24.3 ± 5.7 |
| $C_{ZCM}$ (mg $m^{-2}$) | 16.8 ± 1.2 | 9.5 ± 2.0 | 9.2 ± 1.6 | 13.4 ± 5.1 | 16.9 ± 2.7 | 15.7 ± 4.4 | 7.9 ± 2.4 | 18.7 ± 4.1 | 14.4 ± 8.1 | 13.3 ± 5.1 |
| [n] | [n = 3] | [n = 3] | [n = 3] | [n = 3] | [n = 2] | [n = 3] | [n = 4] | [n = 3] | [n = 3] | [n = 27] |

Integrated chl*a* concentrations over the entire water-column (0 - 200m) shows significant differences within the SASW but not within the central region ($C_{TOT}$;Tables 5.2 and 5.3); significantly ($p<0.05$) differences include higher concetrations during AMT-1 compared with AMT-3,5,8 and 10, AMT-2 compared with AMT-5,8 and 10, AMT-7 and 9 compared with AMT-3,5,8 and 10, and AMT-4 compared with AMT-8 (Tables 5.2 and 5.3). Consideration of the chl*a* contained within upper 0 - 60

m waters ($C_{60m}$) and deep 60 - 200 m ($C_{200m}$) shows no signficant ($p>0.05$) differences between cruises in the SASW or central SASW for $C_{60m}$, whereas there are significant ($p<0.05$) differences between $C_{200m}$ in the SASW; with AMT-1 higher than AMT-3,5,8 and 10, AMT-4 higher than AMT-5, 8 and 10, AMT-9 higher than AMT-5 and 8, and AMT-7 higher than AMT-8 and 10 (Tables 5.2 and 5.3). Significant ($p<0.05$) intercruise differences of the integrated chlorophyll *a* concentration between the surface and the CM ($C_{ZCM}$) are found in both the SASW and central SASW (Tables 5.2 and 5.3); in the SASW AMT-1 is higher than AMT-2,3,4,8,9,10, AMT-5,7,9 are higher than AMT-2,3,4, AMT-5 is higher than AMT-8,9,10, and AMT-9 is higher than AMT-8 and 10. In the central SASW significantly ($p<0.05$) higher $C_{ZCM}$ are found during AMT-1 and 9 compared with AMT-2,3, and 8, AMT-5 compared with AMT-3, AMT-5 and 7 compared with AMT-8, and AMT-10 compared with AMT-10 (Tables 5.2 and 5.3).

Table 5.3: Summary table of statistics for the analysis of intercruise variations in chlorophyll *a* concentration in the SASW and central SASW. Results are from 1-way ANOVA of all cruises and Turkey tests on cruise pairs. Number of samples analysed are given as n.

| Parameter | n | ANOVA | Turkey Tests (Significant at p<0.05) |
|---|---|---|---|
| SASW (0 - 30°S) | | | |
| $C_{z0}$ | 73 | F = 3.43, p<0.005 | [1 > 3,4,5,7,8,10] and [9 > 3,4,5,8,10] |
| $C_{CM}$ | 75 | F = 1.28, NS | |
| $Z_{CM}$ | 74 | F = 0.59, NS | |
| $C_{TOT}$ | 75 | F = 4.60, p<0.005 | [1 > 3,5,8,10] and [2 > 5,8,10] and [3,5,8,10 < 7, 9] and [4 > 8] |
| $C_{60m}$ | 75 | F = 1.24, NS | |
| $C_{200m}$ | 75 | F = 4.22, p<0.005 | [1 >3,5,8,10] and [4 > 5,8,10] and [5,8 < 9] and [7 > 8,10] |
| $C_{ZCM}$ | 75 | F = 9.98, p<0.005 | [1 > 2,3,4,8,9,10] and [2,3,4 < 5,7,9] and [5 > 8,9,10] and [8,10 < 9] |
| Central (10 - 20°S) | | | |
| $C_{z0}$ | 24 | F = 2.72, p<0.05 | [1 > 3,4,5,7,8,9] |
| $C_{CM}$ | 26 | F = 0.47, NS | |
| $Z_{CM}$ | 26 | F = 1.58, NS | |
| $C_{TOT}$ | 26 | F = 1.33, NS | |
| $C_{60m}$ | 26 | F = 1.38, NS | |
| $C_{200m}$ | 26 | F = 0.93, NS | |
| $C_{ZCM}$ | 26 | F = 2.92, p<0.05 | [1,9 > 2,3,8] and [3 < 5] and [8 < 5,7] and [8 < 10] |

The results from intercruise analysis of the photosynthetic standing stock (chl*a*) indicate that although there is evidence of significant intercruise variability in both the SASW and central SASW, the only seasonal pattern appears in the integrated measurements between the surface and CM, and is related to a post-winter increase (odd cruises) that is absent during AMT-3. Differences between the SASW and central SASW include lower values for all parameters of chl*a*, although the ranges of the standard deviations indicate that the measurements are in the range of one another and no statistically significant differences would exist between the two sets of measurements (Tables 5.2 and 5.3). The difference in the cruise track during AMT-8 (Fig. 5.1) is associated with significantly lower water-column integrated chl*a* (INTEGCHL) and chl*a* in the lower portion of the water-column (DEEPCHL) in the SASW, and with significantly lower chl*a* in the upper portion of the water-column compared with AMT-10 in the central SASW (Tables 5.2 and 5.3). Overall there is no highly significantly trend in the intercruise variability for all chl*a* parameters. Therefore, using chl*a* concentration as a proxy for phytoplankton standing stock, there seems to be little variation over the five years of the AMT cruises (1995 - 2000).

## 5.2.2. Community Composition: Biomarker Pigment Ratios

Pigment ratios are used for analysis of intercruise variations in community structure and biomass as they remain relatively consistent during photoacclimation (McManus and Dawson, 1994; Mackey *et al.*, 1996). Integrated pigment ratios (w:w) are presented from AMT-1, 2, 3, 5, 7, 8, and 10, although there is a latitudinal limitation of the measurements during AMT-2 to 19 - 30°S. Average cruise and water-column integrated pigment group ratios are presented in Table 5.3.

Table 5.4: SASW (0 - 30°S) average (± standard deviation) integrated pigment ratios (w:w) within upper (0 - 60m) and deep (60 - 200m) waters. Cruise dates (month/year) are included with cruise number, and the number of stations and samples are given in brackets (n).

| Pigment Ratio | AMT-1 (9/95) | AMT-2 (5/96) | AMT-3 (9/96) | AMT-5 (9/97) | AMT-7 (9/98) | AMT-8 (5/99) | AMT-10 (5/00) | All |
|---|---|---|---|---|---|---|---|---|
| Upper Waters (0 - 60 m) | | | | | | | | |
| TChl *c*[a]:Chl *a* | 0.05 ± 0.03 | 0.33 ± 0.05 | 0.18 ± 0.05 | 0.22 ± 0.08 | 0.21 ± 0.04 | 0.20 ± 0.10 | 0.40 ± 0.15 | 0.23 ± 0.11 |
| Fuco[b]:Chl *a* | 0.09 ± 0.04 | 0.06 ± 0.02 | 0.09 ± 0.04 | 0.10 ± 0.03 | 0.10 ± 0.06 | 0.08 ± 0.09 | 0.14 ± 0.06 | 0.09 ± 0.03 |
| Hex-fuco+But-fuco:Chl *a* | 0.18 ± 0.03 | 0.32 ± 0.02 | 0.52 ± 0.09 | 0.55 ± 0.13 | 0.46 ± 0.04 | 0.61 ± 0.10 | 0.53 ± 0.17 | 0.45 ± 0.15 |
| Zea[c]:TChl *a* | 0.39 ± 0.16 | 0.40 ± 0.19 | 0.66 ± 0.16 | 0.44 ± 0.18 | 0.65 ± 0.15 | 0.80 ± 0.21 | 0.46 ± 0.22 | 0.54 ± 0.16 |
| TChl *b*[d]:TChl *a* | 0.05 ± 0.04 | 0.09 ± 0.02 | 0.65 ± 0.28 | 0.06 ± 0.06 | 0.00 ± 0.00 | 0.01 ± 0.02 | 0.15 ± 0.12 | 0.14 ± 0.23 |
| Dv chl *a*: TChl *a* | 0.40 ± 0.09 | 0.49 ± 0.03 | 0.42 ± 0.08 | 0.35 ± 0.10 | 0.36 ± 0.09 | 0.38 ± 0.06 | 0.38 ± 0.11 | 0.40 ± 0.05 |
| Deep waters (60 - 200 m) | | | | | | | | |
| TChl *c*[a]:Chl *a* | 0.14 ± 0.07 | 0.33 ± 0.07 | 0.32 ± 0.02 | 0.31 ± 0.02 | 0.38 ± 0.04 | 0.46 ± 0.10 | 0.65 ± 0.10 | 0.37 ± 0.16 |
| Fuco[b]:Chl *a* | 0.09 ± 0.10 | 0.04 ± 0.01 | 0.06 ± 0.01 | 0.10 ± 0.03 | 0.07 ± 0.07 | 0.05 ± 0.05 | 0.21 ± 0.07 | 0.09 ± 0.06 |
| Hex-fuco+But-fuco:Chl *a* | 0.28 ± 0.07 | 0.32 ± 0.02 | 0.83 ± 0.07 | 0.74 ± 0.05 | 0.79 ± 0.05 | 1.01 ± 0.19 | 0.96 ± 0.20 | 0.72 ± 0.27 |
| Zea[c]:TChl *a* | 0.15 ± 0.04 | 0.17 ± 0.02 | 0.20 ± 0.07 | 0.16 ± 0.05 | 0.19 ± 0.05 | 0.24 ± 0.08 | 0.19 ± 0.05 | 0.19 ± 0.03 |
| TChl *b*[d]:TChl *a* | 0.13 ± 0.06 | 0.40 ± 0.06 | 0.24 ± 0.13 | 0.26 ± 0.05 | 0.33 ± 0.20 | 0.30 ± 0.20 | 0.41 ± 0.12 | 0.30 ± 0.10 |
| Dv chl *a*: TChl *a* | 0.35 ± 0.10 | 0.41 ± 0.02 | 0.39 ± 0.06 | 0.36 ± 0.06 | 0.35 ± 0.05 | 0.43 ± 0.06 | 0.41 ± 0.14 | 0.38 ± 0.03 |
| [n] | [n = 7] | [n = 3] | [n = 8] | [n = 8] | [n = 8] | [n = 8] | [n = 9] | [n = 51] |

Note: [a] Includes Chl $c_1$, Chl $c_2$ and Chl $c_3$ [b] Fuco, Perid and Allo, [c] includes Zea and Lut, and [d] includes Dv chl *b* and Chl *b*.

Generally, higher ratios of total chlorophyll *c* (TChl *c*):chlorophyll *a* (Chl *a*), 19'-hexanoyloxyfucoxanthin (Hex-fuco)+ 19'-Butanoyloxyfucoxanthin (But-fuco):Chl a and chlorophyll *b* (TChl *b*): total chlorophyll *a* (TChl *a*) are always found in the deeper portion of the water-column, with the inverse for the zeaxanthin(Zea):TChl *a* ratio and no distinct difference between depths for the fucoxanthin(Fuco) +peridinin(Peridin)+alloxanthin(Allo):Chl *a* and divinyl-chlorophyll *a*(Dv chl *a*):TChl *a* ratios (Table 5.3). In upper waters (< 60 m), significant intercruise differences ($p<0.05$) are found in the TChl *c*:Chl *a* ratio with AMT-1 lower than all other cruises, AMT-2 higher than AMT-3 and 8 and AMT-10 higher than all the other cruises (Table 5.5). No significant ($p>0.05$) differences are found

between cruises for the upper Fuco+Peridin+Allo:Chl *a* ratios or for the Dv Chl *a*:TChl *a* ratio (Table 5.5). Signficant ($p<0.05$) intercruise differences are found for the upper water Hex-fuco+But-fuco:Chl *a* ratio with AMT-1 and 2 lower than the other cruises and AMT-8 higher than AMT-10 (Table 5.5). The Zea:TChl *a* ratio in upper waters during AMT-1, 2, 5 and 10 is significantly ($p<0.05$) lower than during AMT-3, 7 and 8 (Table 5.5). Upper water TChl *b*:TChl *a* ratios are significantly ($p<0.05$) higher during AMT-3 than all the other cruises and during AMT-10 compared with AMT-7 and 8 (Table 5.5).

Table 5.5: Summary table of statistics for the analysis of intercruise variations in biomarker pigment ratios in upper waters (0 - 60 m) and deep waters (60 - 200 m) of the SASW. Results are from 1-way ANOVA of all cruises and Turkey tests on cruise pairs. Number of samples analysed are given as n.

| Ratio | n | ANOVA | Turkey Tests (Significant at $p<0.05$) |
|---|---|---|---|
| Upper Waters (0 - 60 m) | | | |
| TChl *c*:Chl *a* | 51 | $F = 9.25$, $p<0.005$ | [1 < 2,3,5,7,8,10] and [2 > 3,8] and [10 > 2,3,5,7,8] |
| Fuco:Chl *a* | 51 | NS | |
| Hex-fuco+But-fuco:Chl *a* | 51 | $F = 11.73$, $p<0.005$ | [1,2 < 3,5,7,8,10] and [8 > 10] |
| Zea:TChl *a* | 51 | $F = 7.32$, $p<0.005$ | [1,2,5,10 < 3,7,8] |
| TChl *b*:TChl *a* | 51 | $F = 22.37$, $p<0.005$ | [3 > 1,2,5,7,8,10] and [7,8 < 10] |
| Dv chl *a*:TChl *a* | 51 | NS | |
| Deep Waters (60 - 200 m) | | | |
| TChl *c*:Chl *a* | 51 | $F = 32.02$, $p<0.005$ | [1 < 2,3,5,7,8,10] and [2,3,5,7 < 8,10] and [8 < 10] |
| Fuco:Chl *a* | 51 | $F = 4.80$, $p<0.005$ | [10 > 1,2,3,5,7,8] |
| Hex-fuco+But-fuco:Chl *a* | 51 | $F = 36.24$, $p<0.005$ | [1 < 2] and [1,2 < 3,5,7,8,10] and [3 < 8] and [5,7 < 8, 10] |
| Zea:TChl *a* | 51 | $F = 3.65$, $p<0.01$ | [1 < 3,8] and [2,5,7,10 < 8] |
| TChl *b*:TChl *a* | 51 | $F = 3.45$, $p<0.01$ | [1 < 2,7,8] and [3,5 < 10] |
| Dv chl *a*:TChl *a* | 51 | $F = 2.67$, $p<0.05$ | [5,7 < 8,10] |

Significant ($p<0.05$) intercruise differences are found for all the biomarker pigment ratios within the deeper (60 - 200 m) portion of the water-colum (Table 5.5). Deep TChl *c*:Chl *a* ratios during AMT-1 are lower than all the other cruises, while ratios during AMT-8 and 10 are significantly ($p<0.05$) higher than those during AMT-2,3,5 and 7, and AMT-10 is higher than AMT-8 (Table 5.5). The Fuco+Peridin+Allo:Chl *a* ratios in the lower portion of the water-column are significantly ($p<0.05$) higher than during the other AMT cruises (Table 5.5). Deep Hex-fuco+But-fuco:Chl *a* ratios are significantly ($p<0.05$) higher during AMT-2 compared with AMT-1, during AMT-3,5,7,8 and 10 compared with AMT-1 and 2, during AMT-8 compared with AMT-3, and during AMT-8 and 10 compared with AMT-5 and 7 (Table 5.5). The deep Zea:TChl *a* ratios are significantly ($p<0.05$) higher during AMT-3 and 8 than AMT-1 and during AMT-8 compared with AMT-2, 5, 7 and 10 (Table 5.5). Within the lower portion of the water-column the TChl *b*:TChl *a* ratios during AMT-1 are significantly ($p<0.05$) lower than during AMT-2, 7 and 8 and significantly higher during AMT-10 compared with AMT-3 and 5 (Table 5.5). Deep Dv Chl *a*:TChl *a* ratios are also significantly ($p<0.05$) higher during AMT-8 and 10 than during AMT-5 and 7 (Table 5.5).

The vertical and horizontal distribution of the TChl *b*:TChl *a* ratio for the AMT cruises is presented in Figure 5.3. The significant ($p<0.05$) increase in the upper water TChl *b*:TChl *a* ratios observed during AMT-3 (Table 5.4 and 5.5) are seen as a large area of elevated ratios (>0.5 - 1) in subsurface waters (<100 m) which is absent from other cruises (Fig. 5.3). However, the depth distribution of the TChl *b*:TChl *a* ratio during AMT-2 is not clear due to restriction of the measurements to the southern portion of the SASW (Fig. 5.3). TChl *b*:TChl *a* ratios during AMT-3 within the upper water patch are much higher (~1.0) and widespread than those found at depth during other AMT cruises (typically 0.1 - 0.5), and there is also a decrease of the ratios below the CM (Fig. 5.3). Due to the lack of any pigments indicative of Chl *b* containing eukaryotic groups (lutein,

violaxanthin), the Chl *b* signal is thought to be mostly due to prochlorophytes (cf. Chapter 4). The presence of this patch of elevated TChl *b*:TChl *a* in upper waters has also been remarked on by Barlow *et al.,* (2002), which is based on the same measurements, although these authors came to the conclusion that it was due to an increase in prasinophytes despite the lack of lutein concentrations.

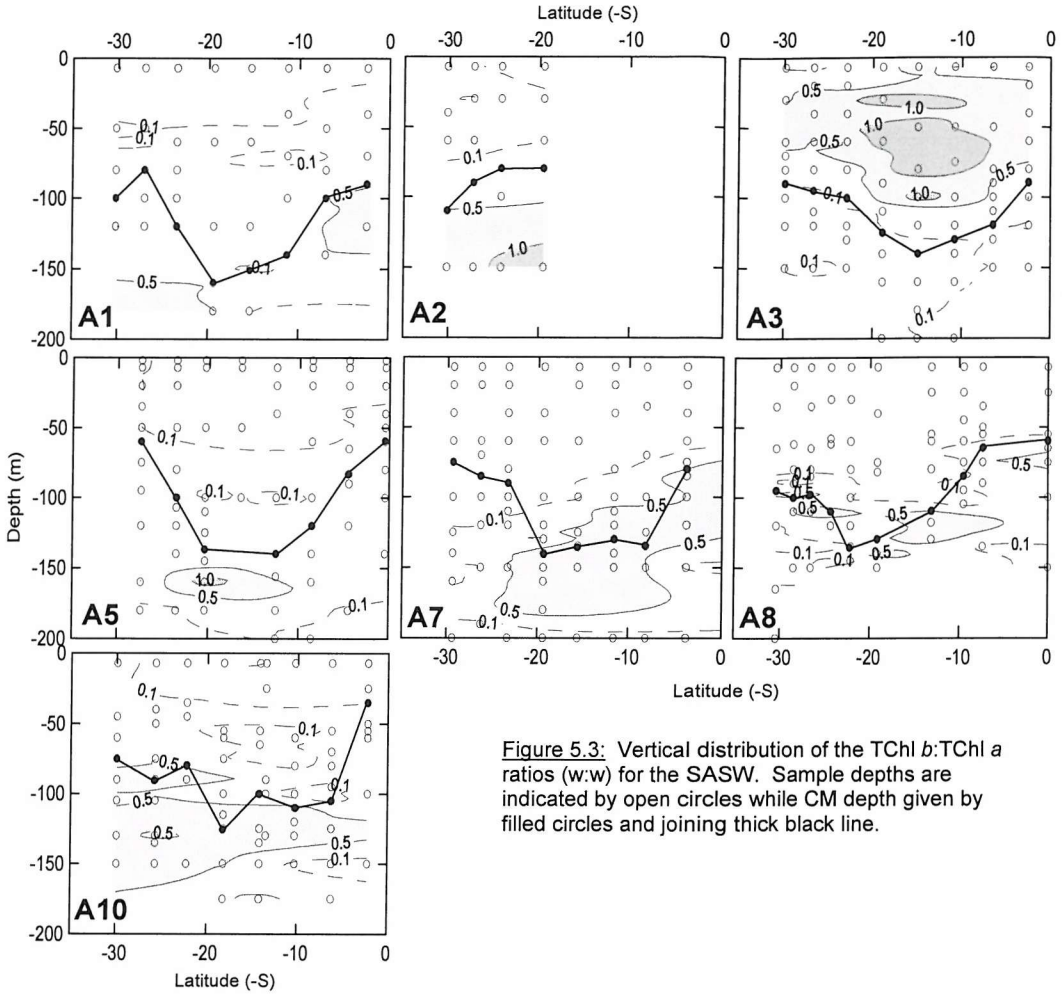


Figure 5.3: Vertical distribution of the TChl *b*:TChl *a* ratios (w:w) for the SASW. Sample depths are indicated by open circles while CM depth given by filled circles and joining thick black line.

The examination of intercruise pigment ratios shows several differences that relate to different phytoplankton groups within the water-column of the SASW. In upper waters there are significant ($p<0.05$) increases in the TChl *c*:Chl *a* ratio during AMT-2 and 10, while in deep waters there are increases over all the AMT cruises; from ~0.1 during AMT-1 to ~0.3 during AMT-2, 3, and 5, to ~0.4 during AMT-7 and 8 and ~0.6 during AMT-10 (Table 5.4 and 5.5). Changes in the ratio of TChl *c*:Chl *a* may be interpreted as indicative of increases in the abundance of eukaryotic phytoplankton groups during the AMT cruises. Intercruise variability in the Hex-fuco+But-fuco:Chl *a* ratios are seen in both upper and deep waters, with upper water ratios increasing from ~0.2 during AMT-1 to ~0.5 during AMT-3, 5, 7 and 10 and reaching a maximum of ~0.6 during AMT-8 (Table 5.4). In deep waters there is an increase in the Hex-fuco+But-fuco:Chl *a* ratios over all the AMT cruises from ~0.3 during AMT-1 and 2, to ~0.7 - 0.8 during AMT-3, 5 and 7 and up to a maximum of ~1.0 during AMT-8 and 10 (Table 5.4). Increases in the Hex-fuco+But-fuco:Chl *a* ratio indicate increases in the numbers of prymnesiophytes and pelagophytes (chrysophytes) during the AMT cruises. Intercruise variations in the Zea:TChl *a* ratio are observed in upper waters with high ratios (~0.6 - 0.8) during AMT-3, 7 and 8 and in deep waters with ratios varying only slightly between 0.15 -

0.24 (Table 5.4). Changes in the Zea:TChl *a* ratio may be interpreted as increases in the abundance of cyanophytes in upper waters of the SASW. Changes in the distribution of the pool of high TChl *b*:TChl *a* ratios from deep waters to upper waters during AMT-3 may indicate that the distribution of low-light adapted prochlorophyte population became shallower during this cruise. Coupled with the other pigment changes there is evidence that prymnesiophytes and pelagophytes may have become more dominant in deep waters during AMT-3.

## 5.3. Nano- and Microphytoplankton Groups

### 5.3.1. Nano- and Microphytoplankton Biomass and Dominant Species

*South Atlantic Subtropical Waters (SASW; 0 - 30°S)* - Spatial and temporal variability in the total biomass of the nano- and micro-phytoplankton species in the SASW is presented in Figure 5.4, while variations in the contribution of the major phytoplankton groups (diatoms, coccolithophores, autotrophic dinoflagellates and endosymbiotic species) to total biomass are presented in Figure 5.5.

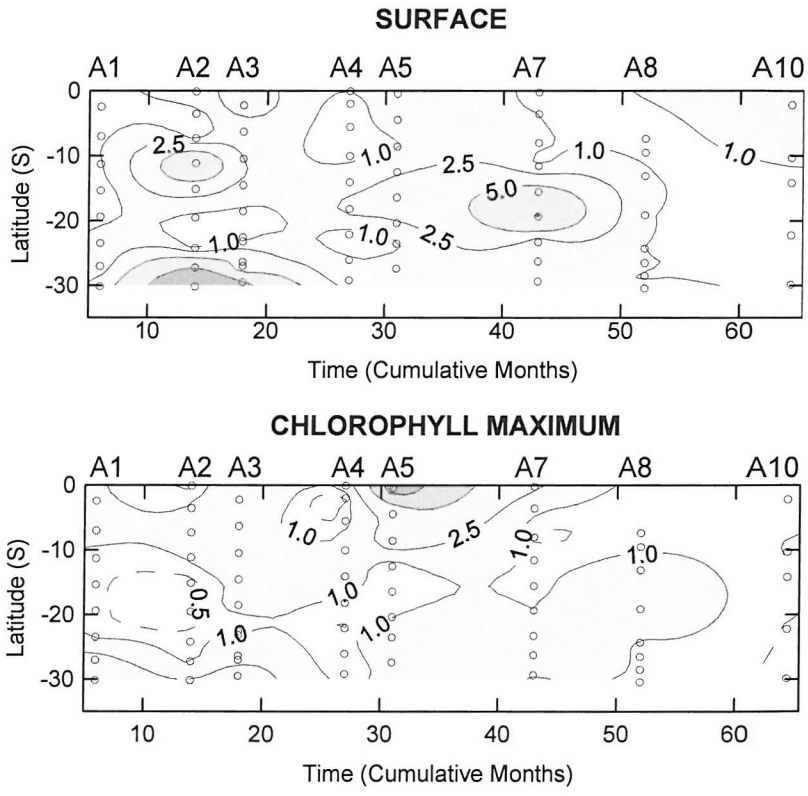


Figure 5.4: Spatial and temporal variability of the total biomass (mg C $m^{-3}$) of nano- and micro-phytoplankton species in surface water and the CM of the SASW (0 - 30°S). Sample points indicated by open circle and AMT cruise numbers given in shortened form on upper x-axis (i.e. A1 = AMT1).

The total biomass of major nano- and microphytoplankton species shows a patchy distribution in both the surface (7 m) and CM (Fig. 5.4), with the range of the biomass values slightly less for CM samples than surface samples; total biomass is ~1.0 - >5.0 mg C $m^{-3}$ in surface waters and between ~0.5 - 2.5 mg C $m^{-3}$ in the CM. Highest biomass measurements are seen in surface waters of the central gyre during AMT-2 and 7, while high biomass in the CM is restricted to equatorial waters during AMT-5 and 7 (Fig. 5.4). Separation of the total biomass into contributions from the major nano- and microphytoplankton groups indicates that coccolithophores are generally the dominant large phytoplankton group (50 - 90%) both in the surface and CM. However, decreases

in coccoiithophore dominance occur periodically and are accompanied by increases in the contribution of one other group or a combination of more than one group (Fig. 5.5).

In the surface community, coccolithophores typically account for 50 - 90% of the total biomass, while autotrophic dinoflagellates generally make the second highest contribution (25 - 50%) and diatoms and endosymbiotic species make smaller contributions (typically <10%) to the total (Fig. 5.5). Within the CM, coccolithophores typically account for 50 - 75% of the total biomass and the second major contributors are diatoms (25 - 50%) rather than autotrophic dinoflagellates (10 - 50%; Fig. 5.5). Decreases in the coccolithophore contribution to total biomass occur patchily in both the surface and CM during AMT-3, 5, 8 and 10 (Fig. 5.5). In surface waters, when the coccolithophore contribution to total biomass decreases there are increases in the contributions from diatoms and autotrophic dinoflagellates, whereas in the CM there is an increase in only diatom contributions. This variability does not appear to be related to changes in the absolute biomass of the groups, as decreases in the total biomass generally occur when coccolithophore contributions decrease (Figs. 5.4 and 5.5).

Increases in diatom contributions and total biomass (Figs. 5.4 and 5.5) are observed at the southern edge of the SASW during AMT-1 (mainly *Dactyliosolen* spp. and *Guinardia striata*) and AMT-3 (small unidentified pennates), and in northern waters during AMT-10 (small unidentified pennates and pennate sp. 'C'). During AMT-3, 4 and 5 high diatom contributions were observed in the CM within the central region of the SASW, although the total biomass remains low (~1.0 mg C $m^{-3}$), and was due mainly to the presence of *Detonula pumila* (Figs. 5.4 and 5.5). One outlier has been removed from Figures 5.4 and 5.5; within the CM at ~8°S during AMT-3, a single diatom species (*Rhizosolenia chunii*) was responsible for biomass measurements up to 824 mg C $m^{-3}$ (cell densities up to 1.24 x $10^6$ cells $l^{-1}$). *R. chunii* is classified as a subarctic species (Tomas, 1997), which is similar in appearance to *Guinardia cylindrus* (D. Harbour, pers. comm.) and appears only during AMT-3 in the SASW and in two samples from southern temperate waters (~50°S) in the entire AMT species dataset. There is no increase in either chl *a* concentration or any of the pigment ratios associated with this sample (Fig. 5.2 and Table 5.4).

High (75 - 90%) coccolithophore contributions to biomass in surface communities are observed during AMT-2 and AMT-7 and are due to the presence of large (up to 50 μm in diameter) cells of *Umbilicosphaera sibogae*, which due to its size is important in variability of the total biomass. High (>75%) coccolithophore contributions to biomass in the CM are observed during AMT-1 and 2 (*U. sibogae*), AMT-3 (small 5 - 10 μm coccolithophores), AMT-5 (*Oolithotus fragilis*) and AMT-8 (*Umbellosphaera irregularis*, *U. tenuis* and 10 - 25 μm coccolithophores) (Fig. 5.5). High (>25%) autotrophic dinoflagellate contributions to total biomass are found during AMT-1 (*Gonyaulax polygramma*), and during AMT-3 and 5 (*Torodinium* spp.) (Fig. 5.5). Generally, autotrophic dinoflagellate contributions to total nano- and microphytoplankton biomass are much lower in the CM than in surface waters which indicates the restriction of this group to upper waters (Fig. 5.5). High (10 - 25%) contributions of endosymbiotic species to total biomass mainly occur in surface waters associated with equatorial waters and are due to the presence of large numbers of the cyanophyte *Trichodesmium* spp. High (10 - 25%) contributions from endosymbiotic species in the CM are found during AMT-3 and AMT-7 (Fig. 5.5), and are due to the occurrence of the large (up to 250 μm long) and rare (cell densities ~20 cells $l^{-1}$) dinoflagellate *Amphisolenia globifera*. *A. globifera* has been

grouped for statistical analysis with other endosymbiotic species due to its known association with external cyanobacterial symbionts (Tomas, 1997).

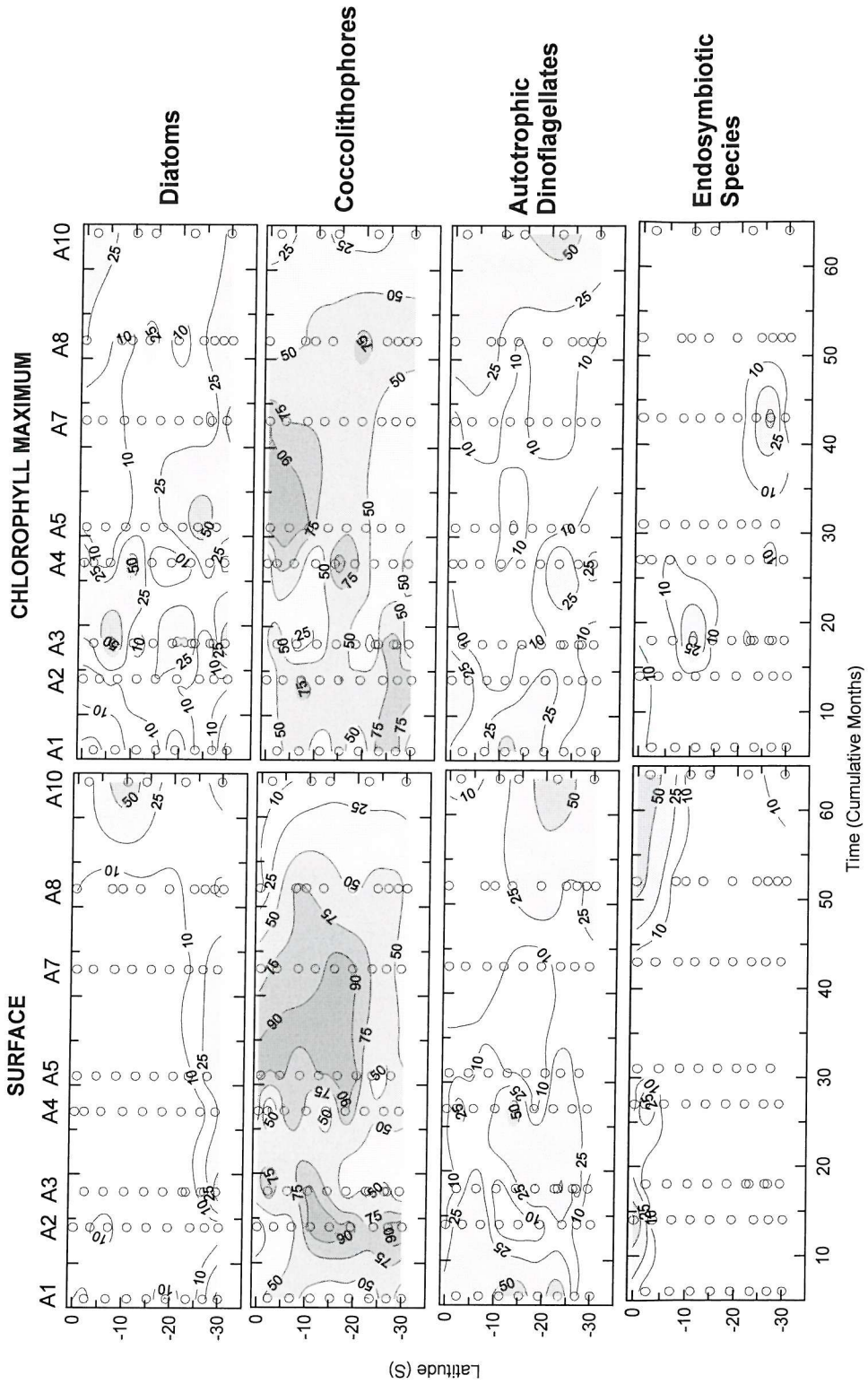


Figure 5.5: Spatial and temporal variability of the percentage contribution (%) of major nano- and microphytoplankton groups to total biomass in surface waters and the CM of the SASW (0 - 30°S). Sample points indicated by open circles and AMT cruise numbers given in shortened form on upper x-axis (i.e. A1 = AMT1).

These results show considerable intercruise variability in the total biomass and composition of the nano- and microphytoplankton community in the SASW. Generally, coccolithophores appear to dominate surface and CM waters in terms of biomass and there is a vertical difference between the second major contributor to total biomass; in surface waters, autotrophic dinoflagellates are the second largest contributor, while in the CM it is diatoms. Consideration of the entire SASW shows

spatial patterns that include increases associated with 'temperate' diatoms at the southern boundary of the SASW, and increases due to the occurrence of *Trichodesmium* spp. around the equator. Thus, further consideration of the total biomass and nano- and microphytoplankton species will focus on the central portion of the SASW (10 - 20°S).

*Central SASW (10 - 20°S) waters* - The total biomass measurements of nano- and microphytoplankton species from the central portion of the SASW (10 - 20°S) are presented in Table 5.6, along with absolute and percentage contributions from the major large (>5 μm) phytoplankton groups. Generally, total biomass of large phytoplankton is higher in surface waters than in the CM, although when surface biomass decreases the difference is small; surface biomass is relatively high (>2.0 mg C $m^{-3}$) during AMT-2, 3, 5 and 7 while total biomass in the CM never exceeds 2 mg C $m^{-3}$ (Table 5.6). High standard deviations for the nano- and microphytoplankton biomass (typically 20 - 90%; up to 240% with the inclusion of *R. chunii* in the CM during AMT-3) highlight the heterogeneous distribution of large phytoplankton and their biomass (Table 5.6). Diatom biomass and contributions to total biomass are generally higher in the CM than in surface waters, although there are large increases during AMT-10 (Table 5.6). The other large phytoplankton groups do not show such a clear pattern; autotrophic dinoflagellate biomass and contributions can be higher in either, coccolithophore biomass and contributions are variable between depths with most cruises showing lower CM biomass than in surface waters, while endosymbiotic species biomass shows no distinct difference between depths (Table 5.6). These results support the earlier conclusion of coccolithophore dominance of both surface and CM waters, while the second dominant group changes between autotrophic dinoflagellates (surface) and diatoms (CM) with depth.

Table 5.6: Nano- and microphytoplankton group biomass (mg C $m^{-3}$) in the central SASW (10 - 20°S). Standard deviations are shown for total biomass, while average percentage contributions are in brackets for individual groups. The number of samples is indicated by n.

| Cruise | | n | Total (mg C $m^{-3}$) | Diatoms | Autotrophic Dinoflagellates | Coccolithophores | Endosymbiotic Species |
|---|---|---|---|---|---|---|---|
| AMT-1 (9/95) | SUR | 3 | 0.7 ± 0.3 | 0.08 (10.1%) | 0.32 (52.2%) | 0.26 (36.7%) | 0.01 (1.0%) |
| | CM | 3 | 0.6 ± 0.0 | 0.11 (17.4%) | 0.27 (41.9%) | 0.24 (38.5%) | 0.01 (2.2%) |
| AMT-2 (5/96) | SUR | 4 | 4.3 ± 3.8 | 0.02 (0.3%) | 0.12 (2.7%) | 4.15 (96.9%) | 0.01 (0.1%) |
| | CM | 4 | 0.6 ± 0.4 | 0.08 (14.2%) | 0.07 (18.9%) | 0.40 (64.5%) | 0.02 (2.5%) |
| AMT-3 (9/96) | SUR | 5 | 3.0 ± 2.3 | 0.06 (2.9%) | 0.23 (16.7%) | 2.41 (69.7%) | 0.34 (10.7%) |
| | CM[a] | 6 | 138.9 ± 336.8 | 137.5 (32.0%) | 0.13 (6.1%) | 0.80 (53.4%) | 0.42 (8.6%) |
| | CM | 5 | 1.35 ± 0.6 | 0.22 (18.4%) | 0.11 (7.3%) | 0.83 (64.0%) | 0.19 (10.3%) |
| AMT-4 (5/97) | SUR | 4 | 1.6 ± 1.1 | 0.01 (0.9%) | 0.38 (27.7%) | 1.20 (70.9%) | 0.001 (0.5%) |
| | CM | 3 | 1.1 ± 0.6 | 0.27 (25.3%) | 0.11 (21.5%) | 0.66 (52.7%) | 0.01 (0.6%) |
| AMT-5 (9/97) | SUR | 4 | 2.3 ± 1.2 | 0.02 (1.1%) | 0.15 (9.2%) | 2.13 (89.3%) | 0.01 (0.5%) |
| | CM | 3 | 0.6 ± 0.3 | 0.19 (27.4%) | 0.06 (12.5%) | 0.38 (59.2%) | 0.01 (1.0%) |
| AMT-7 (9/98) | SUR | 3 | 5.9 ± 4.9 | 0.22 (4.4%) | 0.10 (4.5%) | 5.54 (91.0%) | 0.01 (0.2%) |
| | CM | 5 | 0.8 ± 0.2 | 0.18 (24.7%) | 0.10 (13.6%) | 0.51 (61.1%) | 0.00 (0.6%) |
| AMT-8 (5/99) | SUR | 5 | 1.3 ± 0.7 | 0.10 (7.1%) | 0.28 (21.2%) | 0.89 (65.4%) | 0.00 (0.4%) |
| | CM | 6 | 1.6 ± 0.9 | 0.37 (17.9%) | 0.15 (10.5%) | 1.07 (70.8%) | 0.01 (0.8%) |
| AMT-10 (9/00) | SUR | 3 | 0.8 ± 0.4 | 0.42 (41.7%) | 0.28 (39.3%) | 0.11 (14.5%) | 0.03 (4.6%) |
| | CM | 3 | 0.5 ± 0.1 | 0.09 (17.9%) | 0.28 (54.9%) | 0.11 (21.9%) | 0.03 (5.3%) |

[a] includes *Rhizosolenia chunii*

Temporal variability of nano- and microphytoplankton biomass and percentage contributions are also shown in Table 5.6. High total biomass (>2 mg C $m^{-3}$) in surface waters during AMT-2, 3, 5 and 7 are due to increases in coccolithophore biomass and average percentage contributions. During AMT-1 and 10, coccolithophore biomass and contributions are low (<0.3 mg C $m^{-3}$ and ~60%, respectively) in both surface and CM waters (Table 5.6). Changes in coccolithophore biomass and contributions are generally accompanied by increases of autotrophic dinoflagellate and diatom biomass and contribution, although the pattern changes between cruises; mainly autotrophic dinoflagellates during AMT-1, and both diatoms and autotrophic dinoflagellates during AMT-10 (Table 5.5). Inclusion of the cell counts of *R. chunii* in the total estimate of CM biomass gives a central SASW average biomass ~100 - 230 times higher than other cruise averages (Table 5.6).

Examination of spatial variations in nano- and microphytoplankton biomass show that coccolithophores are generally the dominant group in terms of biomass and contribution to total large phytoplankton biomass in both the surface and CM. The distribution of large phytoplankton cells in the SASW is highly heterogeneous which indicates caution when interpreting temporal trends of biomass. There are vertical differences in the second major contributor to total biomass, with autotrophic dinoflagellates important in surface waters and diatoms in the CM. There is also evidence of interannual variations in the biomass and contributions of the different large phytoplankton groups; during AMT-2, 3, 5 and 7 high total biomass (>2 mg C $m^{-3}$) is associated with high coccolithophore biomass in surface waters, whereas when total biomass is low during AMT-1 and 10 diatom and autotrophic dinoflagellate contributions are higher than coccolithophore contributions.

## 5.3.2. Temporal Variability of the Community Composition; Major Phytoplankton Groups

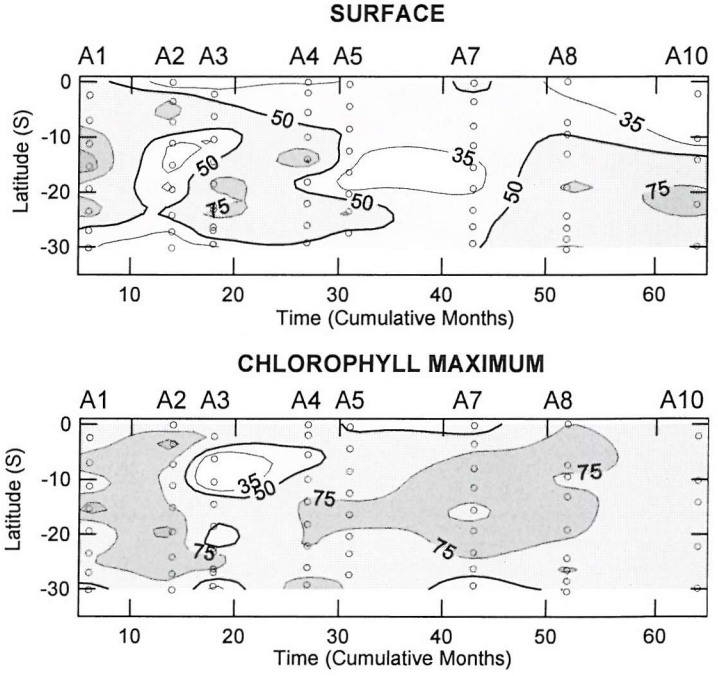


Figure 5.6: Spatial and temporal distribution of Bray-Curtis percentage (%) similarity of the contribution of the major nano- and microphytoplankton groups to total biomass in the surface and the CM of the SASW (0 - 30°S). All surface (CM) samples are compared with the 15°S surface (CM) sample from AMT1. Sample points indicated by open circles and AMT cruise numbers given in shortened form on upper x-axis (i.e. A1 = AMT1).

The last section showed intercruise variability in the biomass and biomass contributions of the nano- and microphytoplankton community in the SASW. To examine spatial and temporal variations in the community composition in terms of the major phytoplankton groups, the similarity between the

community present in all the samples and a static 'reference' sample (community) is examined. 'Reference' samples from the surface and CM have been selected from the central portion of the SASW (15°S) at the start of the time-series (AMT-1). The Bray-Curtis percentage similarity of the surface and CM sample from this latitude compared with all other samples is presented in Figure 5.6 for both the surface and CM. Phytoplankton group biomass has been standardised so that the similarity of group contributions to total biomass are analysed.

Important discontinuities in the similarity between samples have been taken (arbitrarily) as occasions when the similarity between samples falls below 50%, which occurs more often in the surface than in the CM (Fig. 5.6). In surface waters there are changes in the major group composition during AMT-2, 3, 5 and 7 whereas there are increases in similarity during AMT-8 and within the southern portion of the SASW during AMT-10 (Fig. 5.6). Similarity in the CM community composition is generally higher (50 - 75%) than within surface waters (35 - 50%), although there is a sharp decrease below 35% associated with the occurrence of *R. chunii* at ~8°S during AMT-3 (Fig. 5.6). Comparison of Figure 5.6 with the distribution of large phytoplankton group biomass contributions (Fig. 5.5) indicates that decreases in surface similarity are associated with increases in coccolithophore contributions, while increases in similarity during later cruises are associated with increased autotrophic dinoflagellate contributions. Within the CM community the reverse is indicated; when coccolithophore contributions decrease, percentage similarity also decreases. Differences in the patterns of similarity in surface and CM community composition lead to the conclusion that there are different community dynamics at work at the different depths; the surface community appears to be more variable in its composition (coccolithophores, diatoms and autotrophic dinoflagellates), while the CM community is mostly dominated by coccolithophores and appears relatively stable in terms of its composition. Intercruise variability in the species composition of these major nano- and microphytoplankton groups will be examined in the next section.

## 5.4. Species Composition

### 5.4.1. Community Diversity and Species Richness

Diversity is related to the competitive dynamics and structure of a community, and is composed of two components; a measure of the number of species (species richness) and a measure of the partitioning of the total numbers between individual species (dominance or evenness). Spatial and temporal trends of both components of diversity within the SASW are presented in Figure 5.7 in terms of Shannon (H') diversity (dominance) and the number of species (species richness).

Shannon (H') diversity and the number of species show slightly different patterns (Fig. 5.7), indicating that fluctuations in H' may not always be accompanied by changes in the number of species. Low H' is generally observed during the early AMT cruises in surface waters (apart from in northern SASW during AMT-2), whereas there are increases in H' from values of 1 to >2 during AMT-7, 8 and 10 (Fig. 5.7a). The number of species in surface waters roughly follows the increase in H', although an initial increase in species numbers occurs during AMT-5 and precedes the increase in H' (Fig. 5.7a and b). In the CM community there is a peak in species richness during AMT-3 and then another increase during AMT-5 (Fig. 5.7b). The initial increase in species richness during AMT-3 is

not accompanied by an increase in H', although the later increase during AMT-5 is associated with an increase in H' from 1 to >1.5 (Fig. 5.7a). Highest H' is found during AMT-8 and 10 (>2) ,while high species numbers (>24) are observed during AMT-5, 7, 8 and 10 in surface waters and during AMT-3, 5, 7 and 10 in the CM (Fig. 5.7).

These results indicate that in surface waters there was an increase in species during AMT-5, although the community remained dominated by a few species (low H') until AMT-8 and 10 (high H'). In the CM community there was an increase in species numbers during AMT-3, although the community remained dominated by a few species (low H'), and then again during AMT-5 when the community became less dominated (high H') and cell numbers became relatively evenly distributed between all the species present.

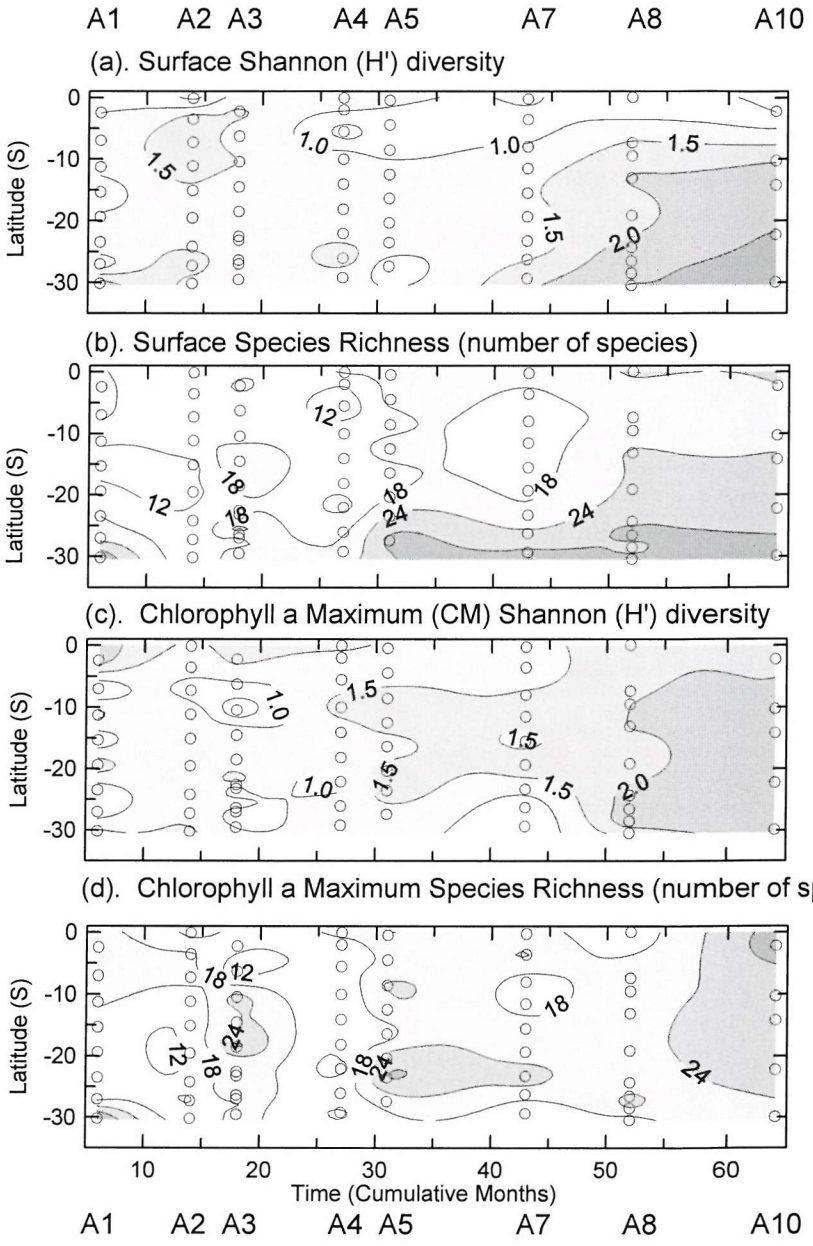


Figure 5.7: Diversity in the surface and CM of the nano- and microphytoplankton community; (a) Surface Shannon (H') diversity, (b) Surface species richness, (c) CM Shannon (H') diversity, and (d) CM species richness. Sample points indicated by open circles and AMT cruise numbers given in shortened form on top x-axis (i.e. A1 = AMT1).

### 5.4.2. Nano- and Microphytoplankton Species Composition

The last section indicated that temporal variability in the nano- and microphytoplankton community occurred in terms of species richness and the evenness of distribution of cell numbers between species. These changes may have or may not have been accompanied by changes in the species composition of the community. To investigate such changes in the species composition of the community two approaches have been selected; a comparison of the Bray-Curtis percentage similarity of the species composition of all samples with a 'reference' sample, and cluster analysis of the species composition of all samples with the aim of identifying those species which have changed in their distribution and abundance. The first analysis of spatial and temporal variability of the Bray-Curtis percentage similarity of samples with a 'reference' sample could be biased if the sample chosen represents a community that is dramatically different in composition to the majority of other samples. The second analysis comparing the composition of all samples and investigating species distribution and abundance changes should indicate whether or not the 'reference' sample from the first analysis is significantly different from the majority of other samples. Thus, the second analysis will support or dismiss the use of the 'references samples to indicate temporal changes in community composition.

*Bray-Curtis Similarity* - The first approach to investigating changes in the species composition is similar to that used to identify changes in the major phytoplankton group composition in terms of contributions to total biomass; selection of a surface and CM sample from 15°S during AMT-1 and comparison of the Bray-Curtis percentage similarity between this sample and all other samples. Spatial and temporal variations in the similarity of the surface and CM species composition are presented in Figure 5.8. Due to the different nature of the community data (i.e. species biomass) the data has been transformed using two different methods to highlight different changes; (1) presence / absence (PA) transformation to downplay the role of rare and dominant species and indicate variability in all species (Fig. 5.8a), and (2) square-root (SQRT) transformation of the common species (consistently >10% of total numbers) biomass to indicate variability in the dominant species (Fig. 5.8b). Treatment of the species data with the SQRT transformation retains 49 species out of the total 141 species examined in the PA analysis; 14 diatom, 15 autotrophic dinoflagellate, 17 coccolithophore and 3 endosymbiotic species. Important discontinuities in the similarity between samples is (arbitrarily) taken as occasions where the similarity falls below 50% (i.e. samples share <50% of their species) and is found more in the CM samples than in surface waters (Fig. 5.8).

In surface waters of the SASW, the species composition (PA) is relatively similar (>50%) during AMT-1 and patchy during AMT-2, 4, 5 and 7, whereas the similarity is low (<50%) throughout the SASW during AMT-8 and 10 (Fig. 5.8a). Within the CM, the overall PA similarity is much lower (~35%) than in surface waters and only exceeds 50% during AMT-1 and once during AMT-7 (Fig. 5.8a). Species dominance (SQRT) in surface waters is generally high (>50%) during most AMT cruises, although low similarity (<50%) is widespread in the SASW during AMT-3, 4 and 10 (Fig. 5.8b). In the CM the overall SQRT similarity is again low (~35%), with similarity ~50% only found for a few samples during AMT-4, 5 and 7 (Fig. 5.8b).

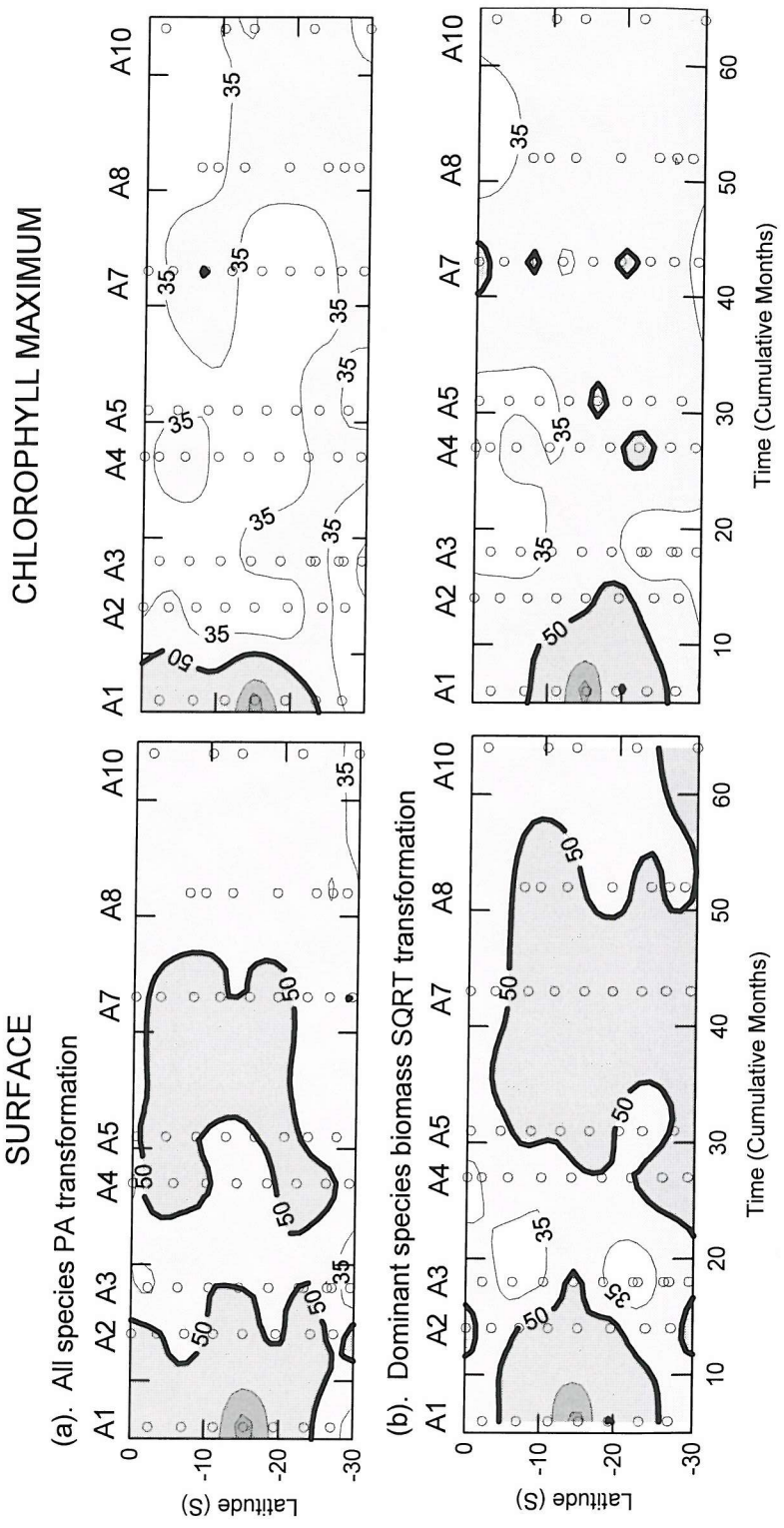


Figure 5.8: Spatial and temporal distribution of Bray-Curtis percentage similarity of nano- and microphytoplankton species composition (a) and dominance (b) in the surface and CM. Species composition (a) analysed through PA transformation of abundances, while species dominance analysed through SQRT transformation of dominant species biomass. All samples compared with a surface and CM sample from 15°S during AMT1. Sample points indicated by open circles and AMT cruise numbers given in shortened form on top x-axis (i.e. A1 = AMT1).

Spatial and temporal variability in the Bray-Curtis percentage similarity of species composition (PA; Fig. 5.8a) and species dominance (SQRT; Fig. 5.8b) show different patterns to that previously found for major nano- and microphytoplankton groups (Fig. 5.6); there is a higher level of intercruise similarity (typically 35 - >50%) in surface waters than CM samples (typically <35% and rarely ~50%). The combined results of Figures 5.6 and 5.8 indicate that in surface waters although the composition of the community in terms of major group biomass varies markedly the species composition is relatively stable, whereas in the CM although the community is generally stable in

terms of phytoplankton groups (i.e. dominated by coccolithophores) the species composition is far more variable. Temporal trends in the distribution of Bray-Curtis similarity in surface waters indicate a decrease in similarity of species composition during AMT-3, 8 and 10 and a decrease in species dominance during AMT-3, 4 and 10 (Fig. 5.8). Within the CM, overall similarity is much lower with highest similarity in species composition in the central SASW during AMT-8 and 10, and extremely low similarity in species dominance restricted to northern and southern portions of the SASW during AMT-3, 4 and 5. Therefore, there seems to be variability in the species composition of surface waters during AMT-3, 8 and 10, whereas the overall species similarity of the CM shows high intercruise variability.

*Cluster analysis and species compositional changes* - Cluster analysis of the PA transformed species abundances and SQRT transformed species biomass shows separation of several clusters of samples at ~40% similarity (Fig. 5.9). The number of samples per cluster and number of clusters varies with the data transformation and some clusters are not true clusters as they include samples that have relatively high dissimilarities (Fig. 5.9). The distribution of the major sample clusters is presented on a latitude-time grid to indicate spatial and temporal variations in species composition in Figure 5.10. Sample clusters with <5 samples and clusters which are limited in their distribution are not presented or discussed.

Species important in determining the differences between clusters have been identified using SIMPER analysis to breakdown the average dissimilarities ($\delta$) between clusters into contributions from individual species ($\delta i$) and the results are presented in Tables 5.7 and 5.8 for both the PA and SQRT transformation. Results included in Tables 5.7 and 5.8 are the species code (see Table 5.1 for full species name), the average dissimilarity between clusters ($\delta$), the average individual species abundance for PA analysis and average biomass for SQRT analysis, the average species contribution to dissimilarity ($\delta i$), the ratio of $\delta i$ to the species' standard deviation and the cumulative percentage contribution to total dissimilarity for each species. In this type of analysis all species will have a role in the dissimilarity between clusters (Clarke and Warwick, 1994) and therefore for this study, only species responsible for ~20% of the dissimilarity between PA clusters and ~40% of the dissimilarity between SQRT clusters are presented. Due to the data transformations, *R. chunii* has been included in the PA analysis but eliminated from the SQRT analysis due to its occurrence in less than 1% of the samples.

(a). Surface PA clusters - Three major sample clusters are identified from the cluster dendrogram for surface samples with PA transformation (Fig. 5.9a); clusters B, D and E. The spatial and temporal distribution of cluster B in the SASW is restricted to waters associated with the southern edge of the SASW during AMT-1, 3, 5 and 7, while cluster E is widespread throughout the SASW during most cruises. Cluster D is found in two samples during early cruises (AMT-2 and 3) and in all samples during AMT-8 (apart from cluster A at the northern edge) and AMT-10 (Fig. 5.10a). Breakdown of the dissimilarity between major sample clusters shows that the average dissimilarity between cluster B and D is 60.8%, between B and E is 60.0%, and between D and E is 54.8% (Table 5.7). 21.8% of the total dissimilarity between clusters B and D is due to the absence of pennate sp. 'C' and *Syracosphaera* spp., lower numbers of *Oxytoxum* sp. and higher numbers of *Leptocylindrus danicus*,

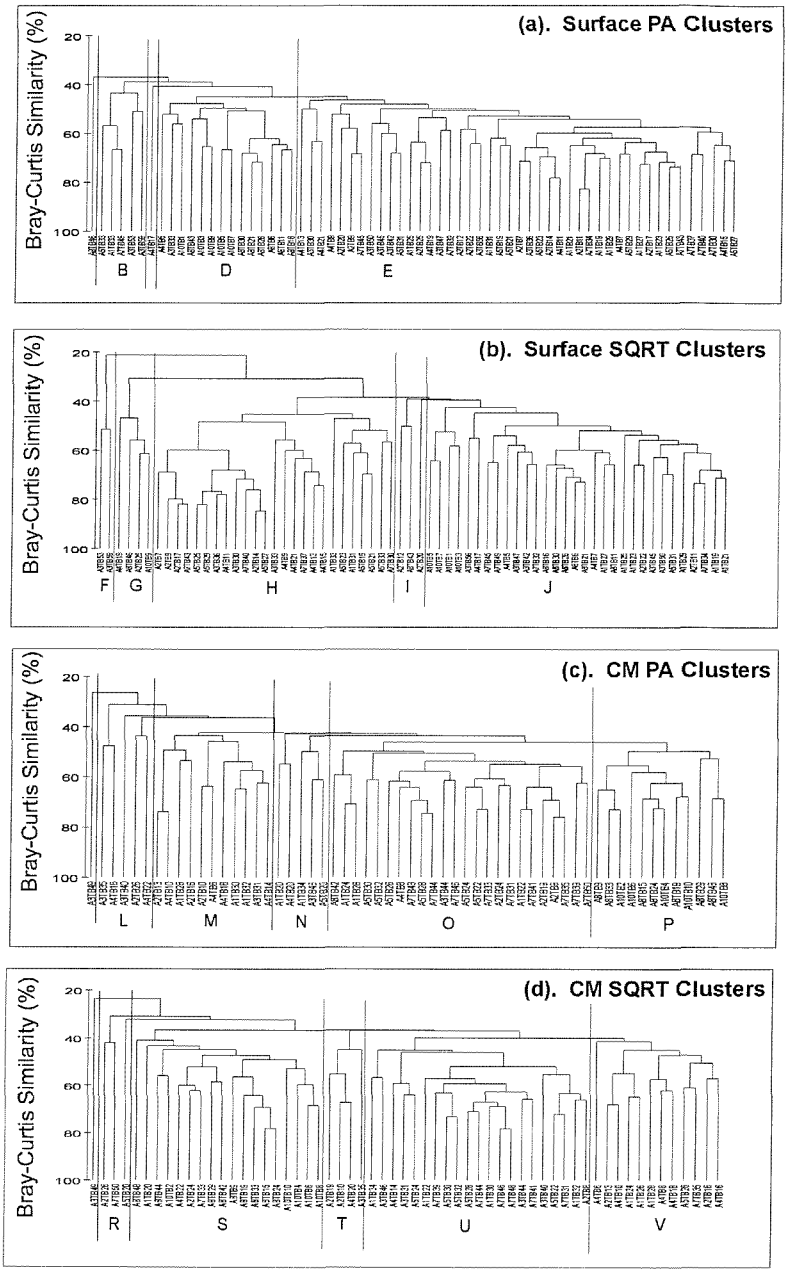


Figure 5.9: Cluster dendrograms for analysis of variations in nano- and microphytoplankton species composition in the SASW; (a) all species in surface samples with PA transformation, (b) dominant species in surface samples with SQRT transformation, (c) all species in CM samples with PA transformation, and (d) dominant species in CM samples with SQRT transformation. Major clusters are identified with letters for all clusters and are used further in the text, Tables 5.7 and 5.8, and Figure 5.8.

*Corethron criophilum*, *Pseudo-nitzschia* spp., *Myrionecta rubra*, *U. sibogae*, *Bacteriastrum* spp. and *Nitzschia longissima* in cluster B (Table 5.7). 22.0% of the total dissimilarity between clusters B and E is due to the absence of *C. criophilum* in E and higher numbers of *N. longissima*, *L. danicus*, Hyalochaete *Chaetoceros* spp., *M. rubra*, *Pseudo-nitzschia* spp., *Bacteriastrum* spp. and *Phaeoceros Chaetoceros* spp. in B (Table 5.7). 21.8% of the total dissimilarity between clusters D and E is due to the absence of *Syracosphaera* spp., and the unidentified "Heart" coccolithophore sp. in E, higher numbers of pennate sp. 'C', *Scrippsiella / Alexandrium* spp., and *Acanthoica* sp. and lower numbers of *U. sibogae*, *Helicosphaera* sp., and small *Prorocentrum* spp. in D (Table 5.7). These results indicate that cluster B represents an influx of species from southern waters outside the SASW due to its predominance of diatoms associated with South Atlantic Ocean waters (cf. Eynaud *et al.*, 1999). The major differences in species composition of surface samples is an increase in the numbers of the

pennate diatom sp. 'C', the autotrophic dinoflagellate group *Scrippsiella / Alexandrium* spp. and the coccolithophore genus *Acanthoica* during AMT-8 and 10, and a decrease in the numbers of the coccolithophores *U. sibogae* and *Helicosphaera* sp. and small autotrophic dinoflagellates of the genus *Prorocentrum* (Table 5.7).

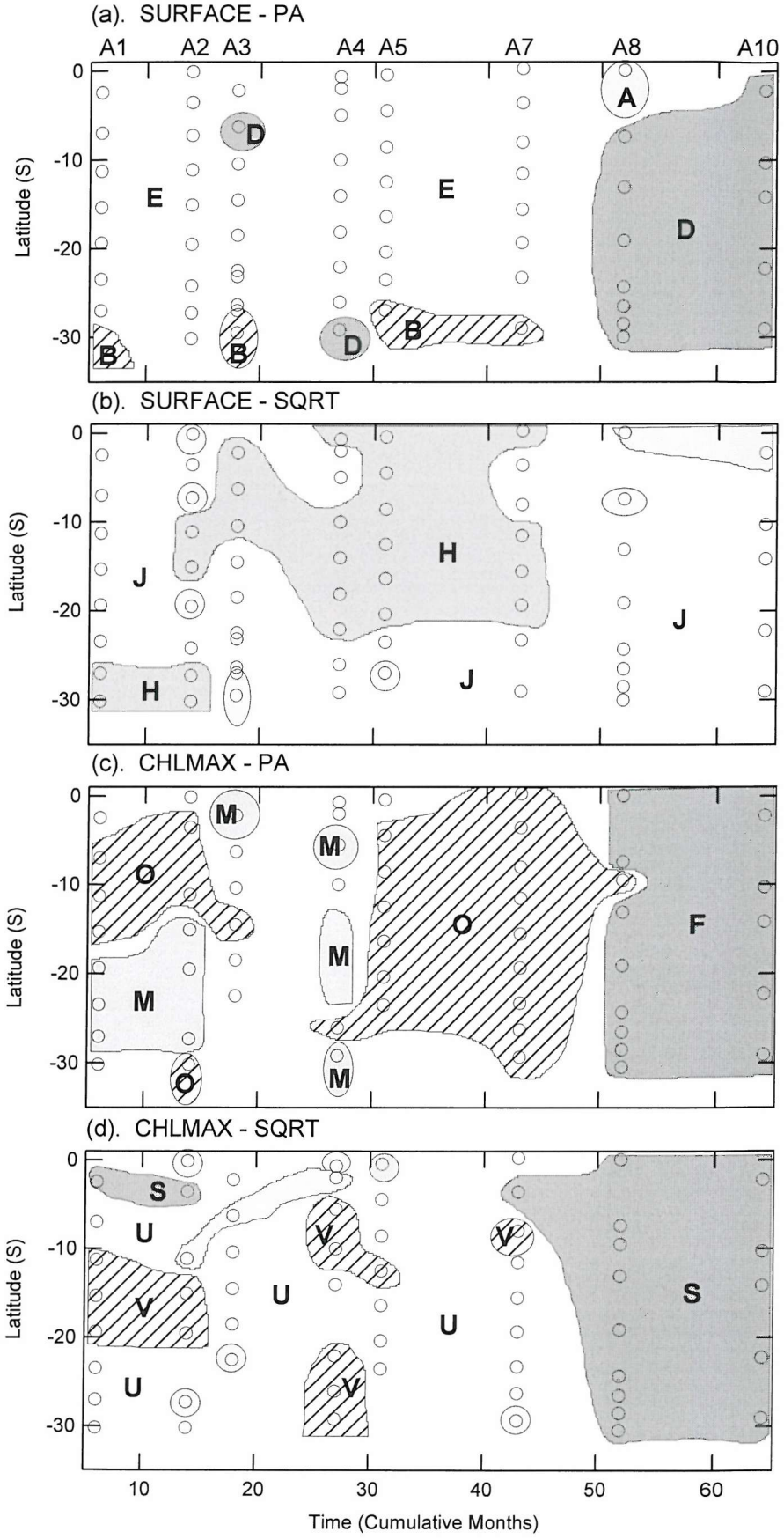


Figure 5.10: The spatial and temporal distribution of major clusters from nano- and microphytoplankton species composition analysis in the SASW; (a) all species in surface samples with PA transformation, (b) dominant species in surface samples with SQRT transformation, (c) all species in CM samples with PA transformation, and (d) dominant species in CM samples with SQRT transformation. Sample points indicated by open circles and major clusters indicated with shading and cluster identity (letters). AMT cruise numbers given in shortened form on top x-axis (i.e. A1 = AMT1). In the case of analysis (b) and (d), minor clusters are included and shaded to highlight the distribution of the major clusters.

(b). Surface SQRT clusters - Two major sample clusters are identified from the cluster dendrogram for surface samples with SQRT transformation (Fig. 5.9b); clusters H and J. Cluster J is found during all AMT cruises, although it latitudinal distribution varies; during AMT-1, 8 and 10 it is relatively widespread whereas during AMT-4, 5 and 7 it is restricted to the southern portion of the SASW while cluster H is found in surface samples (Fig. 5.10b). The average dissimilarity between these two clusters is high (60.9%) and 48.4% of the dissimilarity can be explained by higher biomass of *U. sibogae* and *U. irregularis* in cluster H and higher biomass of the athecate dinoflagellate genus *Torodinium* and 10 - 25μm coccolithophores in cluster J (Table 5.7). Due to the occurrence and identification of *U. sibogae* and *U. irregularis* in samples from AMT-8 (see Chapter 4), differences in the distribution of these species between early and late cruises (i.e. those counted by D. Harbour and those examined in this study; AMT-8 and 10) are likely to reflect real differences and not identification errors.

Table 5.7: Summary of SIMPER results from the breakdown of dissimilarity between clusters of surface samples to the contributions from individual species. Only species responsible for ~20% of the total dissimilarity between PA clusters and ~40% of the total dissimilarity between SQRT clusters are presented. PA clusters are based on average cell numbers (cells $l^{-1}$) while SQRT clusters are based on average biomass (ng C $l^{-1}$). Table includes species codes (see Table 5.1 for full species names), average dissimilarity between clusters ($\delta$), average contributions of each species to total dissimilarity ($\delta i$), ratio of $\delta i$ to species' standard deviation (ratio), and the cumulative percentage of total dissimilarity for each species.

| Species Code | Average Abundance / Biomass | Average Abundance / Biomass | Average Contribution to Dissimilarity | Ratio | Cumulative percentage of total dissimilarity |
|---|---|---|---|---|---|
| **SURFACE PA** | | | | | |
| | Cluster B | Cluster D | Average $\delta$ = 60.8% | | |
| D57 | 0.0 | 219.3 | 1.5 | 1.8 | 2.5 |
| D45 | 1420.0 | 0.0 | 1.5 | 1.7 | 4.8 |
| D26 | 355.0 | 0.0 | 1.4 | 1.7 | 7.2 |
| D64 | 485.0 | 2.9 | 1.4 | 1.5 | 9.4 |
| ED9 | 23.0 | 2.1 | 1.3 | 1.4 | 11.6 |
| CC16 | 0.0 | 62.9 | 1.3 | 1.5 | 13.7 |
| CC18 | 20.0 | 14.3 | 1.3 | 1.5 | 15.8 |
| D8 | 45.0 | 5.0 | 1.3 | 1.4 | 17.9 |
| AD47 | 5.0 | 72.9 | 1.2 | 1.3 | 19.9 |
| D52 | 310.0 | 27.9 | 1.2 | 1.3 | **21.8%** |
| | Cluster B | Cluster E | Average $\delta$ = 60.0% | | |
| D52 | 310.0 | 2.9 | 2.1 | 3.2 | 3.5 |
| D45 | 1420.0 | 2.4 | 1.7 | 1.6 | 6.4 |
| D26 | 355.0 | 0 | 1.7 | 1.7 | 9.3 |
| D20 | 365.0 | 15.2 | 1.6 | 1.5 | 11.9 |
| ED9 | 230.0 | 21.9 | 1.6 | 1.4 | 14.6 |
| D64 | 485.0 | 13.3 | 1.6 | 1.4 | 17.2 |
| D8 | 45.0 | 18.1 | 1.5 | 1.5 | 19.7 |
| D21 | 50.0 | 16.7 | 1.4 | 1.2 | **22.0%** |
| | Cluster D | Cluster E | Average $\delta$ = 54.8% | | |
| D57 | 219.3 | 2.4 | 1.9 | 1.7 | 3.5 |
| CC16 | 62.9 | 0 | 1.7 | 1.5 | 6.5 |
| AD59 | 45.7 | 9.5 | 1.6 | 1.2 | 9.3 |
| CC19 | 84.3 | 0 | 1.5 | 1.3 | 12.1 |
| CC18 | 14.3 | 843.7 | 1.5 | 1.2 | 14.8 |
| CC2 | 12.1 | 10.9 | 1.3 | 1.0 | 17.1 |
| CC10 | 33.6 | 105.9 | 1.3 | 1.0 | 19.5 |
| AD53 | 46.4 | 89.5 | 1.3 | 1.0 | **21.8%** |
| **SURFACE SQRT** | | | | | |
| | Cluster H | Cluster J | Average $\delta$ = 60.9% | | |
| CC18 | 2874.6 | 19.4 | 18.5 | 1.5 | 30.4 |
| CC17 | 239.7 | 184.7 | 4.5 | 1.3 | 37.8 |
| AD60 | 33.1 | 115.9 | 3.5 | 1.4 | 43.5 |
| CC1 | 114.1 | 160.2 | 3.0 | 1.1 | **48.4%** |

(c). Chlorophyll *a* Maximum (CM) PA clusters - Three major sample clusters are identified from the cluster dendrogram for CM samples with PA transformation (Fig. 5.9c); clusters M, O and P. Cluster M is limited in its spatial and temporal distribution and occurs in a few samples during AMT-1, 2, 3 and 4, while cluster O is present in a few samples during AMT-1, 2 and only one sample during AMT-3 and 4, before being found throughout the SASW during AMT-5 and 7 and in one sample during AMT-8 (Fig. 5.10c). Cluster P is only observed during the last two cruises (AMT-8 and 10) when it extends throughout the SASW (Fig. 5.10c). Breakdown of the dissimilarity between major sample clusters shows that the average dissimilarity between cluster M and O is 55.1%, between M and P is 60.8% and between M and O is 54.0% (Table 5.8). 20.6% of the total dissimilarity between clusters M and O is due to lower numbers of *Ophiaster* spp., *Phaeoceros Chaetoceros* spp., small unidentified pennate diatoms, *Helicosphaera* spp. and *Halopappus* spp., and higher numbers of *Gephyrocapsa ornata* in cluster M (Table 5.8). 22.3% of the total dissimilarity between clusters M and P is due to the absence of *Haslea* spp. and pennate sp. 'C', higher numbers of *Ophiaster* sp., and *Pseudo-nitzschia* spp., and lower numbers of small unidentified pennate diatoms, *N. longissima* and *Oxytoxum* spp. in cluster M (Table 5.8). 20.6% of the total dissimilarity between clusters O and P is due to the absence of *U. sibogae* in cluster P, higher numbers of *Pseudo-nitzschia* spp. and *Phaeoceros Chaetoceros* spp., and lower numbers of *Haslea* spp., *N. longissima*, pennate sp. 'C' and *Oxytoxum* spp. in cluster O (Table 5.8). Differences between the clusters in the case of PA transformation are due to fluctuations in the abundance of all the major nano- and microphytoplankton groups. These results show that differences between AMT-5+7 and AMT-8+10 are mainly due to the disappearance of the large coccolithophore *U. sibogae* and a change in diatom species, with increases of *Haslea* spp., *N. longissima* and pennate sp. 'C' and decreases of *Pseudo-nitzschia* spp. and *Phaeoceros Chaetoceros* spp. during the later cruises (Table 5.8).

(d). Chlorophyll *a* Maximum (CM) SQRT clusters - Three major sample clusters are identified from the cluster dendrogram for CM samples with SQRT transformation (Fig. 5.9d); clusters S, U and V. Cluster V is limited in its spatial and temporal distribution to a few localised occurrences; in the central SASW during AMT-1 and 2 and in a few samples from AMT-4 and 5 (Fig. 5.10d). Cluster U is the most widespread cluster and occurs throughout most of the SASW during most of the AMT cruises up to AMT-8 and 10 when cluster S is found throughout the SASW (Fig. 5.10d). Cluster S also occurs in the northern portion of the SASW in two samples during AMT-1 and 2 and in one sample from AMT-7 (Fig. 5.10d). Breakdown of the dissimilarity between major sample clusters shows that the average dissimilarity between cluster S and U is 64.5%, between S and V is 61.4% and between U and V is 60.2% (Table 5.8). 41.5% of the total dissimilarity between clusters S and U is due to higher biomass of 10 - 25 μm coccolithophores and *Torodinium* sp., and lower biomass of *U. sibogae*, small coccolithophores (5 - 10 μm) and *Phaeoceros Chaetoceros* spp. in cluster S (Table 5.8). 43.2% of the total dissimilarity between clusters S and V is due to the absence of *Haslea* spp. in V, higher biomass of 10 - 25 μm coccolithophores, *Torodinium* spp., and *Scrippsiella / Alexandrium* spp., and lower biomass of *Discosphaera tubifer*, small coccolithophores, *U. sibogae* and *Leptocylindrus mediterraneus* in cluster S (Table 5.8). 42.1% of the total dissimilarity between clusters U and V is due to higher biomass of *U. sibogae*, 10 - 25 μm coccolithophores, small coccolithophores and *U. irregularis* in cluster U (Table 5.8). These results indicate that the major

Table 5.8: Summary of SIMPER results from the breakdown of dissimilarity between clusters of CM sample to contributions from individual species. Only species responsible for ~20% of the total dissimilarity between PA clusters and ~40% of the total dissimilarity between SQRT clusters are presented. PA clusters are based on average cell numbers (cells l-1) while SQRT clusters are based on average biomass (ng C $l^{-1}$). Table includes species codes (see Table 5.1 for full species names), average dissimilarity between clusters ($\delta$), average contributions of each species to total dissimilarity ($\delta i$), ratio of $\delta i$ to species' standard deviation (ratio), and the cumulative percentage of total dissimilarity for each species.

| Species Code | Average Abundance / Biomass | Average Abundance / Biomass | Average Contribution to Dissimilarity | Ratio | Cumulative percentage of total dissimilarity |
|---|---|---|---|---|---|
| **CM PA** | | | | | |
| | Cluster M | Cluster O | Average $\delta$ = 55.1 | | |
| CC12 | 412.7 | 1957.1 | 2.5 | 1.9 | 4.5 |
| D21 | 5.4 | 64.2 | 2.1 | 1.4 | 8.2 |
| D56 | 36.4 | 1432.5 | 1.9 | 1.2 | 11.7 |
| CC10 | 12.7 | 92.1 | 1.7 | 1.1 | 14.8 |
| CC20 | 18.2 | 2.5 | 1.6 | 1.0 | 17.7 |
| CC9 | 23.6 | 45.0 | 1.6 | 1.0 | **20.6%** |
| | Cluster M | Cluster P | Average $\delta$ = 60.8 | | |
| CC12 | 412.7 | 342.5 | 2.5 | 2.7 | 4.2 |
| D41 | 0.0 | 76.6 | 2.0 | 1.6 | 7.5 |
| D57 | 0.0 | 390.0 | 1.8 | 1.3 | 10.5 |
| D56 | 36.36 | 888.3 | 1.8 | 1.3 | 13.5 |
| D52 | 36.36 | 612.5 | 1.8 | 1.3 | 16.4 |
| AD47 | 25.45 | 30.0 | 1.8 | 1.3 | 19.4 |
| D64 | 174.5 | 15.0 | 1.8 | 1.2 | **22.3%** |
| | Cluster O | Cluster P | Average $\delta$ = 54.0 | | |
| D64 | 540.0 | 15.0 | 2.1 | 2.5 | 3.9 |
| D41 | 2.5 | 76.7 | 1.7 | 1.6 | 7.1 |
| CC18 | 202.2 | 0.0 | 1.7 | 1.5 | 10.1 |
| D52 | 20.0 | 612.5 | 1.5 | 1.3 | 12.9 |
| D21 | 64.2 | 10.0 | 1.5 | 1.2 | 15.6 |
| D57 | 30.0 | 390.0 | 1.4 | 1.1 | 18.2 |
| AD47 | 22.5 | 30.0 | 1.3 | 1.1 | **20.6%** |
| **CM SQRT** | | | | | |
| | Cluster S | Cluster U | Average $\delta$ = 64.5 | | |
| CC18 | 2.22 | 1023.7 | 12.5 | 1.5 | 19.4 |
| CC1 | 397.6 | 285.5 | 4.8 | 1.3 | 26.9 |
| CC8 | 49.3 | 178.7 | 4.0 | 1.7 | 33.1 |
| D21 | 15.3 | 50.1 | 2.7 | 1.1 | 37.4 |
| AD60 | 87.9 | 35.4 | 2.7 | 1.5 | **41.5%** |
| | Cluster S | Cluster V | Average $\delta$ = 61.4 | | |
| CC1 | 397.6 | 69.5 | 7.6 | 1.5 | 12.3 |
| D41 | 57.0 | 0 | 3.5 | 0.9 | 18.1 |
| AD60 | 87.9 | 77.9 | 3.0 | 1.3 | 23.0 |
| CC7 | 10.5 | 44.8 | 2.9 | 1.1 | 27.8 |
| CC8 | 49.3 | 59.2 | 2.9 | 1.3 | 32.5 |
| CC18 | 2.2 | 43.4 | 2.5 | 0.6 | 36.5 |
| Ad59 | 16.1 | 3.1 | 2.1 | 0.9 | 39.9 |
| ED1 | 11.0 | 15.4 | 2.1 | 1.2 | **43.2%** |
| | Cluster U | Cluster V | Average $\delta$ = 60.2 | | |
| CC18 | 1023.7 | 43.4 | 13.3 | 1.4 | 22.0 |
| CC1 | 285.5 | 69.5 | 4.6 | 1.1 | 29.8 |
| CC8 | 178.7 | 59.2 | 3.8 | 1.4 | 36.0 |
| CC17 | 60.7 | 44.8 | 3.7 | 1.1 | **42.1%** |

differences between early AMT cruises (up to AMT-7) and later cruises (AMT-8 and 10) were biomass decreases of the large coccolithophore species *U. sibogae* and small coccolithophores, and a biomass increase of medium sized coccolithophores (10 - 25 μm) and the autotrophic dinoflagellate genus *Torodinium* (Table 5.8). These results also show that at least two species which have been previously proposed as belonging to the upper water community are found periodically in the CM and cause some of the changes in species composition; decreases in the biomass of *D. tubifer* causes some of the dissimilarity (4.8%) between early AMT cruises and later cruises (AMT-8 and 10, i.e. difference between clusters V and S) and increases in the biomass of *U. irregularis* causes some of

the dissimilarity (6.1%) between regions of the SASW during early cruises (i.e. difference between clusters U and V).

The results from the cluster analysis of variations in the species composition indicate that the 'reference' samples chosen for the analysis of spatial and temporal variations in Bray-Curtis Similarity (Fig. 5.8) do not differ markedly in their species composition compared with most other samples.

## 5.4. Discussion

### 5.4.1. What Regulates Community Structure in Subtropical Waters?

Phytoplankton communities in subtropical waters are known to be nutrient limited in surface waters and the environment is thought to be relatively stable. Although there are slight changes in the species composition within the SASW during the AMT cruises, the overall general partitioning of the total biomass between the major phytoplankton groups shows some level of long-term stability (Figs. 5.5); dominance by coccolithophores. Understanding of the variability observed in species and community composition in the SASW requires knowledge of the dominant patterns of temporal variability in oligotrophic waters. However, apart from the AMT programme few studies have made measurement in the SASW. Subtropical waters of the eastern North Pacific Subtropical Gyre (NPSG) and western Sargasso Sea (North Atlantic Subtropical Gyre; NASG) are part of the US-JGOFS (Joint Global Ocean Flux Studies) programme and have been studied relatively more extensively and have continuing present-day time-series studies; within the NPSG there is the Hawaiian Oceanographic Time-series programme (HOTS) and within the NASG there is the Bermuda Atlantic time-series programme (BATS). Time-series measurements at HOTS began in 1988 and are collected offshore at 23°N, 158°W. Before 1988, several studies took place around Hawaii and include time-series measurements at the CLIMAX study site (27°N, 155°W). The BATS programme is based on an offshore sampling station at 31°N, 64°W. The differences in the geographic positions of the two time-series sites may have significant implications for the results from the time-series; the HOTS site is well within the boundaries of the NPSG, whereas the BATS site is relatively close to the northern NASG boundary with the eutrophic waters of the Gulf Stream and is also situated along the tropical oceanic storm track. However, timeseries measurements have been collected from both HOTS and BATS, and these should make a suitable basis for understanding the temporal variability of phytoplankton community structure in subtropical waters.

*NPSG (HOTS programme)* - Seasonal cycles in fluorescence and chlorophyll *a* (chl *a*) concentration in the NPSG show opposing trends within upper (0 - 50m) and deep waters (100 - 175m) (Letelier *et al.,* 1993; Winn *et al.,* 1995). In upper waters chl *a* concentrations increase during winter (December maximum) and decrease during summer (minimum June/July), whereas chl *a* concentrations in deeper waters increase in spring (May maximum) and decrease in fall (minimum October/November) (Letelier *et al.,* 1993; Winn *et al.,* 1995). The winter increase in chl *a* in upper waters is thought to be a result of photoadaptation due to decreasing average light intensities as the mixed layer deepens (Goericke and Welschmeyer, 1998b; Letelier *et al.,* 1993; Winn *et al.,* 1995), although organic nutrients provided by the death and lysis of nitrogen fixers may also fuel algal growth (Karl, 1999;

Durand *et al.,* 2001). The spring chl *a* increase in deep waters is related to changes in primary production and biomass and are thought to be fuelled by inorganic nutrients mixed into the upper ocean during winter, combined with increased surface irradiances and water-column stability through re-stratification of the water-column and shallowing of the mixed layer (Letelier *et al.,* 1993; Winn *et al.,* 1995). The association of the spring bloom with increased inorganic nutrient concentrations can cause a diatom dominated growth phase, so that the 'classical' food chain overprints the microbial loop (Karl, 1999).

The frequency and magnitude of winter mixing in the NPSG is thought to have changed over time, with a dramatic decrease in the last decade (Karl, 1999). Before this change, Venrick (1990b) found that winter mixing in the NPSG was deep enough to mix species from the deep euphotic zone into upper waters, which stimulated growth of these species. However, winter mixing may also be unfavourable to upper water communities due to decreasing mean light levels and competition for nutrients with deep water species, causing these species to decrease in winter (Venrick, 1993). A review of the hydrographic conditions in the NPSG by Hayward *et al.,* (1983) showed that during summer the mixed layer depth was ~40 m and the nitracline, euphotic zone and CM were all ~ 100 - 150 m. During winter the mixed layer was more heterogeneous (40 - 140 m within a few km), although the depths of the nitracline, euphotic zone and CM remained unchanged.

*NASG (BATS programme)* - Winter mixing at the BATS site is better documented (e.g. Durand *et al.,* 2001) which may be due to the proximity of Bermuda to the northern gyre edge and the tropical storm track in the northern hemisphere. The depth of the thermocline at the BATS site ranges from ~20 m during summer to ~250 m during winter, with deep thermoclines associated with detectable nutrient concentrations in upper waters (Durand *et al.,* 2001). In spring at the BATS site there are increases in the abundance of *Synechococcus* spp., picoeukaryotes and larger eukaryotic algae (coccolithophores and diatoms) while prochlorophytes dominate during summer (Durand *et al.,* 2001). During the spring growth period, the community may become diatom dominated (e.g. *Rhizosolenia* spp. and *Chaetoceros* spp.), and is replaced relatively rapidly by a more diverse community including prymnesiophytes, cyanophytes, dinoflagellates, green algae (including prasinophytes) and diatoms (Bidigare *et al.,* 1990). The seasonal dynamics of the picophytoplankton community in subtropical waters can be compared to a spatial difference between oligotrophic (summer) and mesotrophic (winter/spring) waters and shows opposing trends; *Synechococcus* spp. have an abundance maxima associated with deepening of the mixed layer and shoaling of the nitracline (i.e. mesotrophic conditions), whereas prochlorophyte maxima occur when the nitracline is deep and the water-column is oligotrophic (Campbell and Vaulot, 1993; Partensky *et al.,* 1996; Campbell *et al.,* 1997). Thus, at the BATS site prochlorophyte abundance is high during summer and fall (August - November) and low during winter and spring (March to April), whereas *Synechococcus* spp. reach a maxima in spring (March to May), although there is considerable interannual variability (Durand *et al.,* 2001).

Despite the differences in the locations of the HOTS and BATS sites a comprehensive picture is formed in which winter mixing can be an important source of (new) nutrients for the growth of phytoplankton during spring and early summer in oligotrophic conditions (Karl, 1999). Time-series

measurements from these sites have also shown the importance of stochastic mixing events that may occur throughout the year and cause significant nutrient injections into the euphotic zone (Venrick, 1990b; Letelier *et al.,* 2000; Durand *et al.,* 2001). Stochastic mixing events include internal waves and tides, storms generated by atmospheric instabilities, mesoscale eddies, near-inertial motions, and the upward displacement of isopycnals (Venrick, 1990b); e.g. Letelier *et al.,* (2000) observed a mesoscale eddy in the NPSG which was associated with increases in coloured dissolved organic matter, chlorophyll fluorescence efficiency and a 2-fold increase in subsurface (0 – 25 m) chl *a* concentrations. During the passage of the eddy, the diatom contribution to the total community increased (Letelier *et al.,* 2000), and thus such stochastic events can stimulate another growth phase for large phytoplankton groups (Karl, 1999). Due to the difficulty in observing such phenomenon their occurrence, formation and frequency are poorly known in most subtropical oceans. In areas where winter mixing is low or disrupted, episodic mixing and nutrient injection events are likely to be very important to the phytoplankton community (Campbell and Vaulot, 1993).

Stochastic nutrient mixing events in oligotrophic waters are thought to maintain the biodiversity and species structure of eukaryotic nano- and microphytoplankton communities despite the dominance of the picoplankton community during the majority of the year (Venrick, 1997, 1999; Karl *et al.,* 2001a). Such stochastic and seasonal new nutrient injections may be important for stimulating nutrient-limited components of the ecosystem, these in turn may lead to periods of enhanced ecosystem production, biomass accumulation, or predator-prey oscillations; the classical marine grazing food chain (diatoms-zooplankton) can thus be considered as a 'variable phenomenon in a sea of microbes' (Karl, 1999). Within the NPSG, Platt and Harrison (1985) estimated that ~60% of the annual carbon fixation may occur during the brief (2 weeks) spring bloom, and therefore seasonal and stochastic new nutrient inputs are important for annual productivity. Nutrient inputs from seasonal and episodic sources may also be important in the long-term survival and growth of species, and thus in the overall phytoplankton community structure and ecosystem dynamics (e.g. Hutchinson, 1961; Margalef, 1978; Venrick, 1990a, b; Karl, 1999). The frequency of deep mixing may be sufficient to have allowed species to evolve a strategy of enhanced growth during a short winter, enabling them to survive a prolonged summer of restricted growth (Venrick, 1993). Such a strategy can be seen to be especially important for the long-term survival and species structure of large phytoplankton species that cannot readily use organic nutrients to sustain high growth rates.

It has been hypothesised by Karl *et al.,* (1995) and Karl (1999) that both strong and weak mixing can enhance nutrient input into the euphotic zone in subtropical oceans; strong mixing imports nitrate into the euphotic zone, while weak mixing provides an environment that is selective for N-fixing organisms (e.g. *Trichodesmium* spp.). The death and lysis of the diazotrophic community is thought to provide nutrients in dissolved and particulate organic forms which can fuel another growth phase of the community (Karl *et al.,* 1995; Karl, 1999) where the organic nature of the nutrients would select for phytoplankton groups other than those found during the new-nutrient based spring growth period.

### 5.4.2. AMT: Temporal Variability in Autotrophic Standing Stocks

Generally, chl *a* concentration (photosynthetic standing stock) shows a relatively stable vertical and horizontal pattern in the SASW (Figs. 5.2), although there is some variability in the integrated amounts (Tables 5.2 and 5.3). Such variability is associated with increases in upper water (0 – 60 m) chl *a* concentrations and/or increases in deep (60 – 200 m) chl *a* concentrations, which cause intercruise differences in integrated chl *a* (0 – 200 m). The only seasonal signal observed in the SASW is the intercruise variability of chl*a* concentrations between the surface and the CM ($C_{ZCM}$); where apart from AMT-3 all late winter (odd numbered) AMT cruises have higher $C_{ZCM}$ (Table 5.2). Such a seasonal pattern may be due to late winter/spring increases in deep chl *a* concentrations associated with winter mixing. Where variability in total water-column integrated chl*a* occurs, it is generally accompanied by changes in upper water chl*a* concentrations. However, during AMT-7 the increase in total water-column chl*a* is instead associated with an increase in deep chl*a* concentrations. A deep chl*a* increase during AMT-7 may indicate nutrient injection into the bottom of the euphotic zone during 1998. However, changes in chl*a* concentration in subtropical waters may be due to either cellular increases in pigments (photoadaptation) or the accumulation of biomass, and therefore changes in chl*a* concentration in such areas should be interpreted with caution (Cullen, 1982).

As well as measurements of chl*a* as a proxy of standing stock, measurements of the main large phytoplankton group biomass indicate variations in standing stocks and composition (Table 5.4). Due to the biomass fluctuations in the marginal areas of the SASW (Fig. 5.4), measurements from the central SASW are more suitable for intercruise comparisons (Table 5.6). However, these SASW-wide fluctuations raise an important issue; large phytoplankton taxa are distributed heterogeneously in subtropical waters, whereas the distribution of chl*a* as a marker of standing stock and the pigment ratios give a much more homogeneous picture. Comparing the standard deviations (Coefficient of Variation; SD/mean *100%) of the different measurements shows that heterogeneity of chl*a* concentration is ~21 – 55%, the pigment ratio heterogeneity is 20 – 75% (excluding 168% for upper TChl *b*:TChl *a*) with higher SD associated with rare pigments, while phytoplankton biomass heterogeneity is 1 – 90% (excluding 250% for AMT-3 including *R. chunii*) (Tables 5.2, 5.3, 5.5 and 5.6). During winter sampling in the NPSG, Venrick (1984) found that many large phytoplankton species were patchily distributed, whereas during summer sampling patches were larger and there was a greater tendency towards stratification of the species distributions. Thus, the patchiness of large species distributions was seasonally regulated, with highest heterogeneity after winter mixing events and lowest during summer stratification (Venrick, 1984).

In surface waters of the central SASW average total nano- and microphytoplankton biomass is low (<1.5 mg C $m^{-3}$) during AMT-1, 8 and 10, while measurements for other cruises range between an average of 1.6 – 5.9 mg C $m^{-3}$, with highest amounts found during AMT-2 (4.3 mg C $m^{-3}$) and AMT-7 (5.9 mg C $m^{-3}$) (Table 5.6). Within the CM nano- and microphytoplankton biomass is typically <1 mg C $m^{-3}$, apart from during AMT-3, 4 and 8 (Table 5.6) . The contributions of the different large phytoplankton groups to total biomass varies between cruises within surface and CM communities, although the trends are similar (Table 5.6); dominance of coccolithophores and autotrophic dinoflagellates (AMT-1), to coccolithophore dominance (AMT-2, 3, 4, 5, 7 and 8), and

then diatoms and autotrophic dinoflagellates dominate later on (AMT-10) (Table 5.6). Generally, when the total biomass is low there are larger proportions of autotrophic dinoflagellates in surface waters and diatoms in deep waters, although during AMT-10 there are higher proportions of diatoms in the surface and at depth (Table 5.6). Fluctuations in coccolithophore biomass are due to the occurrence of the large (20 – 50 μm) coccolithophore species *Umbellosphaera sibogae* that has a major impact on the coccolithophore biomass as well as the total biomass.

Comparison of the biomass ranges of nano- and microphytoplankton from the central SASW (Table 5.6) with picoplankton biomass from flow cytometry for the SASW (Table 5.9) show that during AMT-3 and 4 larger phytoplankton made contributions to total autotrophic community biomass of 20 - 50% in upper waters and 10 - 30% in deep waters. However, the contributions and totals are distributed heterogeneously and contributions are also <5% in some areas.

Table 5.9: Biomass (mg C $m^{-3}$) ranges of the total autrophic plankton community and its components during AMT-3 (September, 1996) and AMT-4 (May, 1997) within upper (0 - 60 m) and deep (100 - 150 m) waters of the central SASW (10 - 20°S). Picoplankton biomass measurements are adapted from Zubkov *et al.*, (2000b) while nano and microplankton biomass measurements are from light-microscope cell counts and biomass estimates.

| Depth | Pico-eukaryotes (mg C $m^{-3}$) | Cyano-phytes (mg C $m^{-3}$) | Prochlor-ophytes (mg C $m^{-3}$) | Total Picoplankton (mg C $m^{-3}$) | Nano- and Microplankton (mg C $m^{-3}$) | Total Autotrophic Biomass (mg C $m^{-3}$) |
|---|---|---|---|---|---|---|
| AMT-3 (September, 1996) | | | | | | |
| 0 - 60 m | <0.8 - 1.5 | 0.1 - 0.5 | 2.9 - 4.4 | 3.8 - 6.4 [81 - 48%] | 0.9 - 6.8 [19 - 52%] | 4.7 - 13.2 |
| 100 - 150 m | <0.8 - 1.5 | <0.1 - 1 | 2.9 - 4.4 | 3.8 - 6.9 [88 - 78%] | 0.5 - 2.0 [12 - 22%] | 4.3 - 8.9 |
| AMT-4 (May, 1997) | | | | | | |
| 0 - 60 m | <0.8 - 0.9 | <0.1 | 2.9 - 4.4 | 3.8 - 5.4 [83 - 64%] | 0.8 - 3.1 [17 - 36%] | 4.6 - 8.5 |
| 100 - 150 m | <0.8 - 1.5 | <0.1 | 2.9 - 5.8 | 3.8 - 7.4 [90 - 82%] | 0.4 - 1.6 [10 - 18%] | 4.2 - 9.0 |

The high degree of spatial heterogeneity of large phytoplankton biomass and composition in the SASW and central SASW could be due to localised episodic nutrient injection events. Measurements of chl*a* standing stock are much less heterogeneous in their distribution and the discrepancy between the two is likely to be indicative of dominance of the community biomass by small cells (picoplankton) which do not fluctuate as strikingly as larger phytoplankton taxa.

### 5.4.3. Temporal Variability in Community Structure

Pigment ratios and the species composition indicate two distinct variations in the SASW community during the 5 yrs of the AMT cruises; (1) a striking shift in the distribution of TChl *b* during AMT-3, and (2) on a longer timescale an increase in eukaryotic species (TChl *c*:Chl *a*), prymnesiophytes and pelagophytes (Hex-fuco+But-fuco:Chl *a*) and in the number of diatom species during later cruises (AMT-8 and 10). The two may be related or independent events, as well as being part of a longer successional pattern occurring on decadal or longer timescales. Time-scales of climate variability in the South Atlantic Ocean range from 4 - 12 yrs (Mehta, 1998), and will not be fully resolved by the relative shortness of the present AMT program.

A dramatic shift in the portion of the water-column occupied by high TChl *b*:TChl *a* ratios occurred during AMT-3; high TChl *b*:TChl *a* ratios limited to upper waters while deep waters were almost devoid of Chl *b* (Table 5.4 and Fig. 5.3). During this time, the Hex-Fuco+But-Fuco:Chl *a* ratio

increased which indicates that the deep community may have become dominated by small eukaryotic flagellates (prymnesiophytes and pelagophytes). High TChl *b*:TChl *a* ratios at depth are normally interpreted as being indicative of a low-light prochlorophyte population living at depth in associated with the CM, nutriclines and bottom of the euphotic zone (Goericke and Repeta, 1993). Redistribution of this population seems to have occurred during AMT-3, with low Chl *b* containing prochlorophytes remaining in deeper waters: flow cytometic counts of prochlorophyte abundance do not indicate that there was any significant or widespread change in the distribution of prochlorophytes during AMT-3 or AMT-4 (Table 5.9).

However, at present AMT-3 and 4 are the only AMT cruises that sampled within the SASW for which picoplankton community data is available. Coupled with the fact that pigment data from AMT-4 is missing, and AMT-2 only covers the southern portion of the SASW, the question as to how the community was distributed in previous years can be raised. The distribution of the TChl *b*:TChl *a* ratio during AMT-1 is similar to that found during AMT-5 - 10 (Fig. 5.3), although the ratio is significantly higher during AMT-2 than AMT-1 (Table 5.4). This indicates that AMT-3 does represent an anomaly in terms of the distribution of low-light adapted prochlorophytes when compared to the other AMT cruises. Measurements of standing stock (chl*a*) during AMT-1 and 2 show higher upper and integrated chl*a* measurements than AMT-3 (Table 5.2 and 5.3), however without pigment data on the TChl *b*:TChl *a* ratio these results cannot be easily interpreted as indicative of either Chl *b* fluorometric interference or real community change. Another complication is the fact that prochlorophytes increase their Chl *b*:Dv chl *a* ratio during photoacclimation (Partensky *et al.,* 1993), and therefore increases in the Chl *b*:TChl *a* ratio may not necessarily be associated with changes in prochlorophyte abundance. The change in the TChl *b*:TChl *a* ratio in surface waters does not indicate a large increase in Chl *b*; only a small increase in the cellular levels of Chl *b* are required to cause the high TChl *b*:TChl *a* ratios as the cells contain only small concentrations of chl *a*.

Measurements of community structure during AMT-3 indicate that although the surface and CM community is dominated by coccolithophores the total large phytoplankton biomass is much higher than during AMT-1 or AMT-4, and is comparable with AMT-2; average surface phytoplankton biomass is 3.0 ± 2.3 mg C $m^{-3}$ during AMT-3 and 4.3 ± 3.8 mg C $m^{-2}$ during AMT-2 (Table 5.6). AMT-3 also represents the first cruise where the similarity of the CM community in terms of major groups decreases below 75%, which is partly due to the occurrence of large numbers of *R. chunii* in samples from 8°S. If *R. chunii* numbers and biomass are incorporated into the total large phytoplankton biomass for AMT-3, there is a sharp increase in biomass up to a cruise average of 138.9 mg C $m^{-3}$ (Table 5.6), which is much higher than picoplankton biomass measurements (Table 5.9). *R. chunii* is a very rare species in the SASW species database and appears only once. Although the appearance of such large numbers of a diatom could be easily interpreted as sample contamination, several recent studies have seen large diatom mats and aggregates in subtropical environments (Villareal *et al.,* 1993, 1996, 1999a, b). Such studies have based their sampling on plankton-net and diver collected material, whereas the bottle sampling protocol used during AMT is very unlikely to successfully collect such features. Another point is the possible misidentification of *R. chunii*, which may in fact be a member of the genus *Guinardia* (D. Harbour pers. comm.), which are often associated with the nitrogen fixing cyanobacteria *Richella intracellularis* (Venrick, 1974; Tomas, 1997). Thus, it is possible that the patch of *R. chunii* may represent a diatom mat which is

associated with nitrogen fixation and now recognised as important occurrences in subtropical waters in terms of nutrient fluxes (Villareal *et al.,* 1999a, b). However, without being able to re-examine the sample or provide further complementary measurements (e.g. net collected material) the occurrence of this species represents an enigma, which taken with other oddities during AMT-3 make this cruise one of the most interesting of the AMT dataset.

Long-term variability in the phytoplankton community is seen as fluctuations of high surface biomass during AMT-5 and 7, with a decrease in total large phytoplankton biomass during AMT-8 and 10 (Table 5.6). In surface waters of the central SASW, diatom biomass levels increase during AMT-7, 8 and 10 from <0.05 mg C $m^{-3}$ to 0.10 - 0.42 mg C $m^{-3}$, although the total biomass decreases (Table 5.6). During AMT-8 and 10, the contribution of coccolithophores to total biomass decreases, and there are higher contributions from diatoms and autotrophic dinoflagellates (Table 5.6 and Fig. 5.5). Increases in the contribution of diatoms and autotrophic dinoflagellates to large phytoplankton biomass during AMT-10 are supported by increases in the TChl *c*:Chl *a* and Fuco+Perid+Allo:Chl *a* ratio during this cruise (Table 5.5). Accompanying changes of large phytoplankton biomass in surface waters are fluctuations in surface and CM diversity, species richness and the similarity of the major group contributions to biomass compared with AMT-1. Community diversity and species richness is low during early AMTs, with the number of species increasing during AMT-3 without any change in diversity (Fig. 5.7), which indicates that cell numbers are not evenly distributed between individual species and the community is dominated by a few species. Diversity remains low in surface and CM waters during AMT-5 and 7, although there is an increase in the species richness in both surface and CM waters, while both diversity and species richness increase during AMT-8 (Fig. 5.7). In terms of the similarity of major large phytoplankton groups to total biomass, surface waters during AMT-5 and 7 are associated with a decrease in similarity compared with that during AMT-1 (Fig. 5.6). Within the CM, changes in the similarity of the contribution of large phytoplankton to AMT-1 are slightly different with the similarity in major group contributions lowest during AMT-3 and 10 (Fig. 5.6).

Species similarity in terms of community composition (PA) and dominance (SQRT) show different patterns to the changes in similarity of the major groups (Fig. 5.8). In surface waters species composition is very similar during AMT-2, 5 and 7, with cruises in-between typically sharing <50% of species (Fig. 5.8). In terms of dominant species composition, surface waters show a similar pattern, although low similarity is observed during AMT-4 and higher similarity is observed during AMT-8 (Fig. 5.8). Again the CM community shows totally different patterns to the surface community, with most CM samples sharing <35% of species with AMT-1 (Fig. 5.8). Differences in the trend of intercruise similarity between surface and CM communities despite the two depths having similar patterns of diversity and species richness indicate that the community dynamics of the two depths are different; surface communities vary with coccolithophores, autotrophic dinoflagellates and diatoms oscillating in terms of dominance, whereas in the CM coccolithophores are usually the dominant component. The species composition of the two depths show a different pattern, surface waters have a semi-stable species makeup, even though the dominance of each may fluctuate between species and taxa. Within the CM, the community is mostly composed of coccolithophores, although the species composition of the community fluctuates with the different cruises often sharing <35% of their species. Differences in the communities is likely to be due to differences in nutrient

supply and associated seasonal patterns; nutrient injections from below the euphotic zone will favour growth in the deep community, whereas *in-situ* supply of organic nutrients through N-fixation will favour growth in the shallow community (Karl, 1999; Durand *et al.,* 2001).

Interpretation of the changes of abundance and distribution of individual species is difficult due to lack of knowledge of the nutritional roles or life cycles of subtropical species; i.e. can coccolithophores use organic nutrients? Is *U. sibogae* absent during later AMT cruises or is it present as an un-lithed life-cycle stage or holococcolithophore variety? Intercruise variations in the species composition of surface samples involve fluctuations in the abundances of *U. sibogae* and *U. irregularis* during AMT-3, 4, 5 and 7, whereas variations during later cruises (AMT-8 and 10) involve further decreases of *U. sibogae*, *Helicosphaera* spp. and *Prorocentrum* spp. and increases of pennate sp. 'C', *Scrippsiella / Alexandrium* spp. and *Acanthoica* spp. Thus, in surface waters there are variations in species composition during the late AMT cruises (AMT-8 and 10) and variations in species dominance during the middle cruises (AMT-3, 4, 5 and 7). Variations in the species composition in the CM involve fluctuations in a greater number of species with changes in species composition and species dominance during all AMT cruises. During early AMT cruises (pre-AMT-8) there are fluctuations in the CM of the abundance of *U. sibogae*, 10 - 25 μm coccolithophores, small coccolithophores and *U. irregularis*, *Ophiaster* spp., *Phaeceros Chaetoceros* spp., small pennate diatoms, *Helicosphaera* spp., *Halopappus* spp., and *Gephyrocapsa ornata*. Species variations during late AMT cruises (AMT-8 and 10) include the disappearance of *U. sibogae*, decreases of small coccolithophores, *Ophiaster* spp., *Pseudo-nitzschia* spp., *Phaeoceros Chaetoceros* spp., *D. tubifer* and *L. mediterraneus* and increases in small unidentified pennates, *N. longissima*, *Oxytoxum* spp., pennate sp. 'C', *Haslea* spp., *Scrippsiella / Alexandrium* spp., 10 - 25 μm coccolithophores and *Torodinium* spp. The list of species varying during early AMT cruises (pre-AMT-8) is similar to that found during later cruises (AMT-8 and 10) which indicates that similar species fluctuations occur throughout the 5 yrs of the AMT programme.

Localised increases and apparent disappearances of certain species are likely to be related to the nutrient dynamics of the system with the frequency of stochastic nutrient events and seasonal mixing favouring certain phytoplankton groups and species. Increased supply of new nutrients would favour the long-term survival of such phytoplankton groups as diatoms and fast growing coccolithophores, whereas decreases in new nutrient supply and reliance on regenerated organic nutrient sources would favour more slow growing species. However, too little is known at present about specific species preferences to further interpret the species fluctuations. Instead these results identify several important species in the SASW for which further studies of life histories and physiology should be made.

Hydrographic data from AMT-3 indicate a change in the post winter UMD that could be related to changes in the winter climate in the South Atlantic during 1996 and 1997 (Chapter 3). Such variations may have changed the magnitude of winter mixing and the subsequent seasonal and stochastic nutrient supply to the community during this time. Hydrographic data from later AMT cruises indicates that the seasonal UMD variations seem to have stabilised again during 1999 and 2000 (Chapter 3), which may have caused better regulation of winter mixing and seasonal and stochastic nutrient supply to the upper subtropical ocean.

These variations in nutrient supply are hypothesised to be responsible for the compositional changes in the surface and CM communities, with disruption of the nutrient supply during AMT-3 favouring small prokaryotic and eukaryotic cells and resumption during later cruises allowing increases in diatom numbers and diversity. However, too little is known of the seasonal community dynamics in the subtropical Atlantic Ocean or of the nutrient preferences and life strategies of the species present to fully investigate this hypothesis. As well as ecological studies of the species identified from the multivariate analysis, a better temporal framework for the AMT cruises is required to test the hypothesis of variations in the frequency of winter and stochastic mixing in the SASW. Such a framework could be based on the analysis of remotely sensed parameters such as surface chl *a* patterns (e.g. SeaWiFS images), climate and seascape variations (e.g. AVHRR and TOPEX images) and would also be aided by continued time-series sampling in the SASW.

## 5.6. Summary and Conclusions

1. There appears to be little variation in the standing stock (chlorophyll *a*) of the autrophic community in South Atlantic Subtropical Waters (Fig. 5.1 and Tables 5.2 & 5.3). However, temporal variations in the composition of the phytoplankton community in terms of phytoplankton groups and large (>5 μm) phytoplankton species are evident. Such variations may be linked to the hydrographic variability identified in Chapter 3, although questions about the ecology of phytoplankton community components need to be addressed before this linkage can be fully examined. It is hypothesised that climate-related variations in post-winter mixed layer depths observed in South Atlantic Subtropical Waters have caused variability in the phytoplankton community composition. Linkage of variability of this variability is likely to be through interannual variations in the frequency and magnitude of winter and stochastic (episodic) new nutrient imputs, which the algal community may be reliant on for long-term (annual) population growth and survival.

2. Compositional variations of the phytoplankton community include; (i) shallowing in the distribution of low-light adapted prochlorophytes during AMT-3 (Fig. 5.3), (ii) an increase in eukaryotic phytoplankton groups (prymnesiophytes and pelagophytes/chrysophytes) during AMT-3 and later AMT cruises (Table 5.4), (iii) an increase in diatom and large phytoplankton species diversity (Fig. 5.7) and biomass (Table 5.6), and (iv) variability in the abundance and distribution of the upper flora oligotrophic coccolithophore species *Umbellosphaera irregularis* and *Umbilicosphaera sibogae* (Fig. 5.10, Tables 5.7 and 5.8).

3. Analysis of temporal changes in the large (>5 μm) phytoplankton groups (diatoms, autotrophic dinoflagellates, coccolithophores) and species suggest the existence of different modes of variability between surface and deep assemblages; in surface waters, the species composition of the phytoplankton community is relatively stable, with marked changes in the relative abundance of the different phytoplankton groups. Within the chlorophyll *a* maximum, species composition is more variable and the phytoplankton group composition is relatively stable (dominated by coccolithophores) (Figs. 5.6 and 5.8). These depth differences are likely to relate to differences in nutrient sources and (seasonal) variability in nutrient supply; the semi-stable new nutrient

fluxes at the bottom of the euphotic zone in association with the nutricline and Chlorophyll *a* Maximum will favour dominance by specialised adaptive phytoplankton groups and species. In contrast, the variable *in-situ* regenerated nutrient supplies from autotrophic (leakage) and heterotrophic (grazing and excretion) activity and episodic new nutrient inputs from atmospheric (dust storms and rainfall) and biological (nitrogen-fixation) sources to upper waters (<60 m) of the euphotic zone will favour competition, patchiness and different phytoplankton groups at different times.

# CHAPTER 6: LATITUDINAL CHANGES IN THE SHAPE, FORMATION AND ECOLOGY OF THE CHLOROPHYLL *A* MAXIMUM IN THE SUBTROPICAL AND TROPICAL ATLANTIC OCEAN

## 6.1. Introduction and Outline

The Chlorophyll *a* Maximum (CM) is now recognised as a global feature (Gould, 1987; Longhurst and Harrison, 1989) of tropical and subtropical oceans, and has been investigated in the Atlantic (e.g. Mitchell-Innes *et al.,* 2001), Pacific (e.g. Hayward and Venrick, 1982), Indian (e.g. Murty *et al.,* 2000), Mediterranean (e.g. Estrada et al, 1993) and Caribbean (e.g. McManus and Dawson, 1994). The CM generally lies well below the depth to which remote-sensing techniques penetrate (i.e. below the upper ~22% of the euphotic zone; Hidalgo-Gonzalez and Alvarez-Borrego, 2001); thus understanding regional differences in the CM is important for global ocean studies based on satellite derived measurements. The CM is also recognised as a significant food source for micro- and macroheterotrophs and several authors have shown the importance of the CM for larval fish survival (see Longhurst and Harrison, 1989 and references therein). The CM community composition, size structure and physiology will have important consequences for the nutritional quality of the CM as a food source (Longhurst and Harrison, 1989) and the efficiency of energy transfer through oceanic food webs.

The aim of this chapter is to investigate the regional mechanisms of formation of the CM (interaction of hydrography and physiology), and draw conclusions about the implications of its ecology for regional biogeochemical and ecosystem studies. Data included in the analysis are hydrological parameters, such as vertical water-column structure (Upper Mixed Layer depth), characteristics of the nutrient and light environment (nitracline depth and euphotic zone depth), and phytoplankton community composition (size-fractionated chlorophyll *a*, pigment ratios and microscopically identified algal species). Data for hydrological parameters is presented from all AMT cruises, whereas community composition analysis focuses on AMT-7 (September, 1998), 8 (May, 1999) and 10 (May, 2000). A typical chlorophyll *a* profile is described in Figure 6.1a with reference to the general features used for the analysis within this chapter. Chlorophyll *a* measurements are either from acetone extraction (FIchl*a*; methods 2.4.1), HPLC (TChl *a*; methods 2.4.2), or converted *in-situ* fluorescence (F; methods 2.4.4).

Regional trends in the shape of the CM (see Fig. 6.1a) are likely to be indicative of environmental differences in the characteristics and ecology of the CM. Analysis of the relationships between the CM and other factors will consider patterns on the basinscale and differences between six regional provinces (see Fig. 3.10), which correspond to hydrological and ecological provinces proposed by Hooker *et al.,* (2000), Maranon *et al.,* (2001) and Zubkov *et al.,* (1998, 2000b); (i) North Atlantic Drift (NAtD: 35 - 40°N), (ii) North Atlantic Subtropical Waters (NASW: 20 - 35°N), (iii) Upwelling Waters (UPW: 5 - 20°N), (iv) Equatorial Atlantic (EQU: 5°N - 5°S), (v) South Atlantic Subtropical Waters (SASW: 5 - 30°S), and (vi) South Atlantic Temperate Waters (SATW: 30 - 40°S).

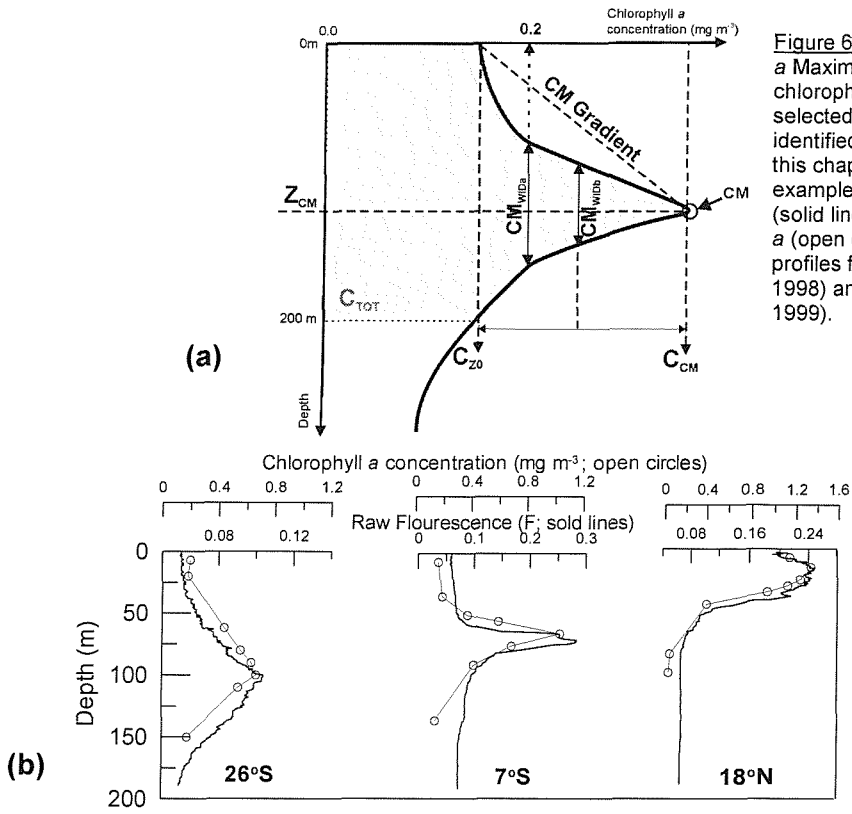


Figure 6.1: The Chlorophyll *a* Maximum; (a) a general chlorophyll *a* profile showing selected characteristics identified and analysed in this chapter, and (b) three examples of fluorescence (solid lines) and chlorophyll *a* (open circles; FIchl*a*) profiles from AMT-7 (Sept., 1998) and AMT-8 (May, 1999).

Regional differences are evident from average measurements of selected characteristics of the chlorophyll *a* profile (Table 6.1; Fig. 6.1b); surface chlorophyll *a* ($C_{z0}$), chlorophyll *a* concentration at the CM ($C_{CM}$) and total water-column integrated chlorophyll *a* ($C_{TOT}$) are highest in the UPW and SATW regions and lowest in the SASW, whereas the depth of the CM ($Z_{CM}$) is highest in the SASW and lowest in the UPW and SATW.

Table 6.1: Average (± Standard Deviation) measurements for selected characteristics of the vertical chlorophyll *a* profile (FIchl*a*) from six regions of the subtropical and tropical Atlantic Ocean for all AMT cruises. See Figure 6.1a for explanation of the characteristics. The numbers of measurements included are given in brackets.

| Region | $C_{z0}$ (mg $m^{-3}$) | $C_{CM}$ (mg $m^{-3}$) | $Z_{CM}$ (m) | $C_{TOT}$ (mg $m^{-2}$) |
|---|---|---|---|---|
| NAtD (35 - 40°N) | 0.18 ± 0.14 [n = 13] | 0.45 ± 0.16 [n = 13] | 62.1 ± 25.2 [n = 13] | 34.7 ± 14.1 [n = 13] |
| NASW (20 - 35°N) | 0.14 ± 0.11 [n = 30] | 0.49 ± 0.22 [n = 30] | 81.1 ± 22.3 [n = 30] | 36.5 ± 12.4 [n = 30] |
| UPW (5 - 20°N) | 0.26 ± 0.15 [n = 28] | 1.13 ± 0.78 [n = 31] | 39.2 ± 21.5 [n = 30] | 54.2 ± 24.0 [n = 31] |
| EQU (5°N - 5°S) | 0.17 ± 0.07 [n = 21] | 0.58 ± 0.15 [n = 21] | 70.8 ± 12.6 [n = 21] | 39.4 ± 6.7 [n = 21] |
| SASW (5 - 30°S) | 0.12 ± 0.06 [n = 58] | 0.37 ± 0.09 [n = 60] | 108.8 ± 23.2 [n = 60] | 33.0 ± 7.1 [n = 59] |
| SATW (30 - 40°S) | 0.35 ± 0.19 [n = 9] | 0.71 ± 0.38 [n = 13] | 45.6 ± 29.2 [n = 13] | 48.7 ± 4.7 [n = 26] |

## 6.2. Regional Variations in the Shape of the Chlorophyll *a* Maximum

### 6.2.1. Chlorophyll *a* Maximum (CM)

Latitudinal changes in the depth of the CM follow a consistent pattern for all the AMT cruises (Fig. 6.2a; Maranon *et al.*, 2000); deep CM in the subtropical gyres (>75 m), intermediate CM around the equator (50 - 75 m) and subsurface and surface CM off NW Africa (<50 m). There is little interannual or seasonal variability in the depth of the CM (Fig. 6.2a). Intercruise variability is restricted to NW African waters and waters at the latitudinal ends of the AMT transect (Fig. 6.2a), which reflects the seasonality of the phytoplankton communities during the austral/boreal spring and autumn (Maranon *et al.*, 1999; Gibb *et al.*, 2000). Variability in waters off NW Africa is likely to be related to slight variations in cruise tracks and to the age of the upwelled water filaments characteristically sampled during the AMT cruises (Maranon *et al.*, 2001). The $C_{CM}$ is related to the $Z_{CM}$ variability (Fig. 6.2a and b); deep CMs are characterised by low $C_{CM}$ (~0.1 - 0.4 mg $m^{-3}$) whereas shallow CMs off NW Africa show elevated $C_{CM}$ (~0.6 - 1.0 mg $m^{-3}$). This basinscale relationship leads to a significant inverse correlation between $Z_{CM}$ and $C_{CM}$ ($r = -0.59$, $p<0.001$, $n = 181$; Table 6.2) that is similar to the relationship identified by Herbland and Voituriez (1979) in the equatorial Atlantic Ocean (i.e. $r = -0.79$, $p<0.01$, $n = 53$).

Table 6.2: Summary table of Pearson-moment correlation coefficients (r) for the relationships between water-column chlorophyll *a* measurements from discrete (CHL) and continous (FCHL) profiles for six regions of the tropical and subtropical Atlantic Ocean. Significance levels have been Bonferroni corrected to a significance level of $p<0.05$ ($p<0.001$). Non-signficant correlations are marked by NS with NS* indicated relationships which are non-significant after Bonferroni correction. Number of data points are shown in brackets.

| Variable 1. | Variable 2. | All Fchla | All FCHL | NAtD | NASW | UPW | EQU | SASW | SATW |
|---|---|---|---|---|---|---|---|---|---|
| $C_{z0}$ | $C_{CM}$ | 0.58 [n = 174] | 0.69 [n = 63] | NS [n = 13] | 0.82 [n = 30] | NS* [n = 31] | NS [n = 21] | NS* [n = 58] | 0.72 [n = 21] |
| $C_{CM}$ | $Z_{CM}$ | -0.59 [n = 181] | -0.73 [n = 63] | NS [n = 13] | -0.75 [n = 30] | NS* [n = 31] | NS [n = 21] | NS* [n = 60] | NS* [n = 26] |
| $Z_{CM}$ | $C_{TOT}$ | -0.51 [n = 180] | -0.57 [n = 63] | NS [n = 13] | NS* [n = 30] | NS* [n = 31] | NS [n = 21] | NS* [n = 59] | NS [n = 26] |
| $C_{z0}$ | $C_{TOT}$ | 0.59 [n = 174] | 0.62 [n = 63] | NS* [n = 13] | NS* [n = 30] | NS [n = 31] | NS* [n = 21] | 0.73 [n = 58] | NS* [n = 21] |
| $C_{CM}$ | $C_{TOT}$ | 0.77 [n = 180] | 0.62 [n = 63] | NS* [n = 13] | NS* [n = 30] | 0.87 [n = 31] | NS* [n = 21] | 0.71 [n = 59] | NS* [n = 26] |
| $C_{z0}$ | $Z_{CM}$ | -0.64 [n = 174] | -0.65 [n = 63] | NS* [n = 13] | -0.79 [n = 30] | NS* [n = 31] | NS [n = 174] | -0.41 [n = 58] | NS* [n = 21] |

Several authors have identified relationships between chlorophyll *a* (chl *a*) measurements at different depths and characteristics of the integrated chl *a* profiles (e.g. Estrada *et al.*, 1993) and there is now a consensus that regional differences in the relationships should be looked at before general conclusions can be proposed (Hayward and Venrick, 1982). In terms of the entire tropical and subtropical Atlantic Ocean significant relationships can be established between $C_{z0}$, $C_{CM}$, $Z_{CM}$, and total water column integrated Fchla (0-200m; $C_{TOT}$) (Table 6.2; cf. Fig. 6.1a); positive correlations between $C_{z0}$ and $C_{CM}$, $C_{z0}$ and $C_{TOT}$, $C_{CM}$ and $C_{TOT}$ and negative relationships between

$C_{CM}$ and $Z_{CM}$, $C_{z0}$ and $Z_{CM}$, $Z_{CM}$ and $C_{TOT}$ are significant. However, if these relationships are separated into regional ones the relationships become variable between regions, although the signs are not (Table 6.2). Relatively poor correlations might be due to small sample sizes for some regions, although such variability might also indicate that different processes are controlling the phytoplankton communities and the vertical chl *a* profile.

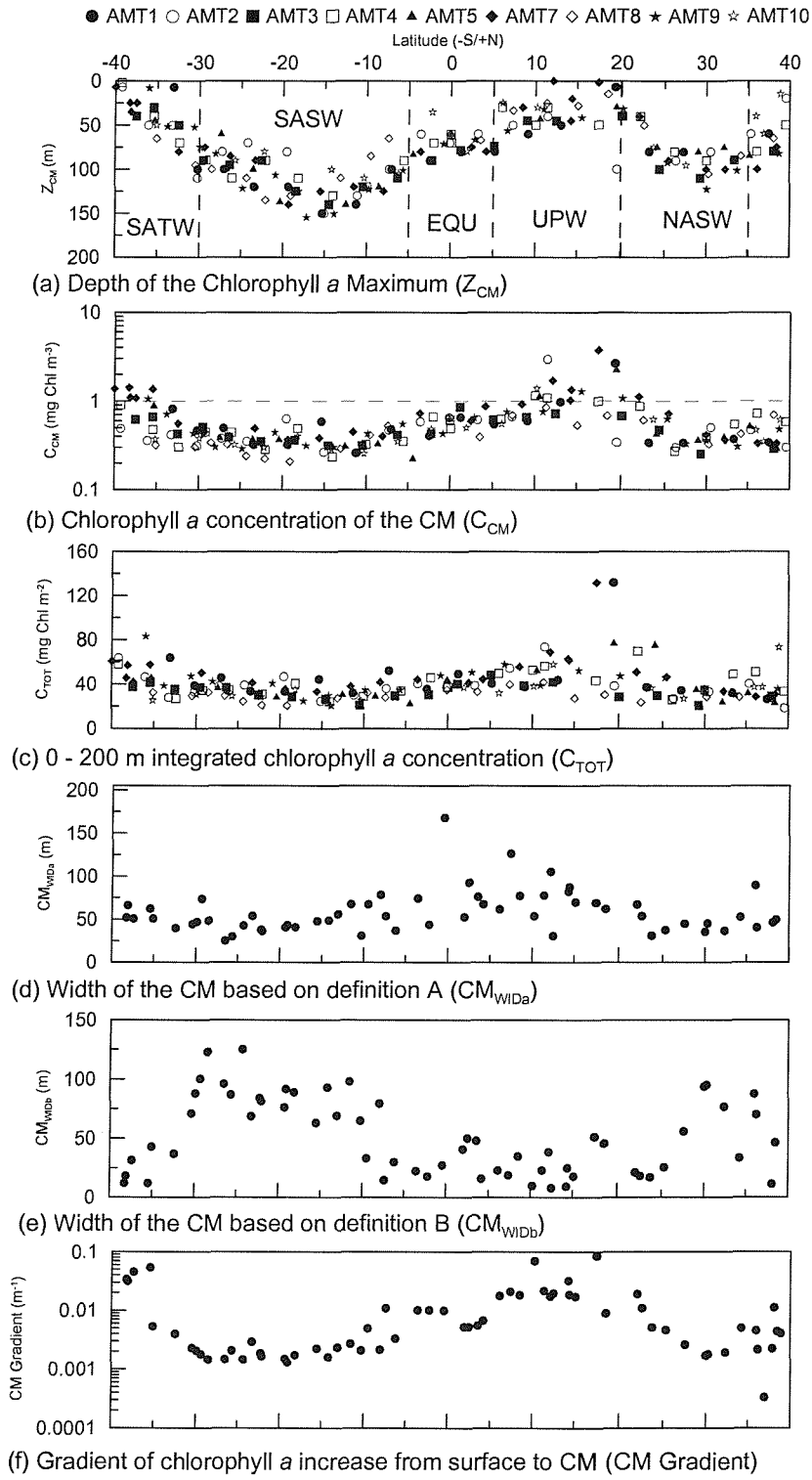


Figure 6.2: Latitudinal variations in selected characteristics of the CM; (a) Depth of the CM ($Z_{CM}$), (b) Chlorophyll a concentration of the CM ($C_{CM}$), (c) 0 - 200 m integrated chlorophyll a ($C_{TOT}$), (d) Width of the CM by definition A ($CM_{WIDa}$), (e) Width of the CM by defintion B ($CM_{WIDb}$), and (f) Surface to CM chlorophyll *a* gradient. See Fig. 6.1a and text for full explanation of characteristics. The key for individual cruise data points used on (a-c) are given at top of the figure. The range of the latitudinal provinces, apart from NAtD (35 - 40°N), are presented on (a).

### 6.2.2. The Fluorescence Maximum and Shape of the CM

Due to the difficulties and possible errors of interpolating between discrete measurements, converted *in-situ* fluorescence measurements are used. Such finescale analysis is based on a lesser number of fluorescence profiles (n = 63; AMT-7, 8 and 10). Comparison of the CM and the Fluorescence Maximum (FM) shows no significant difference in the CM depths (T-test; T = 0.88, P = 0.38, n = 60) and similar relationships between variables determined from F profiles (Table 6.2). There is also a significant correlation between $C_{CM}$ and $F_{FM}$ (r = 0.935, p<0.001, n = 62) with no significant differences between the chl*a* concentrations (T-test; T = 0.71, P = 0.48, n = 62). The shape of the CM (FM) can be described with reference to its width ($CM_{WID}$), although there are many possible definitions; in this case 2 definitions are used: (A) $CM_{WIDa}$ is where upper and lower CM limits are the 0.2 mg Chl *a* $m^{-3}$ boundaries, whereas (B) $CM_{WIDb}$ is where upper and lower CM limits are related to 0.5 $C_{CM}$.

(A) $CM_{WIDa}$ - is higher off NW Africa (75 - 100 m) and occasionally at the northern end of the AMT transect (50 - 75 m), with a width of around 50 - 75 m throughout the rest of the subtropical and tropical Atlantic Ocean (Fig. 6.2d). Significant (p<0.05) basinscale relationships exist between $CM_{WIDa}$ and $F_{TOT}$ (r = 0.666, n = 60) and $CM_{WIDa}$ and $Z_{FM}$ (r = -0.413, n = 60), but not with $F_{z0}$ or $F_{FM}$. The shape, or roundness, of the CM is described by defining the centroid or middle depth of the CM ($Z_{CC}$). No significant difference was found between the $Z_{FM}$ and $Z_{CCa}$ (T-test; T = -1.45, P = 0.15, n = 60), which indicates that the CM represents an even-sided gaussian curve. Significant (p<0.05) inverse relationships exist between $Z_{CCa}$ and $F_{z0}$ (r = -0.584, n = 60), $F_{FM}$ (r = -0.624, n = 60) and $F_{TOT}$ (r = -0.587, n = 60) and a significant positive relationship between $Z_{CCa}$ and $Z_{FM}$ (r = 0.953, n = 60) with the model II regression line close to 1 (0.96).

(B) $CD_{WIDb}$ - suggests an inverse latitudinal pattern compared with $CM_{WIDa}$, with wide CM in the subtropical gyres (75 - 125 m) and narrow CM around the equator (~ 50 m), off NW Africa (25 - 50 m), at the southern latitudinal end of the transect (25 - 50 m), and a wide range of values at the northern end of the transect (25 - 100 m; Fig. 6.2e). There is no significant (p<0.05) relationship between $CM_{WIDb}$ and $F_{z0}$, but there are significant relationships with $F_{TOT}$ (r = -0.429, n = 60), $F_{FM}$ (r = -0.463, n = 60) and $Z_{FM}$ (r = 0.711, n = 60). Measurements of the CM centroid from the second definition of CM width (i.e. $Z_{CCb}$) are significantly (p<0.05) different from the first definition ($Z_{CCa}$); T-test, T = -4.08, n = 60. Thus, there are no significant (p<0.05) relationships between $Z_{CCb}$ and $F_{z0}$, $F_{FM}$ and $F_{TOT}$, but there is a significant relationship between $Z_{CCb}$ and $Z_{FM}$ (r = 0.621, n = 60). These results also lead to the conclusion that the CM represents an even-sided gaussian curve throughout the tropical and subtropical Atlantic Ocean.

The chl*a* gradient of $F_{z0}$ to $F_{FM}$ (see Fig. 6.1a) shows distinct latitudinal patterns (Fig. 6.2c), although this is not an accurate measurement of the upper slope of the CM. The gradient is highest off NW Africa, lower around the equator and reaches a minimum in the subtropical gyres (Fig. 6.2c). The gradient is a measure of the 'flatness or sharpness' of the CM and thus, CM in the subtropics are not as sharp as those around the equator or off NW Africa (see Fig. 6.1b).

## 6.3. Relationships to Hydrographic Parameters

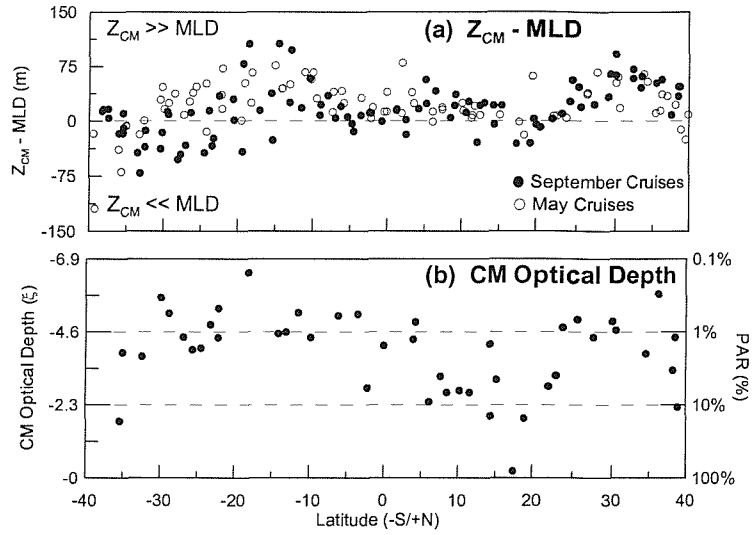


Figure 6.3: The Chlorophyll *a* Maximum and hydrographic parameters; (a) difference between $Z_{CM}$ and MLD, and (b) optical depth and %PAR depth of the CM. MLD are for all AMT cruises and CM optical depths from AMT-7, 8 and 10.

### 6.3.1. Upper Mixed Layer Depth (MLD)

The relationship between the depth of the upper mixed layer (MLD) and the vertical chl*a* profile ($Z_{CM}$) is presented in Figure 6.3a, and reflects the interaction between the physical forcing and the phytoplankton community. The MLD is shallow in the northern hemisphere during both seasons (~25 m), whereas around the equator MLD ranges from 50 m during May cruises to 75 m during September cruises, and in the southern subtropical gyre there is evidence of large scale interannual variations of 75 - 100 m during early AMT cruises (Chapter 3). There are significant ($p<0.05$) differences between MLD and $Z_{CM}$ on the basinscale and in the NASW and SASW, whereas the MLD is closely related to the $Z_{CM}$ in the other regions (Table 6.3). The CM is usually deeper than the MLD in the SASW and NASW, and is in close proximity and often shallower than the MLD around the EQU and UPW during both seasons (Fig. 6.3a). Thus, apart from the interannual variations in MLD in the SASW, seasonal variations in the MLD have little effect on the relationship between MLD and $Z_{CM}$. Significant relationships between MLD and ZCM were only found at the basinscale and around the EQU (Table 6.3) which may indicate that the relationship for the EQU has a pronounced effect on the entire dataset.

### 6.3.2. CM and Light: Optical Depth of the CM

Changes in the light availability at the CM are indicated by the optical depth of the CM and the relationship between $Z_{CM}$ and euphotic zone depth ($Z_{eu}$; 1% surface PAR); the higher the optical depth of the CM, the lower the light levels experienced and in all regions of the subtropical and tropical Atlantic Ocean the $Z_{eu}$ is not at a significantly ($p<0.05$) different depth to the CM ($Z_{CM}$; Table 6.3). Latitudinal changes in the optical depth of the CM are evident with CM in the NASW and SASW at high optical depths (low relative light levels), whereas the CM in other regions is at lower optical depths and therefore higher relative light levels (Fig. 6.3b). Shallow $Z_{CM}$ in the UPW experience better light conditions with the CM often lying around the 10% surface PAR light level (Fig. 6.3b),

whereas $Z_{CM}$ optical depths in the EQU and other provinces are intermediate (10% - 1% PAR; Fig. 6.3b). No statistically significant ($p<0.05$) differences between the $Z_{CM}$ and $Z_{eu}$ are found on the basinscale or within any of the regions (Table 6.3). However, it should be noted that there is a general lack of suitable light data available (n = 3 - 14) and the relationships should be interpreted with caution until more data is available.

Table 6.3: Summary table of statistical analysis (T-tests, correlation coefficients and model II regression equations) of the relationships between $Z_{CM}$ and MLD, $Z_{eu}$ and $Z_{NO3}$ on the basinscale and for six regions of the tropical and subtropical Atlantic Ocean. Correlation coefficients have been Bonferroni corrected to $p<0.05$. The number of samples are indicated by n and NS indicated non-signicant relationships. The mean values and standard deviations for each parameter are presented in final column.

| Region (Range) | Factor | n | T-tests (Bonferroni corrected to p<0.05) | | Model II Regression equations (Bonferroni corrected to p<0.05) | | Means ± SD |
|---|---|---|---|---|---|---|---|
| All | MLD | 175 | T = 5.89, p<0.05 | | r = 0.515 | $Z_{CM}$ = 0.93 * MLD - 12.67 | |
| (40°N - 40°S) | $Z_{eu}$ | 44 | T = -0.34, P = 0.730 | NS | r = 0.907 | $Z_{CM}$ = 0.69 * $Z_{eu}$ + 28.51 | |
| | $Z_{NO3}$ | 95 | T = -5.58, p<0.05 | | r = 0.767 | $Z_{CM}$ = 1.32 * $Z_{NO3}$ + 3.68 | |
| NAtD | MLD | 15 | T = 3.50, P = 0.003 | NS | NS | | 36.8m ± 9.5m |
| (35 - 40°N) | $Z_{eu}$ | 4 | T = -0.46, P = 0.670 | NS | NS | | 69.0m ± 25.8m |
| | $Z_{NO3}$ | 6 | T = -1.30, P = 0.230 | NS | NS | | 73.3m ± 20.4m |
| NASW | MLD | 28 | T = 7.74, p<0.05 | | NS | | 43.1m ± 13.5m |
| (20 - 35°N) | $Z_{eu}$ | 8 | T = -0.58, P = 0.570 | NS | NS | | 85.7m ± 15.1m |
| | $Z_{NO3}$ | 15 | T = -3.52, p<0.05 | | NS | | 126.9m ± 33.1m |
| UPW | MLD | 31 | T = 3.03, P = 0.004 | NS | NS | | 26.2m ± 10.3m |
| (5 - 20°N) | $Z_{eu}$ | 10 | T = -1.58, P = 0.120 | NS | NS | | 45.7m ± 4.5m |
| | $Z_{NO3}$ | 19 | T = -2.68, P = 0.011 | NS | r = 0.729 | $Z_{CM}$ = 0.85 * $Z_{NO3}$ + 18.81 | 55.3m ± 21.7m |
| EQU | MLD | 21 | T = 2.34, P = 0.026 | NS | r = 0.672 | $Z_{CM}$ = 1.60 * MLD - 53.95 | 58.3m ± 20.4m |
| (5°N - 5°S) | $Z_{eu}$ | 5 | T = 0.68, P = 0.510 | NS | NS | | 67.9m ± 7.0m |
| | $Z_{NO3}$ | 13 | T = -1.67, P = 0.110 | NS | NS | | 82.1m ± 22.4m |
| SASW | MLD | 58 | T = 4.91, p<0.05 | | NS | | 82.3m ± 33.7m |
| (5 - 30°S) | $Z_{eu}$ | 14 | T = 2.34, P = 0.027 | NS | NS | | 96.5m ± 15.8m |
| | $Z_{NO3}$ | 30 | T = -6.62, p<0.05 | | NS | | 148.6m ± 28.4m |
| SATW | MLD | 23 | T = -1.79, P = 0.080 | NS | NS | | 65.0m ± 33.6m |
| (30 - 40°S) | $Z_{eu}$ | 3 | T = -4.12, P = 0.006 | NS | NS | | 83.0m ± 11.3m |
| | $Z_{NO3}$ | 13 | T = -2.96, P = 0.008 | NS | NS | | 84.4m ± 40.8m |

### 6.3.3. CM and Nutrients: Depth of the Nitracline ($Z_{NO3}$) and $Z_{CM}$

Latitudinal changes in the estimated nitracline depth ($Z_{NO3}$) follow a pattern of deep $Z_{NO3}$ in the subtropical gyres and shallow around the EQU, UPW, NATD and SATW with little evidence of interannual or seasonal variability (Chapter 3). The availability of nutrients other than nitrate can be approximated by the relationship between the $Z_{CM}$ and $Z_{NO3}$ (see Herbland and Voituriez, 1979), as most nutriclines are found in close proximity to the nitracline depth (Chapter 3).

Significant differences between the $Z_{NO3}$ and $Z_{CM}$ are found on the basinscale, and in the NASW and SASW (Table 6.3). Within the NAtD, UPW, and EQU the differences between the $Z_{NO3}$ and $Z_{CM}$ are on average <15 m, whereas in the NASW, SASW and SATW the average differences are between 35 to 45 m (Table 6.1 and 6.3). In the NAtD, UPW, EQU, and SATW the $Z_{NO3}$ and $Z_{CM}$ are at statistically ($p<0.05$) similar depths which is confirmed by examination of the means (± SD) of the $Z_{NO3}$ and $Z_{CM}$ (Tables 6.1 and 6.3). The slope of the model II regression line for $Z_{NO3}$ and $Z_{CM}$ in the UPW (0.85) is quite similar to that found by Herbland and Voituriez (1979) in the equatorial Atlantic Ocean ($Z_{CM}$ = 0.95 * $Z_{NO3}$ + 3.6; r = 0.95, $p<0.01$, n = 126), although the intercepts are markedly different, which may be due to the much smaller sample size for AMT (n = 19). Relationships between $Z_{CM}$ and $Z_{NO3}$ are indicative of the importance of the upward new nutrient flux on the vertical chl*a* structure and CM formation (Estrada *et al.*, 1993).

Significant inverse relationships where found between $Z_{NO3}$and $C_{CM}$ ($r = -0.510$, $p<0.05$, $n = 95$) for the basinscale measurements, whereas (Bonferroni corrected) significant relationships were only found in the SATW ($r = -0.739$, $p<0.05$, $n = 12$). A lack of a significant relationship in the NATD may be due to the small sample size ($n = 4$), whereas non-significant relationships in the other regions may be indicative of either dynamic variability or differences in the relationship of the $C_{CM}$ and nitracline. Although Herbland and Voituriez (1979) did not examine the relationship between $Z_{NO3}$ and $C_{CM}$, they did find a significant inverse relationship between $Z_{NO3}$ and $C_{TOT}$ ($r = -0.80$, $p<0.01$, $n = 56$). Within the AMT measurements of $Z_{NO3}$ and $C_{TOT}$, significant inverse relationships were found from the total basinscale dataset ($r = -0.456$, $p<0.05$, $n = 97$), whereas examination of the individual regions showed significant results only for the NASW ($r = -0.666$, $p<0.05$, $n = 15$) and SASW ($r = -0.578$, $p<0.05$, $n = 31$). Nonsignificant results from the NAtD may be due to low sample size ($n = 4$), whereas nonsignificant results from better sampled areas (UPW, $n = 19$; EQU, $n = 13$; SATW, $n = 13$) suggest different relationships between $Z_{NO3}$ and $C_{TOT}$; in these areas the depth of the nutricline was not related to the water-column integrated chl*a* and nutrient availability may not be the only factor regulating phytoplankton biomass.

## 6.4. Community Composition of the Chlorophyll *a* Maximum

### 6.4.1. Size-fractionated Chlorophyll *a*

The size-fractionation technique used during AMT-8 and 10 separated the picoplankton (0.2 - 2.0 μm), nanoplankton (2 - 20 μm) and microplankton (>20 μm). The percentage contributions of these three size classes to the total chlorophyll *a* from the different areas of the tropical and subtropical Atlantic Ocean are presented in Figure 6.4. In all six regions of the subtropical and tropical Atlantic Ocean, picoplankton are the dominant contributor to total chl*a* (Fig. 6.4), with fluctuations in picoplankton chl*a* contribution accompanied by changes in either the nanoplankton or microplankton contribution, or both. Highest picoplankton contributions (Fig. 6.4) are found in the NASW (~75%), SASW (>75%) and SATW (~75%). Nanoplankton is the second most important contributor with microplankton contributing almost equivalent amounts (NAtD and UPW) or very little chl*a* (NASW, EQU, SASW and SATW). By contrast, in the NATD (Fig. 6.4), microplankton contributions are often higher (25 - 50%) than nanoplankton (<25%) and only slightly less than the picoplankton contribution (~40 - 65%) indicating a marked difference in the community structure in these waters.

Within the NASW and SASW there is an increase in picoplankton contribution at depth (75 - 90%; Fig. 6.4), indicating the importance of the small chl*a* size-fraction in CM formation in these waters. Occasionally in surface waters of the NASW and SASW (Fig. 6.4), the nanoplankton and microplankton contributions are slightly higher (>12%) than they are at the ZCM (<12%). There is also evidence that in the EQU (Fig. 6.4) the picoplankton contribution is consistently high (50 - 75%), and increases in association with the CM (>75%), although there is a scarcity of data for this region. The trends identified from size-fractionated measurements during AMT-8 and 10 fit well with the patterns identified by Maranon *et al.,* (2001) indicating that these trends in community chl*a* partitioning are similar for most AMT cruises.

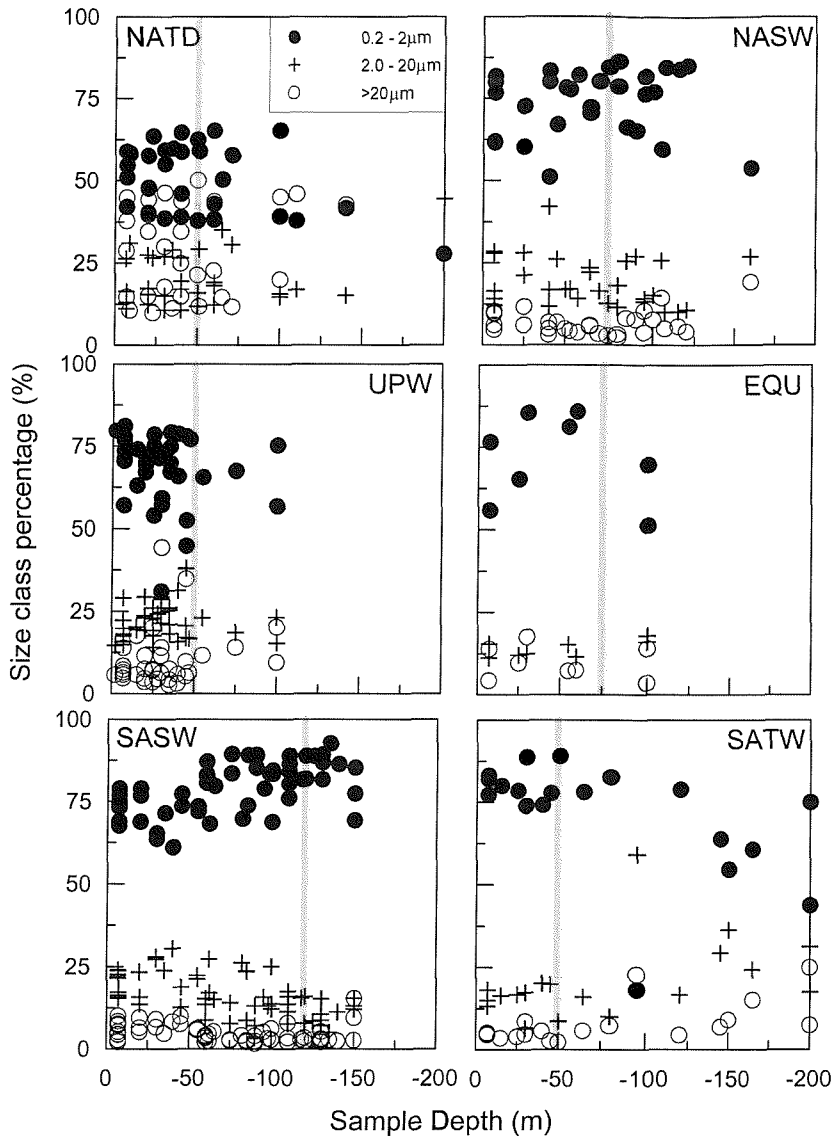


Figure 6.4: Depth patterns of size-fractionated chlorophyll *a* from six regions of the subtropical and tropical Atlantic Ocean (AMT-8 and 10). Grey line indicates cruise-average CM depth and data points indicate picoplankton (solid circles), nanoplankton (cross) and microplankton (open circle).

## 6.4.2. Biomarker Pigments and Pigment Ratios

*Biomarker pigment concentrations:* - Significant ($p<0.05$) positive correlations exists between total chla (TChl *a* = divinyl-chlorophyll *a* and chlorophyll *a*) and most of the other pigment concentrations determined by HPLC (Table 6.4), although the relative abundances of biomarker pigments are regionally variable (Chapter 4). The data also indicate that the CM is both a chl*a* (Fchl*a* and TChl *a*) maximum and an important total pigment maximum (cf. Chapter 4).

At the basinscale, correlations between TChl *a* and zeaxanthin (Zea) and chlorophyll *b* (TChl *b* = Dv Chl b + Chl *b*) are relatively weak ($r = <0.50$; Table 6.4), reflecting their differing physiological roles and taxonomic affiliations. Zea is a photoprotective pigment associated with prochlorophytes and cyanophytes in the subtropical Atlantic Ocean, and is therefore likely to decrease with depth. However, Zea associated with cyanophytes (*Synechococcus* spp.) and prochlorophytes does not change with depth as these phytoplankton groups have been found to retain their cellular Zea concentrations over a wide range of irradiances (Kana *et al.,* 1988; Bricaud *et al.,* 1999). Thus, the

moderate correlation of Zea and TChl *a* in the UPW (Table 6.4) indicate the importance of *Synechococcus* spp. and prochlorophytes in the CM formation. Data points from UPW and NAtD where there are reduced abundances of prochlorophytes (low Dv Chl *a*; see Chapter 4), but high TChl *a* are likely to change the relationship between TChl *b* and TChl *a*. Significant ($p<0.05$) correlations between TChl *b* and TChl *a* in the NASW, EQU, SASW and SATW (Table 6.4) are indicative of the importance of prochlorophytes in formation of the CM in these regions. Dv Chl *a* is a marker of prochlorophytes and there are strong significant relationships with TChl *a* in all regions apart from NAtD (Table 6.4), which is likely to indicate regional differences in the importance of prochlorophytes to CM formation; an absence of prochlorophytes in northern temperate waters and dominance of *Synechococcus* spp.

Table 6.4: Pearson's moment correlation coefficients (r) between pigment concentrations and TCHL*a* (AMT-7 and 8) on the basinscale and within six latitudinal regions. All correlation coefficients have been Bonferroni corrected to a significance level of $p<0.05$. NS indicates non-significant correlations, while NA indicates correlations with less than 8 data points that have been rejected and [n] indicates the number of samples.

| Pigment | All (40°N - 40°S) | NAtD (40 - 35°N) | NASW (35 - 20°N) | UPW (20 - 5°N) | EQU (5°N - 5°S) | SASW (5 - 30°S) | SATW (30 - 40°S) |
|---|---|---|---|---|---|---|---|
| TChl *c*[a] | 0.86 [n = 355] | 0.91 [n = 16] | 0.85 [53] | 0.91 [n = 70] | 0.94 [n = 41] | 0.85 [n = 121] | 0.92 [n = 54] |
| Perid | 0.69 [n = 66] | NA [n = 1] | NA [n = 1] | NS [n = 27] | 0.98 [n = 8] | NA [n = 5] | 0.74 [n = 24] |
| But-fuco | 0.82 [n = 352] | 0.94 [n = 19] | 0.85 [n = 55] | 0.93 [n = 69] | 0.79 [n = 39] | 0.71 [n = 117] | 0.80 [n = 53] |
| Fuco | 0.64 [n = 258] | 0.95 [n = 9] | 0.96 [n = 21] | 0.59 [n = 68] | 0.76 [n = 31] | NS [n = 76] | 0.67 [n = 53] |
| Hex-fuco | 0.93 [n = 375] | 0.98 [n = 22] | 0.93 [n = 59] | 0.98 [n = 72] | 0.95 [n = 41] | 0.92 [n = 126] | 0.90 [n = 55] |
| Diadino | 0.80 [n = 254] | NS [n = 8] | 0.83 [n = 42] | 0.91 [n = 53] | 0.65 [n = 27] | NS [n = 79] | 0.74 [n = 45] |
| Allo | 0.55 [n = 49] | NA [n = 3] | NA [n = 3] | NS [n = 19] | NA [n = 5] | NA [n = 1] | 0.88 [n = 18] |
| Zea | 0.44 [n = 329] | NS [n = 22] | NS [n = 54] | 0.48 [n = 56] | NS [n = 39] | NS [n = 119] | NS [n = 39] |
| TChl *b* | 0.46 [n = 128] | NA [n = 7] | 0.74 [n = 18] | NS [n = 29] | 0.88 [n = 21] | 0.66 [n = 37] | 0.82 [n = 16] |
| Dv Chl *a* | 0.53 [n = 310] | NS [n = 21] | 0.74 [n = 56] | 0.47 [n = 53] | 0.92 [n = 39] | 0.93 [n = 122] | 0.88 [n = 19] |
| Chl *a* | 0.98 [n = 389] | 0.98 [n = 27] | 0.98 [n = 60] | 0.99 [n = 78] | 0.97 [n = 41] | 0.96 [n = 126] | 0.99 [n = 57] |

[a] TChl *c* concentrations are total Chl *c* (TChl *c* = Chl $c_1c_2$ + Chl $c_3$)

Table 6.5: Pearson's moment correlation coefficients (r) for the relationship between pigment ratio and depth on the basinscale and within six latitudinal regions (AMT-7 and 8). All correlation coefficients have been Bonferroni corrected to a significance level of $p<0.05$. NS indicates non-significant correlations, while the number of samples is indicated by [n].

| Region | Dv Chl *a* : TChl *a* | Zea : TChl *a* | TChl *b*: TChl *a* | TChl *c*[a]: Chl *a* | Hex-fuco + But-fuco:Chl *a* | Perid + Fuco + Allo:Chl *a* |
|---|---|---|---|---|---|---|
| All (40°N - 40°S) | NS [n = 310] | -0.41 [n = 329] | 0.73 [n = 128] | 0.46 [n = 355] | 0.56 [n = 376] | NS [n = 260] |
| NAtD (40 - 35°N) | NS [n = 21] | -0.71 [n = 22] | NS [n = 7] | NS [n = 16] | 0.80 [n = 22] | NS [n = 9] |
| NASW (35 - 20°N) | NS [n = 56] | -0.67 [n = 54] | NS [n = 18] | NS [n = 53] | 0.56 [n = 59] | NS [n = 22] |
| UPW (20 - 5°N) | NS [n = 53] | NS [n = 56] | 0.67 [n = 29] | NS [n = 70] | NS [n = 72] | NS [n = 68] |
| EQU (5°N - 5°S) | -0.61 [n = 39] | -0.83 [n = 39] | NS [n = 21] | 0.51 [n = 41] | 0.74 [n = 41] | NS [n = 32] |
| SASW (5 - 30°S) | NS [n = 122] | -0.81 [n = 119] | 0.53 [n = 37] | 0.65 [n = 121] | 0.62 [n = 126] | NS [n = 76] |
| SATW (30 - 40°S) | NS [n = 19] | NS [n = 39] | NS [n = 16] | NS [n = 54] | NS [n = 56] | NS [n = 53] |

[a] TChl *c* concentrations are total Chl *c* (TChl *c* = Chl $c_1c_2$ + Chl$c_3$)

Within all six regions, significant ($p<0.05$) correlations are found between TChl *a* and chlorophyll *c* (TChl *c)*, 19'-butanoyloxyfucoxanthin (But-fuco), 19'-hexanoyloxyfucoxanthin (Hex-fuco) and Chl *a* (Table 6.5), which indicates the basinscale importance of small eukaryotic phytoplankton groups such as the prymnesiophytes, pelagophytes (chrysophytes) and possibly non-peridinin containing dinoflagellates (see Chapter 4). Strong correlations between TChl *a* and peridinin (Perid) are only found in the EQU and SATW (Table 6.5), however within the NAtD, NASW and SASW there is a lack of Perid concentrations above detection limits which is indicative of the rarity of Perid-containing autotrophic dinoflagellates in these areas (Chapter 4). Strong ($r > 0.58$, $p<0.05$) correlations between TChl *a* and fucoxanthin (Fuco) are found in all regions apart from the SASW (Table 6.5), where fucoxanthin is present but at relatively low concentrations (Chapter 4). Fuco is representative of many phytoplankton taxa, but is often taken as the main biomarker for diatoms (e.g. Gibb *et al.,* 2000), thus diatoms seem to be present in most regions and the poor relationship with TChl *a* in the SASW may indicate a patchy distribution unrelated to the CM (see Chapters 4 and 5).

Diadinoxanthin (Diadino) is a eukaryotic photoprotective pigment associated with the xanthophyll cycle in diatoms, dinoflagellates, chrysophytes (pelagophytes) and prymnesiophytes (Jeffrey *et al.,* 1997), and correlates well with TChl *a* in most regions apart from the NAtD and SASW (Table 6.5). Although the basinscale concentration of alloxanthin (Allo) shows a positive relationship with TChl *a*, regional patterns are very different; Allo is almost absent in the NAtD, NASW, EQU and SASW, unrelated to TChl *a* in the UPW and significantly ($p<0.05$) correlated only in the SATW (Table 6.5). Allo is reported to be photoprotective (e.g. Gibb *et al.,* 2000) and is mainly associated with cryptomonads, or symbiont containing dinoflagellate or ciliate species (Jeffrey, *et al.,* 1997).

*Biomarker pigment ratios:* - Due to the photoadaptive nature of algal cells in the vertically variable light regime of the subtropical and tropical Atlantic Ocean, pigment concentrations cannot be taken as indicative of biomass trends. Of greater potential value are pigment ratios, which are thought to be kept relatively constant during photoacclimation (McManus and Dawson, 1994; Mackey, *et al.,* 1996). Vertical changes in the pigment: pigment ratio have been used by McManus & Dawson (1994) to indicate vertical changes in the abundance of key phytoplankton groups in the Caribbean Sea, and this approach is used here. The depth trends of the major biomarker pigment ratios are presented in Figures 6.5 - 6.7.

The ratio of Dv Chl *a*:TChl *a* is indicative of the importance of prochlorophytes to the vertical chl*a* structure. The Dv Chl *a*:TChl *a* ratio is relatively constant with depth in the SATW, tends to increases with depth in the NAtD, NASW and SASW and tends to decrease with depth in the UPW and EQU (Fig. 6.5; Table 6.5). Therefore, prochlorophyte contributions to the TChl *a* are important in the formation of the CM in the NAtD, NASW and SASW and to a lesser extent in the other regions (Fig. 6.5). The CM ratio of Dv Chl *a*:TChl *a* varies between the six regions, with ratios between 10 - 15% in the NASW, EQU and SASW, 10 - 40% in the NAtD, 5 - 40% in the UPW and 5 - 15% in the SATW (Fig. 6.5). The Zea:TChl *a* ratio is indicative of the importance of cyanophytes and prochlorophytes. Some of the highest Zea:TChl *a* ratios are found in upper waters of the NASW and SASW where Zea concentrations are often higher than TChl *a* (Fig. 6.5). The CM ratio of Zea:TChl *a* ranges from ~0 to 0.5 in the NAtD, NASW, UPW, and EQU, and between ~0 - 0.6 in the SASW and SATW (Fig. 6.5). Non-significant ($p<0.05$) correlations between Zea:TChl *a* and depth are found in

the UPW and SATW, and are indicative of changes in the biomass of prochlorophytes and cyanophytes in these different regions; in the SASW biomass is stable with depth but there are increases of cyanophyte and prochlorophyte biomass in the CM in the EQU (cf. Zubkov et al., 1998, 2000a, b).

Chl *b* is rare in upper waters (<50 m) of most regions of the tropical and subtropical Atlantic Ocean, apart from where the CM is shallow (UPW and SATW; Fig. 6.6) and is rarely found in the NATD (Table 6.5). Strong positive significant ($p<0.05$) correlations are found between TChl *b*:TChl *a* and depth in only the UPW and SASW whereas the relationships are insignificant in the other regions (Table 6.5). The ratio of TChl *b*:TChl *a* at the CM changes between region; in the NAtD and NASW the ratio is between 0.10 - 0.60, in the UPW between ~0 - 0.30 in the UPW, in the EQU and SASW between 0.35 - 0.65 and between 0.10 - 0.20 in the SATW (Fig. 6.6). However, there are sharp increases of the TChl *b*:TChl *a* ratio below the CM in all of the regions, with values reaching a maximum of 0.80 in the NASW, EQU and SASW (Fig. 6.6). Due to the lack of biomarker pigments associated with eukaryotic Chl *b* containing taxa (lutein and violaxanthin; Jeffrey *et al.,* 1997) most of the Chl *b* in the subtropical and tropical Atlantic Ocean is though to be associated with prochlorophytes (i.e. is the divinyl form of Chl *b*; cf. Chapter 4; Goericke and Repeta, 1993). Prochlorophytes increase their Chl *b*:Dv Chl *a* ratio under low light (Partensky *et al.,* 1993), therefore, strong correlations between TChl *b*:TChl *a* with depth indicate photoacclimation of low-light adapted prochlorophytes in association with the CM (Table 6.5; Fig. 6.6) rather than an increase in cell numbers or biomass (cf. Zubkov *et al.,* 1998, 2000b).

Increases in the TChl *c*:Chl *a* ratio with depth are seen in all regions apart from the NAtD and SATW, where the ratio is relatively constant with depth although some CM ratios in the NAtD are higher than in upper waters (Fig. 6.6: Table 6.5). CM ratios of TChl *c*:Chl *a* in the NASW are between 0.2 - 0.4, in the UPW between 0.1 - 0.3, between 0.3 - 0.5 in the EQU and between 0.3 - 0.9 in the SASW (Fig. 6.6). Chl *c* is restricted to eukaryotic phytoplankton taxa and the increase in TChl *c*:Chl *a* ratio with depths in the NASW, UPW, EQU and SASW may be indicative of biomass increases at depth in association with the CM of prymnesiophytes, pelagophytes (chrysophytes) and dinoflagellates lacking Perid. Interpretation of depth increases in TChl *c*:Chl *a* ratio in the NASW and UPW are complicated by the occurrence of several samples with relatively high TChl *c*:Chl *a* ratios in surface waters (Fig. 6.5).

Ratios of Hex-fuco+But-fuco:Chl *a* are also indicative of changes in the abundance of prymnesiophytes, pelagophytes (chrysophytes) and dinoflagellates lacking Perid. Significant ($p<0.05$) increases in Hex-fuco+But-fuco:Chl *a* ratios with depth are observed in the NAtD, NASW, EQU, and SASW, with no significant relationship in the UPW or SATW (Fig. 6.7; Table 6.5). The relationship in the UPW can be seen to be due to stable ratios in surface and subsurface waters down to the CM and increases below the CM (Fig. 6.7), which indicates that the abundance of Hex-fuco and But-fuco containing taxa is relatively stable in upper UPW waters and increase below the CM. The Hex-fuco+But-fuco:Chl *a* ratio of the CM varies slightly with values in the NAtD ~0.75, ~0.50 in the UPW, between 0.50 - 0.75 in the EQU, between 0.25 - 0.75 in the SATW and between 0.75 - 1.5 in the NASW and SASW (Fig. 6.7). High ratios in the CM (~1.0) in the NASW and SASW (Fig. 6.7) indicate that at depth algal cells often have higher concentrations of these accessory pigments than chl*a*. High accessory pigment to chl*a* ratios at depth in association with the CM are

indicative of the importance of photoacclimation in the formation of the CM in the NASW and SASW and may reflect the presence of specialised taxa at depth.

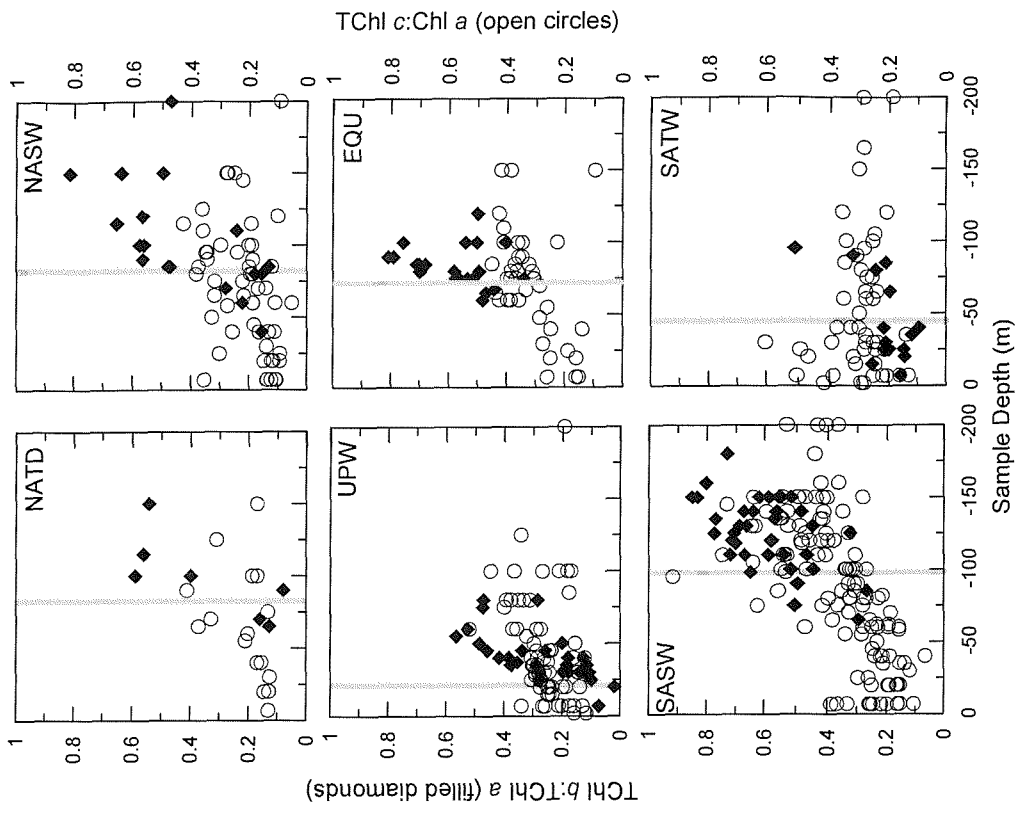


Figure 6.6: The vertical distribution of TChl *b*:TChl *a* (filled diamonds) and TChl *c*: Chl *a* (open circles) ratios in six regions of the subtropical and tropical Atlantic Ocean (AMT7 and 8). Grey line indicates cruise-average CM depth.

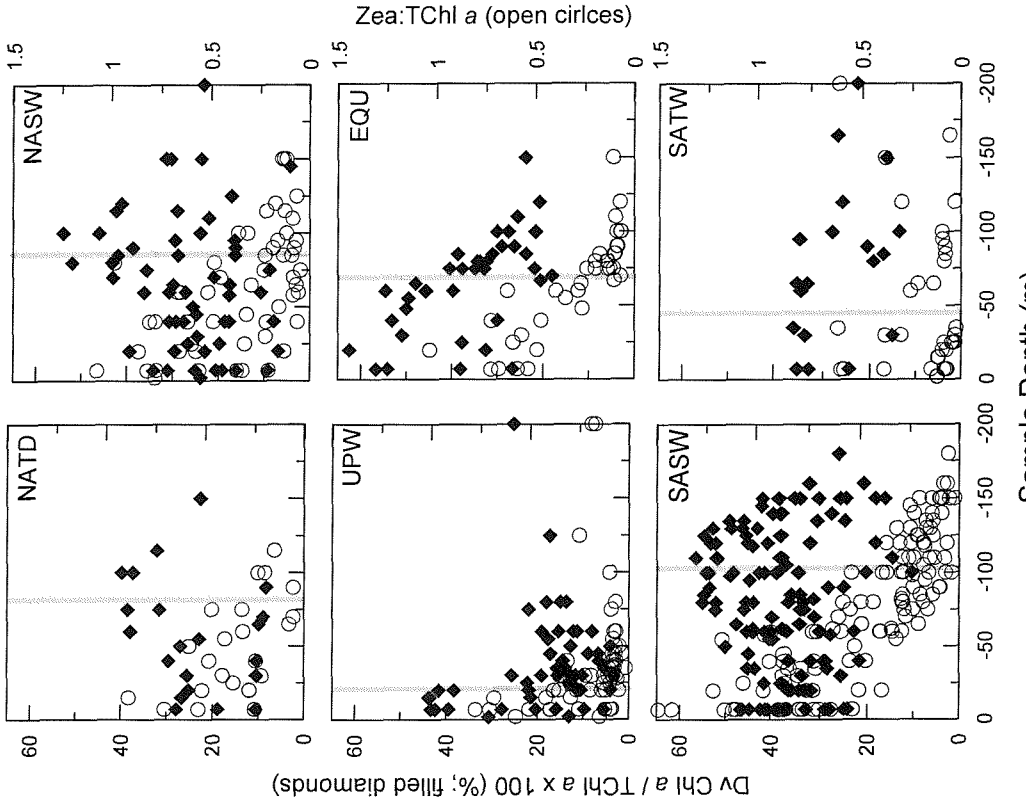


Figure 6.5: The vertical distribution of Dv Chl *a*:TChl *a* (x100, %; filled diamonds) and Zea:TChl *a* (open circles) ratios from six regions of the subtropical and tropical Atlantic Ocean (AMT7 and 8). Grey line indicates cruise-average CM depth.

Vertical stability of the Perid+Fuco+Allo:Chl *a* ratio and very low ratios (<0.2) in the NASW, EQU and SASW indicate that dinoflagellates, diatoms and cryptomonads are relatively rare and do not generally vary in abundance with depth. Non-significant correlations of Perid+Fuco+Allo:Chl *a* are found in all regions which highlights the scarcity of these pigments and phytoplankton groups in the subtropical and tropical Atlantic Ocean and their patchy distribution (Table 6.5). The CM ratio of Perid+Fuco+Allo:Chl *a* is <0.2 in the NASW, EQU and SASW, while slightly higher ratios (0.3 - 0.4) are observed in the CM of the NAtD, UPW and SATW (Fig. 6.7). Pigment ratios do increase with depth in the NAtD in association with the CM, and are relatively high around the shallow CM in the UPW and SATW (Fig. 6.7). Thus, in these regions diatoms, dinoflagellates, and to a lesser extent cryptomonads, are more likely to be relatively important components of the phytoplankton community. Within the SASW there are indications that the Perid+Fuco+Allo:Chl *a* ratio is occasionally higher in surface and subsurface waters than at depth, and that in at least two occasions (AMT-8, 19°S) there are significant contributions from diatoms, dinoflagellates and possibly cryptomonads at depth (Fig. 6.7).

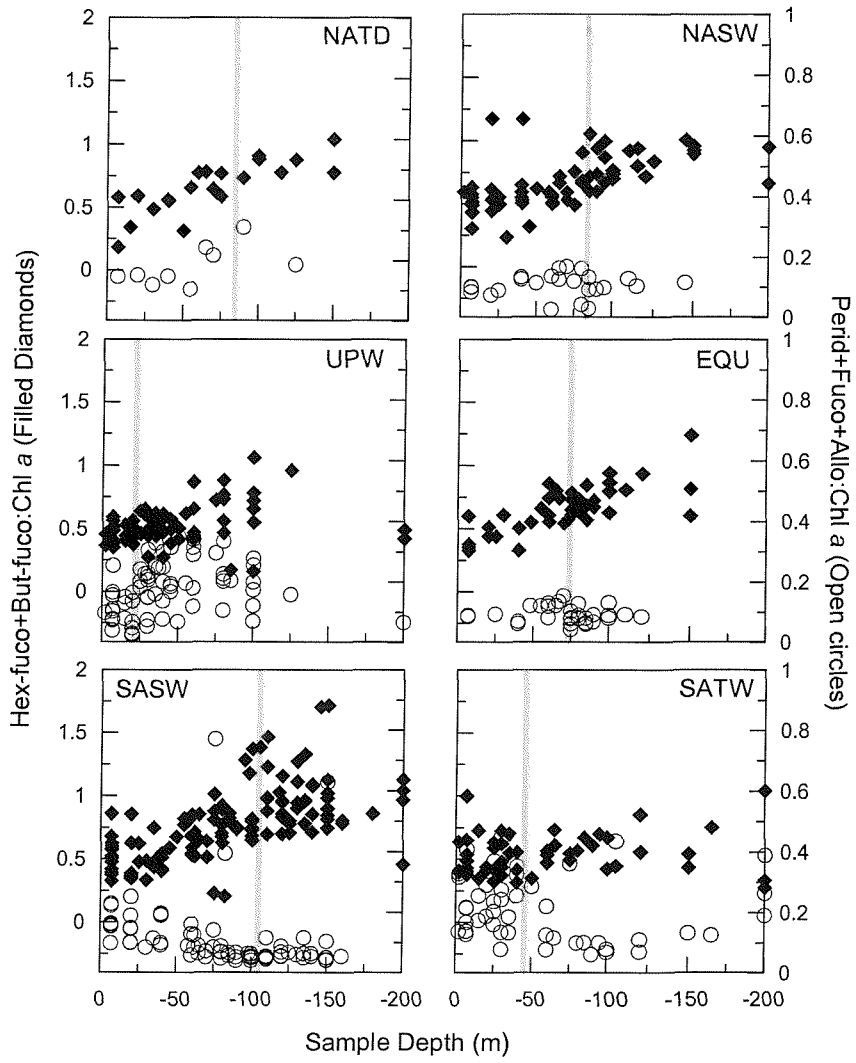


Figure 6.7: The vertical distribution of Hex-fuco+But-fuco:Chl *a* (filled diamonds) and Perid+Fuco+Allo:Chl *a* (open circles) ratios in six regions of the subtropical and tropical Atlantic Ocean (AMT-7 and 8). Grey line indicates cruise-average CM depth.

### 6.4.3. Nano- and Microphytoplankton Biomass

*Nano- and microplankton biomass and depth:* - Nano- and microphytoplankton biomass is calculated from microscopic counts (methods 2.5.2) with the main identifiable groups being diatoms, autotrophic dinoflagellates, coccolithophores and endosymbiotic species from AMT-7, 8 and 10. The biomass of all four groups varies by several orders of magnitude both between regions and within regions (Fig. 6.8). Generally there is relatively little change in the biomass of the four groups with depth and the CM rarely represents a biomass maximum for these phytoplankton groups, although high biomass (>1 mg C $m^{-3}$) is found in upper waters of the NATD, NASW, UPW and SATW (Fig. 6.8).

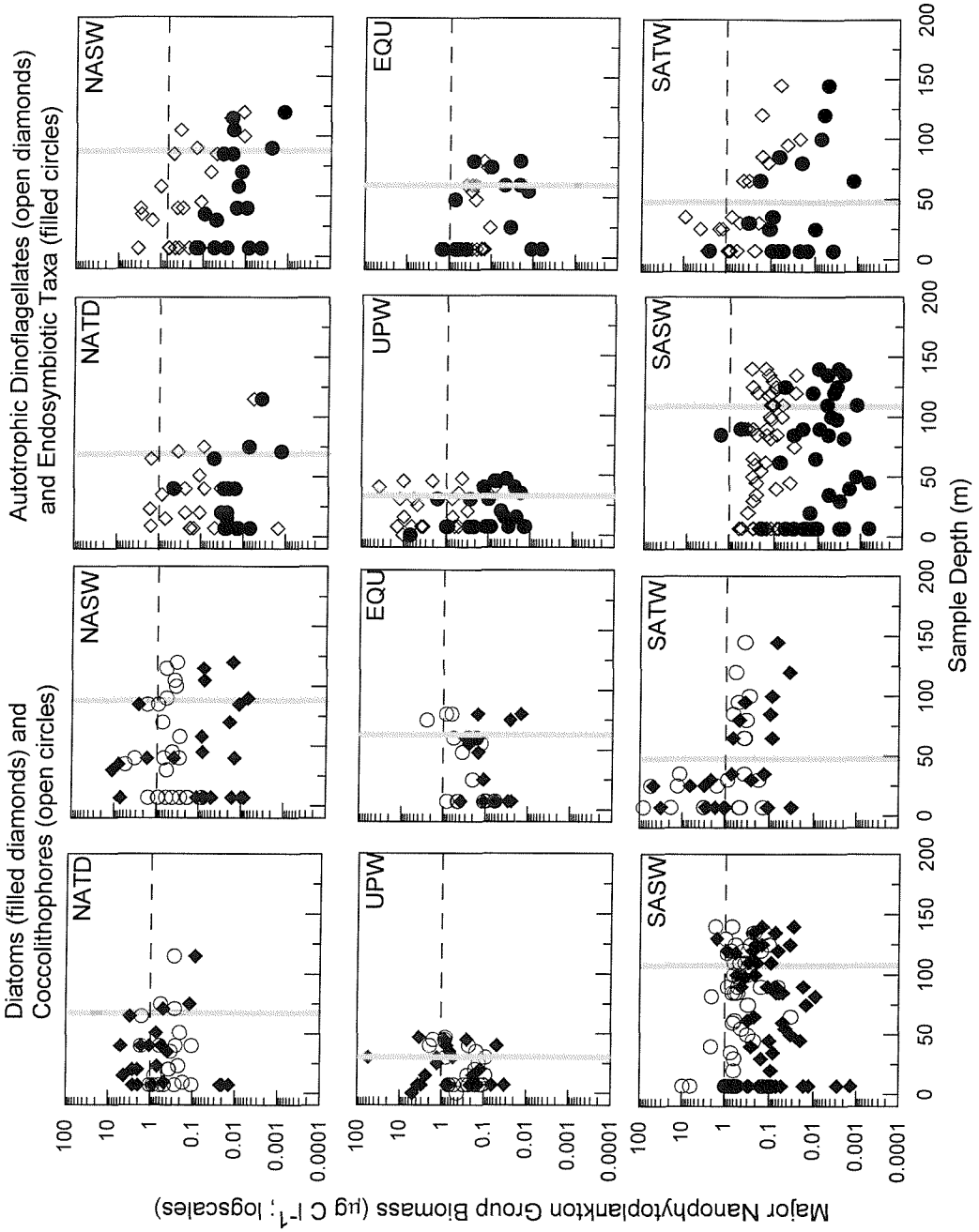


Figure 6.8: Nano- and microphytoplankton total biomass from six regions of the subtropical and tropical Atlantic Ocean (AMT7, 8 and 10). Grey line indicates cruise-average CM depth.

Diatom biomass is highest in the upper waters (<50 m) of the NATD, NASW, UPW and SATW, where the CM is shallow (<50 m; Fig. 6.8). Coccolithophore biomass does not increase appreciably with depth or in association with the CM in most regions, although there is an indication that it increases in the UPW, EQU and SATW when the CM is in the upper 75 m (Fig. 6.8). Coccolithophore biomass is slightly higher than diatom biomass in association with the CM in the EQU and in surface waters of the SASW, whereas the biomasses of the two groups are almost equal in subsurface waters of the SATW (Fig. 6.8). Autotrophic dinoflagellate biomass shows similar trends to diatom biomass; high biomass in the NATD, NASW, UPW and SATW and low biomass in the EQU and SASW (Fig. 6.8). Within the UPW autotrophic dinoflagellate biomass is higher than diatom biomass and this indicates the dominance of dinoflagellates in the UPW (Fig. 6.8). In the NASW and SASW there is some indication that autotrophic dinoflagellates biomass decreases slightly with depth so that the biomass of this group is lower in the deep CM than in subsurface waters (Fig. 6.8; cf. Chapter 5). The biomass of endosymbiotic taxa is generally low (typically <0.1 mg C $m^{-3}$) in the NATD, NASW, SASW and SATW, with higher endosymbiotic taxa biomass (typically >0.1 - 10 mg C $m^{-3}$) in sub-surface waters in the UPW and EQU (Fig. 6.8). Changes in endosymbiotic taxa biomass is mainly due to the presence of *Trichodesmium* spp. in the UPW and EQU, which fits well with historical reports of the distribution of this genus (Tyrrell *et al.*, submit).

*Nano- and microphytoplankton biomass and chl a concentration:* - Generally, the biomass (carbon and chl*a*) of phytoplankton communities in subtropical and tropical waters of the Atlantic Ocean are dominated by picoplankton (Zubkov *et al.*, 1998, 2000a, b; Maranon *et al.*, 2001) which are not accounted for in the microscopic estimates of phytoplankton carbon (methods 2.5.2). However, significant correlations between the estimated nano- and microphytoplankton carbon and Fchl*a* measurements are found in several regions (Table 6.6). The existence of such relationships indicates either community composition change (Chapter 4) or changes in the relative abundance and importance of larger phytoplankton groups to the total community in some regions.

Table 6.6: Pearson's moment correlation coefficients (r) between nano- and microphytoplankton (>5μm) biomass and Fchl*a* for A7, A8 and A10. Total biomass indicates total for identifiable nano- and microphytoplankton biomass only. Significance levels are; * p<0.001, ** p<0.005, + p<0.01, ++ p<0.05 and nonsignificant (NS). Number of samples (n) indicated in brackets.

| Region | Total (>5μm) Biomass | Diatom Biomass | Autotrophic Dinoflagellate Biomass | Coccolithophore Biomass | Endosymbiotic species Biomass |
|---|---|---|---|---|---|
| All (40°N - 40°S) | 0.55 [n = 162] | 0.63 [n = 161] | 0.45 [n = 162] | 0.72 [n = 161] | NS [n = 133] |
| NATD (40 - 35°N) | 0.76 [n = 16] | 0.76 [n = 16] | NS [n = 16] | NS [n = 16] | NS [n = 16] |
| NASW (35 - 20°N) | 0.68 [n = 24] | NS [n = 23] | NS [n = 24] | 0.70 [n = 24] | NS [n = 18] |
| UPW (20 - 5°N) | 0.64 [n = 23] | NS [n = 23] | NS [n = 23] | NS [n = 23] | NS [n = 23] |
| EQU (5°N - 5°S) | NS [n = 16] | NS [n = 16] | NS [n = 16] | NS [n = 16] | NS [n = 16] |
| SASW (5 - 30°S) | NS [n = 55] | NS [n = 55] | NS [n = 55] | NS [n = 55] | NS [n = 54] |
| SATW (30 - 40°S) | NS [n = 23] | NS [n = 23] | NS [n = 23] | NS [n = 23] | NS [n = 18] |

Significant (p<0.05) relationships exist between total nano- and microphytoplankton biomass and Fchl*a* concentrations from the NAtD, NASW and UPW but are nonsignificant in EQU, SASW

and SATW (Table 6.6). In terms of the individual phytoplankton groups, diatom biomass is significantly ($p<0.05$) correlated with Flchl*a* only in the NAtD whereas the relationships are not significant in the NASW, UPW, EQU, SASW or SATW (Table 6.6). The biomass of autotrophic dinoflagellates is significantly correlated with Flchl*a* only on the basinscale (Table 6.6). Coccolithophore biomass correlates with Flchl*a* only in the NASW, while the biomass of endosymbiotic species does not correlate with Flchl*a* in any of the regions (Table 6.6) Changes in the relationship between group biomass and Flchl*a* from different regions indicate the importance of the different groups in the six regions of the subtropical and tropical Atlantic Ocean.

### 6.4.4. Species Composition: Bray-Curtis Similarity

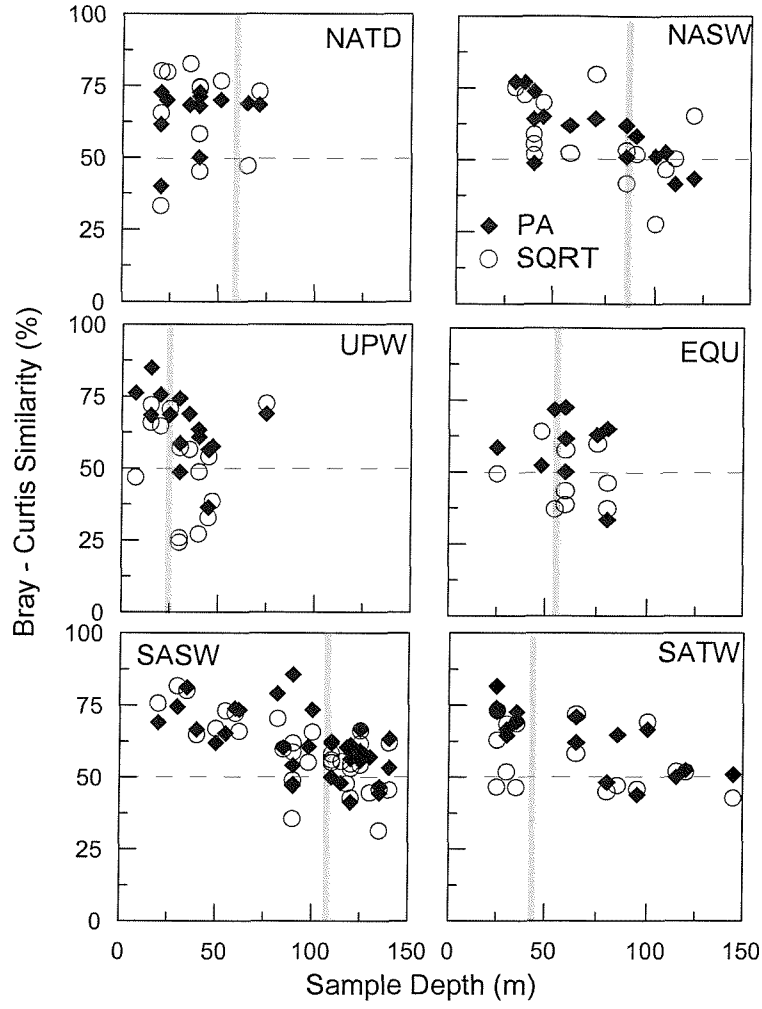


Figure 6.9: Bray-Curtis percentage similarity between surface and deep samples for six regions of the subtropical and tropical Atlantic Ocean (AMT-7, 8 and 10). Grey line indicates cruise-average CM depth.

The species composition of samples from various depths (AMT-7, 8 and 10) has been analysed by comparing each deep sample with its corresponding surface sample through the use of a Bray-Curtis similarity index (%) and is presented in Figure 6.9. Two transformations of the species datamatrix have been applied; (a) presence / absence (PA) transformation of all species, and (b) square-root (SQRT) transformation of the dominant species (>10% of the total numbers) abundances (see methods 2.6.1). PA transformation highlights changes in the species composition, whereas SQRT transformation indicates changes in the species dominance. Vertical trends in Bray-Curtis

similarity show that in the NATD and EQU there is usually little change in the species composition or species dominance with depth; surface and deep NATD and EQU communities have similar nano- and microplankton composition (Fig. 6.9). Within the NASW, SASW and SATW there are vertical decreases in Bray-Curtis similarity for both species composition and species dominance indicating floral differences in surface and deep communities (Fig. 6.9; cf. Chapter 4). In the UPW there is a rapid decrease in Bray-Curtis similarity for species composition but a more variable pattern for species dominance with some stations having more similar surface and deep nano- and microplankton communities than others (Fig. 6.9).

## 6.5. Discussion

### 6.5.1. A Synthesis of Chlorophyll *a* Structures and Community Dynamics

The formation of the Chlorophyll *a* Maximum (CM) has been proposed to be caused by a variety of both independent and related mechanisms; e.g. differential photodegredation of pigments (Gieskes *et al.,* 1978), reduced sinking rates or aggregation at a density discontinuity (e.g. Steele and Yentsch, 1960; Lorenzen, 1967), behavioural aggregation (e.g. Cullen and Horrigan, 1981), enhanced growth in proximity to the nutricline (e.g. Voituriez and Dandonneau, 1974; Herbland and Voituriez, 1979; LeBouteiller, 1986;), enhanced growth in the thermocline (e.g. Pingree *et al.,* 1975), different grazing rates over the water-column where sinking losses are minimal (Longhurst, 1976), photoacclimation of cells to low light conditions and related changes in the cellular carbon to chlorophyll *a* ratio (e.g. Cullen, 1982). Modelling studies of the CM have shown the importance of the light field and upward nutrient flux in determining both the $Z_{CM}$ and $C_{CM}$, with grazing only effecting the $C_{CM}$ (Varela *et al.,* 1992, 1994). The $C_{CM}$ may also be indicative of the role of the CM as a nutrient trap for upward nutrient fluxes and as a self-shading mechanism for waters below the CM. The regular gaussian shape of the CM may also be related to its roles in nutrient trapping and self-shading, in that the upper slope is regulated by nutrient fluxes through the CM and the lower slope regulated by light diffusion through the CM; the CM can only increase in width if these two processes cause high nutrient and light fluxes (e.g. wide CM in the low chl*a* CM of the subtropical gyres). Within the subtropical and tropical Atlantic Ocean different mechanisms in CM formation are likely to operate, although the availability of nutrients and light will regulate the process.

The chl *a* concentration at a specific depth can be described by the following equation;

Chl *a* = (Growth + Photoacclimation + Physical additions) - (Grazing Losses + Physical Losses)

Growth and photoacclimation are functions of the nutrient and light availability and the requirement of algal cells to synthesise pigments (low light) or repair photoinduced damage (high light), while physical losses (e.g. sinking) are related to the physical environment and community structure; a community dominated by small picoplankton cells will have low sinking rates but high grazing losses and lower nutrient requirements than a community dominated by large diatoms which will have high sinking rates, variable grazing losses and higher nutrient requirements. Intrinsic growth rates are

likely to vary between components of the community (see Taylor *et al.,* 1993), and thus the community structure will affect the structure and stability of the CM.

Although a significant inverse relationship between $C_{CM}$ and the depth of the CM has been described previously (Herbland and Voituriez, 1979), and exists on the basinscale (Table 6.2), division into regional relationships reveals a much more complicated picture. Such regional differences in the relationship are likely to be due to differences in the environments and ecosystems. Shallow CM are found in high nutrient environments where there is likely to be substantial growth and therefore high chl*a* concentrations, whereas deep CM are found where nutrient pools are deep and light levels are low. Therefore, an inverse relationship between $Z_{CM}$ and $C_{CM}$ can be expected and although this is found in most regions of the tropical and subtropical Atlantic Ocean, it is absent within the EQU and very weak in the SASW. The absence of a relationship between $C_{CM}$ and $Z_{CM}$ was interpreted by Estrada *et al.,* (1993) as indicative of the relative importance of growth verses loss factors to the $C_{CM}$. However, $C_{CM}$ is also influenced by the relative importance of photoadaptation to cell physiology and other factors. A lack of relationship between $C_{CM}$ and $Z_{CM}$ in EQU and a weak relationship in SASW indicate that growth and/or photoadaptation are important and largely independent of $Z_{CM}$.

The depth of the CM and nitracline, as well as the surface irradiance conditions regulates upper water chl*a* concentrations. Excessive light levels in surface and subsurface waters cause damage to the photosynthetic apparatus and photoinhibition as indicated by a reduction of the photosynthetic efficiency (Falkowski and Raven, 1997). Photoinduced damage of phytoplankton cells will increase the negative effects of nutrient stress in upper waters, so that low surface chl*a* concentrations are due to a combination of nutrient stress, photoinduced breakdown of the photosynthetic apparatus (Falkowski, 1992) and the photoacclimation response of algal cells to high light (Falkowski and Raven 1997). Therefore, changes in the ambient nutrient concentrations will effect growth and photosynthetic rates, as well as the ability of algal cells to repair photoinduced damage (Litchman *et al.,* 2002).

Characteristic chlorophyll *a* profiles may be classified into 3 typical structures which are presented in Figure 6.10 and differ markedly in their formation and maintenance (Cullen, 1982); Seasonal / Upwelling Structure (Cullen, 1982), Typical Tropical Structure (TTS; Herbland and Voituriez, 1979) and Central Gyre Structure (CGS; Cullen, 1982). The data presented in this chapter and in the literature are used to provide further information on the formation of these profiles and the phytoplankton communities that characterise them. These are not rigid classifications, as the typical structures presented are thought to exist along a nutrient continuum (Cullen, 1982), and the dividing lines are not clear, especially between the TTS and CGS. However, it is logical to propose that the CM is an important contributor to total productivity in the TTS, whereas in the CGS the CM contribution to total productivity is negligible. The profiles and communities identified from the subtropical and tropical Atlantic Ocean shows that chl*a* profiles from the NATD, UPW and SATW are representative of Seasonal / Upwelling structure, profiles from the EQU and NASW represent the classical and oligotrophic extreme of the TTS respectively, and profiles from the SASW are representative of the CGS.

*(A). SEASONAL / UPWELLING STRUCTURE:*

Structure and Maintenance - CM in upwelling waters are characteristically shallow (i.e. represent Subsurface Chlorophyll *a* Maximum) and in close proximity to the nitracline (Fig. 6.10a). Light and nutrient conditions are optimal for growth and the CM can be found either at the $Z_{eu}$ or at the 10% PAR isolume (Fig. 6.10a), which indicates that active growth and photosynthesis are important in the CM formation and maintenance. The CM will represent a biomass maximum and in most cases a productivity maximum (Longhurst and Harrison, 1989). Behavioural aggregation either through regulated sinking of cells or swimming may be important (Steele and Yentsch, 1960; Cullen, 1982) when nutrients are becoming depleted, or to avoid self-shading (Prezelin, 1987 and references therein), or for continued presence in the upwelling area (Smith *et al.,* 1987; Barber, 2001). When nutrient conditions are suitable surface blooms can occur resulting in high chl*a* concentrations at the seasurface, and with sinking of the community high chl*a* concentrations can also be found at the bottom of the upper mixed layer and euphotic zone. Therefore, the CM may represent the aggregation of sinking cells from a shallower productivity maximum at the bottom of the upper mixed layer (Cullen, 1982). Light levels are likely to be high at the surface and within the upper few meters which implies a high level of photoinduced damage, however, due to the high nutrient regime algal cells may be able to repair photosystem damage and synthesise photoprotective pigments. Upwelling of new nutrients means that new production dominates in upper waters and regenerated production will occur at depth (LeBouteiller, 1986; Barber, 2001).

Plankton Community Structure - The picoplankton are dominated by *Synechococcus* spp. and picoeukaryotes, as well as high abundances of heterotrophic bacteria (Fig. 6.10a; see Partensky *et al.,* 1996; Zubkov *et al.,* 1998, 2000b). Diatoms and dinoflagellates are often present in bloom abundances and represent the greatest proportion of biomass (Barber, 2001). Recognised bloom forming species dominate inshore upwelling waters (e.g. Smayda, 2000) and there are indications that toxin-producing species are often present (Pitcher and Calder, 2000; cf. Chapter 4). Ultraviolet radiation (UV) is likely to be high in surface waters and many bloom species have been found to have high cellular concentrations of UV absorbing pigments (Jeffrey *et al.,* 1999). As the upwelled water-mass and community are advected offshore there is progression from a characteristically eutrophic community to one characterising oligotrophic waters (Longhurst and Pauly, 1998), with increases in the abundances of prochlorophytes and small eukaryotic taxa. A zooplankton biomass maximum may coincide with the CM when the CM represents a biomass maximum (Longhurst and Harrison, 1989).

Ecosystem Dynamics - As the upwelled water is advected offshore the accumulated phytoplankton biomass is depleted probably by grazing and sinking out of the water column, as well as losses due to vertical advection (Smith *et al.,* 1987; Barber, 2001). The CM in upwelling waters is likely to be an important food source for micro- and macrozooplankton, as well as higher trophic levels (e.g. Cury *et al.,* 2000), due to its diverse size and taxonomic composition. Food webs in upwelling environments are likely to have both microbial and classic food chains with the importance of each depending upon the nutrient fluxes and age since upwelling (Barber, 2001).

Regions - The chlorophyll structure in upwelling areas can be seen to be very similar to that produced during the spring bloom in temperate and coastal tropical waters (Cullen, 1982); the CM is formed by *in-situ* growth in a water-column which is stratified, nutrient-rich and light-rich. Upwelling

occurs in episodes which are similar to the onset of the spring bloom, with upwelling relaxation similar to pre- and post bloom conditions (Cullen, 1982). As the upwelled water is advected away from the upwelling nuclei, the community ages and successional processes similar to those in a seasonal cycle occur. Deepening of the nitracline with movement offshore would eventually lead to conditions representative of the TTS and finally CGS chl*a* structures. Thus, the seasonally influenced regions of the tropical and subtropical Atlantic Ocean would fluctuate between communities characteristic of upwelling regions and the TTS.

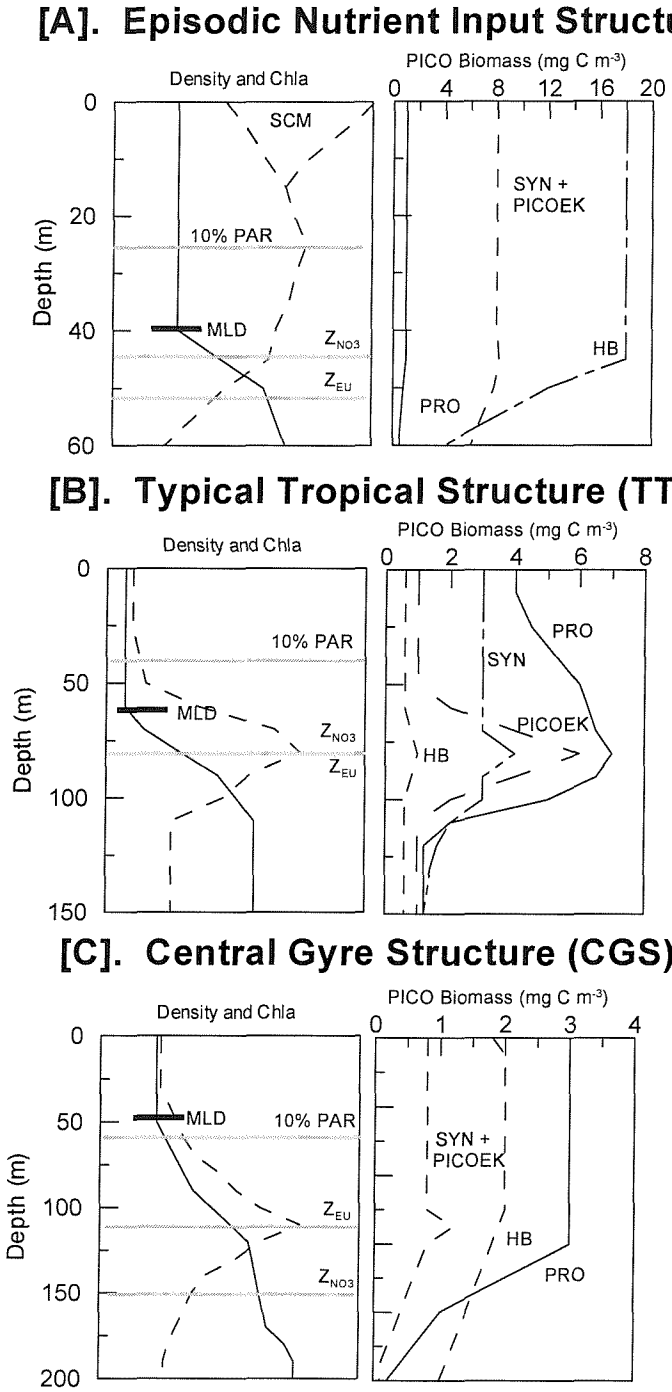


Figure 6.10: The vertical structure of phytoplankton communities in three characteristic chlorophyll profiles; (a) seasonal / upwelling, (b) Typical Tropical Structure (TTS), and (c) Central Gyre Structure (CGS). Picoplankton biomass (mg C $m^{-3}$) profiles are compiled from Campbell and Vaulot (1993), Partensky et al., (1996) and Zubkov et al., (2000), where PRO indicates prochlorophytes, SYN indicates *Synechococcus* spp., PICOEK indicates picoeukaryotes and HB indicates heterotrophic bacteria.

*(B). TYPICAL TROPICAL STRUCTURE (TTS):*

Structure and Maintenance - The CM in the TTS is found near the nitracline either within the thermocline or base of the MLD (Fig. 6.10b; Herbland and Voituriez, 1979; McManus and Dawson,

1994) with the productivity maximum at the same depth (Herbland and Voituriez, 1979) or slightly shallower (Voituriez and Dandonneau, 1974), so that the CM is formed from primary production in a stratum (Cullen, 1982). The CM in the TTS is formed and maintained by *in-situ* growth with suitable nutrient and light conditions for photosynthesis (Cullen, 1982). In the case of the TTS the CM is indicative of a biomass and primary productivity maximum, although photoadaptative changes in cell chl*a* contents may also have a minor role. Within the TTS the water-column can be split into a 2-layered system; an upper nutrient-poor and light-rich layer and deeper nutrient-rich and light-poor layer with the nutricline indicative of the boundary between the two (Herbland and Voituriez, 1979; Cullen, 1982). Upper water chl*a* concentrations are nutrient limited and characterised by high levels of photoinduced damage to the photosystems in the absence of suitable nutrient pools for repair. Production in the CM is based on new nutrient fluxes from below, so that the CM is based on new production and upper waters are based on regenerated production (LeBouteiller, 1986).

Plankton Community Structure - Within the TTS the phytoplankton community is spit into upper and deeper layers. The upper layer is dominated by high-light adapted prochlorophytes, whereas the deeper layer and CM are characterised by increases of several groups, including low-light adapted prochlorophytes, *Synechococcus* spp., picoeukaryotes (Fig. 6.10b; c.f. Zubkov *et al.,* 1998, 2000b) and other eukaryotic taxa (prymnesiophytes, pelagophytes and dinoflagellates). Prochlorophytes, *Synechococcus* spp. and picoeukaryotes increase in abundance and biomass in association with the CM (Fig. 6.10b; Partensky *et al.,* 1996). A significant proportion of increased prymnesiophytes can be attributed to coccolithophores that are abundant in equatorial waters and sediments (Kinkel *et al.,* 2000). Larger phytoplankton taxa are relatively rare, although surface blooms of *Trichodesmium* spp. will occur under suitably stable conditions. The 2-layer system thought to operate in the TTS (Cullen, 1982) implies that specialised sun and shade floras may occupy these different niches; *Trichodesmium* spp. has already been proposed as a member of the sun flora (Longhurst and Harrison, 1989). A zooplankton abundance maximum is often found to coincide with the productivity maximum and CM (Longhurst and Harrison, 1989). Due to the dominance of small cell sizes, grazing is likely to be mainly due to nano- and microheterotrophs acting as a trophic link to larger heterotrophs (i.e. microbial loop).

Ecosystem Dynamics - Dominance of the TTS by small algal cells with characteristically low sinking rates indicates that there are likely to be minimal rates of export production. The main source of export production in the TTS is likely to be from the coccolithophore component of the community as sinking rates of calcified cells are thought to be higher than uncalcified cells (Passow and Peinert, 1993). Grazing losses are likely to be much higher than sinking losses for maintenance of the CM in the TTS.

Regions - Although the TTS was originally described for chl*a* profiles in the equatorial Atlantic (Herbland and Voituriez, 1979), using the characteristics discussed here the TTS appears to occur in several other locations; equatorial Pacific (Blanchot *et al.,* 1992), Caribbean (McManus and Dawson, 1994), North Atlantic Subtropical waters (Jocham and Zeitzschel, 1989) and seasonally off Bermuda and within areas of the Sargasso Sea (Olson *et al.,* 1990).

### *(C). CENTRAL GYRE STRUCTURE (CGS):*

Structure and Maintenance - The CGS represents a situation beyond the oligotrophic extreme of the TTS where the CM is no longer formed through *in-situ* growth but represents a photoacclimative response to light limitation in the presence of deep elevated nutrient concentrations (Cullen, 1982; c.f. Maranon *et al.,* 2000). The CM is found at or very near the bottom of the euphotic zone while the nitracline is much deeper (Fig. 6.10c). Primary productivity rates in the CM are low and contribute very little to integrated measurements (Partensky *et al.,* 1996; Maranon *et al.,* 2000). Due to the deepness of the nitracline in the CGS, light limitation of the deep CM is counteracted by the increased availability of nutrients. The CM is characteristically deep and low in chl*a* which is due to the limited cellular levels of chl*a* available to the small amount of biomass present. Production in the CM is based in nutrient fluxes from below, so that the CM is based on new production and upper waters are based on regenerated production (LeBouteiller, 1986).

Plankton Community Structure - The CGS is dominated by prochlorophytes in terms of numbers and biomass (Fig. 6.10c), with separation into upper high-light adapted communities and deeper low-light adapted communities and a reduction in the abundance of *Synechococcus* spp. and picoeukaryotes (Campbell and Vaulot, 1993; Partensky *et al.,* 1996; Zubkov *et al.,* 2000b). Partensky *et al.,* (1996) suggested that prymnesiophytes were restricted to upper waters and chrysophytes to deeper waters, however the distribution of coccolithophore species throughout the water column (Fig. 6.8; cf. Chapter 4; Venrick, 1988) indicates that prymnesiophytes are not restricted to upper waters. Although nano- and microplankton species represent only a minor contribution to the total biomass, they form distinct and indicative sun and shade flora (Fig. 6.9; cf. Chapter 4; c.f. Venrick, 1973, 1982, 1988, 1990a). Partensky *et al.,* (1996) and Campbell and Vaulot (1993) found evidence of a prochlorophyte and *Synechococcus* spp. abundance and biomass maximum above the CM, and that prochlorophytes represent a higher proportion of primary productivity above the CM than within. Vertical separation of the productivity maximum and CM is positively correlated with $Z_{CM}$; where the CM is deep the productivity maximum is found much shallower (Longhurst and Harrison, 1989). Depth of the zooplankton abundance maximum tracks the depth of the productivity maximum, rather than the CM, although this pattern is clearest at night (Longhurst and Harrison, 1989).

Ecosystem Dynamics - Dominance of the plankton community by small picoplankton cells implies that the main losses in the CGS will be from heterotrophic grazing as opposed to sinking (see Partensky *et al.,* 1996). Coccolithophores are likely to represent the main source of export production (Passow and Peinert, 1993), although seasonal mixing events may cause stochastic export production from other phytoplankton groups (Karl, 1999; Scharek, 1999a, b). Such a system is best described as a microbial loop ecosystem with efficient recycling of organic matter and production within small pico- and nanoplankton food chains (Teira *et al.,* 2001).

Regions - The CGS is commonly found within the central range of the subtropical gyres (e.g. Campbell and Vaulot, 1993; Partensky *et al.,* 1996) with seasonal fluctuations to a profile similar to the oligotrophic extreme of the TTS at the gyre edges (see e.g. Furuya *et al.,* 1990; Olson *et al.,* 1990).

### 6.5.2. Chlorophyll *a* Maximum Formation in the Subtropical and Tropical Atlantic Ocean

Within the tropical and subtropical Atlantic Ocean a wide range of physical conditions exist; from the strongly stratified subtropical gyres to the upwelled waters off NW Africa and the seasonally mixed waters at the northern and southern end of the AMT transect. The characteristics of the Chlorophyll *a* Maximum (CM) differ between regions and can be summarised as follows;

*(1) North Atlantic Drift (NATD):* No significant difference between $Z_{CM}$, $Z_{NO3}$ and $Z_{eu}$ (Table 6.3) indicates that on average the CM is in light- and nutrient-rich waters (mean depths: $Z_{CM}$ 62.1m, MLD 36.8m, $Z_{eu}$ 69.0m, $Z_{NO3}$ 73.3m). However, variability is likely to be important due to the proximity of temperate waters and the high coefficient of variation (COV; %) of parameters ($Z_{CM}$ 40%, MLD 26%, $Z_{eu}$ 37%, $Z_{NO3}$ 28%). The CM shape, therefore, varies between thin pronounced peaks during eutrophic spring conditions and wide flat peaks during late summer/autumn oligotrophic conditions (Fig. 6.2). The community size structure is mainly dominated by picoplankton with almost equal contributions from microplankton cells and lesser amounts of nanoplankton (Fig. 6.4). Pigments and microscopic counts (Fig. 6.5 - Fig. 6.8 and Tables 6.4 and 6.5) indicate the presence of prochlorophytes and eukaryotic algae, with the community most likely composed of eukaryotic flagellate groups as well as larger eukaryotes such as diatoms and non-Peridin dinoflagellates. Good correlations between microscopic carbon estimates and Fchl*a* indicate that the CM represents a biomass maximum (Table 6.6). Although prochlorophytes are present their biomass is low, with *Synechococcus* spp. and picoeukaryotes making large contributions to the picoplankton community (Zubkov *et al.,* 2000b). There may be seasonal changes in composition that would probably follow the seasonal successional patterns shown in temperate waters further north (e.g. Taylor *et al.,* 1993). *Phaeocystis globosa* blooms may also be important during some periods (AMT-10; pers. observation) and would give similar size-fractionated results due to the presence of single cells and colonies, and similar pigment signals to diatoms and dinoflagellates (Irigoien, *et al.,* submit.). Surface and deep communities retain a certain level of similarity (Fig. 6.9) indicating that the CM is formed from similar species to surface waters.

(2) *North Atlantic Subtropical Waters (NASW):* No significant difference between $Z_{CM}$ and $Z_{eu}$ indicate that the CM is at the base of the euphotic zone in conjunction with the $Z_{NO3}$ (Table 6.3). Variability is evident in the $Z_{CM}$, MLD and $Z_{NO3}$ with slightly less variability in the $Z_{eu}$ (COV: $Z_{CM}$ 27%, MLD 31%, $Z_{eu}$ 18%, $Z_{NO3}$ 25%). The CM shape is characteristic of subtropical waters with wide and flat peaks (Fig. 6.2). The community size structure is dominated by picoplankton with minor chl*a* contributions from nanoplankton and microplankton taxa (Fig. 6.4). Pigment and microscopic counts (Figs. 6.5 - 6.8 and Tables 6.4 and 6.6) indicate the dominance of prochlorophytes throughout the water column, with upper waters dominated by high-light adapted prochlorophytes and deeper waters composed of prymnesiophytes and pelagophytes (chrysophytes) and low-light adapted prochlorophytes (cf. Gibb *et al.,* 2001). Significant correlations between total biomass and Fchl*a* (Table 6.6) indicate that larger taxa are also an important component of the community and that the CM may be a biomass maximum on some occasions. Decreases in the percentage similarity of the species composition and dominance with depth (Fig. 6.9) indicate floral differences of nanoplankton species between upper and deeper waters. The nature of the AMT cruise track is such that the

section of the NASW sampled is likely to be influenced by seasonal inputs from surrounding waters (e.g. Azores Current; Kahru *et al.,* 1991) and may not reflect central gyre waters.

(3) *Upwelling Waters (UPW):* The CM is at the depth of the 10% PAR isolume (Fig. 6.3), although there is no significant difference between the $Z_{eu}$ and $Z_{CM}$, and no significant difference between $Z_{CM}$ and $Z_{NO3}$ (Table 6.3). Shifting of the CM from the $Z_{eu}$ in low nutrient waters to the 10% PAR isolume in NW African waters was also observed by Gieskes and Kraay (1986) on an inshore-offshore transect. Although the average $Z_{NO3}$ depth is deeper than the $Z_{CM}$ and $Z_{eu}$, there is much more variability in the $Z_{CM}$ and $Z_{NO3}$ than the $Z_{eu}$ (COV 55%, 39% and 1%, respectively). The CM shape is a thin pronounced peak with high chl*a* concentrations (Fig. 6.2). The community size structure indicates the dominance of picoplankton with lesser contributions of nanoplankton and microplankton taxa (Fig. 6.4). Pigment and microscopic counts (Figs. 6.5 - 6.8 and Tables 6.4 and 6.5) indicate that the community is composed similarly to that in the NATD, although peridinin containing dinoflagellates are found in the UPW. The picoplankton community is similar to that found in the NATD, with dominance by *Synechococcus* spp. and picoeukaryotes, and prochlorophytes restricted to upper waters (Zubkov *et al.,* 1998, 2000b; cf. Partensky *et al.,* 1996). A sharp decrease is seen in the similarity of species composition with depth and differences in dominant species are found with depth (Fig. 6.9). Complications arise in describing a typical UPW structure and community as the communities and structures sampled during AMT cruises represent upwelled water that is being advected away from the upwelling nuclei close to the coast (Maranon *et al.,* 2001). In such situations there is likely to be community succession from a truly upwelled one to one more characteristic of the low nutrient waters offshore as the nutrients are depleted (Longhurst and Pauly, 1988). Thus, communities within the UPW are composed of taxa characterising both environments with more eutrophic communities found inshore (cf. Gieskes and Kraay, 1986).

*(4) Equatorial Atlantic (EQU):* No significant differences are found between $Z_{CM}$, $Z_{eu}$ and $Z_{NO3}$ which indicates that the CM is located in nutrient- and light-rich waters (Table 6.3; Fig. 6.3). Low variability is seen in the $Z_{CM}$ and $Z_{eu}$, while variability in the $Z_{NO3}$ is comparable to that in the NASW and SASW (COV: $Z_{CM}$ 18%, MLD 35%, $Z_{eu}$ 10%, $Z_{NO3}$ 27%). The CM shape is intermediate between UPW and NASW / SASW with a thin pronounced peak found deeper than that in the UPW (Fig. 6.2). The community structure is similar to that of the NASW and SASW, with picoplankton dominant and much lower contributions from nanoplankton and microplankton (Fig. 6.4). Pigment and microscopic counts (Figs. 6.5 - 6.8 and Tables 6.4 and 6.5) indicate that the community is composed of a surface layer dominated by prochlorophytes and a deeper layer composed of eukaryotic taxa (prymnesiophytes, pelagophytes and non-peridinin dinoflagellates) with larger eukaryotic taxa such as dinoflagellates and diatoms relatively rare (cf. Gieskes and Kraay, 1986). There is no significant relationship between microscopic estimates of nanoplankton carbon and Flchl*a* (Table 6.6) which indicate that the CM is not a biomass maximum for these taxa; photoacclimation and small taxa not identified from microscope counts are important in the CM formation. The percentage similarity of surface and deeper samples (Fig. 6.9) indicates that the nano- and microphytoplankton communities are quite similar, although the overall similarity is much reduced and may be due to the dominance of *Trichodesmium* spp. in surface waters (Tyrrell *et al.,* submit).

*(5) South Atlantic Subtropical Waters (SASW):* No significant difference is found between $Z_{CM}$ and $Z_{eu}$, whereas the $Z_{NO3}$ is significantly deeper (Table 6.3). Comparison with the NASW shows

that within the SASW the mean $Z_{eu}$ and $Z_{NO3}$ are deeper, and there is slightly less variability (COV: $Z_{eu}$ 16%, $Z_{NO3}$ 19%). Variability in the MLD is surprisingly high (COV 41%; see Chapters 3 and 5) for an environment thought to be relatively stable, although significant differences are found between $Z_{CM}$ and MLD. The CM shape is characteristic of subtropical waters with a wide and flat peak (Fig. 6.2) with the lowest $C_{CM}$ in the Atlantic Ocean (mean 0.37 ± 0.09 mg Chl $m^{-3}$). The community size structure is similar to the NASW and EQU with dominance by picoplankton and small contributions from nanoplankton and microplankton (Fig. 6.4). Pigments and microscopic counts (Fig. 6.5 - 6.8 and Tables 6.4 and 6.5) indicate that diatoms (indicated by Fuco) and peridinin-containing dinoflagellates are rare, and the community is dominated by prochlorophytes with upper waters dominated by high-light adapted prochlorophytes and at depth by low-light adapted prochlorophytes and small eukaryotes (prymnesiophytes, pelagophytes and non-peridinin containing dinoflagellates) (cf. Anderson *et al.,* 1996; Partensky *et al.,* 1996; Zubkov *et al.,* 2000b). The biomass of nanophytoplankton groups is low throughout the water-column (Fig. 6.8) and non-significant relationships between microscopic estimates of nanoplankton carbon and Flchl*a* (Table 6.6) indicate that the CM is not a nano- and microplankton biomass maxima. Thus, the CM in the SASW represents an adjustment of the cellular carbon to chl*a* ratio (Maranon *et al.,* 2000). Decreases in the percentage similarity of species composition and dominance (Fig. 6.9) indicate floral differences between surface and deep waters (cf. Chapter 4).

*(6) South American Shelf Waters (SATW):* No significant differences are found between the MLD, $Z_{CM}$ and $Z_{eu}$ (Table 6.3), however there is relatively high variability in the $Z_{CM}$, MLD and $Z_{NO3}$ (COV: $Z_{CM}$ 64%, MLD 52%, $Z_{eu}$ 14%, $Z_{NO3}$ 48%). The CM shape is a thin, pronounced peak although there is variability with increasing latitude (Fig. 6.2). The community size structure indicates dominance by picoplankton and nanoplankton groups with lesser contributions from microplankton (Fig. 6.4). Pigments and microscopic counts (Figs. 6.5 - 6.8 and Tables 6.4 and 6.5) indicate the presence of prochlorophytes, as well as both small and large eukaryotic taxa (prymnesiophytes, pelagophytes, diatoms and dinoflagellates) throughout the water-column. Significant correlations are found between Flchl*a* and microscopic estimates of total carbon (Table 6.6), which indicates the importance of large phytoplankton groups and that the CM may represent a biomass maximum. Decreases in the percentage similarity of surface and deep species composition and dominance (Fig. 6.9) indicate floral differences with depth, although there is high similarity between surface and CM samples (~75%).

## 6.6. Summary and Conclusions

1. Regional differences in the relationship between the hydrographic environment and the Chlorophyll *a* Maximum (CM) exist and may be summarised by consideration of 3 general areas (Fig. 6.3, Table 6.3); (i) South Atlantic Subtropical Gyre: Generally, deep (108.8 ± 23.2 m) CM below the upper mixed layer (82.3 ± 33.7 m), around the base of the euphotic zone (96.5 ± 15.8 m) in relatively low light conditions (0.1 - 2% PAR), and ~40 - 50 m above the nutriclines (148.6 ± 28.4 m), (ii) Equatorial waters: Typically, the CM (70.8 ± 12.6 m) is at the same depth as the base of the euphotic zone (67.9 ± 7.0 m) and nutriclines (82.1 ± 22.4 m), in relatively low light conditions (0.5 - 5% PAR), and slightly below the upper mixed layer (58.3 ± 20.4 m), (iii) NW

Africa: Generally, the CM is above (39.2 ± 21.5 m) the base of the euphotic zone (45.7 ± 7.5 m) in variable light conditions (2 - 80% PAR), above the nutriclines (55.3 ± 21.7 m), and within or just below the upper mixed layer (26.2 ± 10.3 m). However, there is considerable variability in these regional structures as shown by the relatively high standard deviations of the hydrographic parameters and depth of the CM.

2. There are corresponding regional differences in the phytoplankton community composition, which may be summarised into three characteristic vertical chlorophyll *a* profiles; (i) Subtropical gyres: Prochlorophytes, cyanophytes, prymnesiophytes and pelagophytes are the dominant groups in the phytoplankton community, (ii) Equatorial waters: The phytoplankton community composition is similar to that found in the oligotrophic subtropical gyres, (iii) NW Africa: The phytoplankton community is dominated by large cells (e.g. diatoms) inshore and an increasingly oligotrophic community offshore (flagellates and prokaryotes); with a reduction of prochlorophyte numbers where new nutrient supplies are high (inshore) and increases of *Synechococcus* spp., diatoms, autotrophic dinoflagellates, prymnesiophytes, pelagophytes (chrysophytes) cryptophytes, chlorophytes and prasinophytes.

3. The shape of the Chlorophyll *a* Maximum may be described as an even-sided gaussian curve throughout the subtropical and tropical Atlantic Ocean. Therefore, algorithms for measuring water-column pigment content from remote sensing can be fitted successfully. However, although the basinscale (40°N - 40°S) relationship between surface chlorophyll *a* to total water-column (0 - 200 m) chlorophyll *a* concentration is significant ($r = 0.58$ $p<0.05$), it does not remain so in the different regions of the tropical and subtropical Atlantic Ocean; the relationship is only signficant ($p<0.05$) within North Atlantic Subtropical Waters ($r = 0.82$, $n = 30$) and South Atlantic Temperate Waters ($r = 0.72$, $n = 21$) and insignificant in the North Atlantic Drift (NAtD), Upwelling Waters (UPW) off NW Africa, Equatorial waters (EQU), and South Atlantic Subtropical Waters (SASW).

4. The community structure of the Chlorophyll *a* Maximum (CM) and interaction with the hydrographic environment are likely to cause regional differences in the mechanisms important in forming and maintaining the CM; (i) Subtropical gyres: light-limitation of the phytoplankton community causes cellular increases in pigmentation and the CM is formed through photoacclimation rather than growth, the characteristic small cell sizes of the algal community (<5 μm) lead to higher grazing than sinking losses, (ii) Equatorial waters: increased new nutrient supplies cause growth of the phytoplankton communities so that the CM is formed partly through photoacclimation to low-light levels and from *in-situ* growth and production, the community remains controlled by high nano- and micro-heterotrophic grazing losses; (iii) NW Africa: high new nutrient fluxes and concentrations in upper light-rich waters cause high growth rates and primary production in surface and sub-surface waters, although there is a decreasing new nutrient gradient spatially (inshore-offshore) and temporally (onset of upwelling and relaxation) which causes variability in the factors important for formation and maintenance of the CM.

# CHAPTER 7. SYNTHESIS AND GENERAL DISCUSSION

## 7.1. Introduction; Thesis Summary

The taxonomic and size structure of the phytoplankton community has a direct effect on the ecosystem dynamics and biogeochemistry of the open-ocean. On the basinscale, the AMT transect extends across several different hydrographic environments (Chapter 3) and phytoplankton communities (Chapters 4 and 6) and the results presented in this study show distinct spatial patterns in the community composition; latitudinal differences between nutrient and light-rich waters off NW Africa and in tropical equatorial waters and the nutrient-poor and light-rich waters of the northern and southern subtropical gyres, as well as vertical differences in the subtropical gyres between upper (0 - 60 m) nutrient-poor, light-rich and deep (60 - 200 m) nutrient-rich and light-poor environments. At the basinscale, the Chlorophyll a Maximum (CM) shows characteristic changes in its depth and community structure which are indicative of both vertical and latitudinal changes in the hydrographic environment (Chapter 6). In this chapter the observations and results from each of the previous chapters are brought together into a general synthesis of phytoplankton community structure in the tropical and subtropical Atlantic Ocean. Three main topics investigated and discussed in this chapter are; (1) the limitations of the techniques employed and the relative success of characterising the phytoplankton community structure and its spatial and temporal variability, (2) patterns of spatial variability relevant to the study of regional (biogeochemical) differences in phytoplankton communities, and (3) temporal variability relevant to gaining an understanding of the dynamics of phytoplankton communities in subtropical waters. Throughout this chapter a critical evaluation of the results and data presented in this thesis is carried out through comparison with relevant material in the literature.

## 7.2. Characterisation of the Phytoplankton Community

### 7.2.1. Light-microscope Measurements

A limitation of the light-microscope techniques used in this study is the lack of a suitable quantitative or qualitative description of the dominant picoplankton component of the phytoplankton community in the subtropical and tropical Atlantic Ocean. Similarly, many of the small (5 - 10 μm) cells observed under the light-microscope cannot be distinguished into clearly defined taxonomic or nutritional categories and represent a poorly understood component of the planktonic community. They could only be included in the analysis of phytoplankton communities by using morphotype and general phytoplankton group names; e.g. small (10 - 30 μm) pennate diatoms. Due to these limitations, some characteristic species have been lost in the analysis; e.g. the small (~5 μm) coccolithophore species *Florisphaera profunda* and *Gladiolithus flabellatus* are known to be important members of the deep shade flora in subtropical and tropical waters, and the abundance of *F. profunda* is known to closely follow depth changes in the nutricline depth (Kinkel *et al.*, 2000). Thus, knowledge of the distribution and abundance of *F. profunda* would greatly add information to spatial and temporal variations in the phytoplankton community structure.

Another limitation of the light-microscope techniques employed in this study is the tendency for the underestimation of meso-phytoplankton (>200 μm) species (e.g. *Ethmodiscus rex*), which occur at relatively low cell densities but due to their size could represent important components of the autotrophic biomass and are often associated with nitrogen-fixing cyanobacteria (Venrick, 1974) and large internal nitrate pools (Villareal *et al.,* 1993, 1996, 1999a, b; Moore and Villareal, 1996). Subsampling of only 100 ml is unlikely to sample quantitatively this component of the community, and suitable alternative techniques would include net-sampling and examination of large water-volumes (1000 - 20000 ml). A comparative study of different sampling techniques (Niskin bottles and 100 ml sub-samples, net-hauls, large-water volume filtering) to measure *Trichodesmium* spp. abundance and distribution in the Atlantic Ocean found that although the Niskin bottle samples indicated the presence of *Trichodesmium* spp., other techniques gave comparative estimates of cell numbers (Tyrrell *et al.,* submit.). Similarly, some of the large (100 - 200 μm) phytoplankton species characteristic of the deep shade flora in subtropical waters (*Gossleriella tropica, Rhizosolenia castracanei, Ceratium gravidum, C. platycorne*; Sournia, 1982), and found from net samples, are missing or extremely rare in the AMT species database. Recent observations of large diatom mats in subtropical waters that are important conveyers of nitrate into the upper euphotic zone (Villareal *et al.,* 1993, 1996, 1999a, b) also highlight the need to better characterise the mesophytoplankton components of the community. Thus, a more comprehensive study of the full composition and dynamics of the subtropical phytoplankton community requires a wider suite of sampling techniques and measurements; suitable additions to the light-microscope techniques used in this study would be flow-cytometic counts, epifluorescence microscopy for picoplankton and electron microscope techniques (Scanning Electron Microscopy and Transmission Electron Microscopy) for coccolithophores, net and large-volume samples for large (>100 μm) taxa.

Despite these limitations, the light-microscope measurements of the phytoplankton community from the AMT programme, in combination with rigorous statistical treatments, reveal several patterns of spatial (Chapter 4) and temporal (Chapter 5) variability in the tropical and subtropical Atlantic Ocean. These fluctuations in large (>5 μm) phytoplankton species composition of the community are generally consistent with spatial and temporal changes in the community pigments (Chapters 4 and 5) and hydrographic parameters (Chapter 6). Thus, large phytoplankton species changes in the community are indicative of changes in the whole community composition and the light-microscope identifiable components of the community can be used as markers of community variability; e.g. the upper and deep floras of large phytoplankton identified in the South Atlantic Subtropical Waters (Chapter 4) agree with previous studies of low-light and high-light adapted prochlorophytes (Goericke and Repeta, 1993; Letelier *et al.,* 1996; McManus and Dawson, 1994; Scanlan *et al.,* 1996; Zubkov *et al.,* 1998; West and Scanlan, 1999), and the interannual variations in pigment ratios in the SASW are accompanied by change in the large phytoplankton species composition (Chapter 5).

### 7.2.2. Pigment Measurements

The combination of phytoplankton pigments and identification of large phytoplankton species by light-microscope techniques leads to a degree of characterisation of the taxonomic components of the phytoplankton community (Chapters 4, 5 and 6) that would not be possible without both techniques.

However, there are gaps and uncertainties with both sets of data. For the pigments, the taxonomic source of some pigments can be ambiguous (e.g. is the deep Chl *b* in subtropical waters solely related to just prochlorophytes, or do chlorophytes and prasinophytes lacking typical accessory pigments contribute?), to the absence of important pigments (phycobilins). Although phycobilins are present in only one oceanic phytoplankton taxa (cyanophytes), the other pigments associated with this group (zeaxanthin, chlorophyll *a*) are found in many other phytoplankton groups, so that the cyanophyte distribution cannot be fully described in the tropical and subtropical Atlantic Ocean. It should also be noted that low-light adapted prochlorophytes also contain low levels of an unknown phycoerythrin derivative, which is absent from high-light adapted prochlorophytes (Penno et al., 2000).

Thus, suitable extensions to the pigment techniques used in this study would be the detection of phycobilins, both forms of chlorophyll *b*, and the separation of zeaxanthin and lutein. Furthermore, size-fractionated pigment measurements would be valuable for defining the size-class and probable source of the pigment signatures (e.g. what proportion of the Hex-fuco pigment signature comes from >10 μm prymnesiophytes, such as some coccolithophores, or from smaller naked cells?). As well as adaptations to the pigment (HPLC) techniques, ecological work is required to quantify the pigment composition of the abundant small dinoflagellates (peridinin or But-fuco) present in subtropical waters (Anderson et al., 1996; cf. Chapter 4) and the nutritional strategy of certain large (>5 μm) phytoplankton species which are present in subtropical waters but in the absence of any typical pigment signature (e.g. small pennate diatoms, *Umbellosphaera irregularis*, dinoflagellate species).

### 7.2.3. Chlorophyll *a* measurements: Problems and Comparison with other Studies

*Problems with Fluorometric Chlorophyll a Measurements*

There are two major problems with chlorophyll a (chl*a*) measurements for studying the dynamics of phytoplankton communities; (a) variability of the autotrophic biomass to chl*a* relationship, and (b) a methodological problem with the interference of the chl*a* signal by chlorophyll *b*.

Within subtropical and tropical waters of the Atlantic Ocean, chl*a* concentrations are not always directly related to variations in autotrophic biomass (Chapters 4, 5 and 6; Cullen, 1982; Maranon et al., 2000). As a general rule, where chl*a* (>0.5 mg $m^{-3}$) and inorganic nutrient concentrations are high (DIN >1 - 10 μM), autotrophic biomass is also likely to be high (e.g. NW Africa). Areas which are characterised by a deep (>100 m) Chlorophyll *a* Maximum (e.g. subtropical gyres) show considerable vertical variations in chl*a* concentration (0.1 - 0.2 mg Chl $m^{-3}$ in upper waters and >0.3 - 0.5 mg Chl $m^{-3}$ in deep waters) without any significant difference in biomass between the two layers (~5 - 10 mg C $m^{-3}$ in each; Chapter 5). In these conditions, the Chlorophyll *a*

Maximum is not a biomass maximum and chl*a* is synthesised as a requirement for efficient light-harvesting in light-poor waters (photoacclimation) as a subsidy for living at depth in association with the deep new nutrient pool. However, this deep community is light-limited, and thus a restriction is set on the chl*a* concentration by the biomass (growth rate) and the detrimental cellular effects of high internal pigment concentrations; i.e. intra-cellular self-shading of the chloroplasts (the 'package effect'; Falkowski and Raven, 1997).

The second major problem with chla measurements is a methodological problem, which is likely to be inherent in measurements made during other studies in subtropical and tropical waters using fluorometry to measure chl*a* concentrations; the interference of the chl*a* signal by chlorophyll *b* (Chl *b*). The degree of interference in the chla measurements depends on the ratio of Chl *b*:Chl *a* (Welschmeyer, 1994). Using the Holm-Hansen *et al.*, (1965) technique (acidification) when the Chl *b*:Chl *a* ratio is close to unity (~1.0), leads to an underestimation of chl*a* concentration by ~ 25 - 60% (Welschmeyer, 1994; Turner Designs website; http://www.turnerdesigns.com/). However, Welschmeyer (1994) proposed a set of light-filters to be used within the fluorometer which decreased the interference and didn't require the acidification step required by the method of Holm-Hansen (1965); using the Welschmeyer (1994) filters when the Chl *b*:Chl *a* ratio was close to unity should cause only a 10% overestimation (Welschmeyer, 1994). Thus, knowledge of the Chl *b*:Chl *a* ratio is required to fully calibrate and interpret the chl*a* measurements and there are severe theoretical problems with comparing chl*a* concentrations determined from the Holm-Hansen (1965) and Welschmeyer (1994) methods.

The results presented in this study have shown that Chl *b* concentrations are highly variable between different regions and depths in the tropical and subtropical Atlantic Ocean (Chapters 4 and 6), and may vary considerably in one region between years (Chapter 5). During the AMT programme there was a change in techniques for the acetone extracted measurements of chl*a*; during AMT-1 and 2 the Holm-Hansen et al., (1965) acidification technique was used, whereas after AMT-3 the Welschmeyer (1994) method was used (Chapter 2). A post-cruise comparison after AMT-3 of measurements taken using both techniques showed good agreement between the two ($r = 0.93$ $p<0.001$, $n = 20$; Bale and Mantoura, 1996), however this cruise coincided with a significant shallowing of the deep water high Chl *b*:Chl *a* ratio in the South Atlantic Ocean (Chapter 5) that may have led to a misleading result; the relatively low Chl *b*:Chl *a* ratios at depth would have led to agreement between the two methods. A statistical comparison of the integrated chl*a* measurement from acetone extraction shows that total water-column (0 - 200 m; $C_{TOT}$) chl*a* was significantly higher during AMT-1 and 2 then during AMT-3 (Chapter 5), which may reflect a change in the interference of the Chl *b* and the distribution of high Chl *b*:Chl *a* ratios rather than high chl*a* levels on these two cruise.

*A Comparison of Chlorophyll a Measurements from Subtropical Waters*

The Chl *b*:Chl *a* ratios found in the SASW during the AMT programme (1995 - 2000) are similar to those reported from other subtropical open-ocean regions, as summarised in Table 7.1 (cf. Chapter 5). These results suggest that the deep high Chl *b*:Chl *a* ratio pool found in the SASW is also present in the NPSG, and in the western and eastern portions of the NASG. Inter-ocean differences in the values for total water-column (0 - 200 m) integrated chl*a* based on fluorescence

measurements (F; Table 7.1) may be due to interference from the deep Chl *b* pool causing over- and underestimation of the chl*a* concentration depending upon the methods used. Comparison of the integrated chl*a* from HPLC determination of pigment concentrations lead to very similar measurements from the different subtropical regions; AMT (Central SASW) 15.7 ± 2.9 mg Chl $m^{-2}$, western NASG (BATS) ~20.3 mg Chl $m^{-2}$, and NPSG (HOTS) 24.5 ± 6.2 mg Chl $m^{-2}$ (Table 7.1). Inconsistent differences between the HPLC and fluorescence determined chl*a* measurements reflect the differences in the techniques; fluorescence measurements are prone to interference from other pigments, whereas these problems are avoided with HPLC measurements of chl*a* concentrations.

Table 7.1: A synthesis of total water-column (0 - 200 m) integrated chlorophyll *a* (mg Chl $m^{-2}$) and Chl *b*: Chl *a* ratio (w:w) measurements (average, standard deviations and ranges) from different studies in subtropical waters. The methods used include fluorescence methods (F) following various modifications of the Holm-Hansen (1965) acidification technique, using Welschmeyer (1994) light-filters, measurements from a spectrofluorometer (SPECTRO) or using High Performance Liquid Chromatography (HPLC).

| Parameter (Units) | Value ± SD or Range | (Method) | Location (Dates) | Source |
|---|---|---|---|---|
| | **$C_{TOT}$ (mg Chl $m^{-2}$)** | | | |
| 0 - 200 m | 34.4 ± 7.5 | (FL) | SASW (1995 - 2000) | AMT - This Study |
| | 30.6 ± 6.7 | (FL) | Central SASW (1995 - 2000) | AMT-8 - This Study |
| | 19.2 ± 5.3 | (HPLC) | SASW (1999) | AMT - This Study |
| | 15.7 ± 2.9 | (HPLC) | Central SASW (1999) | AMT-8 - This Study |
| 0 - 200 m | 14.7 - 12.1 | (FL) | Western NASG (1986) | BATS - Glover *et al.*, 1988 |
| | 55.0 ± 26.1[2] | (HPLC) | Western NASG (1985) | BATS - Bidigare *et al.*, 1990 |
| | 20.3 | (HPLC) | Western NASG (1992) | BATS - Anderson *et al.*, 1992 |
| 0 - 200 m | 12.5 ± 2.8 | (FL) | NPSG (Pre-1976) | CLIMAX |
| | 22.6 ± 4.8 | (FL) | NPSG (Post-1985) | ALOHA Karl, 1999 |
| | 24.5 ± 6.2 | (HPLC) | NPSG (1989 - 1991) | Letelier *et al.*, 1993 |
| | 29.2 | (HPLC) | NPSG (1992) | Anderson *et al.*, 1992 |
| 0 - 200 m | 16.4 ± 1.8 | (SPECTRO) | Eastern NASG (1991 - 1992) | Partensky et al., 1996 |
| | **Chl *b*:Chl *a*** | | | |
| 0 - 60 m | 0.14 ± 0.23 | (HPLC) | SASW (1995 - 2000) | AMT - This Study |
| | 0.06 ± 0.06[1] | | | |
| 60 - 200 m | 0.30 ± 0.10 | | | |
| 5 m | 0.08 | (HPLC) | NPSG (1994 - 1997) | HOTS - Karl *et al.*, 2001a |
| 100 - 125 m | 0.47 | | | |
| 20 m | 0.08 | (HPLC) | NPSG (1992) | HOTS - Anderson *et al.*, 1996 |
| 120 m | 0.43 | | NPSG (1992) | |
| 0 - 200 m | 0.08 - 0.22 | (HPLC) | Western NASG (1985) | BATS - Bidigare *et al.*, 1990 |
| 20 m | 0.03 | (HPLC) | Western NASG (1992) | BATS - Anderson *et al.*, 1996 |
| 120 m | 0.91 | (HPLC) | Western NASG (1992) | BATS - Anderson *et al.*, 1996 |
| 0 - 200 m | 0.08 - 0.30 | (SPECTRO) | Eastern NASG (1991-1992) | Partensky *et al.*, 1996 |

Note: [1] average AMT upper water (0 - 60 m) Chl *b*:Chl *a* ratios are shown for the AMT-average (all cruises) and the AMT-average without measurements from AMT-3, and [2] integrated (0 - 200 m) chl*a* measurements from Bidigare *et al.*, (1990) include pre-bloom (38.6 mg $m^{-2}$), bloom (85.0 mg $m^{-2}$) and post-bloom (41.3 mg $m^{-2}$) stations.

## 7.3. Basinscale Spatial Variability of Phytoplankton Community Composition

### 7.3.1. Patterns of Spatial Variability: A synthesis

Latitudinal differences in the hydrographic characteristics in the subtropical and tropical Atlantic Ocean range from low (new) nutrient subtropical gyres to waters with enhanced new nutrient inputs around the equator and off NW Africa (Chapter 3). These hydrographic differences give rise to consistent patterns in pigment and chl*a* distributions (Chapters 4 and 6); from the low chla (<0.2 mg Chl $m^{-3}$) and pigment concentrations in the subtropical gyres to the high chla (>0.4 mg Chl $m^{-3}$) and pigment concentrations off NW Africa. The characteristic changes in the phytoplankton community size-structure and pigment signatures along this increasing chl*a* (0.05 - 1.5 mg Chl $m^{-3}$) gradient from

the subtropical gyre to waters off NW Africa are discussed in this section in relation to the 'succession' of the phytoplankton community structure. Both the synthesis of size-fractionated and pigment measurements include values <0.05 mg Chl $m^{-3}$ which generally originate from deep (>150 m) waters below shallow (<50 m) Chlorophyll *a* Maximum (i.e. waters off NW Africa), and represent measurements close to the detection limits of the methods and techniques used.

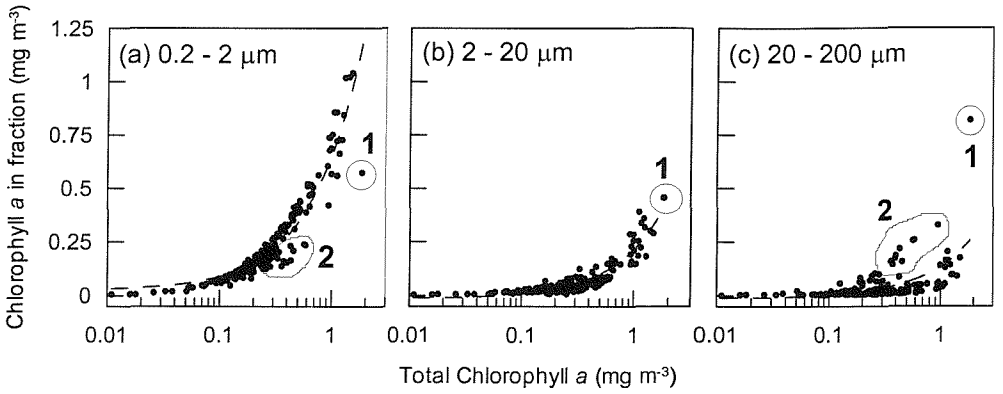


Figure 7.1: Size-fractionated chlorophyll *a*; Chlorophyll *a* concentration (mg $m^{-3}$) in three size fractions against log Tchl*a* (Data from AMT-8 and 10); (a) 0.2 - 2.0 μm, (b) 2.0 - 20.0 μm, and (c) >20.0 μm. Points that do not fit to the main distribution of data have been circled and identified as two clusters; cluster 1 and cluster 2. Cluster 1 was found in the CM off NW Africa (10°N, AMT10), while cluster 2 originates both from NW Africa (10°N, AMT10, 45 m) and at the northern end of the transect (35°N, 36°N, 38°N, AMT10, 20 - 60m). See text for dominant species in these clusters.

*Size fractionated chlorophyll a*

The relationships between size-fractionated chl*a* (0.2 - 2 μm, 2 - 20 μm and >20 μm) and total chl*a* (Tchl*a*) are presented in Figure 7.1, which gives a broad cell size related description of the community composition and succession along the increasing chl*a* (Tchl*a*) gradient from the subtropical gyres to the waters off NW Africa. Although there is a significant positive relationship between Tchl*a* and the different size-class chl*a* concentrations (0.2 μm, r = 0.94; 2.0 μm, r = 0.93; 20 μm, r = 0.60; n = 183), the slopes of the model II regression lines differ markedly; from relatively close to 1 for the picoplankton (0.67), to significantly less than one for nanoplankton (0.24) and microplankton (0.24). Thus, increases in the Tchla are most closely followed by increases in the contribution of the picoplankton community (Fig. 7.1). Chisholm (1992) proposed that there are ecosystem limits to the contributions of different community components to the total standing stock and that high chlorophyll *a* concentrations are only possible when large (>5 μm) cells form a significant proportion of the autotrophic community. The AMT results (Fig. 7.1) indicate that in the subtropical and tropical Atlantic Ocean with chlorophyll *a* ranges from 0.05 - 1.5 mg Chl $m^{-3}$, picoplankton and to a lesser extent nanoplankton are the dominant contributors to standing stock and large (>5 μm) phytoplankton cells generally are a less important contributor to the standing stock. However, two groups of outliers can be identified from Figure 7.2; one data point from the CM (30 m) off NW Africa (10°N, AMT-10) with low picoplankton and high microplankton contributions to Tchla, and a group of points from the northern end of the transect (35 - 38°N, AMT-10) which have slightly lower picoplankton and slightly higher microplankton contributions than the majority of other samples. It is interesting to note that in neither cases do the nanoplankton have contributions which deviate from the regression line (Fig. 7.1); changes in the size-structure in these two locations relative to the regression line show no changes in the nanoplankton contribution to Tchla. The CM off NW Africa

during AMT-10 is associated with large cell abundances (188 x $10^3$ cells $l^{-1}$) of *Pseudo-nitzschia* spp. and medium sized naked dinoflagellates (216 x $10^3$ cells $l^{-1}$), whereas the group 2 data points are associated with increases in diatoms (mainly *Pseudo-nitzschia* spp.; 13 - 40 x $10^3$ cells $l^{-1}$), autotrophic dinoflagellates (mainly 10 - 20 μm and 20 - 40 μm naked forms; 12 - 20 x $10^3$ cells $l^{-1}$) and coccolithophores (mainly *Emiliania huxleyi*; 5 - 92 x $10^3$ cells $l^{-1}$).

*Biomarker Pigments*

The relationship between the average concentration of individual pigment (biomarker) signatures within 13 Total chlorophyll *a* (TChl *a* = Dv Chl *a* + Chl *a*) concentration classes, and the percentage presence of those pigments in each TChl *a* class is presented in Figure 7.2. The number of samples in each size class decreases with increasing TChl *a* concentration; <0.1 (130), 0.1 - 0.2 (103), 0.2 - 0.3 (63), 0.3 - 0.4 (29), 0.4 - 0.5 (15), 0.5 - 0.6 (12), 0.6 - 0.7 (8), 0.7 - 0.8 (6), 0.8 - 0.9 (2), 0.9 - 1.0 (1), 1.0 - 1.1 (5), 1.1 - 1.2 (1) and 1.2 - 1.3 (2). The importance of each phytoplankton group is indicated by both its average biomarker pigment concentration in relation to TChl a and its percentage presence.

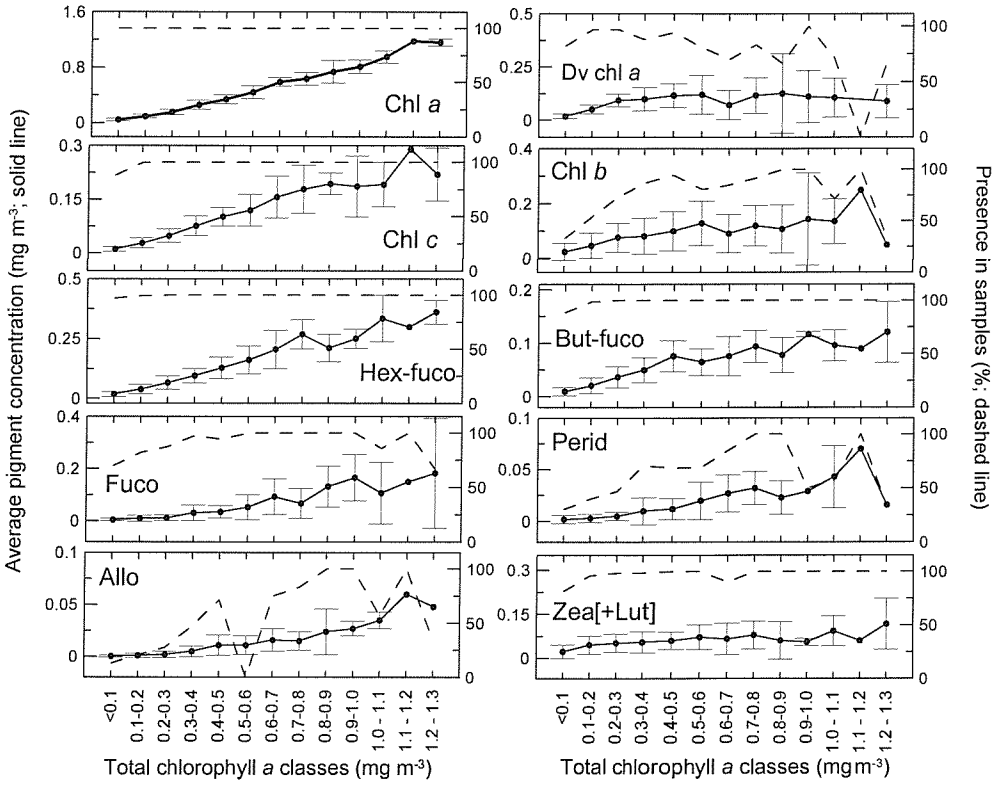


Figure 7.2: Biomarker Pigments; Average (± Standard Deviation) biomarker pigment concentrations (mg Chl $m^{-3}$; left) and percentage (%; right) presence in Total Chlorophyll a (<0.1 - 1.3 mg Chl $m^{-3}$) frequency classes (Data from AMT-7 and 8).

The importance of prochlorophytes and *Synechococcus* spp. as components of the picoplankton is shown by the widespread presence of divinyl-chlorophyll *a* (Dv Chl *a*) and zeaxanthin (Zea plus lutein) in a high proportion of the samples up the increasing TChl a gradient (Fig. 7.2). However, neither Dv Chl *a* or Zea concentrations increase above levels of ~0.3 mg $m^{-3}$ for Dv Chl *a* and ~0.08 mg $m^{-3}$ for Zea as the TChl *a* increases (Fig. 7.2). This is likely to indicate the limitation of prochlorophytes to low nutrient environments, with TChl *a* concentrations >0.3 mg Chl $m^{-3}$ associated

with areas of elevated new nutrients (see Chapters 3 and 4), and the dominance of the picoplankton community by *Synechococcus* spp. in higher new nutrient environments which would be associated with an increase in phycobilin pigments (which have not been measured). The distribution of Chl *b* (Fig. 7.2) is thought to be mainly related to prochlorophytes associated with the CM (TChl *a* 0.2 - 1.0 mg Chl $m^{-3}$). However, Dv Chl *a* concentrations do not show a linear increase with TChl *a*, and there is a decrease in percentage presence of Dv Chl *a* in samples with high TChl *a* (Fig. 7.2). Therefore, at high TChl *a* concentrations, prochlorophyte contributions to TChl *b* may decrease and other Chl *b* containing taxa are likely to become important (prasinophytes and chlorophytes).

Chlorophyll *a* (Chl *a*), chlorophyll *c* (Chl *c*), 19'-hexanoyloxyfucoxanthin (Hex-fuco), and 19'-butanoyloxyfucoxanthin (But-fuco) are present in 75 - 100% of samples collected from the subtropical and tropical Atlantic Ocean, and show almost linear relationships with TChl *a* (Fig 7.2). These relationships indicate the widespread occurrence and importance of prymnesiophytes, pelagophytes (chrysophytes), and possibly naked dinoflagellates that contain But-fuco as opposed to peridinin. Concentrations of fucoxanthin (Fuco) also increase almost linearly with increasing TChl *a*, although it is present in a fewer number of samples relative to Chl *a*, Chl *c*, Hex-fuco and But-fuco (Fig. 7.2). This pattern may be indicative of either the patchy distribution of diatoms in the tropical and subtropical Atlantic Ocean, or that the Fuco is partly associated with prymnesiophytes, pelagophytes (chrysophytes) and naked dinoflagellates. Pigment markers for the larger phytoplankton groups (peridinin - dinoflagellates and alloxanthin - cryptomonads) are relatively rare in low chl*a* situations, and only increase when the TChl *a* is >0.2 - 0.3 mg Chl $m^{-3}$ (Fig. 7.2). This indicates that peridinin-containing dinoflagellates and cryptomonads are rare in waters with low chl*a* (<0.2 mg Chl $m^{-3}$) concentrations, and only where the new nutrient supply is enhanced do they become an important part of the phytoplankton community composition.

### 7.3.2. Spatial Variability: Functional Phytoplankton Groups and Community Structure

*Latitudinal and Vertical Variability: Functional Groups and Species*

Biogeochemically-relevant components of phytoplankton communities include; diatoms and coccolithophores as important mediators of export production, and nitrogen-fixing taxa that are important in the global nitrogen cycle. Phytoplankton groups important in biogeochemical processes are often termed 'functional groups' and include the diatoms, flagellates, coccolithophores and nitrogen-fixers (Riebesell and Wolf-Gladrow, 2002). Figure 7.4 shows the latitudinal distribution (biogeography) of several representative species from the major functional groups of phytoplankton; diatoms, autotrophic dinoflagellates, coccolithophores and nitrogen-fixers (e.g. the cyanophyte *Trichodesmium* spp and diatom - cyanobacteria association of *Hemiaulus* spp. - *Richellia intracellularis*; Venrick, 1974; Carpenter, 1983a, b; Tomas, 1997). The distribution of an individual phytoplankton species (species biogeography) is related to the ability of that species to grow and survive in any given environment (Semina, 1997).

The distribution of individual species from each functional group shows that there are significant species differences in distribution, which questions the validity of the functional group approach with phytoplankton. For example, the distribution of three closely related (taxonomically) diatom species (*Leptocylindrus* spp.) show two distinct patters; one species (*L. mediterraneus*) is

widespread throughout the tropical and subtropical Atlantic Ocean, whereas the other two species (*L. danicus*, *L. minimus*) are restricted to semi-temperate waters at the subtropical convergences (~35 - 40°N/S) and the upwelling off NW Africa (Fig. 7.3a). The distribution of three species from the (autotrophic) dinoflagellate genus *Ceratium* shows similar patterns (Fig. 7.3b; *C. teres* present throughout, *C. furca* restricted to 'eutrophic' waters and *C. lineatum* more abundant in 'eutrophic' waters), as do two species associated with nitrogen-fixation (Fig. 7.3d; the cyanophyte genus *Trichodesmium* spp. is restricted to NW Africa, northern subtropical gyre and southern subtropical convergence, while the diatom genus *Hemiaulus* is found throughout). Coccolithophore species (*Umbellosphaera irregularis*, *U. tenuis* and *Ophiaster hydroideus*) are found throughout the subtropical and tropical Atlantic Ocean, with little evidence of any abundance maxima for species specialising in upper (*U. irregularis* and *U. tenuis*) or deep (*O. hydroideus*) waters (Fig. 7.3c).

Consideration of the vertical distribution of functional groups of phytoplankton (Fig. 7.4) shows regional differences in depth distribution; within upwelling (5 - 20°N) and equatorial waters (5°N - 5°S), diatoms and autotrophic dinoflagellate species richness (number of species) decreases with depth (Fig. 7.4a), whereas in South Atlantic Subtropical Waters (SASW) both groups are as diverse at depth as they are in surface waters (Fig. 7.4b). In terms of the species composition, upwelling and equatorial communities have similar species in upper and deep waters, whereas there is evidence that in the SASW there are depth-specific assemblages present (Chapter 4). In the SASW, temporal studies have shown differences in the depth distribution of diatom and autotrophic dinoflagellate biomass; autotrophic dinoflagellates represent more of the total nano- and microphytoplankton biomass in surface waters and diatoms are more dominant in deep waters associated with the Chlorophyll *a* Maximum (Chapter 5).

The vertical distribution of species proposed to belong to the sun (*U. irregularis*, *U. tenuis* and *Trichodesmium* spp.) and shade flora (*O. hydroideus*) show characteristic depth distributions in both upwelling and equatorial waters and in the SASW (Fig. 7.4); within the EQU, UPW and SASW, *U. irregularis* and *U. tenuis* appear to have two abundance maxima in the upper water-column (7m and 50 m), the *Trichodesmium* spp. abundance maxima are close to the surface (7m), and the *O. hydroideus* maxima is ~100 m in the SASW and between 50 - 75 m in the EQU and UPW. Several 'outliers' can be identified in the depth distribution of the coccolithophore species in the SASW (Fig. 7.4b); relatively high abundances (>15 x $10^3$ cells $l^{-1}$) of *U. irregularis* and *U. tenuis* throughout the water-column during AMT-3 (10 - 14°S), and relatively high abundances (>4.5 x $10^3$ cells $l^{-1}$) of *O. hydroideus* in the upper (<60 m) water-column during AMT-3 (23 - 27°S). The timing of these 'anomalies' appears relevant to temporal variations of the phytoplankton community in the SASW (Chapter 5) that will be discussed further in section 7.4.

The survival of large (>5 μm) phytoplankton species in oligotrophic (inorganic nitrogen <0.1 μM) waters is likely to reflect the development of specialised nutritional and life-cycle strategies; e.g. the cells of *L. mediterraneus* are associated with the flagellate *Rhizomonas setigera* (Tomas, 1997) which provides motility to the diatom, thus reducing the nutrient-depleted boundary layer around the diatom cell, whereas *R. setigera* may utilise DOM released (leaked) from the diatom cell for its own nutrition. Other adaptations to living in low new nutrient environments include migrations into deep water below the euphotic zone to tap into the deep nutrient pools (Villareal *et al.*, 1993, 1996, 1999a,

b; Brokhuizen, 1999) and either nitrogen-fixing abilities or association with intracellular nitrogen fixing endosymbionts (e.g. Venrick, 1974; Carpenter, 1983b; Longhurst, 1998).

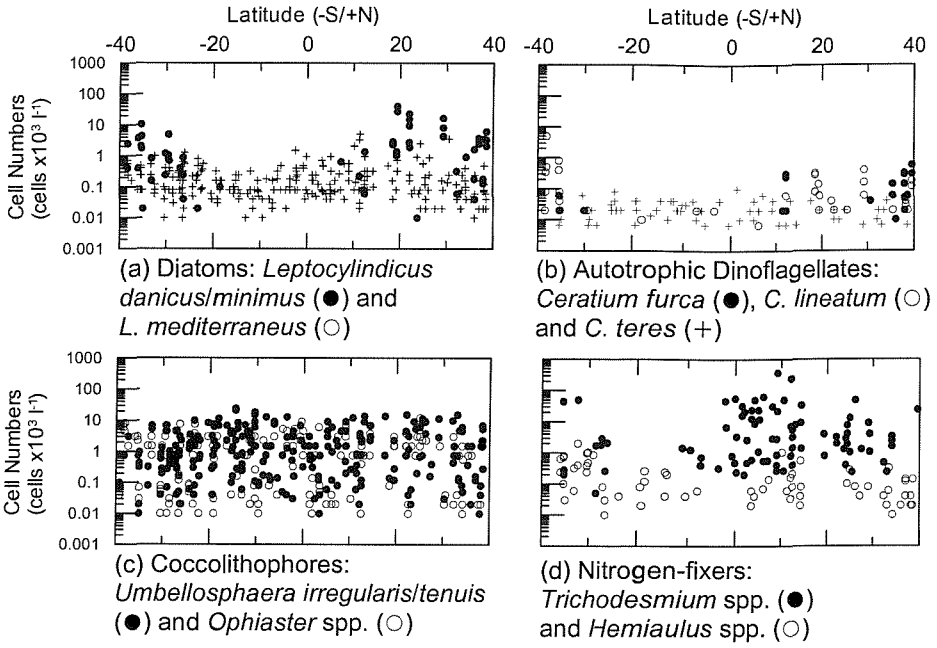


Figure 7.3: Latitudinal distribution of the cell abundances (cells x$10^3$ $l^{-1}$) of individual species from the four major phytoplankton functional groups; (a) Diatoms: *Leptocylindrus danicus* & *L. minimus* and *L. mediterraneus*, (b) Autotrophic Dinoflagellates: *Ceratium furca*, *C. fusus* and *C. teres*, (c) Coccolithophores: *Umbellosphaera irregularis* & *U. tenuis* and Ophiaster spp. (O. hydroideus), (d) Nitrogen-fixers: *Trichodesmium* spp. and *Hemiaulus* spp. (Data from AMT1 - 5, 7, 8 and 10.)

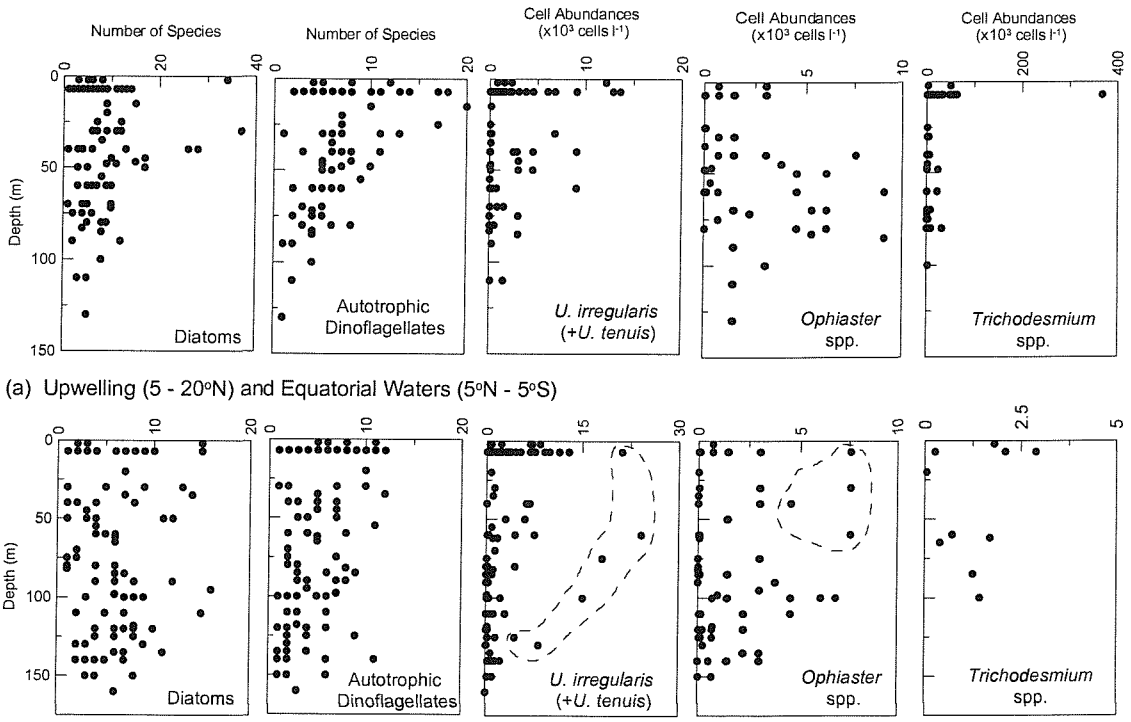


Figure 7.4: Depth distribution of species richness (number of diatom and autotrophic dinoflagellate species) and cell abundances (cells x$10^3$ $l^{-1}$) of individual species of coccolithophores (*U. irregularis* and *O. hydroideus*) and nitrogen fixers (*Trichodesmium* spp.) from different regions of the tropical and subtropical Atlantic Ocean; (a) Upwelling (5 - 20°N) and Equatorial (5°N - 5°S) waters, and (b) South Atlantic Subtropical Waters (5 - 30°S). (Data from AMT1 - 5, 7, 8 and 10.) Anomalies in the depth distribution of the coccolithophore species are identified in South Atlantic Subtropical Waters and are discussed in the text.

Nitrogen-fixing species are important sources of organic nutrients in oligotrophic waters (Capone *et al.,* 1997; Carpenter and Romans, 1991; Karl *et al.,* 1995; Hood *et al.,* 2000); ~50% of the nitrogen fixed by filaments of *Trichodesmium* spp. is released as Dissolved Organic Nitrogen (free amino acids) which represents a significant source of organic (new) nitrogen to the euphotic zone (Capone *et al.,* 1994; Glibert and Bronk, 1994). The basinscale distribution of *Trichodesmium* spp. (Fig. 7.3a) shows maxima associated with waters around the equator (0 - 15°N) in the eastern tropical Atlantic Ocean (Tyrrell *et al.,* submit.), which fits well with historical measurements (cf. Carpenter, 1983a, b). *Trichodesmium* spp. appear to be absent from the central range of the SASW (10 - 25°S; Fig. 7.3a), whereas *Hemiaulus* spp. are found throughout the tropical and subtropical Atlantic Ocean. The absence of *Trichodesmium* spp. in the central SASW raises important issues as to the composition of nitrogen-fixing species in the SASW; are *Trichodesmium* spp. absent, and if so why?

Several possible reasons have been proposed which include mixed layer depths being too deep to allow *Trichodesmium* spp. to 'mine' deep phosphorus pools below the euphotic zone through buoyancy reversals (cf. Carpenter, 1983a, b; Sanudo-Wilhelmy *et al.,* 2001), and the bio-availability of iron supplies suitable for the nitrogenase (nitrogen-fixing) enzyme (Berman-Frank *et al.,* 2001). Another possible reason may be that the nitrogen-fixing role of *Trichodesmium* spp. in the SASW may be filled by other nitrogen-fixers; e.g. diatom-*R. intracellularis* associations (Carpenter and Janson, 2000; Hood *et al.,* 2000), diatom-epiphytic *Calothrix rhizosoleniae* associations (Hood *et al.,* 2000), or unicellular cyanobacteria (Zehr *et al.,* 1998, 2001). Differences between the distribution of *Trichodesmium* spp. and diatom-nitrogen-fixing cyanobacteria associations have also been found on a temporal scale in the North Pacific Subtropical Gyre (NPSG), where blooms of one are accompanied by a total absence of the other (D. Karl, pers.comm.). However, measurements of the abundance of *Hemiaulus* spp. from the NPSG are ~6 times higher (6 x $10^3$ cells $l^{-1}$; Scharek *et al.,* 1999a, b) than from AMT (1 x $10^3$ cells $l^{-1}$), although NPSG measurements are based on summer studies and sediment trap samples.

The results from the consideration of the spatial (latitudinal and vertical) distribution of individual 'functional group' species show that there are difficulties in applying the functional group scheme to the large phytoplankton species; consideration of species-level distribution patterns shows significant deviations from the overall scheme.

*Spatial Variability: Community Structure*

Within the subtropical gyres of the Atlantic Ocean, the phytoplankton communities are composed and dominated by prokaryotic picoplankton (prochlorophytes, cyanophytes) and eukaryotic pico- and nanoplankton (prymnesiophytes, pelagophytes/chrysophytes) (Table 7.2) as indicated by pigment signatures (Chapters 4, 5 and 6). The pico- and nanoplankton also dominate the cell numbers (Zubkov *et al.,* 1998, 2000a, b) and primary productivity (Maranon *et al.,* 2000, 2001) of the subtropical gyres of the Atlantic Ocean. Research from the NPSG and western Sargasso Sea (NASG) show similar phytoplankton communities, and the total autotrophic biomass (~10 mg C $m^{-3}$; Karl, 1999) of the NPSG is comparable with that of the SASW (5 - 10 mg C $m^{-3}$; Chapter 5).

Table 7.1: Summary table of the main conclusions of phytoplankton community characteristics within six regions of the tropical and subtropical Atlantic Ocean.

| Region (Range) | Selected Characteristics | Main Community Components | Characteristic Species | Ecosystem Characteristics |
|---|---|---|---|---|
| NATD (40 - 35°N) | Dv Chl *a*: 10 - 40%<br><br>0.2 μm Chl *a*: 50 - 70 %<br><br>0 - 200 m Chl*a*: 34.7 ± 14.1 mg $m^{-2}$ | Prochlorophytes, Cyanophytes, Prymnesiophytes, Pelagophytes (Chrysophytes) Diatoms, Dinoflagellates | 'Temperate' Species<br>*Bacteriastrum* spp., *Proboscia alata*, *Cerataulina pelagica*, *Myrionecta rubra*,<br><br>'Tropical' Species<br>*Leptocylindrus danicus*, *Leptocylindrus minimus*, *Dactyliosolen* spp., *Pseudo-nitzschia* spp. | Seasonally mixed (?) with shallow MLD, intermediate $Z_{NO3}$ and $Z_{eu}$<br><br>Chlorophyll *a* profile similar to TTS<br><br>Seasonal variation between diatom dominated food chain and microbial loop and therefore seasonal export production |
| NASW (20 - 35°N) | Dv Chl *a*: 10 - 50%<br><br>0.2 μm Chl *a*: >60 - 70%<br><br>0 - 200 m Chl*a*: 36.5 ± 12.4 mg $m^{-2}$ | Prochlorophytes, Cyanophytes, Prymnesiophytes, Pelagophytes (Chrysophytes) | 'Subtropical' Species<br>*Umbellosphaera irregularis*, *Ophiaster* spp., *Discosphaera tubifer*, *Rhabdosphaera claviger*, *Small Prorocentrum* spp. | Stratified with shallow MLD, deep $Z_{NO3}$ and $Z_{eu}$, deep CM<br><br>Chlorophyll *a* profile similar to TTS 2-layer water-column<br><br>Microbial loop dominates, low export production although possibility of seasonal/stochastic events |
| UPW (5 - 20°N) | Dv Chl*a*: <10% - 40%<br><br>0.2 μm Chl*a*: 50 - 80%<br><br>0 - 200 m Chl*a*: 54.2 ± 24.0 mg $m^{-2}$ | Cyanophytes, Prochlorophytes, Prymnesiophytes, Pelagophytes (Chrysophytes) Diatoms, Dinoflagellates, Cryptophytes, | 'Tropical' Species<br>*Pseudo-nitzschia* spp., *Leptocylindrus danicus*, *Leptocylindrus minimus*, *Trichodesmium* spp., *Planktoniella sol*<br><br>'Temperate' Species<br>*Dactyliosolen* spp., *Thalassionema* spp. *Gymno/Gyro aureolum*, *Prorocentrum dentatum* | Shallow MLD, $Z_{NO3}$, CM typically shallower than $Z_{eu}$<br><br>Chlorophyll *a* profile represents Upwelling/Seasonal Structure<br><br>Diatom dominated food chain inshore with increased importance of microbial loop offshore. Therefore, high export production inshore and decreasing offshore into surrounding oligotrophic waters |
| EQU (5°N - 5°S) | Dv Chl*a*: 20 - 60%<br><br>0.2 μm Chl*a*: 50 - 80%<br><br>0 - 200 m Chl*a*: 39.4 ± 6.7 mg $m^{-2}$ | Cyanophytes, Prochlorophytes, Prymnesiophytes, Pelagophytes (Chrysophytes) | Tropical<br>*Trichodesmium* spp., *Emiliania huxleyi*, *Leptocylindrus mediterraneus*, *Hemiaulus hauckii*, *Ceratium teres*, Pennate sp. 'C' | Stratified with intermediate MLD, $Z_{NO3}$, $Z_{eu}$ and CM at similar depths<br><br>Chlorophyll *a* profile represents TTS 2- layer water-column<br><br>Microbial loop dominates, low export production despite relatively high nutrient fluxes compared with subtropical gyres |
| SASW (5 - 30°S) | Dv Chl *a*: >20 - 50%<br><br>0.2 μm Chl*a*: 75 - 90%<br><br>0 - 200 m Chl*a*: 33.0 ± 7.1 mg $m^{-2}$ | Prochlorophytes, Cyanophytes, Prymnesiophytes, Pelagophytes (Chrysophytes) | Subtropical Sun Flora<br>*Umbellosphaera irregularis*, *Discosphaera tubifer*, <5 μm coccolithophores, Small pennate diatoms *Rhabdosphaera claviger*<br><br>Subtropical Shade Flora<br>*Ophiaster hydroideus*, Pennate sp. 'C' *Haslea* spp., | Stratified with variable MLD, deep $Z_{NO3}$, $Z_{eu}$ and CM<br><br>Chlorophyll *a* profile represents CGS 2- layer water-column<br><br>Microbial loop dominates, low export production although possibility of seasonal/stochastic events |
| SATW (30 - 40°N) | Dv Chl*a*: 10 - 40%<br><br>0.2μm Chl*a*: 50 - 80%<br><br>0 - 200 m Chl*a*: 48.7 ± 4.7 mg $m^{-2}$ | Prochlorophytes, Cyanophytes, Prymnesiophytes, Pelagophytes (Chrysophytes) Diatoms, Dinoflagellates | 'Subtropical' Species<br>*Nitzschia longissima*, *Haslea* spp., Small pennate diatoms, *Discosphaera tubifer*, *Mastogloia rostrata*, *Hemiaulus hauckii*, | Seasonally mixed (?) with variable MLD, intermediate $Z_{NO3}$ and $Z_{eu}$<br><br>Chlorophyll *a* profile varies between TTS and Seasonal/Upwelling<br><br>Seasonal variation between diatom dominated food chain and microbial loop and therefore seasonal export production |

Vertical differences in the phytoplankton community are evident from the pigment signatures of the major phytoplankton groups in the subtropical gyres of the Atlantic Ocean (Chapters 4, 5 and 6). Upper waters (0 - 60 m) are dominated by prochlorophytes and cyanophytes (Dv Chl *a* and Zea) with prymnesiophytes also present (low concentrations of Hex-fuco and Diadino), and the community pre-occupied with photoprotection from photo-induced damage (dominance of accessory pigments by Zea; Chapter 4). Deep waters (60 - 200 m) are characterised by a diverse community of prochlorophytes (Dv Chl *a*, Chl *b*), cyanophytes (Zea, Chl *a*), prymnesiophytes (Hex-fuco) and pelagophytes (But-fuco) with light-harvesting important to the community as indicated by the formation of a chlorophyll and accessory pigment maximum without any measurable increase in autotrophic biomass (Chapters 4, 5 and 6; Zubkov *et al.,* 1998; Maranon *et al.,* 2000). Therefore, eukaryotic pico- and nanoplankton groups (prymnesiophytes, pelagophytes/chrysophytes) represent a higher proportion of the community at depth (McManus and Dawson, 1994). The CM in subtropical waters of the Atlantic Ocean is formed by increases in the cellular pigment concentrations rather than by absolute changes in autotrophic biomass, and therefore represents the Central Gyre Structure described by Cullen, (1982) (cf. Chapter 6).

Vertical separation of the phytoplankton community in subtropical waters is associated with separation of the water-column into a 2-layered system which was first suggested by Dugdale and Goering (1967), and expanded by Dugdale (1967) and Eppley *et al.,* (1973); an upper light-rich and nutrient-poor layer spatially removed from the nutriclines and CM where the specific growth rate of the phytoplankton community is nutrient-limited, and a light-limited layer below the thermocline associated with the CM and nutriclines (Dugdale, 1967; Dugdale and Goering, 1967; Eppley *et al.,* 1973; Harrison, 1991). Multivariate analysis of the nutrient and light availability within the water-column shows the clear distinction of these two layers in subtropical waters between 50 and 100 m (Chapter 3). The upper phytoplankton community would be dependent upon the nitrogenous excretory products from nano- and microheterotrophic grazers as the primary source of (regenerated) nutrients, whereas the deep community would be dependent upon the vertical new nutrient flux from deep water (Harrison, 1991). Due to the size-structure of the phytoplankton community (i.e. numerically dominated by pico-and nanoplankton), both the upper and deep plankton communities would show tight coupling between autotrophic production and consumption (microbial-loop food chain). Vertical separation of different phytoplankton taxa and species is likely to be related to differences in physiological and nutritional strategies (Eppley *et al.,* 1973; Venrick, 1982, 1993).

Analysis of the temporal variability in large (>5 μm) phytoplankton species composition in the oligotrophic waters of the SASW has shown that there is a difference between surface communities and communities associated with the CM (Chapter 5); in surface waters the species composition is relatively stable although the biomass-dominant large phytoplankton group is variable, whereas in the CM community the species composition varies considerably while the dominant group (coccolithophores) is relatively stable. Venrick (1982) found layering of species composition in the NPSG and pointed out the two associations (layers) are composed of similar proportions of diatoms, dinoflagellates and coccolithophores, despite major differences between these groups with respect to functional and adaptive properties (pigment composition, skeletal materials, motility). Although there are similarities between the results of this study and Venrick's (1982) work (e.g. layering, species present) there are differences relative to methodology; e.g. within this study autotrophic and

heterotrophic dinoflagellates have been distinguished (following the work of Lessard and Swift, 1986), whereas Venrick (1982) did not. Venrick (1982) also found a transitional zone in her work in the NPSG between the surface and deep association, which was unrelated to the UMD or to any isopycnal, but typically occurred above the CM at ~ 100 m (Venrick, 1988). The existence or position of such a zone in this work is difficult to establish due to the smaller number of depths sampled within this study (2 - 6), compared with 12 depths sampled by Venrick (1982), and the differences between statistical methods used; for example, it is statistically easier to distinguish between a sample from the subtropics and equatorial waters than between relatively subtle depth differences within the subtropics (Chapter 4).

The layering of phytoplankton communities in subtropical waters has led to the proposal of the existence of two highly specialised and adapted floras (physiologically and nutritionally) in subtropical waters (Sournia, 1982; Longhurst and Harrison, 1989); the upper 'sun' flora and the deep 'shade' flora. The results from this study have shown the first evidence of the existence of these flora in the SASW and include a few new species to be considered. *Discosphaera tubifer*, *U. irregularis* and *U. tenuis* are already thought to belong to the sun flora (e.g. Jordan, 1988; Winter *et al.,* 1994), however, the results from this study suggest that *Syracosphaera prolongata*, *Acanthoica* spp., *Rhabdosphaera claviger*, small (10 - 30 μm) unidentified pennates and high-light adapted (low Dv Chl *a* and Chl *b*, high Zea) prochlorophytes should be added. In addition to *Ophiaster* spp. and *Florisphaera profunda* (Jordan, 1988; Winter et al., 1994; Kinkel et al., 2000), *Halopappus* spp., *Calciopappus* spp., *Michaelsarsia elegans*, *Haslea* spp., *Nitzschia longissima*, *Anoplosolenia brasiliensis*, *Calciosolenia murrayi*, Pennate sp. 'C' (50 μm) and low-light adapted (high Dv Chl *a* and Chl *b*, low Zea) prochlorophytes should be added to the shade flora.

The phytoplankton community of the tropical equatorial Atlantic Ocean is similar to that found in the subtropical gyres (Table 7.2); upper waters characterised by prochlorophytes, cyanophytes and prymnesiophytes, while at depth there are increases in these groups as well as pelagophytes (chrysophytes). However, around the equator, the increases in pigment concentrations at depth are more likely to represent biomass increases (Chapter 4 and 6) due to increased new nutrient fluxes (Chapter 3). This conclusion is supported by information on the distributions of picoplanktonic biomass (Zubkov *et al.,* 1998) and of nano- and picoplankton biomass (Chapter 4; Maranon *et al.,* 2000). Pigment concentrations in the CM of the tropical equatorial Atlantic Ocean show a marked increase in deep Zea (>0.1 mg $m^{-3}$), which may be related to increases of both prochlorophytes (increased Chl *b*; >0.1 mg $m^{-3}$) and cyanophytes (*Synechococcus* spp. and *Trichodesmium* spp.) (Chapter 4). Increases in the biomass of the pico- and nanoplankton groups, and higher contributions by the CM to water-column integrated primary productivity (Maranon *et al.,* 1999, 2000) in equatorial waters indicates that the CM is similar to the Typical Tropical Structure described by Herbland and Voituriez (1979) (Chapter 6).

The phytoplankton communities found in the tropical waters off NW Africa and the high latitude (>30 - 40°N/S) subtropical waters at the ends of the AMT transects are quite similar in composition (Table 7.2); e.g. increases in the diversity, cell numbers and pigment signature concentrations of diatom and autotrophic dinoflagellates (Chapter 4). However, prochlorophytes are relatively rare off NW Africa (Dv Chl *a*: 10 - 40% of TChl *a*) compared with other regions along the transect (e.g. SASW, Dv Chl *a* 20 - 60% of TChl *a*; Chapter 4). Decreases of prochlorophyte pigment

signatures off NW Africa (Dv Chl *a*), detectable concentrations of Chl *b* (~0.01 - 0.05 mg $m^{-3}$) and lutein (0.004 - 0.009 mg $m^{-3}$) suggest an increase in the abundance of chlorophytes and prasinophytes (Chapter 4). Detectable concentrations of alloxanthin in waters off NW Africa (~0.005 - 0.03 mg $m^{-3}$) may also indicate increases in the abundance of cryptophytes (Chapter 4). The characteristics of the CM off NW Africa and in the warm semi-temperate waters around the subtropical convergences (30 - 40°N/S) suggest that CM in these waters are formed through similar mechanisms to those in seasonally mixed and stratified waters (Chapter 6); production, sinking and accumulation of algal cells at a density discontinuity (bottom of the mixed layer).

Regional differences in the composition of the phytoplankton communities are related to differences in the relationship between the nutriclines (nutrient availability) and euphotic zone depth (light availability) (Table 7.2). Temporal variations in the regional hydrographic conditions interact with the phytoplankton community size-structure to vary the degree of export production possible and seasonal succession of phytoplankton groups (Table 7.2). However, the study of temporal (seasonal) variations in hydrographic parameters and phytoplankton community structure is difficult due to the low (seasonal) temporal resolution of the AMT cruises; although interannual variations have been detected within fixed study areas of the AMT cruise transect.

### 7.3.3. Alternative Nutrient Sources for Subtropical Phytoplankton Communities

The main sources of nutrients for phytoplankton communities in oligotrophic subtropical waters are from the vertical new nutrient flux at the base of the euphotic zone and regenerated nutrients produced in the upper light-rich portion of the euphotic zone. However, there are other sources of nutrients to the pelagic community; e.g. lateral nutrient inputs from eutrophic environments at the boundaries of the subtropical gyres, or the utilisation of particulate or dissolved organic nutrient pools available in the water-column. The possible role of these alternative nutrient sources to the autotrophic community is discussed in this section.

*Isopycnal Inputs of Nutrients*

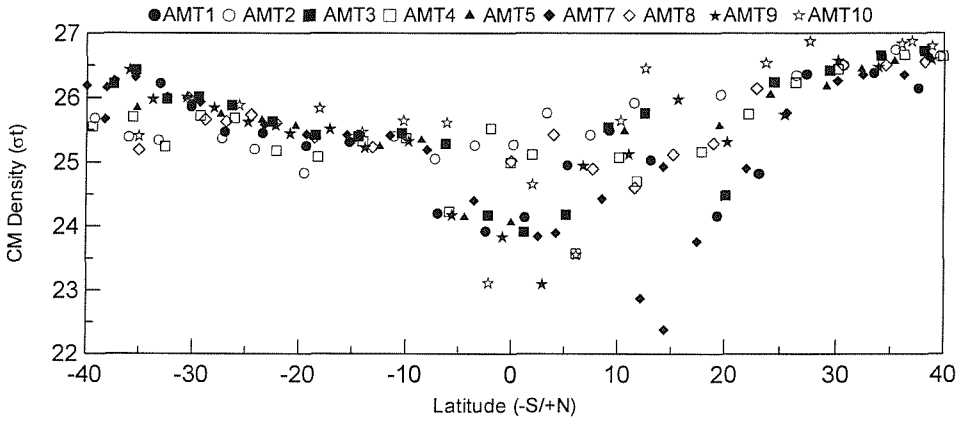


Figure 7.5: Density (σt) of the Chlorophyll *a* Maximum in the tropical and subtropical Atlantic Ocean. Depth changes of the CM with latitude (Chapter 6) and latitudinal density changes in the upper ocean (Chapter 3) produc this characteristic pattern of decreasing CM density from high latitude to low-latitude waters. There is also evidence of intercruise variations in CM density that are related to regional seasonal differences in water-column structure and variations in the AMT cruise trac

The basinscale pattern of CM density (Fig. 7.5) shows that the CM is found in high-density waters (26 – 27 σt) at mid-latitudes (40°N/S) and relatively lower density (<25 σt) waters at low-latitudes around the equator. This characteristic pattern of CM density suggests the possibility of

lateral movement of material across isopycnals from the equatorial region into the central gyres that could include inorganic nutrient fluxes. However, at present the nutrient data from the AMT programme is unsuitable to further test this possible lateral inorganic nutrient flux; inorganic nutrient concentrations are typically below the detection limits of the current techniques employed. Similarly, the density of the *in-situ* fluorescence maximum would provide a more accurate measurement of the density of the CM, although CTD depth profiles of fluorescence for all the AMT cruises are not currently available. This lateral flux of nutrients may not be restricted to inorganic nutrient sources; the proposition of the heterotrophic subtropical gyral ecosystems (e.g. Del Giorgio *et al.,* 1997) requires an external input of dissolved organic matter to fuel the system (Geider, 1997). As well as cross-isopycnal movements of nutrients, mesoscale physical instabilities (e.g. mesoscale eddies) may also represent significant nutrient inputs into the subtropical gyres (McGillicuddy and Robinson, 1997; McGillicuddy *et al.,* 1998).

*Organic Nutrients*

The assimilation of organic nutrients (faculative heterotrophy) by phytoplankton is possibly more widespread than previously thought (Karl, 1999), especially in environments where depleted inorganic nutrient concentrations cause nutrient limitation of the phytoplankton community (Bonin and Maestrini, 1981). The ability of a few planktonic algae to utilise organic nutrients is well documented from laboratory studies (see review by Bonin and Maestrini, 1981), however there are few examples from the open-ocean. It has been hypothesised that as new nutrient (e.g. nitrate) supplies are depleted, the phytoplankton community composition changes so that species capable of utilising organic nutrients become dominant (Bonin and Maestrini, 1981). Suggestions that prochlorophytes lack the enzyme (nitrate reductase) to utilise nitrate (Karl et al., 2002b), coupled with a 'preference' for ammonia and DON (Rippka *et al.,* 2000), may explain their dominance in the low new nutrient environments of the subtropical gyres and provide significant evidence of the importance of facultative heterotrophy in the open-ocean. However, there is likely to be intense competition between algae and bacterioplankton for organic nutrients, as bacteria are generally thought to have much higher affinities for organic nutrient sources at low substrate concentrations (Bonin and Maestrini, 1981; Kiel and Kirchman, 1999). Organic nutrients are supplied to the planktonic community *in-situ* from autotrophic (leakage of dissolved organic matter) and heterotrophic (excretion, sloppy feeding) activity. Other sources of organic nutrients into central gyre provinces may include lateral transfer from surrounding high productivity regions (e.g. upwelling areas in boundary currents).

*Mixotrophy*

Mixotrophy is the use of dual methods of nutrition; the use of light energy for photosynthesis (photoautotrophy) coupled with the ingestion of organic dissolved (ozmotrophy) or particulate (phagotrophy) material. Although the presence of pigments suggests photoautotrophic nutrition, pigments may also indicate other nutritional strategies; e.g. photoheterotrophy (assimilation of organic substances using light energy) or mixotrophy (Karl, 1999). Mixotrophy may be selected for *in-situ* in oligotrophic waters (Karl, 1999) where the microbial food web is efficiently recycling organic matter. In this situation, mixotrophy would act as a trophic link between the classical food web and

the microbial loop; faculative mixotrophs could ingest organically enhanced prey (bacteria, flagellates) as supplementary nutrient sources when the majority of nutrients are bound in particulate organic material (Stoecker *et al.,* 1997; Legrand *et al.,* 2001). Seasonal phagotrophy has been invoked as a possible over-wintering survival strategy for the coccolithophore *Coccolithus pelagicus* (Brand, 1994), while culture studies of faculative mixotrophic species have shown that ingestion of prey particles coupled with phototrophic nutrition can lead to increased growth rates compared with rates measured from prey-depleted cultures at comparable light intensities (Skovgaard, 1996; Hansen and Nielsen, 1997; Li *et al.,* 1999; Zhang and Watanabe, 2001). Phagotrophic strategies by coccolithophores, or other phytoplankton groups, have yet to be investigated in subtropical and tropical waters, although it is recognised that the biology of oligotrophic phytoplankton is poorly understood (Brand, 1994; Karl, 1999). Mixotrophy can also have implications for food web structure and inter-species competition; e.g. Jeong *et al.,* (1997) found that the relative abundance ratios of a mixotrophic and heterotrophic dinoflagellate species decided which was the predator or prey. There are few field measurements of mixotrophic abundances, although measurements from the Sargasso Sea have shown mixotrophic flagellates account for 12 - 17% of the total autotrophic flagellate population and up to 39% of the total phagotrophic flagellate numbers (Sanders *et al.,* 2000). Another advantage of a mixotrophic nutritional strategy is that mixotrophs reduce the abundance of competitors for nutrients and gain limiting nutrients in pelleted form (Thingstad *et al.,* 1996).

## 7.4. Temporal Variability of Phytoplankton Community Composition in Subtropical Waters

### 7.4.1. Variability in South Atlantic Subtropical Waters: AMT

*Hydrographic Measurements: Seasonal and Interannual Variability*

Analysis of variations in the mixed layer depths (MLD) within South Atlantic Subtropical Waters (SASW; 0 - 30°S) show a breakdown in the seasonal pattern during post-winter cruises (Fig. 7.6); during AMT-1 and 9 the mixed layer was significantly (1-way ANOVA, $p<0.001$, $n = 85$) deeper (122.8 ± 38.8 m and 115.6 ± 31.5 m, respectively) than during other post-winter cruises (AMT-3, 62.3 ± 25.0 m; AMT-5, 70.9 ± 27.1 m; AMT-7, 70.5 ± 14.7 m). Examination of the mean monthly wind-speeds from two points within the SASW suggest that there was a slight decrease in winter mixing during August-November in 1996 in the southern portion of the SASW (>20°S), and a total absence of high (>8 m $s^{-1}$) wind speeds during the same period in 1997 throughout the SASW (Chapter 3). The 1997 decrease in wind speed may be related to the 1997 - 1998 El-Nino-Southern-Oscillation (ENSO) event in the Pacific Ocean (Chapter 3), although the variability during late-1996 precedes the ENSO event. The full extent of interannual changes in the wind speeds in the SASW need to be further examined through the examination of a longer time-series of wind speeds (>20 yrs) to determine the seasonal cycle in the SASW. However, these measurements and observations suggest a disturbance in the physical forcing in the SASW during 1996 - 1997 that coincides with the changes in MLD. It is hypothesised that these disturbances caused variability in the new nutrient supply to the subtropical phytoplankton communities during AMT-3, and 5, and further variability when high winter wind speeds re-occurred again during 1998 (AMT-7); the SASW became more oligotrophic during these years.

*Chlorophyll a and Pigment Measurements: Interannual Variability*

Examination of the phytoplankton community in the SASW has shown very little change in upper (0 - 60 m) or deep (60 - 200 m) autotrophic standing stock (using chlorophyll *a* concentration as a proxy), or in the abundance of prochlorophytes (Dv Chl *a*:TChl *a* ratio) (Fig. 7.6).

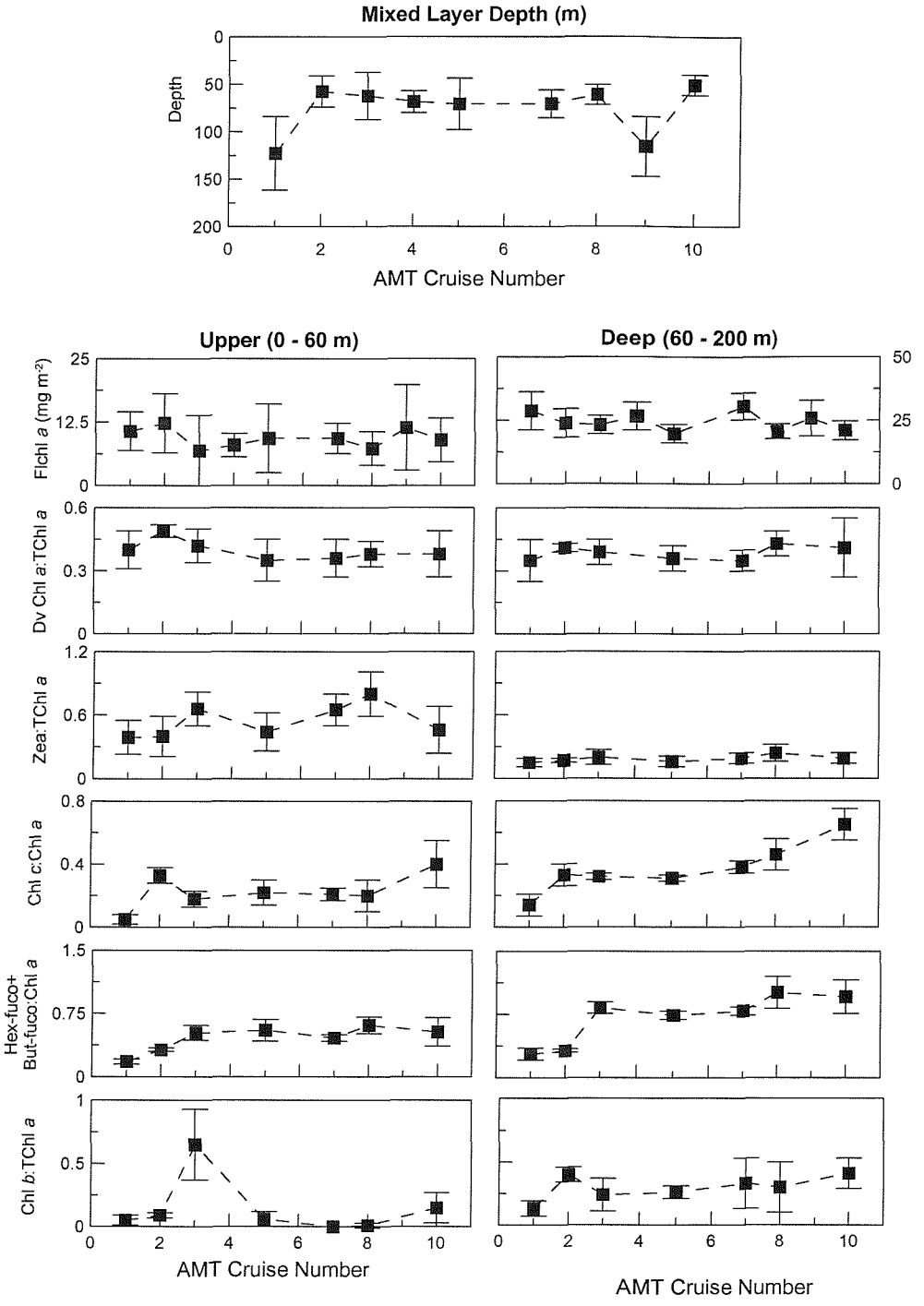


Figure 7.6: Summary plots of temporal variability in the South Atlantic Subtropical Waters (SASW; 0 - 30°S) for mixed layer depth (UMD), integrated chlorophyll *a* concentrations (mg $m^{-3}$; FIchl*a*) and integrated biomarker pigment ratios (w:w) in upper (0 - 60 m) and deep (60 - 200 m) portions of the water-column.

However, variability in the Dv Chl *a*:TChl *a* ratio cannot be interpreted as biomass changes as this ratio is dependent upon photoacclimation; prochlorophytes increase their cellular Dv Chl *a* concentrations with photoacclimation to low-light (Partensky *et al.*, 1993). In contrast, neither prochlorophytes or cyanophytes vary their intracellular Zea concentrations with photoacclimation

(Kana *et al.*, 1987a, b 1988; Bricaud *et al.*, 1999), so the increases in the Zea:TChl *a* ratios observed during AMT-3 and AMT-8 in the upper portion of the water-column may be related to an increase in these groups (Fig. 7.6). If there was a decrease in the winter mixing of the water-column during AMT-3 and 5 and a decrease in the vertical nitrate supply, differences in the nutrient preferences of prochlorophytes (ammonia and DON; e.g. Rippka *et al.*, 2000) and *Synechococcus* spp. (nitrate; e.g. Partensky *et al.*, 1996), lead to the interpretation of the increase in Zea:TChl *a* ratio as an increase in prochlorophytes. Unfortunately, there is no independent way to test this conclusion (i.e. no flow-cytometric cells counts of the picoplankton in these years).

During AMT-3 there was a highly significant and dramatic increase in the TChl *b*:TChl *a* ratio in upper (<60 m) waters; TChl *b*:TChl *a* ratios increased from 0.05 ± 0.04 and 0.09 ± 0.02 during AMT-1 and 2 to 0.65 ± 0.28 during AMT-3 (Fig. 7.6; Chapter 5). This increase in the TChl b:TChl a ratio was associated with a shift of the deep high TChl *b*:TChl *a* pool into subsurface waters (Chapter 5). Interpretation of these changes in the TChl *b*:TChl *a* ratio as abundance changes of the prochlorophytes is not possible due to Chl *b* being related to photoacclimation to low-light levels; prochlorophytes increase their intracellular Chl *b* (Dv Chl *b*) concentrations with photoacclimation to low light levels (Bricaud *et al.*, 1999).

As well as changes in some of the prokaryotic pigment ratios, there are increases in eukaryotic pigment ratios during the AMT cruises (Fig. 7.6); a slight increase of the upper water TChl *c*: Chl *a* ratio during AMT-10 (from 0.20 ± 0.10 during AMT-8 to 0.40 ± 0.15 during AMT-10), and increases of the deep TChl *c*:TChl *a* and Hex-fuco+But-fuco:Chl *a* ratios during all the AMT cruises. Increases in the deep TChl *c*:TChl *a* ratios during AMT-8 and 10 accompany changes in the species composition (increases in diatom biomass), while increases in the Hex-fuco+But-fuco:Chl *a* ratios are likely to relate to increases in prymnesiophytes and pelagophytes (Chapter 5).

Thus, it appears that the proposed breakdown of winter mixing during AMT-3 and 5 may have led to an increase in prochlorophytes as well as eukaryotic members of the phytoplankton community (prymnesiophytes and pelagophytes). If winter mixing resumed during AMT-7 and 9, these eukaryotic groups, including diatoms, continued to increase in abundance towards the end of the AMT cruises (Fig. 7.6).

*Comparison of Ecological and Productivity Data*

Intercruise comparisons of the primary productivity measurements collected during the AMT cruises (AMT-1-3) show several interesting phenomena; (1) interannual and intercruise differences in carbon assimilation rates without major changes in biomass (Maranon *et al.*, 2000), (2) in low productivity waters the contribution of nanoplankton and microplankton to total productivity was higher than their contributions to total chlorophyll *a* (e.g. the microplankton represented <4% of total chlorophyll *a* in tropical and subtropical waters, whereas they contributed 10 - 12% of total productivity; Maranon *et al.*, 2001), and (3) evidence that in oligotrophic regions (NASG, SASG) there are occasions when the dominance of picoplankton in terms of biomass (chlorophyll *a*) co-occurs with either their dominance of productivity or a dominance of nano- and microplankton in terms of production (Maranon *et al.*, 2001). Non-linearity of the production to biomass (chlorophyll *a*) relationships for large phytoplankton groups would appear to indicate that such large cells are more

adapted to the ambient environment than small cells; i.e. the nano- and microplankton can attain higher productivity per unit of biomass than the picoplankton.

Intercruise differences in rates of primary productivity include an increase during AMT-3 in the South Atlantic Ocean (5 - 40°S); integrated (euphotic layer) primary productivity during AMT-1 was 301.0 ± 149.1 mg C $m^{-2}$ $d^{-1}$, 190.3 ± 58.1 mg C $m^{-2}$ $d^{-1}$ during AMT-2 and 392.7 ± 91.1 mg C $m^{-2}$ $d^{-1}$ during AMT-3 (Maranon et al., 2000). These intercruise differences in primary productivity rates in the SASW can now be seen to be associated with changes in the community composition in terms of biomarker pigments and are associated with several fluctuations of the nano- and micro-plankton species composition (Chapter 5). However, primary productivity rates from further AMT cruises are not presently available to compare with the longer-term changes in the phytoplankton community structure.

*Variability in Large (>5 μm) Phytoplankton Species Distributions*

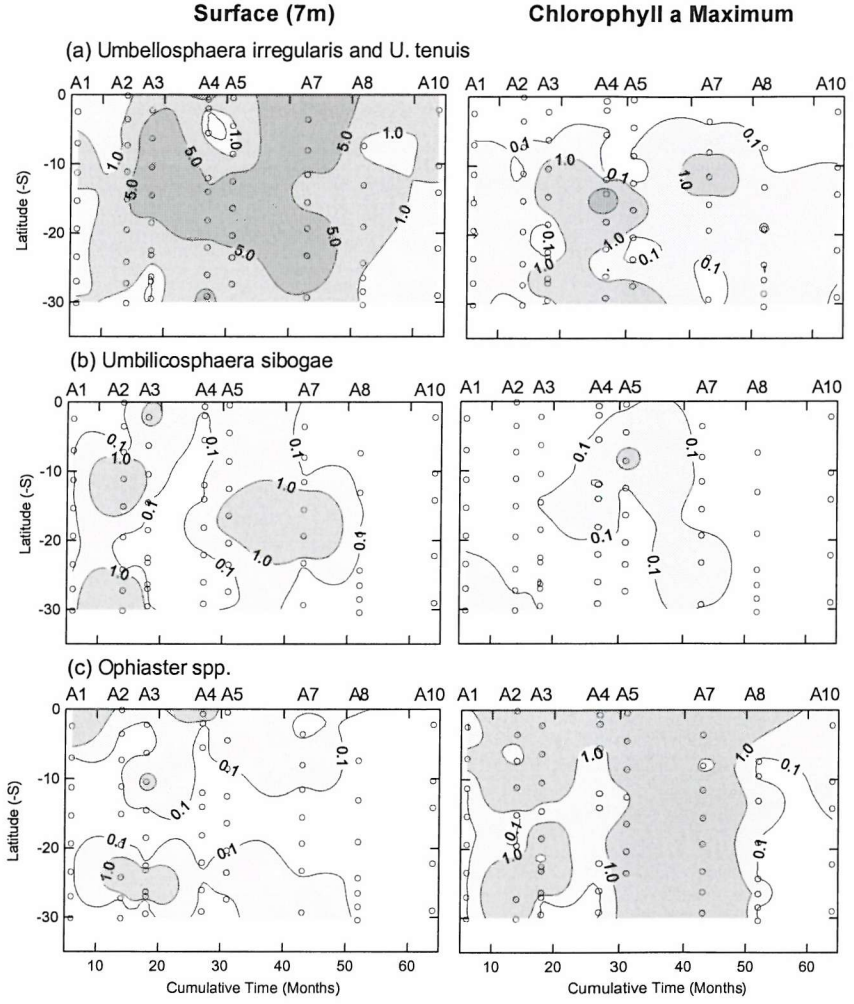


Figure 7.7: Temporal variability in the abundance (cells x$10^3$ $l^{-1}$) of species in South Atlantic Subtropical Waters; (a) *Umbellosphaera irregularis* & *U. tenuis*, (b) *Umbilicosphaera sibogae*, and (c) *Ophiaster* spp. (*O. hydroideus*).

Analysis of the large (>5 μm) phytoplankton species composition of the phytoplankton community in the SASW (Chapter 5) shows that there are several fluctuations during the AMT cruises (Chapter 5). These include an increase in species richness (number of species) and the distribution of cell

numbers between individual species (evenness) during AMT-5, which continue to increase until AMT-10 (Chapter 5). Multivariate statistical analysis of changes in species composition identifies several important phytoplankton species (Chapter 5), which include *Umbellosphaera irregularis* and *U. tenuis*, *Umbilicosphaera sibogae* and *Ophiaster* spp.

The abundance of these phytoplankton within the SASW for all AMT cruises (AMT-1 - 5, 7, 8 and 10) are plotted in Figure 7.7. Fluctuations in the abundance of *U. irregularis* and *U. tenuis* are found in both upper and deep (Chlorophyll *a* Maximum) waters, with *U. irregularis* and *U. tenuis* abundance high (>5 x $10^3$ cells $l^{-1}$) during AMT-3, 4, 5 and 7 in surface waters and during AMT-3, 4 and 5 (>1 x $10^3$ cells $l^{-1}$) in the CM (Fig. 7.7). Cell densities of *U. sibogae* are high (>0.1 x $10^3$ cells $l^{-1}$) during AMT-2, 3, 4, 5 and 7 and then decrease below 0.1 x $10^3$ cells $l^{-1}$ during AMT-8 and 10 in surface waters, and are high (>0.1 x $10^3$ cells $l^{-1}$) only during AMT4, 5, and 7 in the CM (Fig. 7.7). The abundance of *O. hydroideus* is generally low (<0.1 x $10^3$ cells $l^{-1}$) in surface waters, high (>1.0 x $10^3$ cells $l^{-1}$) in the CM during AMT-2, 3, 5, and 7 and low (<0.1 x $10^3$ cells $l^{-1}$) in the CM during AMT-8 and 10 (Fig. 7.7).

Although not enough is known about the nutritional or life-cycle strategies of these species to fully interpret these fluctuations in abundance, reasonable speculations are available; *U. irregularis* is known to dominate surface waters in oligotrophic waters as part of the proposed sun flora (e.g. Winter *et al.,* 1994; Kinkel *et al.,* 2000) and therefore its abundance may be inversely related to the availability of new nutrients (possibly through competition). *Ophiaster* spp. are known to be components of the shade flora (e.g. Jordan, 1988; Winter *et al.,* 1994) which live deep in the water-column in association with the nutriclines and therefore its abundance may be positively related to the vertical new nutrient fluxes. The reported distribution of *U. sibogae* includes the central parts of the Pacific and Atlantic Ocean, as well as the Indian Ocean and Mediterranean Sea (Winter *et al.,* 1994), and this species is also thought to prefer warm oligotrophic waters and does not respond to increased new nutrient availability (Kleijne, 1993; Broerse *et al.,* 2000); therefore, its abundance may also be inversely related to new nutrient availability. Using these suppositions, if there was a break-down of winter mixing during AMT-3 and 5 and a decrease in the new nutrient supply to the upper euphotic zone (0 - 60 m), *U. irregularis*, *U. tenuis* and *U. sibogae* may have increased in upper waters due to the increased oligotrophy of the environment, through competition with species dependent upon the winter new nutrient influxes (cf. Venrick, 1982, 1993). Similarly, *Ophiaster* spp. may have found less competition at depth for new nutrients in a relatively stable environment during AMT-3 and 5. However, until studies have addressed the physiological and nutritional strategies of these species these assumptions cannot be validated.

### 7.4.2. Lessons from the 'Domain-Shift' in the North Pacific Subtropical Gyre

Oceanic turbulence is affected by variability in the atmosphere and related climatic variations. In the North Pacific Subtropical Gyre (NPSG) climate shifts are thought to have caused a change in the standing stock and ecosystem function of the pelagic community over the last 30 - 40 years (Karl, 1999; Karl *et al.,* 2001a). Climate variation in the North Pacific, specifically the intensification of the Aleutian Low Pressure System, caused mixed layer depths to be 30 - 80% deeper between 1977 - 88 than during 1960 - 76 (Polovina *et al.*, 1994). Long-term measurements show that the mixed layer

depth changes occur at decadal- and basin-scales, and may be an important mechanism linking variations in the atmosphere to oceanic ecosystem productivity and structure (Polovina *et al.,* 1994).

Time-series measurements from the NPSG have shown an increasing trend in the integrated chl*a* concentrations and estimated rates of primary production; while concentrations of dissolved inorganic silica (silicate) and phosphorus have decreased over the last 30 yrs (Karl *et al.,* 2001a). The average euphotic zone (0 - 200 m) chl*a* concentration in the NPSG during summer has nearly doubled between 1968 (11.2 - 13.8 mg $m^{-3}$) and 1980 (19.8 - 24.3 mg $m^{-3}$), which was accompanied by an increase in winter winds and a decrease in SST (Venrick *et al.,* 1987). These changes have been accompanied by an increase in the deep chlorophyll *b* (chl *b*) concentration (Karl *et al.,* 2001a); where phaeopigment concentrations from the acidification fluorometric technique (after Holm-Hansen *et al.,* 1965) are used as a surrogate for chl *b* concentrations. [Phaeopigment concentrations are very low in subtropical waters (Vernet and Lorenzen, 1987; Ondrusek *et al.,* 1991) and the phaeopigment signal from the fluorometric techniques is likely to be largely due to chl *b* (Karl *et al.,* 2001a).] These observations were hypothesised to be a result of a 'regime' shift in the NPSG; a shift in the phytoplankton community structure has occurred in response to climate variations (Venrick *et al.,* 1987) which has been termed the *'Domain-Shift'* (Karl *et al.,* 2001a). The initial increase in chl *b* concentrations occurred after an initial increase in chl*a* concentrations between 1976 - 1985 and seems to be continuing (Karl *et al.,* 2001a). Increased stratification, linked to the El-Nino-Southern-Oscillation events via 'teleconnections' (Karl *et al.,* 1995, 2001a; Karl, 1999), are thought to have resulted in a decrease in inorganic nitrogen and phosphorus supply, and therefore a greater dependency on the much larger dissolved nitrogen and phosphorus pools; both conditions would favour the growth and accumulation of prochlorophytes as opposed to larger eukaryotic species (Karl *et al.,* 2001a). Increased Chl *b*:Chl *a* ratios could be a result of either increased prochlorophyte numbers relative to phytoplankton biomass, or a long term photoadaptation of a static population, or a combination of both (Karl *et al.,* 2001a). Both Venrick *et al.,* (1987) and Polovina *et al.,* (1994) suggest that changes in the NPSG after the 1976 climate change were a result of increased mixed layer depths and a higher frequency of deep mixing events due to an intensification of the Aleutian low-pressure system in winter. However, the Aleutian low-pressure system returned to its normal position in 1988, whereas the chl*a* has remained at the elevated "regime-shift" concentrations (Venrick *et al.,* 1987; Karl, 1999).

Therefore, the prolonged summer conditions in the NPSG, following an intensification of winter mixing, are thought to have selected for small cells with enhanced nutrient uptake and light absorption capabilities as well as diazotrophic phytoplankton (Karl *et al.,* 2001a). The *'Domain-Shift'* hypothesis suggests that the ecosystem has moved from being eukaryotic to prokaryotic dominated which has altered nutrient flux pathways and affected food-web structure, and in turn new and export production (Karl *et al.,* 2001a). The climate shift has caused increased stratification in the NPSG, and further stratification of the surface ocean as a result of global warming has been suggested to lead to further selection pressures and changes in the ecosystem structure and dynamics (Karl *et al.,* 2001a).

If the *'Domain-Shift'* that occurred in the NPSG was in response to enhanced water-column stratification due to global warming (and/or movement of the Aleutian Low Pressure System), then it can be hypothesised that similar processes may occur in other subtropical regions as stratification is

further enhanced and inorganic nutrients become depleted (Karl *et al.,* 2001a). The '*Domain-Shift*' in the NPSG also emphasises the importance of external forcing and physical variability in structuring the plankton communities of the NPSG (Venrick *et al.,* 1987), as well as challenging the view of long-term stability in the dynamics of subtropical ecosystems. Climate variability is thought to be important in maintaining the diversity and structure of the oligotrophic marine ecosystem and the phytoplankton community composition, and could not be detected without time-series measurements and datasets (Venrick *et al.,* 1987).

In relation to the time-series studies in the NPSG, AMT measurements in the SASW are in their infancy. AMT is the first oceanic programme to collect directly comparative measurements of phytoplankton community structure in the SASW, and therefore the temporal trends identified in the mixed layer depths (Chapter 3) and phytoplankton community composition (Chapter 5) can only be identified post-1995 (AMT-1). However, there is evidence from this study that temporal variability of the pelagic ecosystem in the SASW is related to climatic variability. It is also clear that the roles of stochastic and seasonal mixing events in subtropical waters have been undervalued and need further attention (section 7.4.3). Despite the limitations of the AMT time-series measurements in the SASW, a trend comparable to that found in the NPSG can be identified; a reduction in winter wind speeds and post-winter mixed layer depths (Chapter 3) and an apparent increase in the diversity and biomass of the eukaryotic portion of the autrophic community in the SASW (Chapter 5).

### 7.4.3. The Enigma of Mixing in Subtropical Waters

The importance of seasonal or stochastic mixing events (e.g. wind mixing, mesoscale eddies) in subtropical waters has now been invoked as controlling new and export production (Karl, 1999), as well as species survival (Venrick, 1993). However, winter mixing in subtropical waters still represents an enigma due in part to the climatic changes that have occurred in the NPSG and to the relative difficulty in sampling such remote areas. Within the NPSG there has been decadal climate variations related to the Pacific Decadal Oscillation (PDO), which has decreased the winter mixing and enhanced stratification (Karl, 1999). Mixing events are now known to be important in stimulating otherwise inefficient or dormant components of the ecosystem, which may lead to enhanced ecosystem production, and biomass accumulation (Karl, 1999). Despite the occurrence of winter mixing in the NPSG during the early 80s, Venrick (1990a, b) and McGowan and Walker (1985) found that the phytoplankton species and zooplankton species structures were highly resilient to change. Venrick (1993) hypothesised that brief, stochastic deep-mixing events occurred in the NPSG that injected nutrients into the euphotic zone and allowed species survival. Venrick (1982, 1993) also hypothesised that the ability of species to store nutrients may be important for growth and survival during times when mixing was reduced or absent. Adaptation of upper and deep species to sub-optimal nutrient conditions (upper waters) and sub-optimal light conditions (deep waters) allow species in these environments to maximise their growth potential (Venrick, 1982). McGowan and Walker (1985) proposed a slightly different answer; the maintenance of high diversity and numerical dominance of zooplankton in the NPSG was not due to physical disturbance but rather a result of (unidentifiable) biological interactions, despite episodes of significant physical variability. Now that AMT has identified temporal variability in winter wind speeds, mixed layer depths (Chapter 3) and

phytoplankton community composition (Chapter 5), it has to be recognised that more attention to mixing events in subtropical waters is required; a climatological framework needs to be built with regard to seasonal, annual and decadal variations in the physical environment of the South Atlantic Ocean to fully elucidate the causes of temporal variability.

## 7.5. Thesis Conclusions

1. Spatial variations in the hydrographic environment in the tropical and subtropical Atlantic Ocean are related to spatial variations in the phytoplankton community composition. Spatial variability of the phytoplankton community occur along a latitudinal gradient of increasing (new) nutrient availability, from the oligotrophic subtropical gyres to intermediate nutrient concentrations around the tropical equatorial Atlantic Ocean, and on to the eutrophic waters of the NW African upwelling zone. The low (new) nutrient environments of the subtropical gyres are dominated by prochlorophytes, cyanophytes, prymnesiophytes and pelagophytes (chrysophytes), whereas the high (new) nutrient waters of the upwelling off NW Africa are characterised by a more diverse community with a reduction in prochlorophyte abundance and increases of cyanophytes, prymnesiophytes, pelagophytes (chrysophytes), diatoms, autotrophic dinoflagellates, cryptophytes, and possibly chlorophytes and prasinophytes.

2. Spatial variability of the phytoplankton community composition also exists in the vertical direction, in relation to the opposing nutrient and light gradients; upper waters are nutrient-poor and light-rich, while deep waters are nutrient-rich and light-poor (as described by Dugdale and Goering, 1967 and Dugdale, 1967). The slope of the nutrient and light gradients change with latitude, and the degree of vertical separation of the phytoplankton community is proportional to the degree of separation of nutrient and light-rich conditions. In eutrophic waters, upper waters (<50 m) are both nutrient- and light-rich and the phytoplankton community is similar throughout the water-column. In contrast, in oligotrophic subtropical waters the water-column is highly layered; upper waters (<60 m) are new nutrient-poor and light-rich, whereas deep waters (>100 m) are relatively nutrient-rich and light-poor. Therefore, in oligotrophic subtropical environments of the Atlantic Ocean two specialised communities exist; an upper community which is dominated by high-light adapted prochlorophytes, and includes mainly cyanophytes and prymnesiophytes (coccolithophores), and a deep diverse community of mainly low-light adapted prochlorophytes, cyanophytes, prymnesiophytes (coccolithophores) and pelagophytes (chrysophytes). This study represents the first analysis of vertical differences in the phytoplankton community structure in South Atlantic Subtropical Waters, and the results show that depth-layering of the community in subtropical waters of the Atlantic Ocean is identical to that described from other subtropical ocean basins; e.g. North Pacific Subtropical Gyre (Letelier *et al.,* 1993) and western North Atlantic Subtropical Gyre (Sargasso Sea; Bidigare *et al.,* 1990).

3. This study represents the first to use multivariate statistics to examine basinscale changes in the large (>5 μm) phytoplankton species composition. The results show several spatial patterns including: (i) an increase in 'temperate' (e.g. *Pseudo-nitzschia* spp.) and 'tropical' (e.g.

*Planktoniella sol*) diatom species in the tropical waters off NW Africa; (ii) the dominance of the nitrogen-fixing cyanophyte *Trichodesmium* spp. in the eastern tropical equatorial Atlantic Ocean, its presence in eastern North Atlantic subtropical waters and its relative absence in western and central South Atlantic subtropical waters; (iii) the first reports of the presence of specialised 'sun' (e.g. *Umbellosphaera irregularis*, *U. tenuis* and *Discosphaera tubifer*) and 'shade' (e.g. *Ophiaster* spp., *Anoplosolenia brasiliensis*, *Calciosolenia murrayi*) coccolithophore species in western and central South Atlantic subtropical waters, which have been previously proposed from studies in the North Atlantic Subtropical Gyre (Sargasso Sea; Haider and Thierstein, 2001) and North Pacific Subtropical Gyre (e.g. Venrick, 1982, 1999; Cortes *et al.*, 2001).

**4.** Temporal studies (1995 - 2000) of the large (>5 μm) phytoplankton group and species composition in surface waters and the Chlorophyll *a* Maximum of the South Atlantic Subtropical Waters (0 - 30°S) indicate depth-specific differences in the community; the community composition in surface waters is relatively stable over the 5 yr period in terms of species composition but variable in terms of the dominant phytoplankton group (coccolithophores-autotrophic dinoflagellates-diatoms), whereas in the Chlorophyll *a* Maximum the species composition is variable but relatively stable in terms of the dominant phytoplankton group (coccolithophores). These depth differences are hypothesised to be a result of the differences in nutrient supply mechanisms; (i) surface waters are dependent upon the *in-situ* regeneration of nutrients (e.g. ammonia, urea, dissolved organic nitrogen and phosphorus) and episodic new nutrient inputs (e.g. mesoscale eddies, atmospheric inputs, nitrogen-fixation) which are mediated by biological, climatic and hydrographic factors, whereas (ii) deep waters associated with the Chlorophyll *a* Maximum and nutriclines are dependent upon the upward new nutrient (e.g. nitrate, phosphate) fluxes which are primarily derived from the hydrographic environment.

**5.** This study presents the first set of evidence of significant temporal variability of the hydrographic environment (mixed layer depths) in South Atlantic subtropical waters (0 - 30°S), which appears to be associated with temporal variability in the wind speeds in the South Atlantic Ocean (decreases in winter wind speeds during 1996 - 1997). Temporal studies (1995 - 2000) of the phytoplankton community in South Atlantic Subtropical Waters indicate variations in composition, which include; (i) dramatic shallowing of the pigment signature of the low-light prochlorophyte population and an increase in the deep prymnesiophytes and pelagophyte pigment signature during September 1996 (AMT-3), (ii) significant increases of the pigment signatures of prymnesiophytes, pelagophytes and eukaryotic phytoplankton groups in the deep portion of the water-column (60 - 200 m) over the 5 yr time-period of the AMT cruises, (iii) increase in large (>5 μm) phytoplankton species diversity (species richness and evenness of numbers) in both surface waters and the Chlorophyll *a* Maximum during September 1997, which continued to increase until May 2000, (iv) an increase in diatom and autotrophic dinoflagellate biomass and contributions to the total autotrophic nano- and microplankton biomass, and (iv) variability in the biomass and abundance of the oligotrophic coccolithophore species *Umbellosphaera irregularis*, *U. tenuis* and *Umbilicosphaera sibogae*, with maxima occurring in surface waters during September 1996 (AMT-3), May 1997 (AMT-4), September 1997 (AMT-5) and September 1998

(AMT-7). Variability in the hydrographic environment and phytoplankton community composition are not associated with any significant variations in the chlorophyll *a* standing stock of the autotrophic community in South Atlantic Subtropical Waters during the 5 yrs of the AMT programme.

6. It is hypothesised that the temporal variations (1995 - 2000) in the hydrographic environment of the South Atlantic Subtropical Waters (0 - 30°S), possibly as a result of climatic variability, caused changes in the winter nutrient supplies and that the variability detected in the phytoplankton community was a result of (i) a period of extended oligotrophy causing increases in low-nutrient adapted phytoplankton species (*Umbellosphaera irregularis*, *U. tenuis*, and *Umbilicosphaera sibogae?*) and then (ii) a return of winter-mixing during the late AMT cruises which caused an increase in eukaryotic phytoplankton groups (prymnesiophytes, pelagophytes and diatoms). However, at present too little is known of the ecology of the species present in subtropical waters or the factors controlling phytoplankton community structure to fully elucidate these temporal changes.

7. Consideration of the regional mechanisms (hydrographic, nutrients and light) for formation of the Chlorophyll *a* Maximum (CM) and regional differences in the phytoplankton community structure in the subtropical and tropical Atlantic Ocean expand on the basic schemes of vertical chlorophyll *a* profiles proposed by Cullen (1982); (i) in the subtropical gyres of the Atlantic Ocean the CM is formed through photoacclimation (cellular regulation of pigmentation levels) and the CM is a pigment maximum independent of biomass changes (Central Gyre Structure described by Cullen, 1982), (ii) in the tropical equatorial Atlantic Ocean the CM is partly formed through photoacclimation and *in-situ* growth so that the CM represents a pigment and biomass maximum (Typical Tropical Structure as described by Herbland and Voituriez, 1979), and (iii) in the waters of the upwelling zone off NW Africa the CM is typically formed through *in-situ* growth so that the CM represents a biomass maximum, although there is important spatial and temporal variability in the upwelling intensity so that there is considerable variation in the CM structure and community (described by Cullen, 1982, as Seasonal/Upwelling structure). Knowledge of the formation mechanisms and community structure of the CM in different regions of the subtropical and tropical Atlantic Ocean provides a basis for theoretically proposing the rates of organic material lost out of the euphotic zone through sinking (export production) and grazing; from high export production and grazing losses in waters where the CM represent a biomass maximum, to low export production and high grazing losses in waters where the CM represents a pigment maximum only.

## 7.6. Future Work and Recommendations

The results of this thesis shown that the AMT programme (1995 - 2000) is a perfect platform for the investigation of both spatial and temporal variability of phytoplankton community composition. Continuation of the AMT programme (2002 - 2005) will greatly improve the temporal component of this study in terms of variability within the South Atlantic Ocean, as well as continuing to observe and measure the spatial fluctuations in community structure described in this study. However, this study has also identified significant gaps and uncertainties in the measurements and choice of techniques to characterise the phytoplankton community structure.

Methodological: Any future AMT programme, or subtropical time-series study, requires a significant effort to both standardise techniques and compare new and old methodology in both the field and within controlled laboratory conditions. Particularly, (i) What is the magnitude of error associated with the acetone extracted chlorophyll *a* measurements following Holm-Hansen et al., (1965) and Welschmeyer (1994) in high chlorophyll *b* conditions? (ii) Light-microscope measurements of phytoplankton species need to be standardised in terms of species identification and put into a framework of possible sampling errors? and (iii) What are the difference between the HPLC methods of Wright *et al.*, (1991) and Barlow *et al.*, (1997a, b), and how could they effect timeseries measurements?

As well as standardisation of present methodology, there is a requirement to widen and develop new techniques for a fuller characterisation of the phytoplankton community; (i) Examination of large-water volumes (>>10,000 ml) to address questions about the abundance, biomass, distribution and ecological role of large (>100 - 200 μm) phytoplankton, (ii) Epifluorescence techniques to investigate the abundance, distribution and importance of N-fixing symbionts associated with phytoplankton species, (iii) Development of a technique to measure the concentration and abundance of phycobiliproteins associated with cyanophytes and possibly low-light adapted prochlorophytes, (iv) Scanning and Transmission Electron Microscope (SEM/TEM) examination of collected water samples to increase measurements of the coccolithophore community taxonomy and distribution, and investigate the taxonomy of small pico- and nano-eukaryotes; what is the ecological role of small naked dinoflagellates in the subtropical and tropical Atlantic Ocean?, and (v) Expansion of size-fractionated measurements to include pigment (HPLC) measurements to address uncertainties of the origin of the pigment signatures; is the chlorophyll *b* signal in the subtropical and tropical Atlantic Ocean only associated with prochlorophytes (<1 μm) or also with chlorophytes and prasinophytes (>2 - 5 μm)?

Characterisation of the Environment and Community: Improved nutrient measurements would be a significant expansion of the AMT programme. Measurement of the concentrations of nanomolar (nM) inorganic and organic nutrient concentrations would greatly improve our understanding of the nutrient conditions in the subtropical and tropical Atlantic Ocean. Similarly, nutrient enrichment experiments in the field (community) and under controlled laboratory conditions (community isolates) would greatly increase our understanding of the nutrient dynamics and utilisation by the phytoplankton community. Isolation and the provision of mono-specific cultures of subtropical phytoplankton

species (e.g. prochlorophytes, *Umbellosphaera irregularis*) would lead to novel experimentation opportunities. For example, do prochlorophytes utilise dissolved organic nutrient pools? Is *U. irregularis* mixotrophic or does it too utilise dissolved organic nutrient sources? The provision of a prochlorophyte culture would also allow depth-specific physiological and genetic questions to be addressed, as well as allow inter-ocean genetic studies to be carried out. There is also a need to investigate the nutrition of the plankton community in subtropical and tropical waters in terms of the roles of mixotrophy and ozmotrophy in the growth and survival of phytoplankton species.

# References

Agawin, N. S. R., C. M. Duarte and S. Agusti (2000). Nutrient and temperature control of the contribution of picoplankton to phytoplankton biomass and production. Limnology and Oceanography 45, (3), 591-600.

Agusti, S. (1994). Planktonic size structure and the photon budget of the euphotic ocean. Scientia Marina 58, (1-2), 10-117.

Aiken, J., D. Cummings, S. Gibb, N. Rees, R. Wood-Walker, E. Woodward, J. Woolfenden, S. Hooker, J. Berthon, C. Dempsey, D. Suggett, P. Wood, C. Donlan, N. Gonzalez-Benitez, I. Huskin, M. Quevedo, R. Barciela-Fernandez, C. de Vargas and C. McKee (1998). AMT-5 Cruise Report, Rep. No. 206892. NASA Goddard Space Flight Centre, Maryland.

Aiken, J., N. Rees, S. Hooker, P. Holligan, A. Bale, D. Robins, G. Moore, R. Harris and D. Pilgrim (2000). The Atlantic Meridional Transect: Overview and Synthesis of data. Progress in Oceanography 45, (3-4), 257.

Andersen, R., G. Saunders, M. Paskind and J. Sexton (1993). Ultrastructure and 18S Ribosomal-RNA gene sequence for *Pelagomonas calceolata* gen et sp. - nov and the description of a new algal class, the *Pelagophyceae* classis nov. Journal of Phycology 29, (5), 701-715.

Anderson, R. A., R. R. Bidigare, M. D. Keller and M. Latasa (1996). A comparison of HPLC pigment signatures and electron microscopic observations for oligotrophic waters of the North Atlantic and Pacific Oceans. Deep-Sea Research II 43, (2-3), 517-537.

Azam, F., Fenchel, T., Field, J.G., Gray, J.S., Meyer-Reil, L.A., and Thingstad, F. (1983). The Ecological Role of Water-Column Microbes in the Sea. Marine Ecology Progress Series 10, 257 - 263.

Bale, A. and R. Mantoura (1996). AMT-3 Cruise Report,. Plymouth Marine Laboratory (CCMS), Plymouth.

Bale, A. and R. Mantoura (1997). AMT-4 Cruise Report,. Plymouth Marine Laboratory (CCMS), Plymouth.

Banse, K. (1992). Grazing, temporal changes of phytoplankton concentrations, and the microbial loop in the open sea. *In* "Primary Productivity and Biogeochemical cycles in the sea" (P. Falkowski and A. Woodhead, Eds.), Vol. 43. Plenum Press, Pittsburgh.

Banse, K. (1995). Zooplankton: Pivotal role in the control of ocean production. ICES Journal of Marine Science 52, 265-277.

Barber, R.T. and R.L. Smith (1981). Coastal Upwelling Ecosystems. *In* "Analysis of Marine Ecosystems" (A.R. Longhurst, Ed.) pg 31 - 68, Academic Press, London.

Barber, R.T. (2001). Upwelling Ecosystems. *In* "Encyclopedia of Ocean Sciences" (J.H. Steele, K.K. Turekian and S.A. Thorpe, Eds.) pg 3128 - 3135, Vol. 6 (6). Academic Press, San Diego.

Barlow, R., R. Mantoura, M. Gough and T. Fileman (1993). Pigment signatures of the phytoplankton composition in the northeastern Atlantic during the 1990 spring bloom. Deep-Sea Research II 40, (1/2), 459-477.

Barlow, R., R. Mantoura, D. Cummings and T. Fileman (1997a). Pigment chemotaxonomic distributions of phytoplankton during summer in the western Mediterranean. Deep-Sea Research II 44, (3-4), 833-850.

Barlow, R., D. Cummings and S. Gibb (1997b). Improved resolution of mono- and divinyl chlorophylls *a* and *b* and zeaxanthin and lutein in phytoplankton extracts using reverse phase C-8 HPLC. Marine Ecology Progress Series 161, 303-307.

Barlow, R., J. Aiken, P. Holligan, D. Cummings, S. Maritorena and S. Hooker (2002). Phytoplankton pigment and absorption characteristics along meridional transects in the Atlantic Ocean. Deep Sea Research I 49 (4), 637-660.

Barton, E., A. Huyer and R. Smith (1977). Temporal variation observed in the hydrographic regime near Cabo Corveiro in the north-west African upwelling region, February to April 1974. Deep-Sea Research 24, 7-23.

Beers, J., F. Reid and G. Stewart (1982). Seasonal abundance of the microplankton population in the North Pacific Central Gyre. Deep-Sea Research 29, (2A), 227-245.

Behrenfeld, M.J. and P.G. Falkowski (1997). Photosynthetic rates derived from satellite-based chlorophyll concentration. Limnology and Oceanography 42 (1), 1 - 20.

Behrenfeld, M.J., Esaias, W.E., and K.R. Turpie (2002). Assessment of Primary Production at the Global Scale. *In* "Phytoplankton Productivity: Carbon assimilation in marine and freshwater ecosystems" (P.J. le B. Williams, D.N. Thomas and C.S. Reynolds, Eds.) pg 156 - 186, Blackwell Sciences, Oxford.

Berger, W.H. (1989). Global Maps of Ocean Productivity. *In* "Productivity of the Ocean:Past and Present" (W.H. Berger, V.S. Smetacek and G. Wefer, Eds.) pg 429 - 455, John Wiley & Sons Ltd, Dahlem.

Berman-Frank, I., J. Cullen, Y. Shaked, R. Sherrell and P. Falkowski (2001). Iron availability, cellular iron quotas and nitrogen fixation in *Trichodesmium*. Limnology and Oceanography 46, (6), 1249-1260.

Bidigare, R., J. Marra, T. Dickey, R. Iturriaga, K. Baker, R. Smith and H. Pak (1990). Evidence for phytoplankton succession and chromatic adaptation in the Sargasso Sea during spring 1985. Marine Ecology Progress Series 60 (1-2), 113-122.

Biggs, D. C. (1977). Respiration and ammonium excretion by open ocean gelatinous zooplankton. Limnology and Oceanography 22, (1), 108-117.

Bishop, J. and W. Rossow (1991). Spatial and Temporal Variability of Global Surface Solar Irradiance. Journal of Geophysical Research 96, (C9), 16, 839-16, 858.

Bishop, J., W. Rossow and E. Dutton (1997). Surface solar irradiance from the International Satellite Cloud Climatology Project 1983-1991. Journal of Geophysical Research 102, (D6), 6883-6910.

Blanchot, J., M. Rodier and A. LeBouteiller (1992). Effect of El-Nino Southern Oscillation events on the distribution and abundance of phytoplankton in the Western Pacific tropical Ocean along 165-degree-E. Journal of Plankton Research 14, (1), 137 - 156.

Boltovskoy, D. (1999). General biological features of the South Atlantic. *In* "South Atlantic Zooplankton" (D. Boltovskoy, Ed.), Vol. 1, pp. 1-42. Backhuys Publishers, Leiden, The Netherlands.

Bonin, D. and S. Maestrini (1981). Importance of Organic Nutrients for Phytoplankton Growth in Natural Environments: Implications for Algal Species Succession. *In* "Physiological Basis of Phytoplankton Ecology" (T. Platt, Ed.), Vol. 210, pp. 279-291. Canadian Bulletin of Fisheries and Aquatic Sciences.

Brand, L. E. (1994). Physiological ecology of marine coccolithophores. *In* "Coccolithophores" (A. S. Winter, W.G., Ed.). Cambridge University Press, Cambridge.

Bricaud, A., K. Allali, R. Morel, D. Marie, M. Veldhuis, F. Partensky and D. Vaulot (1999). Divinyl chlorophyll a specific absorption coefficients and absorption efficiency factors for *Prochlorococcus marinus*: kinetics of photoacclimation. Marine Ecology Progress Series 188, 21 - 32.

Broekhuizen, N (1999). Simulating motile algae using a mixed Eulerian-Langrangian appraoch: Does motility promote dinoflagellate persistence or co-existence with diatoms? Journal of Plankton Research 21 (7), 1191 - 1216.

Broerse, A.T.C., Brummer, G.J.A., and J.E. van Hinte (2000). Coccolithophore export production in response to monsoonal upwelling off Somalia (northwestern Indian Ocean). Deep Sea Resarch II 47 (9 - 11), 2179 - 2205.

Brown, J., A. Colling, D. Park, J. Phillips, D. Rothery and J. Wright (1989a). Ocean Circulation, First/Ed. Pergman Press, Oxford.

Brown, J., A. Colling, D. Park, J. Phillips, D. Rothery and J. Wright (1989b). Seawater: Its composition, properties and behavious, First/Ed. Pergman Press, Oxford.

Bustillosguzman, J., H. Clauste and J. Marty (1995). Specific phytoplankton signatures and their relationship to hydrographic conditions in the coastal northwestern Mediterranean Sea. Marine Ecology Progress Series 124 (1 - 3), 247 - 258.

Calbert, A. and M. Landry (1999). Mesozooplankton influences on the microbial food web: Direct and indirect trophic interactions in the oligotrophic open ocean. Limnology and Oceanography 44, (6), 1370-1380.

Campbell, L. and D. Vaulot (1993). Photosynthetic picoplankton community structure in the subtropical North Pacific Ocean near Hawaii (station ALOHA). Deep Sea Research I 40, (10), 2043 - 2060.

Campbell, L., H. Nolla and D. Vaulot (1994). The importance of *Prochlorococcus* to community structure in the central North Pacific Ocean. Limnology and Oceanography 39, (4), 954 - 961.

Campbell, L., L. Hongbin, H. Nolla and D. Vaulot (1997). Annual variability of phytoplankton and bacteria in the subtropical North Pacific Ocean at Station ALOHA during the 1991-1994 ENSO event. Deep-Sea Research Part I 44, (2), 167-192.

Canellas, M., Agusti, S. and C.M. Duarte (2000). Latitudinal variability in phosphate uptake in the central Atlantic. Marine Ecology Progress Series 194, 283 - 294.

Capone, D., M. Ferrier and E. Carpenter (1994). Amino Acid Cycling in Colonies of the Planktonic Marine Cyanobacterium *Trichodesmium thiebautii*. Applied and Environmental Microbiology 60, (11), 3989-3995.

Capone, D., J. Zehr, H. Paerl, B. Bergman and E. Carpenter (1997). *Trichodesmium*, a Globally Significant Marine Cyanobacterium. Science 276, 1221-1229.

Carlson, C. and H. Ducklow (1994). Growth of bacterioplankton and consumption of dissolved organic carbon in the Sargasso Sea. Aquatic Microbial Ecology 10, (1), 69-85.

Carlson, C., H. Ducklow and A. Michaels (1994). Annual flux of dissolved organic carbon from the euphotic zone in the northwestern Sargasso Sea. Nature 371, (6496), 405-408.

Carpenter, E. J. (1983a). Physiology and Ecology of Marine Planktonic *Oscillatoria* (*Trichodesmium*). Marine Biology Letters 4, 69-85.

Carpenter, E. (1983b). Nitrogen Fixation by marine *Oscillatoria* (*Trichodesmium*) in the World's Oceans. *In* "Nitrogen in the Marine Environment". Academic Press, Inc.

Carpenter, E. J. and K. Romans (1991). Major Role of Cyanobacterium *Trichodesmium* in Nutrient Cycling in the North Atlantic Ocean. Science 254, 1356-1358.

Carpenter, E. and S. Janson (2000). Intracellular cyanobacterial symbionts in the marine diatom *Climacodium frauenfeldianum* (*Bacillariophyceae*). Journal of Phycology 36, 540-544.

Cavender-Bares, K. K., A. Rinaldo and S. W. Chisholm (2001). Microbial size spectra from natural and nutrient enriched ecosystems. Limnology and Oceanography 46, (4), 778-789.

Chapman, P. and S. Mostert (1990). Does Freezing of Nutrient Samples cause analytical errors? South African Journal of Marine Science 9, 239-247.

Chavez, F., K. Buck, R. Bidigare, D. Karl, D. Hebel, M. Latasa, L. Campbell and J. Newton (1995). On the chlorophyll *a* retention properties of glass fibre GF/F filters. Limnology and Oceanography 40, (2), 428 - 433.

Chisholm, S. (1992). Phytoplankton size. *In* "Primary Productivity and Biogeochemical cycles in the sea" (P. Falkowski and A. Woodhead, Eds.), Vol. 43, pp. 213-237. Plenum Press, Pittsburgh.

Chisholm, S. W., R. J. Olson, E. R. Zettler, J. Waterbury, R. Goericke and Welschmeyer (1988). A novel free-living prochlorophyte abundant in the oceanic euphotic zone. Nature 334, 340-343.

Church, M., H. Ducklow and D. Karl (2002). Multiyear increases in dissolved organic matter inventories at Station ALOHA in the North Pacific Subtropical Gyre. Limnology and Oceanography 47, (1), 1-10.

Clarke, K. and R. Warwick (1994). Change in marine communities: an approach to statistical analysis and interpretation., Second/Ed. Plymouth Marine Laboratory, Plymouth.

Claustre, H. and J. Marty (1995). Specific phytoplankton biomasses and their relation to primary production in the tropical North Atlantic. Deep-Sea Research I 42, (8), 1475-1493.

Climate Variability (CLIVAR) (1997). The CLIVAR Implementation Plan. http://www.clivar.org/publications/other_pubs/iplan/brochure/contents.htm.

Conkright, M., W. Gregg and S. Levitus (2000). Seasonal cycle of phosphate in the open ocean. Deep-Sea Research Part I 47, (2), 159-175.

Cortes, M. Y., J. Bollmann and H. R. Thierstein (2001). Coccolithophore ecology at the HOT station ALOHA, Hawaii. Deep-Sea Research II 48 (8 - 9), 1957-1981.

Cros, L., A. Kleijne, A. Zeltner, C. Billard and J. Young (2000). New examples of holococcolith-heterococcolith combination coccospheres and their implications for coccolithophorid biology. Marine Micropaleontology 39, (1-4), 1 - 34.

Cullen, J. and S. Horrigan (1981). Effects of nitrate on the diurnal vertical migration, carbon to nitrogen ratio, and photosynthetic capacity of the dinoflagellate *Gymnodinium splendens*. Marine Biology 62, 81 - 89.

Cullen, J. J. (1982). The Deep Chlorophyll Maximum: Comparing Vertical Profiles of Chlorophyll *a*. Canadian Journal of Fisheries and Aquatic Sciences 39, 791-803.

Cushing, D.H. (1971). Upwelling and the production of fish. Advances in Marine Biology 9, pg 255 -334.

Curtin, F. and Schulz, P. (1998). Multiple correlations and Bonferroni's correction. Biological Psychiatry, 44: 775 - 777.

Cury, P., A. Bakun, R. Crawford, A. Jarre, R. Quinones, L. Shannon and H. Verheye (2000). Small pelagics in upwelling systems: patterns of interaction and structural changes in "wasp-waist" ecosystems. ICES Journal or Marine Science 57, (3), 603 - 618.

Dandonneau, Y. and L. Lemasson (1987). Water-column chlorophyll in an oligotrophic environment: correction for the sampling depths and variations of the vertical structure of density, and observation of a growth period. Journal of Plankton Research 9, (1), 215-234.

del Girorgio, P.A., J.J. Cole, and Cimbleris, A. (1997). Respiration rates in bacteria exceed phytoplankton production in unproductive aquatic systems. Nature 385 (6612), 148 - 151.

DeMaster, D.J. (2001). Marine Silica Cycle. *In* "Encyclopedia of Ocean Sciences" (J.H. Steele, K.K. Turekian, S.A. Thorpe, Eds.), Vol. 4 (6), Academic Press, San Diego.

Dodge, J.D. (1982). Marine Dinoflagellates of the British Isles. Her Majesty's Stationary Press, London.

Doney, S., D. Glover and R. Najjar (1996). A new coupled, one-dimensional biological-physical model for the upper ocean: Applications to the JGOFS Bermuda Atlantic Time-series Study (BATS) site. Deep-Sea Research II 43, (2-3), 591-624.

Duarte, C., S. Agusti, J. Aristegui, N. Gonzalez and R. Anadon (2001). Evidence for a heterotrophic subtropical northeast Atlantic. Limnology and Oceanography 46, (2), 425-428.

Dugdale, R. and J. Goering (1967). Uptake of new and regenerated forms of nitrogen in primary productivity. Limnology and Oceanography 12, 196-206.

Dugdale, R. (1967). Nutrient limitation in the sea: dynamics, identification, and significance. Limnology and Oceanography 12, 685 - 695.

Durand, M. D., R. J. Olson and S. W. Chisholm (2001). Phytoplankton population dynamics at the Bermuda Atlantic Time-series station in the Sargasso Sea. Deep-Sea Research II 48 (8 - 9), 1983-2003.

Elliott, J., S. Jewson and R. Sutton (2001). The impact of the 1997/98 El Nino event on the Atlantic Ocean. Journal of Climate 14, (6), 1069 - 1077.

Eppley, R.W. (1972). Temperature and phytoplankton growth in the Sea. Fishery Bulletin 70 (4), 1063 - 1085.

Eppley, R.W., E. Renger, E. Venrick and M. Mullin (1973). A study of plankton dynamics and nutrient cycling in the central gyre of the North Pacific Ocean. Limnology and Oceanography 18, (4), 534-551.

Eppley, R.W. (1981a). Autotrophic Production of Particulate Matter. *In* "Analysis of Marine Ecosystems" (A. Longhurst, Ed.), pp. 343-357. Academic Press, London.

Estrada, M., C. Marrase, M. Latasa, E. Berdalet, M. Delgado and T. Riera (1993). Variability of deep chlorophyll maximum characteristics in the Northwestern Mediterranean. Marine Ecology Progress Series 92 (3), 289-300.

Eynaud, F., J. Giraudeau, J. Pichon and C. Pudsey (1999). Sea-surface distribution of coccolithophores, diatoms, silicoflagellates and dinoflagellates in the South Atlantic Ocean during the late austral summer 1995. Deep-Sea Research I 46 (3), 451-482.

Falkowski, P., R. Greene and R. Geider (1992). Physiological limitations on phytoplankton productivity in the Ocean. Oceanography 5, (2), 84-91.

Falkowski, P. (1994). The Role of Phytoplankton photosynthesis in global biogeochemical cycles. Photosynthesis Research 39, (3), 235-258.

Falkowski, P. and J. Raven (1997). Aquatic Photosynthesis, Blackwell Science, USA.

Fernanadez, E., E. Maranon, D. S. Harbour and R. D. Pingree (1994). Phytoplankton carbon incorporation patterns and biochemical composition of particulate matter in the eastern North Atlantic subtropical region. Journal of Plankton Research 16, (12), 1627-1644.

Fogg, G.E. (1986). Review Lecture: Picoplankton. Proceedings of the Royal Society of London. Series B: Biological Sciences, Vol. 288 (1250), pg 1 - 30.

Fogg, G.E. (1995). Some comments on picoplankton and its importance in the pelagic ecosystem. Aquatic Microbial Ecology 9, (1), 33 - 39.

Foss, P., R. Guillard and S. Liaaenjensen (1986). Algal Carotenoids. 34. Carotenoids from Eukaryotic Ultraplankton clones (Prasinophyceae). Phytochemistry 25, (1), 119 - 124.

Fowler, J. and L. Cohen (1993). Practical Statistics for Field Biology, Third/Ed. John Wiley and Sons Ltd, Chichester, England.

Furuya, K. and R. Marumo (1983). The structure of the phytoplankton community in the subsurface chlorophyll maxima in the western North Pacific Ocean. Journal of Plankton Research 5, (3), 393-406.

Geider, R.J. (1997). Photosynthesis or planktonic respiration. Nature 388 (6638), 132 - 132

Gibb, S. W., R. G. Barlow, D. G. Cummings, N. W. Rees, C. C. Trees, P. Holligan and D. Suggett (2000). Surface phytoplankton pigment distributions in the Atlantic Ocean: An Assessment of basin scale variability between 50°N and 50°S. Progress in Oceanography 45, (3-4), 339.

Gibb, S., D. Cummings, X. Irigoien, R. Barlow and R. Mantoura (2001). Phytoplankton pigment chemotaxonomy of the northeastern Atlantic. Deep-Sea Research II 48 (4 - 5), 795-823.

Gieskes, W. W., G. W. Kraay and S. B. Tijssen (1978). Chlorophylls and their degradation products in the deep pigment maximum layer of the tropical North Atlantic. Netherlands Journal of Sea Research 12, 195-204.

Gieskes, W. W. and G. W. Kraay (1986). Floristic and physiological differences between the shallow and the deep nanophytoplankton community in the eutrophic zone of the open tropical Atlantic revealed by HPLC analysis of pigments. Marine Biology 91, 567-576.

Glibert, P. and D. Bronk (1994). Release of Dissolved Organic Nitrogen by Marine Diazotrophic Cyanobacteria, *Trichodesmiu*m spp. Applied and Environmental Microbiology 60, (11), 3996-4000.

Glover, H.E., Prezelin, B.B., Campbell, L., and M. Wyman (1988). Pico- and ultraplankton Sargasso Sea communities: variability and comparative distributions of *Synechococcus* spp. and alge. Marine Ecology Progress Series 49 (1 - 2), 127 - 139.

Goericke, R. and D. J. Repeta (1993). Chlorophylls *a* and *b* and divinyl chlorophylls *a* and *b* in the open subtropical North Atlantic Ocean. Marine Ecology Progress Series 101 (3), 307-313.

Goericke, R. and N. Welschmeyer (1998b). Response of Sargasso Sea phytoplankton biomass, growth rates and primary production to seasonally varying physical forcing. Journal of Plankton Research 20 (12), 2233-2249.

Goldman, J.C., J. McCarthy and D. Peavey (1979). Growth rate influence on the chemical composition of phytoplankton in oceanic waters. Nature 279, (17 May), 210-215.

Goldman, J.C. and P.M. Glibert (1983). Kinetics of Inorganic Nitrogen Uptake by Phytoplankton. *In* "Nitrogen in the Marine Environment" (E.J. Carpenter and D.G. Capone, Eds.). pg 233 - 269, Academic Press, New York.

Gould, R. W. (1987). The Deep Chlorophyll maximum in the world ocean: a review. The Biologist 66, (1-4), 4-13.

Haidar, A. T. and H. R. Thierstein (2001). Coccolithophore dynamics off Bermuda (N. Atlantic). Deep-Sea Research II 48 (8 - 9), 1925-1956.

Hansen, D. and C. Carlson (1998). Net community production of dissolved organic carbon. Global Biogeochemical Cycles 12, (3), 443-453.

Hansen, D. A. and C. A. Carlson (2001). Biogeochemistry of total organic carbon and nitrogen in the Sargasso Sea: control by convective overturn. Deep-Sea Research II 48, 1649-1667.

Hansen, P. and T. Nielsen (1997). Mixotrophic feeding of *Fragilidium subglobosum* (*Dinophyceae*) on three species of *Ceratium*: effects of prey concentration, prey species and light intensity. Marine Ecology Progress Series 147 (1 - 3), 187-196.

Harrison, W. (1991). Regeneration of nutrients. *In* "Primary Productivity and Biogeochemical cycles in the sea" (P. Falkowski and A. Woodhead, Eds.), Vol. 43, pp. 385-407. Plenum Press, Pittsburgh.

Hasle, G. (1978). The inverted microscope method. *In* "Phytoplankton Manual" (A. Sournia, Ed.), Vol. 6. UNESCO, Paris.

Hayward, T. and E. Venrick (1982). Relation between surface chlorophyll, integrated chlorophyll and integrated primary production. Marine Biology 69, (3), 247 - 252.

Hayward, T., E. Venrick and J. McGowan (1983). Environmental heterogeneity and plankton community structure in the central North Pacific. Journal of Marine Research 41, 711-729.

Herbland, A. and B. Voituriez (1979). Hydrological structure analysis for estimating the primary production in the Atlantic Ocean. Journal Marine Research 137, 87-101.

Herbland, A. and A. Le Bouteiller (1981). The size distribution of phytoplankton and particulate organic matter in the Equatorial Atlantic Ocean: importance of ultraseston and consequences. Journal of Plankton Research 3 (4), 659 - 673.

Herbland, A. Le Bouteiller, A., and P. Raimbault (1985). Size structure if phytoplankton biomass in the equatorial Atlantic Ocean. Deep Sea Research I 32, 819 - 836.

Herbland, A., Le Bouteiller, A. and P. Raimbault (1987). Does the nutrient enrichment of the equatorial upwelling influence the size structure of phytoplankton in the Atlantic Ocean? Oceanologica Acta: Proceedings of the International Symposium on Equatorial Vertical Motion, Paris, 6 -10 May, 1985. Vol. 6 (SP) 115 - 120.

Hidalgo-Gonzalez, R. and S. Alvarez-Borrego (2001). Chlorophyll profiles and the water column structure in the Gulf of California. Oceanologica Acta 24, (1), 19 - 28.

Holm-Hansen, O., C. Lorenzen, R. Holmes and J. Strickland (1965). Fluorometric Determination of Chlorophyll. Journal de Conseil International Pour l'Exploration de la Mer 30, (1), 3 - 15.

Hood, R., A. Michaels and D. Capone (2000). Answers Sought to the Enigma of Marine Nitrogen Fixation. EOS 81, (13), 133-138.

Hooker, S., N. Rees and J. Aiken (2000). An objective methodology for identifying oceanic provinces. Progress in Oceanography 45, (3-4), 313.

Hutchinson, G. E. (1961). The Paradox of the Plankton. The American Naturalist XCV, (882), 137-145.

Innocentini, V. and E. Neto (1996). A Case Study of the 9 August 1988 South Atlantic Storm: Numerical Stimulations of the Wave Activity. Weather and Forecasting 11, (1), 78-88.

Iriarte, A. and D. Purdie (1993). Photosynthesis and growth response of the oceanic picoplankter *Pyncnococcus provasoli* Guillard (Clone Omega 48-23; *Chlorophyta*) to variations in irradiance, photoperiod and temperature. Journal of Experimental Marine Biology and Ecology 239 - 257.

Irigoien, X., B. Meyer-Harms, R. Harris and D. Harbour (submitted). Using HPLC pigment analysis and CHEMTAX to investigate phytoplankton taxonomy: the importance of knowing your species. Marine Ecology Progress Series.

Jackson, G. A. (1980). Phytoplankton growth and zooplankton grazing in oligotrophic waters. Nature 284, 439-441.

James, F. C. and C. E. McCulloch (1990). Multivariate Analysis in Ecology and Systematics: Panacea or Pandora's Box? Annual Review of Ecological Systems 21, 129-166.

Jeffrey, S.W. and G. Humphrey (1975). New spectrophotometric equations for determining chlorophylls *a*, *b*, $c_1$ and $c_2$ in higher plants, algae and natural phytoplankton. Biochemical Physiology Pflanzen 167, (191 - 194).

Jeffrey, S.W., Mantoura, R.F.C. and S.W. Wright (1997). Phytoplankton Pigments in Oceanography, UNESCO, Paris.

Jeffrey, S.W. and Vesk, M. (1997). Introduction to marine phytoplankton and their pigment signatures. *In* "Phytoplankton pigments in oceanography" (S. W. Jeffrey, Mantoura, R.F.C. and Wright, S.W., Eds.), Vol. 10, pp. 127-166. UNESCO, Paris.

Jeffrey, S.W. (1997). Application of pigment methods to oceanography. *In* "Phytoplankton pigments in oceanography" (S. W. Jeffrey, Mantoura, R.F.C. and Wright, S.W., Ed.), Vol. 10, pp. 127-166. UNESCO, Paris.

Jeffrey, S. W., H. MacTavish, W. Dunlap, M. Vesk and K. Groenewoud (1999). Occurrence of UVA- and UVB-absorbing compounds in 152 species (206 strains) of marine microalgae. Marine Ecology Progress Series 189, 35-51.

Jeong, H., C. Lee, Y. WH and J. Kim (1997). *Fragilidium* cf. *mexicanum*, a thecate mixotrophic dinoflagellate which is prey for and a predator on co-occurring thecate heterotrophic dinoflagellate *Protoperidinium* cf. *divergens*. Marine Ecology Progress Series 151 (1 - 3), 229-305.

Jocham, F. and B. Zeitzschel (1993). Productivity regime and phytoplankton size structure in the tropical and subtropical North Atlantic in Spring 1989. Deep Sea Research Part II - Topical Studies in Oceanography 40, (1 - 2), 495 - 519.

Joseph, L., Villareal, T.A., and F. Lipschultz (1997). A high sensitivity nitrate reductase assay and its application to vertically migrating *Rhizosolenia* mats. Aquatic Microbial Ecology 12 (1), 95 - 104.

Jordan, R. W. (1988). Coccolithophorid Communities in the North East Atlantic. PhD Thesis, University of Surrey.

Jumars, P., D. Penry, J. Baross, M. Perry and B. Frost (1989). Closing the Microbial loop: dissolved carbon pathway to heterotrophic bacteria from incomplete ingestion, digestion and absorption in animals. Deep-Sea Research 36, (4), 483-495.

Kahru, M., S. Nommann and B. Zeitzschel (1991). Particle (Plankton) size structure across the Azores Front (Joint Global Ocean Flux Study North Atlantic Bloom Experiment). Journal of Geophysical Research - Oceans 96, (C4), 7083 - 7088.

Kana, T. and P. Glibert (1987a). Effect of irradiances up to 2000 $\mu E\ m^{-2}\ s^{-1}$ on marine *Synechococcus* WH7803 - I. Growth, pigmentation and cell composition. Deep-Sea Research 34 (4), 479-495.

Kana, T. and P. Glibert (1987b). Effect of irradiances up to 2000 $\mu E\ m^{-2}\ s^{-1}$ on marine *Synechococcus* WH7803 - II. Photosynthetic responses and mechanisms. Deep-Sea Research 34, (4), 497-516.

Kana, T., P. Glibert, R. Goericke and N. Welschmeyer (1988). Zeaxanthin and Beta-carotene in *Synechococcus* WH7803 respond differently to irradiance. Limnology and Oceanography 33, (6/2), 1623-1627.

Karl, D., R. Letelier, D. Hebel, L. Tupas, J. Dore, J. Christian and C. Winn (1995). Ecosystem changes in the North Pacific Subtropical Gyre attributed to the 1991-92 El-Nino. Nature 373, (6511), 230 - 234.

Karl, D., D. Hebel, K. Bjorkman and R. Letelier (1998). The role of dissolved organic matter release in the productivity of the oligotrophic North Pacific Ocean. Limnology and Oceanography 43, (6), 1270-1286.

Karl, D. M. (1999). A Sea of Change: Biogeochemical Variability in the North Pacific Subtropical Gyre. Ecosystems 2, 181-214.

Karl, D. M., R. R. Bidigare and R. M. Letelier (2001a). Long-term changes in plankton community structure and productivity in the North Pacific Subtropical Gyre: The domain shift hypothesis. Deep-Sea Research II 48 (8 - 9), 1449-1470.

Karl, D.M. and A.F. Michaels (2001c). Nitrogen Cycle. *In* "Encyclopedia of Ocean Sciences" (J.H. Steele, K.K. Turekian and S.A. Thorpe, Eds.) Vol. 4 (6) pg 1876 - 1884, Academic Press, San Diego.

Karl, D., R. Bidigare and R. Letelier (2002b). Sustained and Aperiodic Variability in Organic Matter Production and Phototrophic Microbial Community Structure in the North Pacific Subtropical Gyre. *In* "Phytoplankton Productivity: Carbon assimilation in marine and freshwater ecosystems" (P. Williams, D. Thomas and C. Reynolds, Eds.), pp. 386. Blackwell Science, Oxford.

Keil, R. and D. Kirchman (1999). Utilisation of dissolved protein and amino acids in the northern Sargasso Sea. Aquatic Microbial Ecology 18, (3), 293-300.

Kemp, A. E. S., J. Pike, R. B. Pearce and C. B. Lange (2000). The "Fall dump" - a new perspective on the role of a "shade flora" in the annual cycle of diatom production and export flux. Deep-Sea Research II 47 (9 - 11), 2129-2154.

Kinkel, H., K.-H. Baumann and M. Cepek (2000). Coccolithophores in the equatorial Atlantic Ocean: response to seasonal and Late Quaternary surface water variability. Marine Micropaleontology 39 (1-4), 87-112.

Kiorbe, T. (1993). Turbulence, Phytoplankton Cell Size, and the Structure of Pelagic Food Webs. Advances in Marine Biology 29, 2 - 72.

Kirk, J. (1992). The nature and measurement of the light environment in the ocean. *In* "Primary Productivity and Biogeochemical cycles in the sea" (P. Falkowski and A. Woodhead, Eds.), Vol. 43, pp. 9-29. Plenum Press, Pittsburgh.

Kirk, J. T. O. (1994). Light and photosynthesis in aquatic ecosystems, Cambridge University Press, Cambridge.

Kleijne, A. (1993). Morphology, Taxonomy and Distribution of Extant Coccolithophorids (Calcareous Nannoplankton), Vrije Universiteit, Amsterdam.

Klein, P. and B. Coste (1984). Effects of wind stress variability on nutrient transport into the mixed layer. Deep-Sea Research 31, (1), 21-37.

Knauss, J. (1996). Chapter 2: A Stratified Ocean. *In* "Introduction to Physical Oceanography". Pearson.

Kovala, P. and J. Larrence (1966). Computation of Phytoplankton Number, Cell Volume, Cell Surface and Plasma Volume per Litre, from microscopical counts,. Office of Naval Research, Seattle, Washington.

Latasa, M., R. R. Bidigare, M. E. Ondrusek and M. Kennicutt (1996). HPLC analysis of algal pigments - a comparison exercise among laboratories and recommendations for improved analyptical performance. Marine Chemistry 51, 4315 - 4324.

Le Bouteiller, A. (1986). Environmental control of nitrate and ammonium uptake by phytoplankton in the Equatorial Atlantic Ocean. Marine Ecology Progress Series 30, 167-179.

Legrand, C., N. Johansson, G. Johnsen, K. Borsheim and E. Graneli (2001). Phagotrophy and toxicity variation in the mixotrophic *Prymnesium patelliferum* (*Haptophyceae*). Limnology and Oceanography 46, (5), 1209-1214.

Lessard, E. J. and E. Swift (1986). Dinoflagellates from the North Atlantic classified as phototrophic or heterotrophic by epifluorescence microscopy. Journal of Plankton Research 8, 1209-1215.

Letelier, R., R. Bidigare, D. Hebel, M. Ondrusek, C. Winn and D. Karl (1993). Temporal variability of Phytoplankton community structure - based on pigment analysis. Limnology and Oceanography 38, (7), 1420 - 1437.

Letelier, R., D. Karl, M. Abbott, P. Flament, M. Freilich, R. Lukas and T. Strub (2000). Role of late winter mesoscale events in the biogeochemical variability of the upper water column of the North Pacific Subtropical Gyre. Journal of Geophysical Research-Oceans 105, (C12), 28723 - 28739.

Li, A., D. Stoecker and J. Adolf (1999). Feeding, pigmentation, photosynthesis and growth of the mixotrophic dinoflagellate *Gyrodinium galatheanum*. Aquatic Microbial Ecology 19, (2), 163-176.

Lincoln, R., G. Boxshall and P. Clark (1998). A Dictionary of Ecology, Evolution and Systematics, Second Edition/Ed. University Press, Cambridge.

Litchman, E., Neale, P.J. and A.T. Banaszak (2002). Increased sensitivity to Ultraviolet radiation in nitrogen-limited dinoflagellates: Photoprotection and repair. Limnology and Oceanography 47 (1), 86-97

Longhurst, A. (1976). Interactions between zooplankton and phytoplankton profiles in the eastern tropical Pacific Ocean. Deep-Sea Research 23, 729-754.

Longhurst, A. and D. Pauly (1987). Ecology of Tropical Oceans, Academic Press, San Diego.

Longhurst, A. (1993). Seasonal cooling and blooming in tropical oceans. Deep-Sea Research I 40, (11/12), 2145-2165.

Longhurst, A. and W. G. Harrison (1989). The biological pump: Profiles of plankton production and consumption in the upper ocean. Progress in Oceanography 22, 47-123.

Longhurst, A., Sathyendranath, S., Platt, T. and C. Caverhill (1995). An estimate of global primary production in the ocean from satellite radiometer data. Journal of Plankton Research 17 (6), 1245 - 1271.

Longhurst, A. (1998). Ecological Geography of the Sea, Academic Press, London.

Lorenzen, C. (1967). Vertical distribution of chlorophyll and phaeopigments: Baja California. Deep-Sea Research 14, 735-745.

Mackey, M. D., D. J. Mackey, H. W. Higgins and S. W. Wright (1996). CHEMTAX - a program for estimating class abundances from chemical markers: application to HPLC measurements of phytoplankton. Marine Ecology Progress Series 144, 265-283.

Magurran, A. (1988). Ecological Diversity and Its Measurement, Chapman & Hall, London.

Maranon, E. and P. M. Holligan (1999). Photosynthetic parameters of phytoplankton from 50N to 50S in the Atlantic Ocean. Marine Ecology Progress Series 176, 191-203.

Maranon, E., P. Holligan, M. Varela, B. Mourino and A. Bale (2000). Basin-scale variability of phytoplankton biomass, production and growth in the Atlantic Ocean. Deep-Sea Research I 47, (5), .

Maranon, E., P. Holligan, R. Barciela, N. Gonzalez, B. Mourino, M. Pazo and M. Varela (2001). Patterns of phytoplankton size-structure and productivity in contrasting open ocean environments. Marine Ecology Progress Series 216, 43-56.

Margalef, R. (1978). Life forms of phytoplankton as survival alternatives in an unstable environment. Oceanologica Acta 1, (4), 493-509.

McCarthy, J. and J. Goldman (1979). Nitrogenous Nutrition of Marine Phytoplankton in Nutrient-Depleted Waters. Science 203, (16 February), 670-672.

McGillicuddy, D. and A. Robinson (1997). Eddy-induced nutrient supply and new production in the Sargasso Sea. Deep-Sea Research Part I 44, (8), 1427-1450.

McGillicuddy, D., A. Robinson, D. Siegal, H. Jannasch, R. Johnson, T. Dickey, J. McNeil, A. Michaels and A. Knap (1998). Influence of mesoscale eddies on new production in the Sargasso Sea. Nature 394, (16 July 1998), 263-266.

McGowan, J. (1977). What Regulates Pelagic Community Structure in the Pacific? *In* "Oceanic Sound Scattering Prediction" (Andersen, Ed.), pp. 423 - 443. Plenum Press.

McGowan, J. and T. Hayward (1978). Mixing and Oceanic Productivity. Deep-Sea Research 25, 771-793.

McGowan, J. and P. Walker (1985). Dominance and Diversity Maintenance in an Oceanic Ecosystem. Ecological Monographs 55, (1), 103-118.

McManus, G. B. and R. Dawson (1994). Phytoplankton pigments in the deep chlorophyll maximum of the Caribbean Sea and the western tropical Atlantic Ocean. Marine Ecology Progress Series 113, 199-206.

Medlin, L., M. Lange and E. Nothig (2000). Genetic diversity in marine phytoplankton: a review and a consideration of Antarctic phytoplankton. Antarctic Science 12, (3), 325-333.

Mehta, V. (1998). Variability of the Tropical Ocean Surface Temperatures at Decadal-Multidecadel Timescales. Part I: The Atlantic Ocean. Journal of Climate 11, (9), 2351-2375.

Metzler, P., P. Glibert, S. Gaeta and J. Ludlam (1997). New and regenerated production in the South Atlantic off Brazil. Deep-Sea Research Part I 44, (3), 363-384.

Michaels, A. and M. Silver (1988). Primary production, sinking fluxes and the microbial food web. Deep-Sea Research 35, (473-490), .

Migon, C. and V. Sandroni (1999). Phosphorus in rainwater: Partitioning inputs and impact on the surface coastal ocean. Limnology and Oceanography 44, (4), 1160-1165.

Millie, D., H. Paerl and J. Hurley (1993). Microalgal pigment assessments using High-Performance Liquid Chromatography: A synopsis of organismal and ecological applications. Canadian Journal of Fisheries and Aquatic Science 50, 2513-2527.

Mills, E. (1989). Biological Oceanography: An Early History, 1870-1960, Cornell University Press, Ithaca and London.

Mitchell-Innes, B., N. Silulwane and M. Lucas (2001). Variability of chlorophyll profiles on the west coast of southern Africa in June/July 1999. South African Journal of Science 97, (5 - 6), 246 - 250.

Monger, B., C. McClain and R. Murtugudde (1997). Seasonal phytoplankton dynamics in the eastern tropical Atlantic. Journal of Geophysical Research - Oceans 102, (C6), 12, 389 - 14, 411.

Moore, J. and T. Villareal (1996). Buoyancy and growth characteristics of three positively buoyant marine diatoms. Marine Ecology Progress Series 132, 203-213.

Moore, L. and S. Chisholm (1999). Photophysiology of the marine cyanobacterium *Prochlorococcus*: Ecotypic difference among cultured isolates. Limnology and Oceanography 44, (3), 628-638.

Muller-Karger, F. (1988). The dispersal of the Amazon's water. Nature 333, 56 - 59.

Murty, V., G. Gupta, V. Sarma, B. Rao, D. Jyothi, P. Shastri and Y. Supraveena (2000). Effect of vertical stability and circulation on the depth of the chlorophyll maximum in the Bay of Bengal during May-June, 1996. Deep Sea Resarch-I 47, (5), 859 - 873.

Odum, E.P. (1971). Fundamentals of Ecology. 574 pg, W.B. Saunders Company, Philadelphia.

Ohki, K. and S. Honjho (1997). Oceanic picophytoplankton having a high abundance of chlorophyll *b* in the major light harvesting chlorophyll protein complex. Photosynthesis Research 121 - 127.

Olson, R. J., S. W. Chisholm, E. R. Zettler, M. A. Altabet and J. A. Dusenberry (1990). Spatial and temporal distributions of prochlorophyte picoplankton in the North Atlantic Ocean. Deep-Sea Research I 37, (6), 1033-1051.

Ondrusek, M., R. Bidigare, S. Sweet, D. Defreitas and J. Brooks (1991). Distribution of phytoplankton pigments in the North Pacific Ocean in relation to physical and optical variability. Deep-Sea Research I 243 - 266.

Paerl, H., R. J and M. MA (1990). Stimulation of phytoplankton production in coastal waters by natural rainfall inputs: nutritional and trophic implications. Marine Biology 107, 247-254.

Paerl, H., J. Willey, M. Go, B. Peierls, J. Pinckney and M. Fogel (1999). Rainfall stimulation of primary production in western Atlantic Ocean waters: roles of different nitrogen sources and co-limiting nutrients. Marine Ecology Progress Series 176, 205-214.

Pahlow, M, Riesbesell, U. and D.A. Wolf-Gladrow (1997). Impact of cell shape and chain formation on nutrient acquisition by marine diatoms. Limnology and Oceanography 42 (8), 1660 - 1672.

Pan, Y., M. Parsons, M. Busman, P. Moeller, Q. Dortch, C. Powell and G. Douchette (2001). *Pseudo-nitzschia* sp. cf. *pseudodelicatissima* - a confirmed producer of domoic acid from the northern Gulf of Mexico. Marine Ecology Progress Series 83, 83 - 92.

Parsons, T., M. Takahashi and B. Hargrave (1984). Biological Oceanographic Processes, Third Edition/Ed. Butterworth Heinemann, Oxford.

Partensky, F., N. Hoepffner, W. Li, O. Ulloa and D. Vaulot (1993). Photoacclimation of *Prochlorococcus* sp. (Prochlorophyta) Stains Isolated from the North Atlantic and Mediterranean Sea. Plant Physiology 101, (1), 285 - 296.

Partensky, F., J. Blanchot, F. Lantoine, J. Neveux and D. Marie (1996). Vertical structure of picoplankton at different trophic sites of the tropical northeastern Atlantic Ocean. Deep-Sea Research I 43, (8), 1191-1213.

Passow, U. and R. Peinert (1993). The role of plankton in particle flux - 2 Case studies from the Northeast Atlantic. Deep Sea Research Part II - Topical Studies in Oceanography 40, (1 - 2), 573 - 585.

Penno, S., L. Campbell and W. Hess (2000). Presence of phycoerythrin in two strains of *Prochlorococcus* (Cyanobacteria) isolated from the subtropical North Pacific Ocean. Journal of Phycology 36, 723-729.

Pingree, R., P. Pugh, P. Holligan and G. Forster (1975). Summer phytoplankton blooms and red tides along tidal fronts in the approaches to the English Channel. Nature 258, 672 - 677.

Pitcher, C. and D. Calder (2000). Harmful algal blooms of the southern Benguela Current: a review and appraisal of monitoring from 1989 to 1997. South African Journal of Marine Sciences 22, 255 - 271.

Planas, D., S. Agusti, C. Duarte, T. Granata and M. Merino (1999). Nitrate uptake and diffusive supply in the Central Atlantic. Limnology and Oceanography 44, (1), 116-126.

Platt, T. and W. Harrison (1985). Biogenic fluxes of carbon and oxygen in the ocean. Nature 318, (7 November), .

Polovina, J., G. Mitchum and G. Evans (1995). Decadal and basinscale variation in mixed layer depth and the impact on biological production in the Central and North Pacific, 1960 - 88. Deep Sea Research I 42, (10), 1701-1716.

Pond, S. and G. Pickard (1983). Introductory dynamical oceanography, 2nd/Ed. Butterworth-Heinemann, Oxford.

Porra, R. J., E. E. Pfundel and N. Engel (1997). Metabolism and function of photosynthetic pigments. *In* "Phytoplankton pigments in oceanography" (S. W. Jeffrey, Mantoura, R.F.C. and Wright, S.W., Ed.), Vol. 10, pp. 85-126. UNESCO, Paris.

Prezelin, B. (1987). Photosynthetic Physiology of Dinoflagellates. *In* "The Biology of Dinoflagellates" (F. Taylor, Ed.), Vol. 21, pp. 175-217. Blackwell Scientific Publications.

Probyn, T. A. (1987). Ammonium regeneration by microplankton in an upwelling environment. Marine Ecology Progress Series 37, 53-64.

Raven, J. (1998). The Twelfth Tansley Lecture. Small is beautiful: the picophytoplankton. Functional Ecology 503 - 513.

Reddy, M.P.M. (2001). Descriptive Physical Oceanography, First Edition. A.A. Balkema, Lisse.

Ricker, W.E. (1973). Linear regression in fishery research. Journal of Fisheries Research Board Canada, 30: 409 - 434.

Riebesell, U. and D. A. Wolf-Gladrow (2002). Supply and Uptake of Inorganic Nutrients. *In* "Phytoplankton Productivity: Carbon assimilation in marine and freshwater ecosystems" (P. J. le B. Williams, D. N. Thomas and C.S. Reynolds, Eds.) pg 109 - 140, Blackwell Science, Oxford.

Rippka, R., Coursin, T., Hess, W., Lichtle, C., Scanlan, D.J., Palinska, K.A., Iteman, I., Partensky, F., Houmard, J., and M. Herdman (2000). *Prochlorococcus marinus* Chisholm *et al.,* 1992 susp. pastoris subsp. nov strain PCC9511, the first axenic chlorophyll *a*(2)/*b*(2)-containing cyanobacterium (Oxyphotobacteria). International Journal of Systematic and Evolutionary Microbiology 50 (5), 1833 - 1847.

Ruttenberg, K.C. (2001). Phosphorus Cycle. *In* "Encyclopedia of Ocean Sciences (J.H. Steele, K.K. Turekian and S.A. Thorpe, Eds.) Vol., 4 (6), Academic Press, San Diego.

Ryther, J. (1969). Photosynthesis and fish production in the sea. Science 166, (72-76), .

Sanders, R., U. Berninger, E. Lim, P. Kemp and D. Caron (2000). Heterotrophic and mixotrophic nanoplankton predation on picoplankton in the Sargasso Sea and on Georges Bank. Marine Ecology Progress Series 192, 103-118.

Sanudo-Wilhelmy, S. A., A. B. Kustka, C. J. Gobler, D. A. Hutchins, M. Yang, K. Lwiza, J. Burns, D. G. Capone, J. A. Raven and E. J. Carpenter (2001). Phosphorus limitation of nitrogen fixation by *Trichodesmium* in the central Atlantic Ocean. Nature 411, (3 May 2001), 66-69.

Santhyendranath, S. and T. Platt (2001). Primary Production Distribution. *In* "Encyclopedia of Ocean Sciences" (J.H. Steele, K.K. Turekian and S.A. Thorpe, Eds.). Vol. 4 (6), Academic Press, San Diego.

Scanlan, D., W. Hess, F. Partensky, J. Newman and D. Vaulot (1996). High degree of genetic variation in *Prochlorococcus* (Prochlorophytes) revealed by RFLP analysis. European Journal of Phycology 31, (1), 1-9.

Scharek, R., L. Tupas and C. Karl (1999a). Diatom fluxes to the deep sea in the oligotrophic North Pacific gyre at Station ALOHA. Marine Ecology Progress Series 182, 55-67.

Scharek, R., M. Latasa, D. Karl and R. Bidigare (1999b). Temporal variations in diatom abundance and downwards vertical flux in the oligotrophic North Pacific gyre. Deep-Sea Research Part I 46, (6), 1051-1075.

Semina, H. and S. Levashova (1993). The biogeography of tropical phytoplankton species in the Pacific Ocean. International Revue Der Gesamten Hydrobiologie 243 - 262.

Semina, H. J. (1997). An Outline of the Geographical Distribution of Oceanic Phytoplankton. Advances in Marine Biology 32, 527-563.

Sieburth (1979). Sea Microbes, Oxford University Press, New York.

Signorini, S., R. Murtugudde, C. McClain, J. Christian, J. Picaut and A. Busalacchi (1999). Biological and physical signatures in the tropical and subtropical Atlantic. Journal of Geophysical Research 104, (C8), 18,367 - 18,382.

Skovgaard, A. (1995). Role of chloroplast retention in a marine dinoflagellate. Aquatic Microbial Ecology 15, (3), 293-301.

Smayda, T. (1978). Estimating cell numbers: 7.1. General Principles: 7.1.1. What to count? *In* "Phytoplankton Manual" (A. Sournia, Ed.), Vol. 6. UNESCO, Paris.

Smayda, T. (2000). Ecological features of harmful algal blooms in coastal upwelling ecosystems. South African Journal of Marine Science 22, 219 - 253.

Smith, W. and R. Barber (1987). The influence of horizontal and vertical displacements on phytoplankton assemblages in tropical upwelling systems. Oceanologica Acta. Proceedings International Symposium on Equatorial Vertical Motion, Paris, 6-10 May 1985 No 6 SP, 137-143.

Sournia, A. (1978). Phytoplankton Manual, UNESCO, Paris.

Sournia (1982). Is there a shade flora in the marine plankton? Journal of Plankton Research 4, (2), 391-399.

Sournia, A., C. Belin, C. Billard, M. Catherine, E. Erardledenn, J. Fresnel, P. Lassus, A. Pastoureaud and R. Soulard (1992). The Repetitive and expanding occurrence of a green, bloom-forming dinoflagellate (*Dinophyceae*) on the coasts of France. Cryptogamie Algologie 13, (1), 13.

Steele, J. and C. Yentsch (1960). The vertical distribution of chlorophyll. Journal of the Marine Biological Association (UK) 39, 217 - 226.

Steinberg D.K., Carlson, C.A., Bates, N.R., Johnson, R.J., Michaels, A.F., and A.H. Knap (2001). Overview of the US-JGOFS Bermuda Atlantic Time-series Study (BATS): A decadel-scale look at ocean biology and biogeochemistry. Deep Sea Research II 48, 1405 - 1447.

Stoecker, D., A. Li, D. Coats, D. Gustafson and M. Nannen (1997). Mixotrophy in the dinoflagellate *Prorocentrum minimum*. Marine Ecology Progress Series 152, 1-12.

Taylor, A., D. Harbour, R. Harris, R. Burkill and P. Edwards (1993). Seasonal succession in the pelagic ecosystem of the North Atlantic and the utilisation of nitrogen. Journal of Plankton Research 15, (8), 875 - 891.

Tchernia, P. (1980). Descriptive Regional Oceanography, Pergamon Marine Series.

Teira, E., M. Pazo, P. Serret and E. Fernandez (2001). Dissolved organic carbon production by microbial populations in the Atlantic Ocean. Limnology and Oceanography 46, (6), 1370-1377.

Tett, P. and E. D. Barton (1995). Why are there about 5000 species of phytoplankton in the sea? Journal of Plankton Research 17, (8), 1693-1704.

Thingstad, T., H. Havskum, K. Garde and B. Riemann (1996). On the Strategy of "Eating Your Competitor": A Mathematical Analysis of Algal Mixotrophy. Ecology 77, (7), 2108-2118.

Throndsen, J. (1978). Preservation and storage. *In* "Phytoplankton Manual" (A. Sournia, Ed.), Vol. 6. UNESCO, Paris.

Tomas, C. R., Ed. (1997). Identifying Marine Phytoplankton, pp. 1-835. Academic Press.

Tomczak, M. and J. S. Godfrey (1994). Regional Oceanography: An Introduction, Pergman Press.

Trees, C., M. Kennicutt and J. Brooks (1985). Errors associated with the standard fluorometric determination of chlorophylls and phaeopigments. Marine Chemistry 17, 1 - 12.

Trees, C., D. Clark, R. Bidigare, M. Ondrusek and J. Mueller (2000). Accessory pigments versus chlorophyll *a* concentrations within the euphotic zone: A ubiquitous relationship. Limnology and Oceanography 45, (5), 1130-1143.

Tyrrell, T. (1999). The relative influences of nitrogen and phosphorus on oceanic primary production. Nature 400 (6744), 525 - 531.

Tyrrell, T., E. Maranon, A. Poulton, A. Bowie, D. Harbour and E. Woodward (submitted). Factors controlling the large-scale latitudinal distribution of *Trichodesmium* spp. in the Atlantic Ocean. Journal of Plankton Research .

Varela, R., A. Cruzado, J. Tinore and E. Ladona (1992). Modelling the deep chlorophyll maximum - a coupled physical-biological approach. Journal of Marine Research 50, (3), 441 - 463.

Varela, R., A. Cruzado and J. Tintore (1994). A simulation analysis of various biological and physical factors influencing the deep chlorophyll maximum structure in oligotrophic areas. Journal of Marine Systems 5, (2), 143 - 157.

Vaulot, D., F. Partensky, J. Neveux, R. Mantoura and C. Llewellyn (1990). Winter presence of prochlorophytes in surface waters of the Northwestern Mediterranean Sea. Limnology and Oceanography 35, (5), 1156 - 1164.

Veldhuis, M. J. W. and G. W. Kraay (1990). Vertical distribution and pigment composition of a picoplanktonic prochlorophyte in the subtropical North Atlantic: a combined study of HPLC-analysis of pigments and flow cytometry. Marine Ecology Progress Series 68, 121-127.

Venegas, S., L. Mysak and D. Straub (1997). Atmosphere-ocean coupled variability in the South Atlantic. Journal of Climate 10, (11), 2904-2920.

Venrick, E. (1971). Recurrent groups of diatom species in the North Pacific. Ecology 52, (4), 614-625.

Venrick, E. (1974). The distribution and significance of *Richella intracellularis* Schmidt in the North Pacific Central Gyre. Limnology and Oceanography 19, (3), 437-445.

Venrick, E. (1978). Estimating cell numbers - 7.1.2. How many cells to count? *In* "Phytoplankton Manual" (A. Sournia, Ed.), Vol. 6. UNESCO, Paris.

Venrick, E. (1982). Phytoplankton in an oligotrophic ocean: Observations and Questions. Ecological Monographs 52, (2), 129-154.

Venrick, E. (1984). Winter mixing and the vertical stratification of phytoplankton - another look. Limnology and Oceanography 29, (3), 636-640.

Venrick, E., J. McGowan, D. Cayan and T. Hayward (1987). Climate and chlorophyll *a* - Long term trends in the central North Pacific Ocean. Science 238, (4823), 70-72.

Venrick, E. (1988). The vertical distributions of chlorophyll and phytoplankton species in the North Pacific central environment. Journal of Plankton Research 10, (5), 987-998.

Venrick, E. (1990a). Phytoplankton in an oligotrophic ocean: species structure and interannual variability. Ecology 71, (4), 1547-1563.

Venrick, E. (1990b). Mesoscale patterns of chlorophyll *a* in the central North Pacific. Deep-Sea Research part A 37, (6), 1017-1031.

Venrick, E. L. (1992). Phytoplankton species structure in the central North Pacific: Is the edge like the centre? Journal of Plankton Research 14, (5), 665-680.

Venrick, E. L. (1993). Phytoplankton seasonality in the central North Pacific: The endless summer reconsidered. Limnology and Oceanography 38, (69), 1135-1149.

Venrick, E. (1999). Phytoplankton species structure in the central North Pacific, 1973-1996: variability and persistence. Journal of Plankton Research 21, (6), 1029-1042.

Vernet, M. and C. Lorenzen (1987). The presence of chlorophyll *b* and the estimation of phaeopigments in marine phytoplankton. Journal Of Plankton Research 9, 255-265.

Vidal, M., C. Duarte and S. Agusti (1999). Dissolved organic nitrogen and phosphorus pools and fluxes in the central Atlantic Ocean. Limnology and Oceanography 44, (1), 106-115.

Villareal, T.A., M. Altabet and K. Culverrymsza (1993). Nitrogen transport by vertically migrating diatom mats in the North Pacific Ocean. Nature 363, (6431), 709-712.

Villareal, T. A., S. Woods, J. K. Moore and K. Culver-Rymsza (1996). Vertical migration of *Rhizosolenia* mats and their significance to $NO^{-3}$ fluxes in the Central North Pacific gyre. Journal of Plankton Research 18, (3), 1103-1121.

Villareal, T.A., C. Pilskaln, M. Brzezinski, F. Lipschultz, M. Dennett and G. Gardner (1999a). Upward transport of oceanic nitrate by migrating mats. Nature 397, (6718), 423-425.

Villareal, T.A., Joseph, L., Brzezinski, M.A., Shipe, R.F., Lipschultz, F., and M.A. Altabet (1999b). Biological and chemical characerteristics of the giant diatom *Ethmodiscus* (Bacillariophyceae) in the central North Pacific gyre. Journal of Phycology 35 (5), 896 - 902.

Vinogradov, M.E. (1981). Ecosystems of Equaotrial Upwellings. *In* "Analysis of Marine Ecosystems" (A.R. Longhurst, Ed.) pg 60 - 90, Academic Press, London.

Voituriez, B. and Y. Dandonneau (1974). Relations entre la structure thermique et la production primaire et al regeneration des sels nutririfs dans le Dome de Guinee. Cah. ORSTOM Ser Oceanography. 4, 241 - 255.

Waterbury, J., S. Watson, R. Guillard and L. Brand (1979). Widespread occurrence of a unicellular, marine, planktonic, cyanobacterium. Nature 277, (25 January), 29-30.

Welschmeyer, N. (1994). Fluorometric analysis of chlorophyll *a* in the presence of chlorophyll *b* and phaeopigments. Limnology and Oceanography 39, (8), 1985-1992.

West, N. and D. Scanlan (1999). Niche-partitioning of *Prochlorococcus* populations in a stratified water column in the eastern North Atlantic Ocean. Applied and Environmental Microbiology 65, (6), 2585 - 2591.

Williams, P.J. LeB. (1998). The balance of plankton respiration and photosynthesis in the open oceans. Nature 394, 55 - 57.

Winn, C., L. Campbell, J. Christian, R. Letelier, D. Hebel, J. Dore, L. Fujieki and D. Karl (1995). Seasonal Variability in the Phytoplankton community of the North Pacific Subtropical Gyre. Global Biogeochemical Cycles 9, (4), 605 - 620.

Winter, A. and W.G. Siesser (1994). Atlas of living coccolithophores. *In* " Coccolithophores" (A. Winter W.G Seisser, Eds.) pg 107 - 160. Cambridge University Press, Cambridge.

Winter, A., R. W. Jordan and P. H. Roth (1994). Biogeography of living coccolithophores in ocean waters. *In* "Coccolithophores" (A. Winter and W.G Siesser, Eds.) pg 161 - 178. Cambridge University Press, Cambridge.

Wooster, W., A. Bakun and D. McLain (1976). The seasonal upwelling cycle along the eastern boundary of the North Atlantic. Journal of Marine Research 34, (2), 131-141.

Wright, S. W., S. W. Jeffrey, R. F. C. Mantoura, C. A. Llewellyn, T. Bjornland, D. Repeta and N. Welschmeyer (1991). Improved HPLC method for the analysis of chlorophylls and carotenoids from marine phytoplankton. Marine Ecology Progress Series 77, 183-196.

Wu, J., W. Sunda, E. Boyle and D. Karl (2000). Phosphate depletion in the western North Pacific Ocean. Science 289, (5480), 759-762.

Wyatt, T. and I. Jenkinson (1997). Note on *Alexandrium* population dynamics. Journal of Plankton Research 19, (5), 551 - 575.

Young, J. R. (1994). Functions of coccoliths. *In* "Coccolithophores" (A. Winter and W. G. Siesser, Eds.). Cambridge University Press, Cambridge.

Zehr, J., M. Mellon and S. Zani (1998). New nitrogen fixing micro-organisms detected in oligotrophic oceans by amplification of nitrogenase (nifH) genes. Applied and Environmental Microbiology 64, (9), 3444-3450.

Zehr, J., J. Waterbury, P. Turner, J. Montoya, E. Osmoregie, G. Steward, A. Hansen and D. Karl (2001). Unicellular cyanobacteria fix N-2 in the subtropical North Pacific Ocean. Nature 412, (6847), 635 - 638.

Zhang, X. and M. Watanabe (2001). Grazing and growth of the mixotrophic chrysomonad *Poterioochromonas malhamensis* (*Chrysophyceae*) feeding on algae. Journal of Phycology 37, 738-743.

Zubkov, M., M. Sleigh, G. Tarran, P. Burkill and R. Leakey (1998). Picoplanktonic community structure on an Atlantic transect from 50N to 50S. Deep-Sea Research Part I 45, (8), 1339-1355.

Zubkov, M., M. Sleigh and P. Burkill (2000a). Assaying picoplankton distribution by flow cytometry of underway samples collected along a meridional transect across the Atlantic Ocean. Aquatic Microbial Ecology 21, 13-20.

Zubkov, M., M. Sleigh, P. Burkill and R. Leakey (2000b). Picoplankton Community Structure on the Atlantic Meridional Transect: A Comparison between Seasons. Progress in Oceanography 45, (3-4), 369.